



Caged-polyprenylated Xanthenes from the Twigs of

Garcinia merguensis

Dudsadee Sukavisite

Master of Science Thesis in Organic Chemistry


Prince of Songkla University

T	2003
Library	QD405 D82 2003 C 2
Bin Key	232315
	14 W.O. 2547

Thesis Title Caged-polyprenylated Xanthenes from the Twigs of
 Garcinia merguensis
Author Miss Dudsadee Sukavisite
Major Program Organic Chemistry


Advisory committee

..... *V. Rukachaisirikul.*Chairman
(Associate Professor Dr.Vatcharin Rukachaisirikul)


..... Committee
(Assistant Professor Dr.Chatchanok Karalai)

Examining committee


..... *V. Rukachaisirikul.*Chairman
(Associate Professor Dr.Vatcharin Rukachaisirikul)

..... Committee
(Assistant Professor Dr.Chatchanok Karalai)

..... *K. Panthong*Committee
(Dr.Kanda Panthong)

..... Committee
(Dr.Chatchai Wattanapiromsakul)

The Graduate School, Prince of Songkla University, has approved this thesis as partail fulfillment of the requirment for the Master of Science degree in Organic Chemistry.

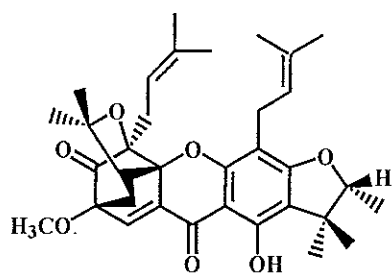
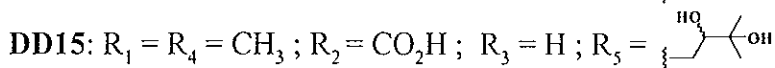
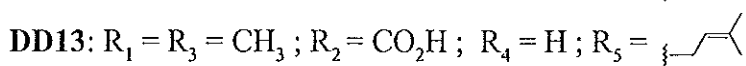
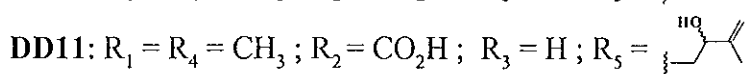
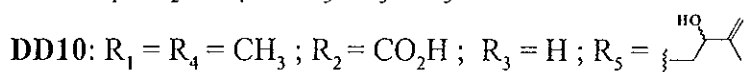
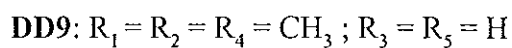
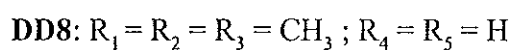
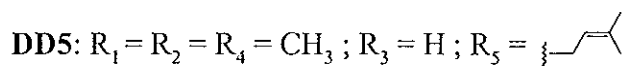
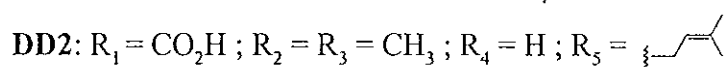
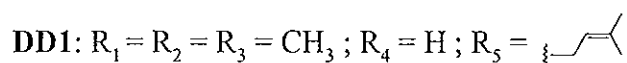
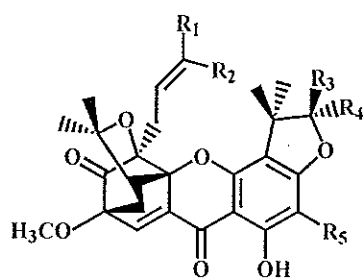
..... 

(Piti Trisdikoon, Ph.D.)
Associate Professor and Dean
Graduate School

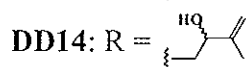
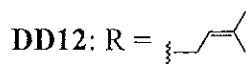
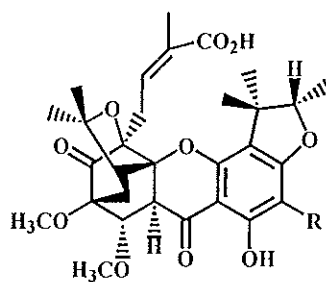
Thesis Title Caged-polyprenylated Xanthenes from the Twigs of
Garcinia merguensis
Author Miss Dudsadee Sukavisite
Major Program Organic Chemistry
Academic Year 2002

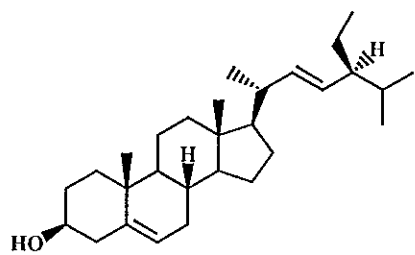
ABSTRACT

The crude methanol extract from the twigs of *Garcinia merguensis*, upon chromatographic separation, yielded four new caged-polyprenylated xanthenes (**DD3**, **DD5**, **DD14** and **DD15**) together with twelve known compounds : eight caged-polyprenylated xanthenes [scortechinone A (**DD1**), PP9 (**DD2**), PP3 (**DD8**), PP4 (**DD9**), PP14 (**DD10**), scortechinone C (**DD11**), PP8 (**DD12**) and scortechinone B (**DD13**)], one steroid [stigmasterol (**DD4**)], one triterpene [friedelin (**DD6**)], one sesquiterpene [germacra-4(15), 5*E*, 10(14)-trien-1-ol (**DD7**)] and one biflavone [I-5, II-5, I-7, II-7, I-3', I-4', II-4'-heptahydroxy-[I-3,II-8]-flavanonylflavone (**DD16**)]. All new structures were determined by 1D and 2D NMR spectroscopic data while known ones were identified by comparison of ¹H and/or ¹³C spectral data with those reported in the literature.

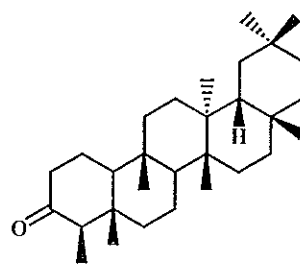


DD3

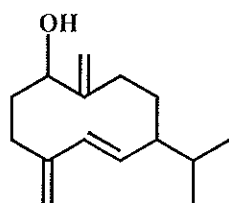




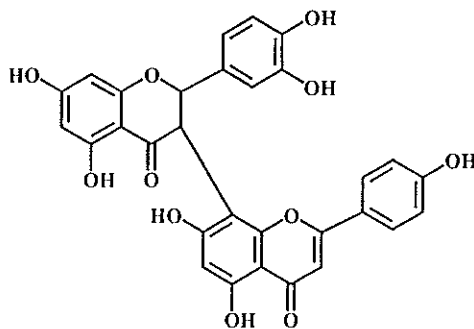
DD4



DD6



DD7

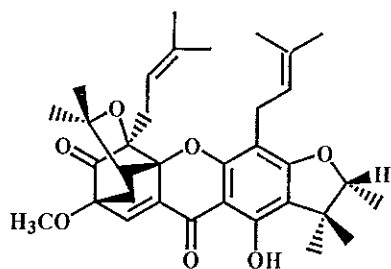
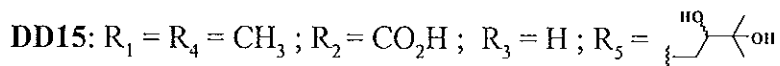
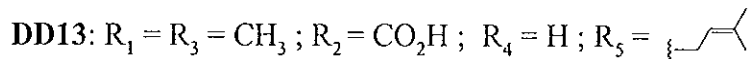
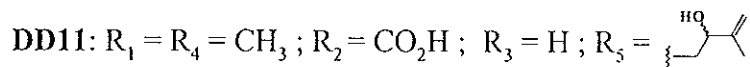
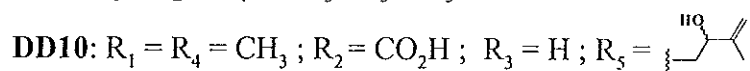
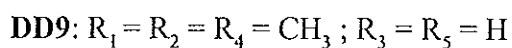
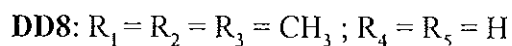
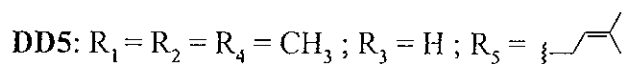
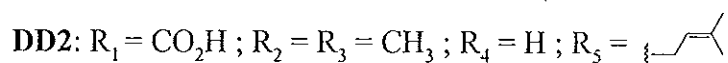
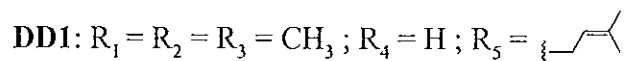
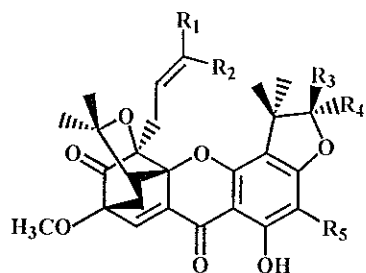


DD16

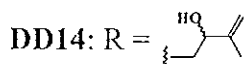
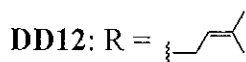
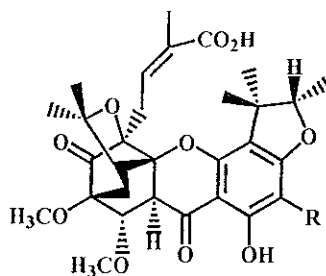
ชื่อวิทยานิพนธ์	เคจพอลิพรีนิลเลทเตทแซนโทนจากกิ่งกะนวล (<i>Garcinia merguensis</i>)
ผู้เขียน	นางสาวศุภฎี สุชะวณิชฐ์
สาขาวิชา	เคมีอินทรีย์
ปีการศึกษา	2545

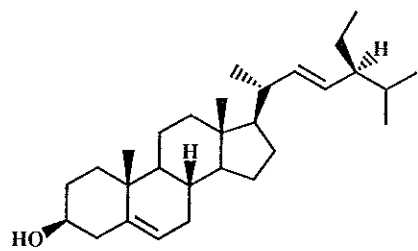
บทคัดย่อ

นำส่วนสกัดหยาบเมธานอลของกิ่งกะนวลมาทำการแยกให้บริสุทธิ์ด้วยวิธีทางโครมาโทกราฟี สามารถแยกสารใหม่ประเภท caged-polyprenylated xanthone ได้จำนวน 4 สาร (DD3, DD5, DD14 และ DD15) และสารที่ทราบโครงสร้างแล้วจำนวน 12 สาร ซึ่งเป็นสารประเภท caged-polyprenylated xanthone จำนวน 8 สาร [scortechinone A (DD1), PP9 (DD2), PP3 (DD8), PP4 (DD9), PP14 (DD10), scortechinone C (DD11), PP8 (DD12) และ scortechinone B (DD13)] สารประเภท steroid จำนวน 1 สาร [stigmasterol (DD4)] สารประเภท triterpene จำนวน 1 สาร [friedelin (DD6)] สารประเภท sesquiterpene จำนวน 1 สาร [germacra-4(15), 5E, 10(14)-trien-1-ol (DD7)] และสารประเภท biflavone จำนวน 1 สาร [I-5, II-5, I-7, II-7, I-3', I-4', II-4'-heptahydroxy-[I-3,II-8]-flavanonylflavone (DD16)] โครงสร้างของสารใหม่ทั้งหมดวิเคราะห์โดยใช้ข้อมูล 1D และ 2D NMR สเปกโทรสโกปี ส่วนสารที่ทราบโครงสร้างแล้วทำการวิเคราะห์โครงสร้างด้วยการเปรียบเทียบข้อมูล ^1H และ/หรือ ^{13}C NMR กับสารที่มีการรายงานโครงสร้างแล้ว

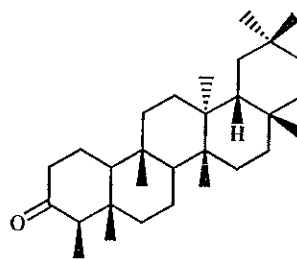


DD3

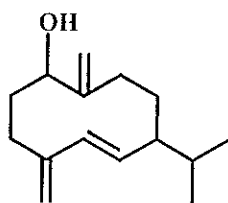




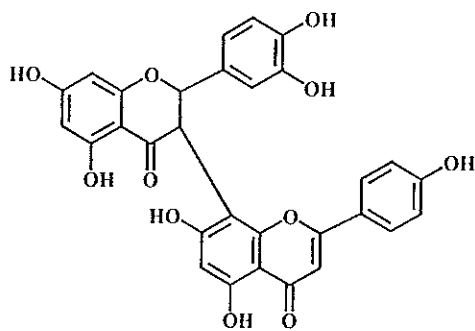
DD4



DD6



DD7



DD16

Acknowledgements

I wish to express my deepest gratitude and sincere appreciation to my advisor, Associate Professor Dr.Vatcharin Rukachaisirikul, for her valuable instruction, expert guidance and helpful suggestion. I would also like to direct my appreciation to her for correction of my thesis.

My sincere thanks are expressed to Assistant Professor Dr.Chatchanok Karalai, my co-advisor, for his kindness and valuable advice.

Special thanks are addressed to Professor Dr.Walter C. Taylor, Department of Organic Chemistry, the University of Sydney, Australia for recording 400 MHz NMR and mass spectra.

My deeply gratitude is also due to the staffs of the Department of Chemistry, Faculty of Science, Prince of Songkla University, including the officers for making this thesis possible and to Ms.Dusanee Langjae, the Scientific Equipment Center, Prince of Songkla University, for recording 500 MHz NMR spectra.

Appreciately thank to Higher Education Development Project : Postgraduate Education and Research Program in Chemistry, funded by The Royal Thai Government and the Graduate School, Prince of Songkla University for scholarship.

Finally, none of this would have been possible without love and encouragement of my family, Miss Yaowapa Sukpomma, Miss Thunwadee Ritthiwigrom and friends.

Dudsadee Sukavisite

Contents

	Page
Abstract (in English)	(3)
Abstract (in Thai)	(6)
Acknowledgements	(9)
Contents	(10)
List of Tables	(12)
List of Illustrations	(16)
Abbreviations and Symbols	(20)
Chapter	
1 INTRODUCTION	1
1.1 Introduction	1
1.2 Review of Literatures	2
1.2.1 Chemical constituents from the genus <i>Garcinia</i>	2
1.2.2 Caged-polyprenylated xanthenes	6
1.3 The objectives	22
2 EXPERIMENTAL	23
2.1 Chemicals and instruments	23
2.2 Plant material	24
2.3 Extraction and isolation	24
3 RESULTS AND DISCUSSION	82
3.1 Compound DD13	82
3.2 Compound DD15	85
3.3 Compound DD2	90
	(10)

Contents (Continued)

	Page
3.4 Compound DD11	93
3.5 Compound DD10	95
3.6 Compound DD14	98
3.7 Compound DD12	103
3.8 Compound DD1	105
3.9 Compound DD3	108
3.10 Compound DD5	112
3.11 Compound DD8	114
3.12 Compound DD9	117
3.13 Compound DD7	119
3.14 Compound DD16	123
3.15 Compound DD4	127
3.16 Compound DD6	129
Bibliography	198
Vitae	207

List of Tables

Table	Page
1 Compounds isolated from plants of the genus <i>Garcinia</i>	3
2 Caged-polyprenylated xanthenes from the genus <i>Garcinia</i>	7
3 Solubility of the methanol extract in various solvents at room temperature	24
4 Fractions obtained from fraction A by column chromatography over silica gel	26
5 Subfractions obtained from A3 by column chromatography over silica gel	27
6 Subfractions obtained from A4 by flash column chromatography over silica gel	29
7 Subfractions obtained from A5 by flash column chromatography over silica gel	30
8 Subfractions obtained from SolA5.8 by flash column chromatography over silica gel	38
9 Subfractions obtained from A6 by flash column chromatography over silica gel	43
10 Subfractions obtained from A8 by column chromatography over silica gel	44
11 Subfractions obtained from A8.5 by column chromatography over silica gel	45
12 Subfractions obtained from K2 by flash column chromatography over silica gel	46

List of Tables (Continued)

Table	Page
13 Subfractions obtained from KB2 by flash column chromatography over silica gel	47
14 Subfractions obtained from A8.6 by column chromatography over silica gel	49
15 Subfractions obtained from A8.6/2 by column chromatography over silica gel	50
16 Subfractions obtained from C3 by column chromatography over silica gel	51
17 Subfractions obtained from A8.7 by column chromatography over reverse-phase silica gel	53
18 Subfractions obtained from L2 by flash column chromatography over silica gel	54
19 Subfractions obtained from A8.8 by column chromatography over reverse-phase silica gel	56
20 Subfractions obtained from D2 by column chromatography over silica gel	57
21 Subfractions obtained from D2.4 by column chromatography over silica gel	59
22 Subfractions obtained from DC2 by column chromatography over silica gel	60
23 Subfractions obtained from D4 by flash column chromatography over silica gel	63

List of Tables (Continued)

Table	Page
24 Subfractions obtained from A8.9 by column chromatography over reverse-phase silica gel	65
25 Subfractions obtained from M2 by column chromatography over reverse-phase silica gel	66
26 Subfractions obtained from M2.2 by flash column chromatography over silica gel	66
27 Subfractions obtained from M3 by column chromatography over silica gel	68
28 Subfractions obtained from A9 by column chromatography over reverse-phase silica gel	70
29 Subfractions obtained from A9.2 by flash column chromatography over silica gel	71
30 Subfractions obtained from A9.4 by flash column chromatography over silica gel	73
31 Subfractions obtained from A10 by column chromatography over reverse-phase silica gel	75
32 Subfractions obtained from A10.1 by flash column chromatography over silica gel	76
33 Subfractions obtained from A10.3 by column chromatography over reverse-phase silica gel	77
34 Subfractions obtained from A10.3/2 by column chromatography over reverse-phase silica gel	78

List of Tables (Continued)

Table	Page
35 Subfractions obtained from U2 by column chromatography over reverse-phase silica gel	79
36 The ¹ H NMR data of compounds DD13 and scortechinone B	84
37 The NMR data of compounds DD15 and scortechinone B	88
38 The ¹ H NMR data of compounds DD2 , PP9 and scortechinone B	91
39 The ¹ H NMR data of compounds DD11 , scortechinone C and scortechinone B	94
40 The NMR data of compounds DD10 , PP14 and scortechinone C	96
41 The NMR data of compounds DD14 and scortechinone C	100
42 The ¹ H NMR data of compounds DD12 , PP8 and DD14	104
43 The NMR data of compounds DD1 , scortechinone A and scortechinone B	106
44 The NMR data of compounds DD3 and scortechinone A	110
45 The ¹ H NMR data of compounds DD5 , GF3 and scortechinone A	113
46 The ¹ H NMR data of compounds DD8 , PP3 and scortechinone A	115
47 The ¹ H NMR data of compounds DD9 , PP4 and DD8	118
48 The NMR data of compound DD7	121
49 The NMR data of compounds DD7 and germacra-4(15), 5E, 10(14)-trien-1-ol	122
50 The ¹ H NMR data of compounds DD16 , morelloflavone (14) and I-5, II-5, I-7, II-7, I-3', I-4', II-4'-heptahydroxy-[I-3,II-8]-flavanonylflavone (15)	126
51 The ¹ H NMR data of compound DD4 and stigmaterol	128
52 The ¹ H NMR data of compound DD6 and friedelin	129

List of Illustrations

Figure	Page
1 UV (MeOH) spectrum of DD13	131
2 FT-IR (neat) spectrum of DD13	131
3 ^1H NMR (500 MHz) (CDCl_3) spectrum of DD13	132
4 UV (MeOH) spectrum of DD15	133
5 FT-IR (neat) spectrum of DD15	133
6 ^1H NMR (400 MHz) (CDCl_3) spectrum of DD15	134
7 ^{13}C NMR (100 MHz) (CDCl_3) spectrum of DD15	135
8 DEPT spectrum of DD15	136
9 NOEDIFF spectrum of DD15 after irradiation at δ_{H} 1.29	137
10 NOEDIFF spectrum of DD15 after irradiation at δ_{H} 1.53	138
11 NOEDIFF spectrum of DD15 after irradiation at δ_{H} 1.71	139
12 NOEDIFF spectrum of DD15 after irradiation at δ_{H} 5.20	140
13 2D HMQC spectrum of DD15	141
14 2D HMBC spectrum of DD15	142
15 Mass spectrum of DD15	143
16 UV (MeOH) spectrum of DD2	144
17 FT-IR (neat) spectrum of DD2	144
18 ^1H NMR (400 MHz) (CDCl_3) spectrum of DD2	145
19 UV (MeOH) spectrum of DD11	146
20 FT-IR (neat) spectrum of DD11	146
21 ^1H NMR (500 MHz) (CDCl_3) spectrum of DD11	147

List of Illustrations (Continued)

Figure	Page
22 UV (MeOH) spectrum of DD10	148
23 FT-IR (neat) spectrum of DD10	148
24 ^1H NMR (500 MHz) (CDCl_3) spectrum of DD10	149
25 ^{13}C NMR (125 MHz) (CDCl_3) spectrum of DD10	150
26 UV (MeOH) spectrum of DD14	151
27 FT-IR (neat) spectrum of DD14	151
28 ^1H NMR (500 MHz) (CDCl_3) spectrum of DD14	152
29 ^{13}C NMR (125 MHz) (CDCl_3) spectrum of DD14	153
30 DEPT spectrum of DD14	154
31 NOEDIFF spectrum of DD14 after irradiation at δ_{H} 1.12	155
32 NOEDIFF spectrum of DD14 after irradiation at δ_{H} 1.22	156
33 NOEDIFF spectrum of DD14 after irradiation at δ_{H} 1.43	157
34 NOEDIFF spectrum of DD14 after irradiation at δ_{H} 4.47	158
35 NOEDIFF spectrum of DD14 after irradiation at δ_{H} 6.63	159
36 2D HMQC spectrum of DD14	160
37 2D HMBC spectrum of DD14	161
38 UV (MeOH) spectrum of DD12	162
39 FT-IR (neat) spectrum of DD12	162
40 ^1H NMR (500 MHz) (CDCl_3) spectrum of DD12	163
41 UV (MeOH) spectrum of DD1	164
42 FT-IR (neat) spectrum of DD1	164

List of Illustrations (Continued)

Figure	Page
43 ^1H NMR (500 MHz) (CDCl_3) spectrum of DD1	165
44 ^{13}C NMR (125 MHz) (CDCl_3) spectrum of DD1	166
45 UV (MeOH) spectrum of DD3	167
46 FT-IR (neat) spectrum of DD3	167
47 ^1H NMR (500 MHz) (CDCl_3) spectrum of DD3	168
48 ^{13}C NMR (125 MHz) (CDCl_3) spectrum of DD3	169
49 DEPT spectrum of DD3	170
50 NOEDIFF spectrum of DD3 after irradiation at δ_{H} 1.30	171
51 NOEDIFF spectrum of DD3 after irradiation at δ_{H} 1.37	172
52 NOEDIFF spectrum of DD3 after irradiation at δ_{H} 1.68	173
53 NOEDIFF spectrum of DD3 after irradiation at δ_{H} 4.40	174
54 NOEDIFF spectrum of DD3 after irradiation at δ_{H} 5.32	175
55 2D HMQC spectrum of DD3	176
56 2D HMBC spectrum of DD3	177
57 Mass spectrum of DD3	178
58 UV (MeOH) spectrum of DD5	179
59 FT-IR (neat) spectrum of DD5	179
60 ^1H NMR (500 MHz) (CDCl_3) spectrum of DD5	180
61 UV (MeOH) spectrum of DD8	181
62 FT-IR (neat) spectrum of DD8	181
63 ^1H NMR (500 MHz) (CDCl_3) spectrum of DD8	182

List of Illustrations (Continued)

Figure	Page
64 UV (MeOH) spectrum of DD9	183
65 FT-IR (neat) spectrum of DD9	183
66 ^1H NMR (500 MHz) (CDCl_3) spectrum of DD9	184
67 UV (MeOH) spectrum of DD7	185
68 FT-IR (neat) spectrum of DD7	185
69 ^1H NMR (500 MHz) (CDCl_3) spectrum of DD7	186
70 ^{13}C NMR (125 MHz) (CDCl_3) spectrum of DD7	187
71 DEPT spectrum of DD7	188
72 2D HMQC spectrum of DD7	189
73 2D HMBC spectrum of DD7	190
74 2D ^1H - ^1H cosy spectrum of DD7	191
75 UV (MeOH) spectrum of DD16	192
76 FT-IR (neat) spectrum of DD16	192
77 ^1H NMR (500 MHz) (CD_3OD) spectrum of DD16	193
78 FT-IR (neat) spectrum of DD4	194
79 ^1H NMR (500 MHz)(CDCl_3) spectrum of DD4	195
80 FT-IR (neat) spectrum of DD6	196
81 ^1H NMR (500 MHz) (CDCl_3) spectrum of DD6	197

Abbreviations and Symbols

<i>s</i>	=	<i>singlet</i>
<i>d</i>	=	<i>doublet</i>
<i>t</i>	=	<i>triplet</i>
<i>q</i>	=	<i>quartet</i>
<i>m</i>	=	<i>multiplet</i>
<i>br</i>	=	<i>broad</i>
<i>brs</i>	=	<i>broad singlet</i>
<i>brd</i>	=	<i>broad doublet</i>
<i>brt</i>	=	<i>broad triplet</i>
<i>brdd</i>	=	<i>broad doublet of doublet</i>
<i>dd</i>	=	<i>doublet of doublet</i>
<i>dq</i>	=	<i>doublet of quartet</i>
<i>dt</i>	=	<i>doublet of triplet</i>
<i>ddd</i>	=	<i>doublet of doublet of doublet</i>
<i>qd</i>	=	<i>quartet of doublet</i>
<i>qt</i>	=	<i>quartet of triplet</i>
<i>md</i>	=	<i>multiplet of doublet</i>
<i>mt</i>	=	<i>multiplet of triplet</i>
<i>mdd</i>	=	<i>multiplet of doublet of doublet</i>
δ	=	chemical shift relative to TMS
<i>J</i>	=	coupling constant
<i>m/z</i>	=	a value of mass divided by charge
$^{\circ}\text{C}$	=	degree celcius

Abbreviations and Symbols (Continued)

R_f	=	retention factor
g	=	gram
mg	=	milligram
kg	=	kilogram
mL	=	milliliter
cm^{-1}	=	reciprocal centimeter (wavenumber)
nm	=	nanometer
ppm	=	part per million
λ_{max}	=	maximum wavelength
ν	=	absorption frequencies
ϵ	=	Molar extinction coefficient
Hz	=	hertz
MHz	=	megahertz
rel. int.	=	relative intensity
$[\alpha]_D$	=	specific rotation
c	=	concentration
H-n	=	position of protons
C-n	=	position of carbons
TLC	=	Thin-layer Chromatography
UV	=	Ultraviolet
IR	=	Infrared
NMR	=	Nuclear Magnetic Resonance
1D NMR	=	One Dimensional Nuclear Magnetic Resonance

Abbreviations and Symbols (Continued)

2D NMR	=	Two Dimensional Nuclear Magnetic Resonance
MS	=	Mass Spectroscopy
HMQC	=	Heteronuclear Multiple Quantum Coherence
HMBC	=	Heteronuclear Multiple Bond Correlation
DEPT	=	Distortionless Enhancement by Polarization transfer
NOE	=	Nuclear Overhauser Effect
NOEDIFF	=	Nuclear Overhauser Effect Difference Spectroscopy
TMS	=	tetramethylsilane
d_6 -DMSO	=	hexadeuterodimethylsulphoxide
MeOH	=	methanol
NaOH	=	sodium hydroxide
HCl	=	hydrochloric acid
$CDCl_3$	=	deuteriochloroform
CD_3OD	=	tetradeteromethanol
ASA	=	anisaldehyde-sulphuric acid in acetic acid solution

Chapter 1

INTRODUCTION

1.1 Introduction

Garcinia merguensis (family Guttiferae) has various local names: “Ka nuan” (กะนวน) in Peninsular; “Khanom pang” (ขนมปัง), “Khi phueng” (ขี้ผึ้ง) in Chanthaburi; “Sa-pae” (ซาแป) in Malay-Narathiwat; “Nuan” (นวน) in Northern; “Nuan khao” (นวนขาว), “Nuan dong” (นวนดง) in Surat Thani; “Nuan daeng” (นวนแดง) in Chumphon; “Nuan paeng” (นวนแป้ง) in Nakhon Si Thammarat; “Bun yong” (บุญยอง) in Lampang; “Muang nok” (ม่วงนก) in Ranong; “Yang khao” (ยางเขา) in Trat (เต็ม, 2523). *G. merguensis* is a small tree or shrub. Leaves are thinly coriaceous. Male flowers are numerous; cymes 0.17-0.25 in. long; pedicels 0.25 in., 4-gonal. Female flowers are on pedicels 0.50-1 in. Fruits are 0.33-0.50 in. long, oblong, fleshy. Seeds are solitary, subreniform. *G. merguensis* was commonly found at Eastern Peninsular; indense woods from Mergui to Malacca (Hooker, 1875).

1.2 Review of Literatures

1.2.1 Chemical constituents from the genus *Garcinia*

The genus *Garcinia* (family Guttiferae, sub-family Clusiodeae), which is encountered mainly in lowland rainforests of the tropical world, has been extensively investigated from phytochemical, biological and pharmacological points of view. Biflavonoids (Thoison, 2000 ; Terashima, 1999 ; Spino, 1995 ; Fukuyama, 1993 ; Gunatilaka, 1983), benzophenones (Minami, 1998 ; Inuma, 1996 ; Gustafson, 1992), lactones (Wu, 2001), triterpenes (Rukachaisirikul, 2000b ; Thoison, 2000 ; Nyemba, 1990) and xanthenes (Suksamrarn, 2002 ; Nilar, 2002 ; Wu, 2001 ; Rukachaisirikul, 2000a) are compounds isolated from this genus. Some of these exhibit a wide range of biological and pharmacological activities such as cytotoxic (Thoison, 2000 ; Xu, 2000 ; Cao, 1998a, b), antimicrobial (Permana, 2001 ; Kosela, 2000 ; Peres, 2000 ; Ilyas, 1994 ; Parveen, 1991), antiinflammatory (Peres, 2000 ; Ilyas, 1994 ; Parveen, 1991), antibacterial (Permana, 2001 ; Peres, 2000 ; Rukachaisirikul, 2000a ; Ito, 1997 ; Parveen, 1991), antifungal (Kosela, 2000 ; Peres, 2000 ; Gopalakrishnan, 1997), antitumor (Ito, 1998), antiimmunosuppressive (Ilyas, 1994 ; Parveen, 1991), antimalarial (Kosela, 2000 ; Likhiwitayawuid, 1998a, b), anti-HIV (Kosela, 2000 ; Lin, 1997 ; Gustafson, 1992) activities, antioxidant (Peres, 2001 ; Kosela, 2000 ; Minami, 1996) and the healing of skin infections and wounds (Ilyas, 1994).

According to information from NAPRALERT database developed by University of Illinois at Chicago and chemical abstracts in the year 2001, chemical constituents isolated from 62 species of the genus *Garcinia* were reported. They were then summarized by Thunwadee Ritthiwigrom in the year 2001. Therefore, only

additional chemical constituents from the genus *Garcinia* apart from those reported are summarized in Table 1.

Table 1 Compounds isolated from plants of the genus *Garcinia*

Scientific name	Investigated part	Compound	Structure	Bibliography
<i>G. atroviridis</i>	fruits	2-butoxycarbonyl-methyl-3-butoxycarbonyl-2-hydroxy-3-propanolide	3a	Mackeen, <i>et al.</i> , 2002
		1',1''-dibutyl Me hydroxycitrate	-	
<i>G. mangostana</i>	green fruit	mangostenol	4.2a	Suksamrarn, <i>et al.</i> , 2002
	hulls	mangostenone A	2.2m	
		mangostenone B	4.2n	
		trapezifolixanthone	4.1a	
		tovophyllin B	4.2o	
		α -mangostin	4.2b	
		β -mangostin	4.2c	
		garcinone B	4.2q	
		mangostinone	4.1b	
		mangostanol	4.2p	
(-)-epicatechin	2a			

Table 1 (Continued)

Scientific name	Investigated part	Compound	Structure	Bibliography
<i>G. mangostana</i>	heartwood	1-(OH)-8-(2-(OH)-3-methylbut-3-enyl)-3,6,7-tri(OMe)-2-(3-methylbut-2-enyl)-xanthone	4.2d	Nilar and Harrison, 2002
		(16 <i>E</i>)-1-(OH)-8-(3-(OH)-3-methylbut-1-enyl)-3,6,7-tri(OMe)-2-(3-methylbut-2-enyl)-xanthone	4.2e	
		1-(OH)-2-(2-(OH)-3-methylbut-3-enyl)-3,6,7-tri(OMe)-8-(3-methylbut-2-enyl)-xanthone	4.2f	
		β -mangostin	4.2c	
		1,6-di(OH)-2-(2-(OH)-3-methylbut-3-enyl)-3,7-di(OMe)-8-(3-methylbut-2-enyl)-xanthone	4.2g	

Table 1 (Continued)

Scientific name	Investigated part	Compound	Structure	Bibliography
<i>G. mangostana</i>	heartwood	(16 <i>E</i>)-1,6-di(OH)-8-(3-(OH)-3-methylbut-1-enyl)-3,7-di(OMe)-2-(3-methylbut-2-enyl)-xanthone	4.2h	Nilar and Harrison, 2002
		1,6-di(OH)-8-(2-(OH)-3-methylbut-3-enyl)-3,7-di(OMe)-2-(3-methylbut-2-enyl)-xanthone	4.2i	
		1,3-di(OH)-2-(2-(OH)-3-methylbut-3-enyl)-6,7-di(OMe)-8-(3-methylbut-2-enyl)-xanthone	4.2j	
		mangostanin	4.2r	
		6- <i>O</i> -methylmangostanin	4.2s	
		1,6-di(OH)-3,7-di(OMe)-2-(3-methylbut-2-enyl)xanthone	4.2k	

Table 1 (Continued)

Scientific name	Investigated part	Compound	Structure	Bibliography
<i>G. mangostana</i>	heartwood	1,6-di(OH)-3,7-di-(OMe)-2-(3-methylbut-2-enyl)-8-(2-oxo-3-methylbut-3-enyl)-xanthone	4.2l	Nilar and Harrison, 2002
		garciniafuran	4.2t	
<i>G. nervosa</i>	leaves	5'-Br-2'-(OH)-4,4',6'-tri-(OMe)chalcone	1a	Ilyas, <i>et al.</i> , 2002
		2'-(OH)-4,4'-di(OMe)chalcone	1b	
		2'-(OH)-3,4,4',6'-tetra-(OMe) dihydrochalcone	1c	

1.2.2 Caged-polyprenylated xanthenes

Caged-polyprenylated xanthenes are produced by several plants exclusively from the genus *Garcinia*, e.g. *Garcinia bracteata*, *G. forbesii*, *G. gaudichaudii*, *G. hanburyi*, *G. morella* and *G. scortechinii*, as shown in Table 2. The classic member of these caged-xanthenes is gambogic acid as its structural work started in 1809 but the corrected molecular formula was first reported in 1963 (Yates, 1963). However, the first caged-polyprenylated xanthone of which structure to be elucidated was morellin

(Kantha, 1963). This was achieved after a detailed and extensive chemical investigation by Venkataraman and his group over a period of years. Since the major components found from our investigation on the twigs of *G. merguensis* were caged-polyprenylated xanthenes, compounds of this type were then summarized in Table 2.

Table 2 Caged-polyprenylated xanthenes from the genus *Garcinia*

Scientific name	Investigated part	Compound	Structure	Bibliography
<i>G. bracteata</i>	leaves	bractatin	4.3uu	Thoison, <i>et al.</i> , 2000
		isobractatin	4.3ww	
		1- <i>O</i> -methylbractatin	4.3vv	
		1- <i>O</i> -methylisobractatin	4.3xx	
		1- <i>O</i> -methyl-8-methoxy-8,8a-dihydrobractatin	4.3yy	
		1- <i>O</i> -methylneobractatin	4.3zz	
<i>G. forbesii</i>	branches and stem	forbesione	4.3r	Leong, <i>et al.</i> , 1996
<i>G. gaudichaudii</i>	leaves	gaudichaudione I	4.3t	Wu, <i>et al.</i> , 2000
		gaudichaudione J	4.3u	
		gaudichaudione A	4.3p	Cao, <i>et al.</i> , 1998a, b
		gaudichaudione B	4.3m	

Table 2 (Continued)

Scientific name	Investigated part	Compound	Structure	Bibliography
<i>G. gaudichaudii</i>	leaves	gaudichaudione C	4.3q	Cao, <i>et al.</i> , 1998a, b Cao, <i>et al.</i> , 1998b
		gaudichaudione D	4.3j	
		gaudichaudione E	4.3k	
		gaudichaudione F	4.3n	
		gaudichaudione G	4.3v	
		gaudichaudione H	4.3s	
		gaudichaudiic acid A	4.3l	
		gaudichaudiic acid B	4.3o	
		gaudichaudiic acid C	4.3d	
		gaudichaudiic acid D	4.3e	
		gaudichaudiic acid E	4.3b	
		morellic acid	4.3c	
		forbesione	4.3r	
		bark	7-isoprenylmorellic acid	
		morellic acid	4.3c	
		isomorellin	4.3bb	
		isomoreollin	4.3ll	
		isomorellinol	4.3ii	
		gaudichaudiic acid E	4.3b	
		isomorellic acid	4.3gg	

Table 2 (Continued)

Scientific name	Investigated part	Compound	Structure	Bibliography
<i>G. gaudichaudii</i>	bark	gaudichaudiic acid F	4.3h	Xu, <i>et al.</i> , 2000
		gaudichaudiic acid G	4.3i	
		gaudichaudiic acid H	4.3f	
		gaudichaudiic acid I	4.3g	
<i>G. hanburyi</i>	latex	isomorellinol	4.3ii	Lin, <i>et al.</i> , 1993
		isogambogic acid	4.3aa	
		gambogic acid	4.3z	Ollis, <i>et al.</i> , 1965 ; Lin, <i>et al.</i> , 1993 ; Asano, <i>et al.</i> , 1996
		gambogin	4.3dd	
		morellin dimethyl acetal	4.3ee	
		isomoreollin B	4.3jj	Asano, <i>et al.</i> , 1996
		moreollic acid	4.3kk	
		gambogenic acid	4.3nn	
		gambogenin	4.3oo	
		isogambogenin	4.3pp	
		desoxygambogenin	4.3qq	

Table 2 (Continued)

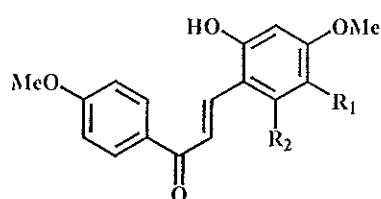
Scientific name	Investigated part	Compound	Structure	Bibliography
<i>G. hanburyi</i>	latex	gambogenin dimethyl acetal	4.3rr	Asano, <i>et al.</i> , 1996
		gambogellic acid	4.3ss	
		hanburin	4.3tt	
		isomorellin	4.3bb	
		morellic acid	4.3c	
		deoxymorellin	4.3cc	
		(deoxymorellin)		
<i>G. morella</i>	pericarp	isomorellin	4.3bb	Bringi, <i>et al.</i> , 1955
		deoxymorellin	4.3cc	
		(deoxymorellin)		
	seeds	morellin	4.3ff	Rao, 1937 ; Bringi, <i>et al.</i> , 1955
		dihydroisomorellin	4.3aaa	Bhat, <i>et al.</i> , 1964
		ethoxydihydroisomorellin	4.3ll	
	(isomorellin)			
	deoxymorellin	4.3cc		
	(deoxymorellin)			

Table 2 (Continued)

Scientific name	Investigated part	Compound	Structure	Bibliography
<i>G. morella</i>	seed coat	moreollin	4.3mm	Murthy, <i>et al.</i> , 1953 ; Rao, <i>et al.</i> , 1974
		morellin	4.3ff	Rao, <i>et al.</i> , 1974
	bark	morellinol	4.3hh	Adawadkar, <i>et al.</i> , 1976
	latex	morellic acid	4.3c	Karanjgaonkar, <i>et al.</i> , 1966
isomorellic acid		4.3gg		
<i>G. scortechinii</i>	twigs	scortechinone A	4.3w	Rukachaisirikul, <i>et al.</i> , 2000a
		scortechinone B	4.3x	
		scortechinone C	4.3y	

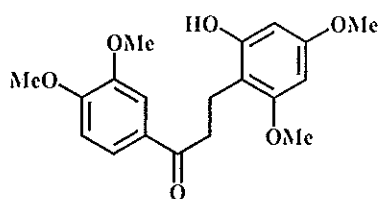
Structures of compounds isolated from plants of the genus *Garcinia*

1. Chalcone



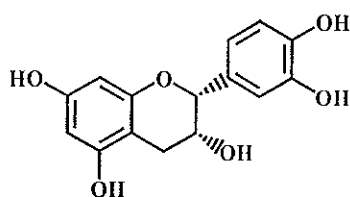
1a: $R_1 = \text{Br}$; $R_2 = \text{OMe}$: 5'-Br-2'-(OH)-4,4',6'-tri(OMe)chalcone

1b: $R_1 = R_2 = \text{H}$: 2'-(OH)-4,4'-di(OMe)chalcone



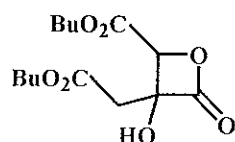
1c: 2'-(OH)-3,4,4',6'-tetra(OMe)dihydrochalcone

2. Flavonoid



2a: (-)-epicatechin

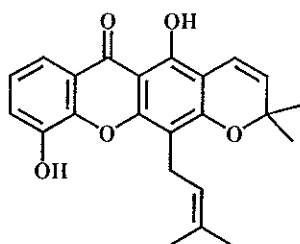
3. Lactone



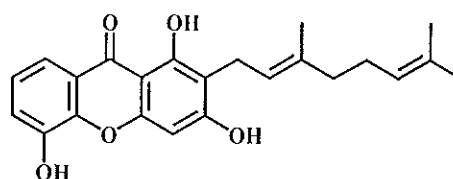
3a: 2-butoxycarbonylmethyl-3-butoxycarboxyl-2-hydroxy-3-propanolide

4. Xanthones

4.1 Trioxyxanthones

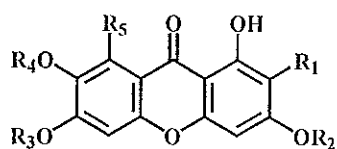


4.1a: trapezifolixanthone



4.1b: mangostinone

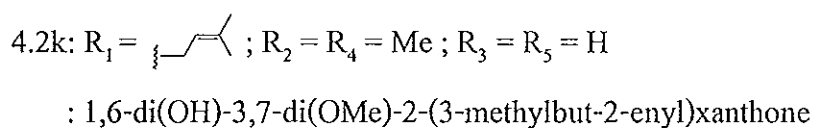
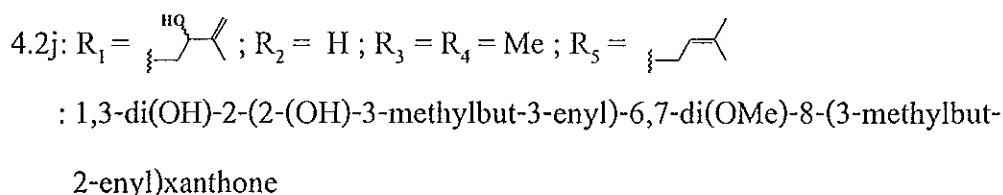
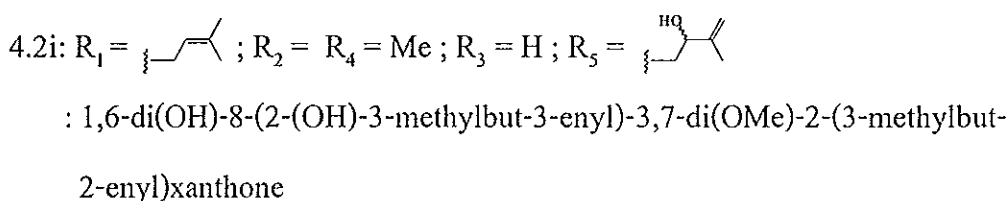
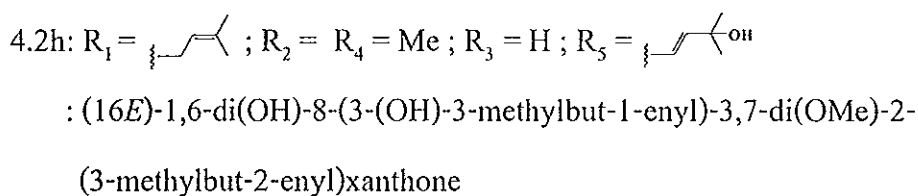
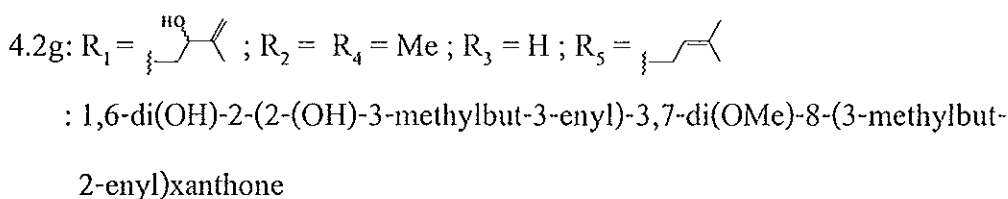
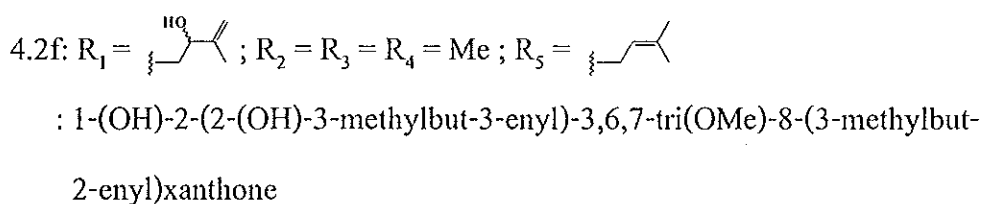
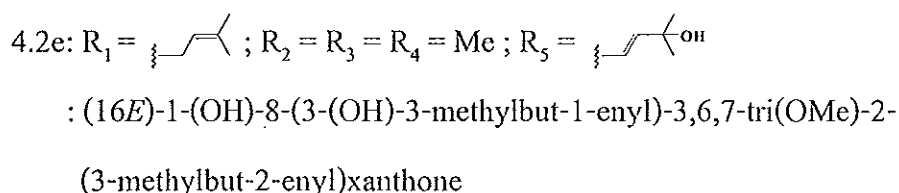
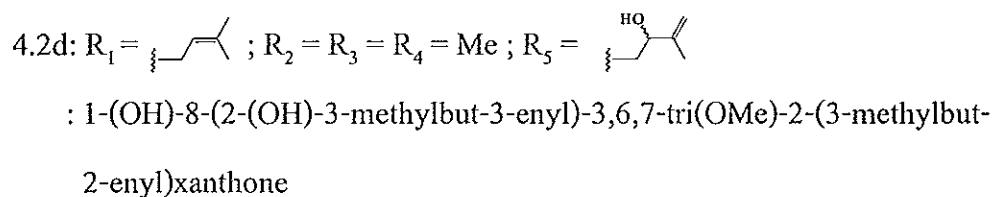
4.2 Tetraoxyxanthones



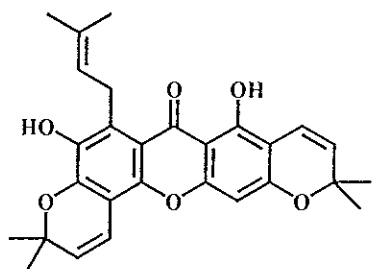
4.2a: $R_1 = \text{HO}-\text{CH}_2-\text{CH}=\text{C}(\text{Me})_2$; $R_2 = R_3 = \text{H}$; $R_4 = \text{Me}$; $R_5 = \text{CH}_2-\text{CH}=\text{C}(\text{Me})_2$: mangostenol

4.2b: $R_1 = R_5 = \text{CH}_2-\text{CH}=\text{C}(\text{Me})_2$; $R_2 = R_3 = \text{H}$; $R_4 = \text{Me}$: α -mangostin

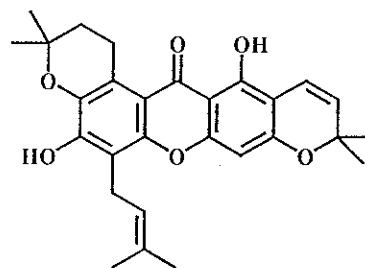
4.2c: $R_1 = R_5 = \text{CH}_2-\text{CH}=\text{C}(\text{Me})_2$; $R_2 = R_4 = \text{Me}$; $R_3 = \text{H}$: β -mangostin



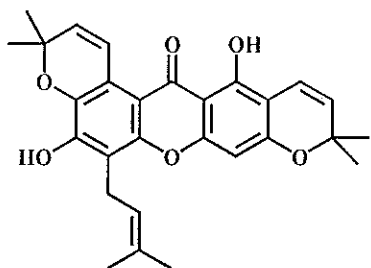
4.2l: $R_1 = \text{---CH=CH---}$; $R_2 = R_4 = \text{Me}$; $R_3 = \text{H}$; $R_5 = \text{---C(=O)CH}_2\text{---}$
 : 1,6-di(OH)-3,7-di(OMe)-2-(3-methylbut-2-enyl)-8-(2-oxo-3-methylbut-3-enyl)xanthone



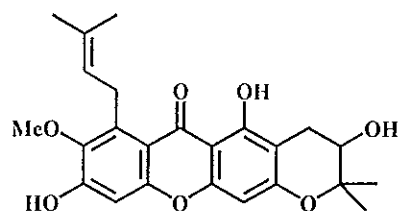
4.2m: mangostenone A



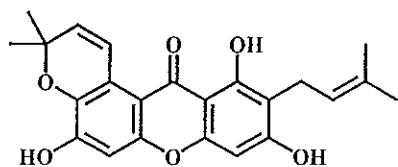
4.2n: mangostenone B



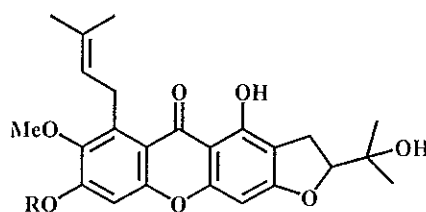
4.2o: tovophyllin B



4.2p: mangostanol

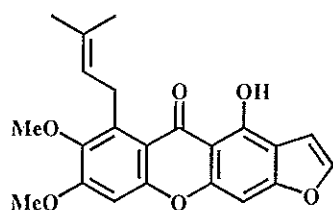


4.2q: garcinone B



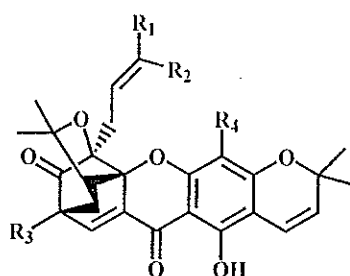
4.2r: R = H : mangostanin

4.2s: R = Me : 6-O-methylmangostanin



4.2t: garciniafuran

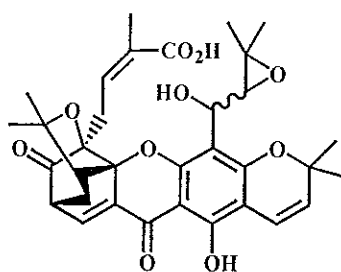
4.3 Caged-polyprenylated xanthones



4.3a: $R_1 = \text{Me}$; $R_2 = \text{CO}_2\text{H}$; $R_3 = R_4 = \text{---CH}_2\text{---CH}(\text{Me})\text{---CH}(\text{Me})\text{---}$: 7-isoprenylmorellic acid

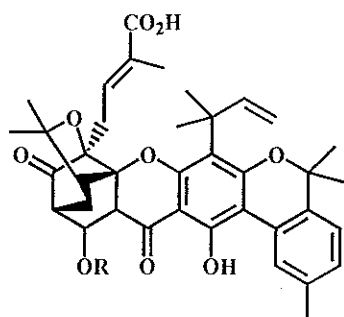
4.3b: $R_1 = \text{Me}$; $R_2 = \text{CO}_2\text{H}$; $R_3 = \text{H}$; $R_4 = \text{---CH}_2\text{---CH}(\text{OH})\text{---CH}(\text{Me})\text{---}$: gaudichaudiic acid E

4.3c: $R_1 = \text{Me}$; $R_2 = \text{CO}_2\text{H}$; $R_3 = \text{H}$; $R_4 = \text{---CH}_2\text{---CH}(\text{Me})\text{---}$: morellic acid



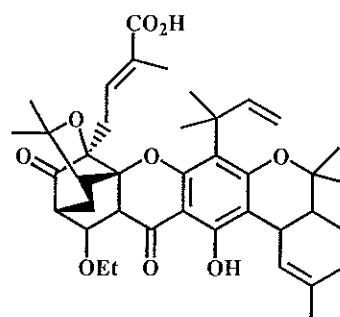
4.3d: gaudichaudiic acid C

4.3e: gaudichaudiic acid D

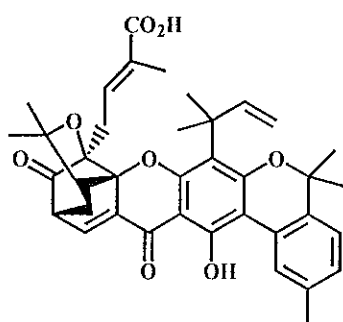


4.3f: R = Me : gaudichaudiic acid H

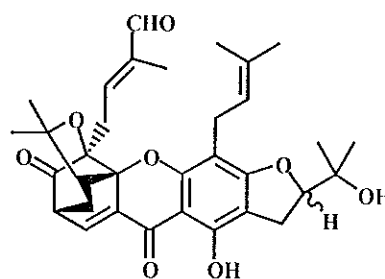
4.3g: R = Et : gaudichaudiic acid I



4.3h: gaudichaudiic acid F

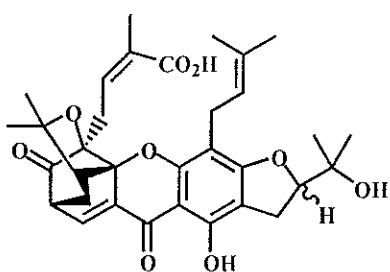


4.3i: gaudichaudiic acid G

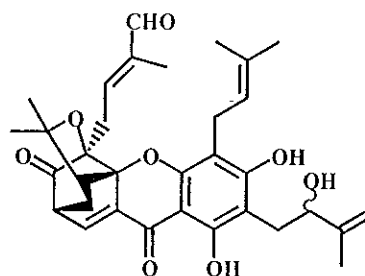


4.3j: gaudichaudione D

4.3k: gaudichaudione E

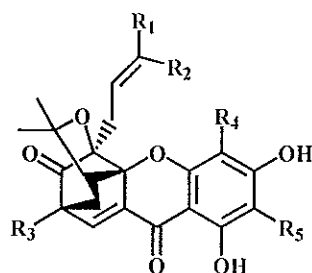


4.3l: gaudichaudiic acid A



4.3m: gaudichaudione B

4.3n: gaudichaudione F



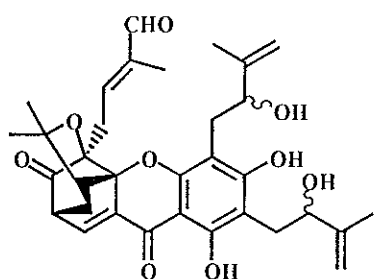
4.3o: $R_1 = \text{Me}$; $R_2 = \text{CO}_2\text{H}$; $R_3 = \text{H}$; $R_4 = \text{CH}_2\text{CH}(\text{OH})\text{CH}_2\text{CH}_3$; $R_5 = \text{CH}_2\text{CH}(\text{Me})\text{CH}_2\text{CH}_3$: gaudichaudiic acid B

4.3p: $R_1 = \text{CHO}$; $R_2 = \text{Me}$; $R_3 = \text{H}$; $R_4 = R_5 = \text{CH}_2\text{CH}(\text{Me})\text{CH}_2\text{CH}_3$: gaudichaudione A

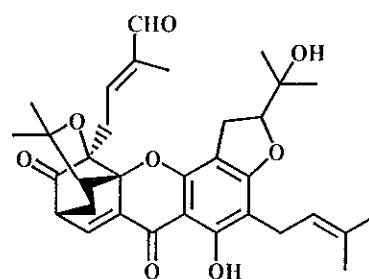
4.3q: $R_1 = \text{CHO}$; $R_2 = \text{Me}$; $R_3 = \text{H}$; $R_4 = \text{CH}_2\text{CH}(\text{OH})\text{CH}_2\text{CH}_3$; $R_5 = \text{CH}_2\text{CH}(\text{Me})\text{CH}_2\text{CH}_3$: gaudichaudione C

4.3r: $R_1 = R_2 = \text{Me}$; $R_3 = R_5 = \text{H}$; $R_4 = \text{CH}_2\text{CH}(\text{Me})\text{CH}_2\text{CH}_3$: forbesione

4.3s: $R_1 = R_2 = \text{Me}$; $R_3 = \text{OMe}$; $R_4 = \text{CH}_2\text{CH}(\text{Me})\text{CH}_2\text{CH}_3$; $R_5 = \text{H}$: gaudichaudione H

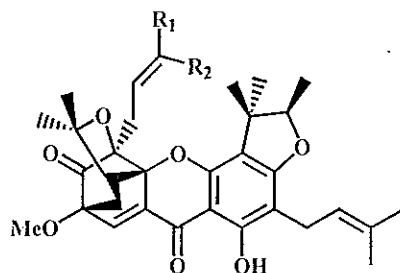


4.3t: gaudichaudione I



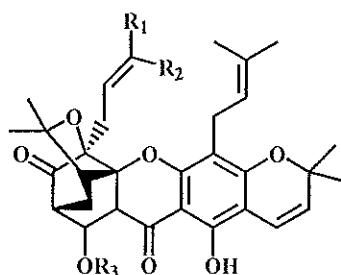
4.3v: gaudichaudione G

4.3u: gaudichaudione J

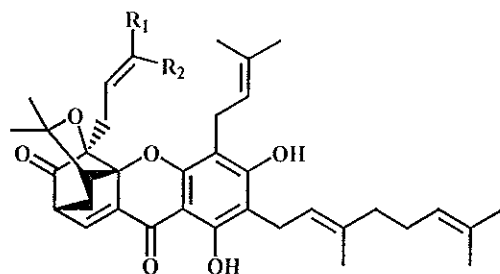


4.3w: $R_1 = R_2 = \text{Me}$: scortechinone A

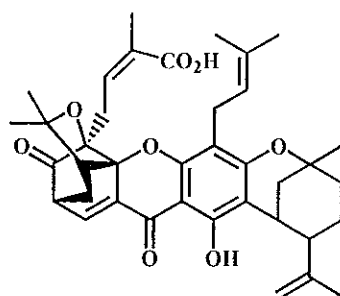
4.3x: $R_1 = \text{Me}$; $R_2 = \text{CO}_2\text{H}$: scortechinone B



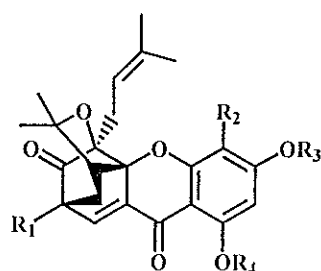
- 4.3jj: $R_1 = \text{CHO}$; $R_2 = R_3 = \text{Me}$: isomoreollin B
- 4.3kk: $R_1 = R_3 = \text{Me}$; $R_2 = \text{CO}_2\text{H}$: moreollic acid
- 4.3ll: $R_1 = \text{CHO}$; $R_2 = \text{Me}$; $R_3 = \text{Et}$: ethoxydihydroisomorellin
(isomoreollin)
- 4.3mm: $R_1 = \text{Me}$; $R_2 = \text{CHO}$; $R_3 = \text{Et}$: moreollin



- 4.3nn: $R_1 = \text{Me}$; $R_2 = \text{CO}_2\text{H}$: gambogenic acid
- 4.3oo: $R_1 = \text{Me}$; $R_2 = \text{CHO}$: gambogenin
- 4.3pp: $R_1 = \text{CHO}$; $R_2 = \text{Me}$: isogambogenin
- 4.3qq: $R_1 = R_2 = \text{Me}$: desoxygambogenin
- 4.3rr: $R_1 = \text{Me}$; $R_2 = \text{CH}(\text{OMe})_2$: gambogenin dimethyl acetal



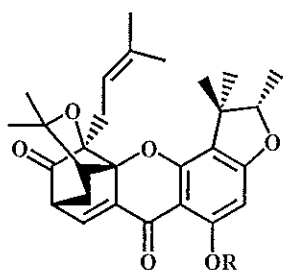
4.3ss: gambogelic acid



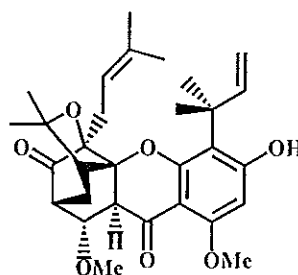
4.3tt: $R_1 = R_2 = \text{isopentenyl}$; $R_3 = R_4 = \text{H}$: hanburin

4.3uu: $R_1 = R_3 = R_4 = \text{H}$; $R_2 = \text{isopentenyl}$: bractatin

4.3vv: $R_1 = R_3 = \text{H}$; $R_2 = \text{isopentenyl}$; $R_4 = \text{Me}$: 1-*O*-methylbractatin

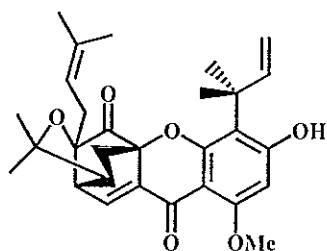
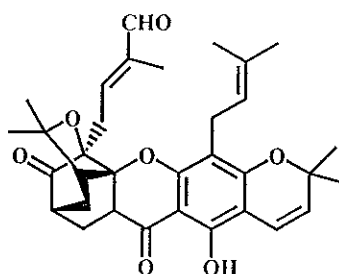


4.3ww: $R = \text{H}$: isobractatin



4.3yy : 1-*O*-methyl-8-methoxy-
8,8a-dihydrobractatin

4.3xx: $R = \text{Me}$: 1-*O*-methylisobractatin

4.3zz: 1-*O*-methylnobractatin

4.3aaa: dihydroisomorellin

1.3 The objectives

Based on NAPRALERT database, phytochemical examination on *G. merguensis* has not yet been reported. This prompted us to investigate its chemical constituents in order to provide additional chemical information of this plant. This research involved isolation, purification and structural determination of the chemical constituents isolated from the twigs of *G. merguensis* which was collected at the Ton Nga-Chang Wildlife Sanctuary in Songkhla Province.

Chapter 2

EXPERIMENTAL

2.1 Chemical and instruments

Melting points were determined on an electrothermal melting point apparatus (Electrothermal 9100) and reported without correction. Infrared spectra (IR) were obtained on a FTS165 FT-IR spectrometer and Perkin Elmer Spectrum GX FT-IR system and recorded on wavenumber (cm^{-1}). ^1H and ^{13}C -Nuclear magnetic resonance (^1H and ^{13}C NMR) spectra were recorded on a FTNMR, Varian UNITY INOVA 500 MHz by using a solution in either deuteriochloroform or deuteromethanol with tetramethylsilane (TMS) as an internal standard. Spectra were recorded as chemical shift parameter (δ) value in ppm down field from TMS (δ 0.00). Ultraviolet spectra (UV) were measured with UV-160A spectrophotometer (SHIMADZU). Principle bands (λ_{max}) were recorded as wavelengths (nm) and $\log \varepsilon$ in methanol solution. Optical rotation was measured in methanol solution with sodium D line (590 nm) on an AUTOPOL[®] II automatic polarimeter. Quick column chromatography, thin-layer chromatography (TLC) and precoated thin-layer chromatography were performed on silica gel 60 GF₂₅₄ (Merck) or reverse-phase C-18. Column chromatography was performed on silica gel (Merck) type 100 (70-230 Mesh ASTM) or reverse-phase C-18. The solvents for extraction and chromatography were distilled at their boiling point ranges prior to use except for petroleum ether (bp. 40-60°C) while diethyl ether and ethyl acetate were analytical grade reagent.

2.2 Plant material

The twigs of *Garcinia merguensis* were collected from Ton Nga-Chang Wildlife Sanctuary in Songkhla Province in June 2000 and identified by Ajarn Prakart Sawangchote, Department of Biology, Faculty of Science, Prince of Songkla University. A voucher specimen has been deposited at the Prince of Songkla University Herbarium.

2.3 Extraction and isolation

The twigs of *Garcinia merguensis* were chopped into small pieces and air-dried. Dried twigs of the plant (1.8 kg) were extracted with methanol and the extract was evaporated to dryness under reduced pressure to give a dark brown gum in 102 g. Part of the extract was tested for its solubility in various solvents at room temperature. The results were demonstrated in Table 3.

Table 3 Solubility of the methanol extract in various solvents at room temperature

solvent	solubility at room temperature
petroleum ether	+ (pale yellow-brown solution)
dichloromethane	† (pale brown solution)
ethyl acetate	++ (brown-yellow solution)
methanol	+++ (brown solution)
water	-
10% NaOH	++ (dark brown solution)

Table 3 (Continued)

solvent	solubility at room temperature
10% NaHCO ₃	+ (yellow-brown solution)
10% HCl	-

Symbol meaning: - insoluble, + slightly soluble, ++ moderately soluble,
+++ well soluble

The solubility results indicated that the methanol extract contained non-polar and polar chemical constituents as it was soluble in non-polar and polar solvents. In addition, the major constituents would be weak acid as their solubility in 10% NaOH was better than that in 10% NaHCO₃. All soluble parts in above organic solvents were examined on normal phase TLC (silica gel) using chloroform as a mobile phase. According to solubility of the methanol extract and chromatograms of the above soluble parts, the methanol extract was divided into two fractions by soaking in dichloromethane for a day. The dichloromethane soluble fraction (**A**, 13.59 g) and dichloromethane insoluble fraction (**B**, 88.41 g) were obtained as a green-yellow gum and a brown solid mixed with brown gum, respectively. Fraction **A** was further separated by column chromatography over silica gel. Elution was performed initially with chloroform, followed by increasing amount of methanol and finally with 90% methanol in chloroform. Fractions with the similar chromatogram were combined and evaporated to dryness under reduced pressure to afford eleven fractions, as shown in Table 4.

Table 4 Fractions obtained from fraction A by column chromatography over silica gel

fraction	weight (mg)	physical appearance
A1	527.8	orange gum
A2	141.6	white needle crystals mixed with red solid
A3	127.5	white needle crystals mixed with red solid
A4	81.7	white solid mixed with orange-red gum
A5	611.1	yellow solid mixed with brown gum
A6	465.1	yellow solid mixed with brown gum
A7	212.9	yellow solid mixed with yellow-brown gum
A8	7,907.2	yellow solid mixed with yellow gum
A9	1,298.4	yellow-brown solid mixed with yellow-brown gum
A10	1,763.1	brown-yellow solid mixed with brown-yellow gum
A11	1,037.8	brown solid

Fraction A1 showed many UV-active spots on normal phase TLC using 10% ethyl acetate in petroleum ether as a mobile phase. One additional spot was observed after dipping the TLC plate in ASA reagent and subsequently heating. Because it contained unseparable components, it was not further carried out.

Fraction A2 showed five UV-active components on normal phase TLC using 10% ethyl acetate in petroleum ether as a mobile phase with the R_f values of 0.58, 0.48, 0.46, 0.32 and 0.24. Three additional spots were observed above UV-active spots after dipping the TLC plate in ASA reagent and subsequently heating. Therefore, it was not purified.

Fraction A3 displayed three UV-active components on normal phase TLC using 10% ethyl acetate in petroleum ether as a mobile phase with the R_f values of 0.58, 0.48 and 0.32. Further separation by column chromatography over silica gel was performed. Elution was conducted initially with 10% ethyl acetate in petroleum ether, followed by increasing amount of ethyl acetate and finally with pure ethyl acetate. Fractions with the similar chromatogram were combined and evaporated to dryness under reduced pressure to afford five subfractions, as shown in Table 5.

Table 5 Subfractions obtained from A3 by column chromatography over silica gel

subfraction	weight (mg)	physical appearance
A3.1	22.4	yellow gum
A3.2	62.5	white needle crystals mixed with yellow gum
A3.3	17.3	purple gum
A3.4	10.2	purple-red gum
A3.5	22.1	orange-yellow gum

Subfraction A3.1 showed no major UV-active components on normal phase TLC. Therefore, it was not investigated further.

Subfraction A3.2, upon standing at room temperature, afforded a white solid (**DD6**), melting at 240-241°C. According to its ^1H NMR spectral data, it was identified to be friedelin. The filtrate contained too many spots on normal phase TLC without any major components. Therefore, it was not investigated.

$[\alpha]_D^{29}$	+17° (c = 9.5x10 ⁻³ g/100 cm ³ , MeOH)
IR (neat) $\nu_{\text{cm}^{-1}}$	2926, 2866 (C-H stretching), 1713 (C=O stretching)
¹ H NMR (CDCl ₃) (δ ppm) (500 MHz)	2.40 (<i>ddd</i> , <i>J</i> = 14.0, 5.0 and 2.0 Hz, 1H), 2.31 (<i>ddd</i> , <i>J</i> = 13.0, 7.0 and 1.5 Hz, 1H), 2.25 (<i>q</i> , <i>J</i> = 7.0 Hz, 1H), 2.00-1.94 (<i>m</i> , 1H), 1.76 (<i>md</i> , <i>J</i> = 13.0 Hz, 1H), 1.69 (<i>dq</i> , <i>J</i> = 13.0 and 5.0 Hz, 1H), 1.60-1.20 (<i>m</i> , 20H), 1.18 (<i>s</i> , 3H), 1.05 (<i>s</i> , 3H), 1.01 (<i>s</i> , 3H), 1.00 (<i>s</i> , 3H), 0.95 (<i>s</i> , 3H), 0.89 (<i>d</i> , <i>J</i> = 6.5 Hz, 3H), 0.87 (<i>s</i> , 3H), 0.73 (<i>s</i> , 3H)

Subfraction A3.3 displayed two major UV-active spots on normal phase TLC with the R_f values of 0.74 and 0.68 using 10% ethyl acetate in petroleum ether as a mobile phase (2 runs). Because it was obtained in low quantity, it was not further investigated.

Subfraction A3.4 showed two UV-active spots on normal phase TLC using 10% ethyl acetate in petroleum ether as a mobile phase (2 runs) with the R_f values of 0.59 and 0.56. Further chromatographic separation by precoated TLC on silica gel plates using 10% ethyl acetate in petroleum ether as a mobile phase (4 runs) gave two bands as a yellow gum (3.3 mg) and a purple-pink gum (3.7 mg) of which chromatograms contained many spots. Further purification was not performed.

Subfraction A3.5 showed only one UV-active spot on normal phase TLC using 10% ethyl acetate in petroleum ether as a mobile phase with the same R_f value as the

component isolated from **subfraction A3.4**. Its ^1H NMR spectrum indicated the presence of impurities. It was not further investigated.

Fraction A4 showed four major UV-active spots on normal phase TLC using 10% ethyl acetate in petroleum ether as a mobile phase with the R_f values of 0.48, 0.32, 0.24 and 0.16. Further separation by flash column chromatography over silica gel was performed. Elution was initially conducted with 10% ethyl acetate in petroleum ether, followed by increasing the polarity with ethyl acetate until 50% ethyl acetate in petroleum ether. Fractions with the similar chromatogram were combined and evaporated to dryness under reduced pressure to afford three subfractions, as shown in Table 6.

Table 6 subfractions obtained from A4 by flash column chromatography over silica gel

subfraction	weight (mg)	physical appearance
A4.1	22.8	white needle crystals mixed with yellow gum
A4.2	47.5	orange gum
A4.3	15.0	orange-yellow gum

Subfraction A4.1, upon standing at room temperature, gave a white solid which was shown to be identical to **DD6** by TLC. In addition, the filtrate showed the same chromatogram as that of the filtrate obtained from **subfraction A3.2**. Thus, it was not further separated.

Subfraction A4.2 showed many components on normal phase TLC under UV-S using 10% ethyl acetate in petroleum ether as a mobile phase. After dipping the TLC plate

in ASA reagent and subsequently heating, chromatogram showed many additional spots. Therefore, it was not investigated.

Subfraction A4.3 showed no distinct spots on normal phase TLC using 10% ethyl acetate in petroleum ether as a mobile phase. Thus, further separation was not performed.

Fraction A5 displayed five major components on normal phase TLC under UV-S using 15% ethyl acetate in petroleum ether as a mobile phase. It was further separated by flash column chromatography over silica gel. Elution was performed with 10% ethyl acetate in petroleum ether with increasing amount of ethyl acetate up to 50% ethyl acetate in petroleum ether. Fractions with the similar chromatogram were combined and evaporated to dryness under reduced pressure to give eleven subfractions, as shown in Table 7.

Table 7 Subfractions obtained from A5 by flash column chromatography over silica gel

subfraction	weight (mg)	physical appearance
A5.1	36.4	pale yellow gum
A5.2	61.9	orange gum
A5.3	27.6	orange-yellow gum
A5.4	16.1	yellow gum
A5.5	34.3	yellow gum
A5.6	46.2	white solid mixed with yellow gum
A5.7	51.4	white solid mixed with yellow gum
A5.8	148.2	white solid mixed with yellow gum

Table 7 (Continued)

subfraction	weight (mg)	physical appearance
A5.9	88.7	white solid mixed with yellow gum
A5.10	27.5	yellow gum
A5.11	81.2	yellow gum

Subfraction A5.1 showed many unseparable spots on normal phase TLC under UV-S using 15% ethyl acetate in petroleum ether as a mobile phase. After dipping the TLC plates in ASA reagent and subsequently heating, many additional spots were observed. Thus, it was not investigated.

Subfraction A5.2 displayed two major spots on normal phase TLC under UV-S using 15% ethyl acetate in petroleum ether as a mobile phase with the R_f values of 0.38 and 0.26. It was then purified by flash column chromatography over silica gel. Elution was conducted with 10% ethyl acetate in petroleum ether with increasing amount of ethyl acetate up to 50% ethyl acetate in petroleum ether. Fractions with the similar chromatogram were combined and evaporated to dryness under reduced pressure to give three subfractions, as a yellow gum (10.5 mg), an orange gum (23.2 mg) and a brown gum (29.8 mg). Their chromatograms on normal phase TLC using 5% ethyl acetate in petroleum ether showed unseparable components under UV. Therefore, they were not further purified.

Subfraction A5.3 showed one major UV-active spot on normal phase TLC using 5% ethyl acetate in petroleum ether as a mobile phase with the R_f value of 0.26. Further

separation by precoated TLC on silica gel plates using 5% ethyl acetate in petroleum ether as a mobile phase (11 runs) gave three bands of which their chromatograms on normal phase TLC using 5% ethyl acetate in petroleum ether as a mobile phase showed unseparable spots under UV-S.

Subfraction A5.4 showed one major UV-active spot on normal phase TLC using 10% ethyl acetate in petroleum ether as a mobile phase with the R_f value of 0.42. It was rechromatographed on precoated TLC on silica gel plates using 10% ethyl acetate in petroleum ether as a mobile phase (4 runs) to give two bands.

Band 1 was a pale yellow gum (1.3 mg). Chromatogram on normal phase TLC using 10% ethyl acetate in petroleum ether as a mobile phase showed two UV-active spots with the R_f values of 0.64 and 0.59. It was not purified further because it was obtained in low quantity.

Band 2 was a yellow gum (3.0 mg). It contained two overlapping UV-active spots on normal phase TLC using 10% ethyl acetate in petroleum ether as a mobile phase with the R_f values of 0.62 and 0.59. Further separation on precoated TLC using 5% ethyl acetate in petroleum ether as a mobile phase (17 runs) gave three bands in low quantity. Thus, they were not investigated.

Subfraction A5.5 showed the similar chromatogram to that of **subfraction A5.4**. It was then separated on precoated TLC with 10% ethyl acetate in petroleum ether (4 runs) to afford a yellow gum (11.6 mg). Chromatogram on normal phase TLC with 5% ethyl acetate in petroleum ether (5 runs) showed two overlapping spots. Therefore, it was rechromatographed on precoated TLC with 5% ethyl acetate in petroleum ether (17 runs) to afford two bands.

Band 1 was a yellow gum (3.0 mg). Its chromatogram on normal phase TLC with 5% ethyl acetate in petroleum ether (6 runs) showed two UV-active spots. Because of low quantity, it was not carried out.

Band 2 (DD3) was a yellow gum (1.6 mg). Chromatogram showed a single UV-active spot on normal phase TLC with 5% ethyl acetate in petroleum ether (6 runs).

$[\alpha]_D^{29}$	-182° (c = 1.1x10 ⁻² g/100 cm ³ , MeOH)
UV λ_{\max} nm (MeOH) (log ϵ)	360 (3.96)
IR (neat) $\nu_{\text{cm}^{-1}}$	3453 (O-H stretching), 2926, 2856 (C-H stretching), 1741, 1646 (C=O stretching)
¹ H NMR (CDCl ₃) (δ ppm) (500 MHz)	12.65 (<i>s</i> , 1H), 7.47 (<i>d</i> , <i>J</i> = 1.5 Hz, 1H), 5.32 (<i>mt</i> , <i>J</i> = 6.5 Hz, 1H), 4.46 (<i>q</i> , <i>J</i> = 6.5 Hz, 1H), 4.40 (<i>mt</i> , <i>J</i> = 7.5 Hz, 1H), 3.64 (<i>s</i> , 3H), 3.29 (<i>mdd</i> , <i>J</i> = 15.0 and 6.5 Hz, 1H), 3.21 (<i>mdd</i> , <i>J</i> = 15.0 and 6.5 Hz, 1H), 2.59 (<i>d</i> , <i>J</i> = 7.5 Hz, 2H), 2.53 (<i>d</i> , <i>J</i> = 9.5 Hz, 1H), 2.34 (<i>d</i> , <i>J</i> = 14.0 Hz, 1H), 1.71 (<i>s</i> , 3H), 1.68 (<i>s</i> , 6H), 1.63 (<i>dd</i> , <i>J</i> = 14.0 and 9.5 Hz, 1H), 1.45 (<i>s</i> , 3H), 1.37 (<i>d</i> , <i>J</i> = 6.5 Hz, 3H), 1.36 (<i>brs</i> , 3H), 1.30 (<i>s</i> , 3H), 1.21 (<i>s</i> , 3H), 0.96 (<i>brs</i> , 3H)
¹³ C NMR (CDCl ₃) (δ ppm) (125 MHz)	202.08, 178.93, 166.61, 158.40, 158.24, 135.28, 133.52, 132.67, 132.37, 121.76, 117.59, 114.58, 103.72, 101.53, 90.77, 89.09, 84.80, 84.27, 83.57, 53.97, 49.72, 43.51, 30.20, 30.09, 29.03,

	28.83, 25.71, 25.55, 25.26, 22.10, 20.64, 17.96, 16.53, 14.38
DEPT (135°) (CDCl ₃)	CH ₃ : 53.97, 30.09, 29.03, 25.71, 25.55, 25.26, 20.64, 17.96, 16.53, 14.38
	CH ₂ : 30.20, 28.83, 22.10
	CH : 133.52, 121.76, 117.59, 90.77, 49.72
FABMS (<i>m/z</i>) (% rel. int.)	563 (65.8), 535 (78.9), 509 (36.8), 495 (41.4), 481 (27.0), 467 (38.2), 455 (27.0), 439 (34.2), 427 (25.0), 413 (30.3), 391 (100), 383 (25.0), 369 (29.7), 341 (25.7), 327 (27.0), 315 (28.3), 303 (34.9), 279 (77.6), 263 (48.7), 251 (61.8), 237 (77.6), 223 (84.2), 209 (81.6), 195 (100), 179 (90.8), 169 (>100), 155 (>100), 141 (>100), 127 (>100), 113 (>100), 97 (>100), 85 (>100)

Subfraction A5.6 crystallized at room temperature to give two parts: a white solid (**DD4**, 9.3 mg) and a yellow solution (**SolA5.6**). **DD4**, melting at 162-163°C, showed one spot with the R_f value of 0.19 after dipping the TLC plate in ASA reagent and subsequently heating. Its ¹H NMR spectrum indicated that it was stigmasterol.

$[\alpha]_D^{29}$	-31° (c = 1.6x10 ⁻² g/100 cm ³ , MeOH)
IR (neat) ν _{cm-1}	3443 (O-H stretching), 2937, 2886, 2863 (C-H stretching)
¹ H NMR (CDCl ₃) (δ ppm) (500 MHz)	5.36-5.33 (<i>m</i> , 1H), 5.15 (<i>dd</i> , <i>J</i> = 15.0 and 8.5 Hz, 1H), 5.02 (<i>dd</i> , <i>J</i> = 15.0 and 8.5 Hz, 1H), 3.54-

3.50 (*m*, 1H), 2.28 (*ddd*, $J = 13.0, 5.0$ and 1.5 Hz, 1H), 2.24 (*qd*, $J = 11.0$ and 2.0 Hz, 1H), 2.07-1.93 (*m*, 3H), 1.86-1.80 (*m*, 2H), 1.74-1.66 (*m*, 1H), 1.56-1.39 (*m*, 11H), 1.30-1.04 (*m*, 5H), 1.01 (*d*, $J = 7.0$ Hz, 3H), 1.00 (*s*, 3H), 0.98-0.90 (*m*, 2H), 0.84 (*d*, $J = 6.5$ Hz, 3H), 0.80 (*t*, $J = 7.5$ Hz, 3H), 0.79 (*d*, $J = 7.5$ Hz, 3H), 0.69 (*s*, 3H)

SolA5.6 was evaporated to dryness under reduced pressure to afford a yellow gum (36.9 mg). Its chromatogram on normal phase TLC using 10% ethyl acetate in petroleum ether as a mobile phase showed three major UV-active spots with the R_f values of 0.44, 0.40 and 0.27. It was then separated on precoated TLC with 10% ethyl acetate in petroleum ether (4 runs) to afford two bands.

Band 1 was a yellow gum (4.9 mg). Chromatogram on normal phase TLC with 10% ethyl acetate in petroleum ether showed two overlapping spots under UV-S. Further separation on precoated TLC gave three bands in low quantity. Thus, they were not investigated.

Band 2 (DD7) was a pale yellow gum (2.8 mg) which showed a single spot on normal phase TLC under UV-S with the R_f values of 0.35 using 10% ethyl acetate in petroleum ether as a mobile phase.

$[\alpha]_D^{29}$	-200° ($c = 5.0 \times 10^{-3}$ g/100 cm ³ , MeOH)
UV λ_{\max} nm (MeOH) (log ϵ)	280 (3.17), 236 (3.87)
IR (neat) $\nu_{\text{cm}^{-1}}$	3414 (O-H stretching), 2952, 2926, 2849 (C-H stretching)

^1H NMR (CDCl_3) (δ ppm) (500 MHz)	6.00 (<i>d</i> , $J = 16.5$ Hz, 1H), 5.44 (<i>dd</i> , $J = 16.5$ and 10.5 Hz, 1H), 5.28 (<i>s</i> , 1H), 5.00 (<i>d</i> , $J = 2.0$ Hz, 1H), 4.93 (<i>d</i> , $J = 1.0$ Hz, 1H), 4.85 (<i>s</i> , 1H), 3.78 (<i>dd</i> , $J = 12.0$ and 4.0 Hz, 1H), 2.65-2.61 (<i>m</i> , 1H), 2.44 (<i>dt</i> , $J = 13.0$ and 5.0 Hz, 1H), 2.20 (<i>ddd</i> , $J = 13.0$, 5.0 and 2.5 Hz, 1H), 2.08-2.01 (<i>m</i> , 2H), 1.83-1.77 (<i>m</i> , 1H), 1.73-1.58 (<i>m</i> , 2H), 1.68-1.60 (<i>m</i> , 1H), 1.53-1.46 (<i>m</i> , 1H), 0.89 (<i>d</i> , $J = 6.5$ Hz, 3H), 0.82 (<i>d</i> , $J = 6.5$ Hz, 3H)
^{13}C NMR (CDCl_3) (δ ppm) (125 MHz)	153.49, 146.72, 137.97, 129.61, 112.91, 110.57, 76.03, 52.50, 36.27, 36.17, 34.52, 31.82, 29.93, 20.75, 20.49
DEPT (135°) (CDCl_3)	<p>CH_3 : 20.75, 20.49</p> <p>CH_2 : 112.91, 110.57, 36.27, 36.17, 34.52, 29.93</p> <p>CH : 137.97, 129.61, 76.03, 52.50, 31.82</p>

Subfraction A5.7, upon standing at room temperature, afforded a white solid which was shown to be identical to **DD4** by TLC. In addition, the filtrate showed two UV-active spots. It was then chromatographed on precoated TLC with 10% ethyl acetate in petroleum ether (4 runs) to give a yellow solid (**DD1**, 6.3 mg), melting at 153-155°C. Its chromatogram showed only one UV-active spot with the R_f value of 0.39 using 5% ethyl acetate in petroleum ether as a mobile phase (5 runs).

$[\alpha]_D^{29}$	-177° ($c = 1.7 \times 10^{-2} / 100 \text{ cm}^3$, MeOH)
UV λ_{max} nm (MeOH) ($\log \epsilon$)	362 (4.06)

IR (neat) $\nu_{\text{cm}^{-1}}$	3432 (O-H stretching), 2959, 2928, 2856 (C-H stretching), 1742, 1635 (C=O stretching)
^1H NMR (CDCl_3) (δ ppm) (500 MHz)	13.19 (<i>s</i> , 1H), 7.51 (<i>d</i> , $J = 1.5$ Hz, 1H), 5.22 (<i>mt</i> , $J = 7.0$ Hz, 1H), 4.41-4.37 (<i>m</i> , 1H), 4.37 (<i>q</i> , $J = 6.5$ Hz, 1H), 3.63 (<i>s</i> , 1H), 3.22 (<i>brt</i> , $J = 7.0$ Hz, 2H), 2.69 (<i>md</i> , $J = 14.5$ Hz, 1H), 2.56 (<i>dd</i> , $J = 14.5$ and 10.5 Hz, 1H), 2.55 (<i>d</i> , $J = 9.5$ Hz, 1H), 2.33 (<i>brd</i> , $J = 13.0$ Hz, 1H), 1.75 (<i>s</i> , 3H), 1.71 (<i>s</i> , 3H), 1.68 (<i>brd</i> , $J = 1.0$ Hz, 3H), 1.65 (<i>dd</i> , $J = 13.0$ and 9.5 Hz, 1H), 1.58 (<i>s</i> , 3H), 1.41 (<i>d</i> , $J = 6.5$ Hz, 3H), 1.36 (<i>brs</i> , 3H), 1.29 (<i>s</i> , 3H), 1.64 (<i>s</i> , 3H), 1.06 (<i>brs</i> , 3H)
^{13}C NMR (CDCl_3) (δ ppm) (125 MHz)	202.31, 178.23, 166.82, 163.25, 153.81, 135.64, 133.93, 132.38, 132.05, 121.74, 117.16, 113.04, 105.75, 101.38, 90.61, 89.27, 84.89, 84.17, 83.26, 53.97, 49.91, 43.47, 30.84, 30.78, 29.00, 28.93, 25.74, 25.51, 24.05, 21.42, 21.09, 17.76, 16.87, 13.59

Subfraction A5.8, upon standing at room temperature, afforded a white solid (**DD4**) and a yellow solution (**SolA5.8**). The solution was evaporated to dryness under reduced pressure to yield a white solid mixed with yellow gum (109.3 mg). It showed the similar chromatogram to the filtrate obtained from **subfraction A5.7**. Further chromatography by flash column chromatography over silica gel was then carried out. Elution was performed with 5% ethyl acetate in petroleum ether, followed by

increasing the polarity with ethyl acetate until 20% ethyl acetate in petroleum ether. Fractions with the similar chromatogram were combined and evaporated to dryness under reduced pressure to give four subfractions, as shown in Table 8.

Table 8 Subfractions obtained from SolA5.8 by flash column chromatography over silica gel

Subfraction	weight (mg)	physical appearance
A5.8/1	61.6	white solid mixed with yellow gum
A5.8/2	19.4	white solid mixed with yellow gum
A5.8/3	31.2	orange yellow gum
A5.8/4	24.9	orange yellow gum

Subfraction A5.8/1 showed two spots on normal phase TLC under UV-S using 15% ethyl acetate in petroleum ether as a mobile phase. After dipping the TLC plate in ASA reagent and subsequently heating, many additional spots were observed. Thus, it was not investigated further.

Subfraction A5.8/2 showed one major UV-active spot on normal phase TLC using 15% ethyl acetate in petroleum ether as a mobile phase with the R_f value of 0.35. One additional spot was observed below the UV-active spot after dipping the TLC plate in ASA reagent and subsequently heating. It was further separated on precoated TLC with 15% ethyl acetate in petroleum ether (2 runs) afforded two bands.

Band 1 was a yellow gum (6.2 mg). It showed one major UV-active spot on normal phase TLC using 15% ethyl acetate in petroleum ether as a mobile phase with the R_f value of 0.35. One additional spot was observed below the UV-active spot after

dipping the TLC plate in ASA reagent and subsequently heating. It was rechromatographed on precoated TLC with 5% ethyl acetate in petroleum ether (5 runs) and then 10% ethyl acetate in petroleum ether (6 runs), respectively, to give **DD1** as a yellow gum (4.8 mg).

Band 2 was a yellow gum (10.0 mg) which showed two overlapping spots on normal phase TLC under UV-S using 15% ethyl acetate in petroleum ether as a mobile phase. It was purified further on precoated TLC with 5% ethyl acetate in petroleum ether (5 runs) and then 10% ethyl acetate in petroleum ether (6 runs), respectively, to afford two bands.

Band 2.1 was a yellow gum (4.0 mg). It was shown to be **DD1** by TLC. **Band 2.2** was a yellow gum (5.2 mg). It contained two UV-active spots which partially overlapped each other. Further purification was not performed because it was obtained in low quantity.

Subfraction A5.8/3 contained two overlapping spots on normal phase TLC under UV-S using 15% ethyl acetate in petroleum ether as a mobile phase. Its ^1H NMR spectrum indicated that it was a mixture of **DD1** and **DD5**. Thus, it was then purified by precoated TLC with 8% ethyl acetate in petroleum ether (17 runs) to give two bands.

Band 1 was a yellow gum (6.3 mg) which was identified to be **DD1** by TLC.

Band 2 (DD5) was a yellow gum (3.4 mg). Its chromatogram showed one UV-active spot with the R_f value of 0.33 on normal phase TLC 5% ethyl acetate in petroleum ether (10 runs).

$[\alpha]_D^{29}$	-158° (c = 1.9x10 ⁻² /100 cm ³ , MeOH)
UV λ_{max} nm (MeOH) (log ϵ)	364 (3.79)

IR (neat) $\nu_{\text{cm}^{-1}}$	3444 (O-H stretching), 2959, 2926, 2856 (C-H stretching), 1745, 1635 (C=O stretching)
$^1\text{H NMR}$ (CDCl_3) (δ ppm) (500 MHz)	13.24 (<i>s</i> , 1H), 7.51 (<i>d</i> , $J = 1.5$ Hz, 1H), 5.22 (<i>mt</i> , $J = 7.0$ Hz, 1H), 4.54 (<i>q</i> , $J = 6.5$ Hz, 1H), 4.36 (<i>md</i> , $J = 10.5$ Hz, 1H), 3.64 (<i>s</i> , 3H), 3.22 (<i>d</i> , $J = 7.0$ Hz, 2H), 2.67 (<i>md</i> , $J = 14.0$ Hz, 1H), 2.58 (<i>d</i> , $J = 9.5$ Hz, 1H), 2.54 (<i>dd</i> , $J = 14.0$ and 10.5 Hz, 1H), 2.34 (<i>brd</i> , $J = 12.5$ Hz, 1H), 1.75 (<i>s</i> , 3H), 1.71 (<i>s</i> , 3H), 1.68 (<i>d</i> , $J = 1.0$ Hz, 3H), 1.66 (<i>dd</i> , $J = 12.5$ and 9.5 Hz, 1H), 1.49 (<i>s</i> , 3H), 1.41 (<i>s</i> , 3H), 1.36 (<i>s</i> , 3H), 1.29 (<i>d</i> , $J = 6.5$ Hz, 3H), 1.29 (<i>s</i> , 3H), 1.02 (<i>s</i> , 3H)

Subfraction A5.8/4 showed two major UV-active spots on normal phase TLC which overlapped each other. Attempted purification using various mobile phase systems was not successful.

Subfraction A5.9, upon standing at room temperature, afforded **DD4** as a white precipitate. The remaining solution showed the same chromatogram as **SolA5.8** which consisted of **DD1** as a major component.

Subfraction A5.10 displayed two major UV-active spots on normal phase TLC using 15% ethyl acetate in petroleum ether as a mobile phase with the R_f values of 0.56 and 0.49. Further chromatography on precoated TLC with 5% ethyl acetate in petroleum ether (40 runs) afforded two bands.

Band 1 (DD8) was a yellow solid (2.8 mg), melting at 180-181°C. It showed only one UV-active spot on normal phase TLC using 5% ethyl acetate in petroleum ether as a mobile phase (6 runs) with the R_f value of 0.39.

$[\alpha]_D^{29}$	-167° ($c = 6.0 \times 10^{-3}$ g/100 cm ³ , MeOH)
UV λ_{\max} nm (MeOH) (log ϵ)	360 (3.83)
IR (neat) $\nu_{\text{cm}^{-1}}$	3422 (O-H stretching), 2926, 2856 (C-H stretching), 1742, 1640 (C=O stretching)
¹ H NMR (CDCl ₃) (δ ppm) (500 MHz)	13.03 (<i>s</i> , 1H), 7.52 (<i>d</i> , $J = 1.0$ Hz, 1H), 6.04 (<i>s</i> , 1H), 4.40 (<i>q</i> , $J = 6.5$ Hz, 1H), 4.40-4.37 (<i>m</i> , 1H), 3.64 (<i>s</i> , 3H), 2.70 (<i>md</i> , $J = 14.5$ Hz, 1H), 2.59 (<i>d</i> , $J = 9.5$ Hz, 1H), 2.58 (<i>dd</i> , $J = 14.5$ and 11.0 Hz, 1H), 2.36 (<i>d</i> , $J = 13.0$ Hz, 1H), 1.72 (<i>s</i> , 3H), 1.66 (<i>dd</i> , $J = 13.0$ and 9.5 Hz, 1H), 1.59 (<i>s</i> , 3H), 1.57 (<i>brs</i> , 1H), 1.41 (<i>d</i> , $J = 6.5$ Hz, 3H), 1.38 (<i>brs</i> , 3H), 1.30 (<i>s</i> , 3H), 1.17 (<i>s</i> , 3H), 1.09 (<i>s</i> , 3H)

Band 2 (DD9) was a yellow solid (2.3 mg), melting at 186-187°C. Its chromatogram displayed a single spot on normal phase TLC under UV-S using 5% ethyl acetate in petroleum ether as a mobile phase (6 runs) with the R_f value of 0.36.

$[\alpha]_D^{29}$	-143° ($c = 7.0 \times 10^{-3}$ g/100 cm ³ , MeOH)
UV λ_{\max} nm (MeOH) (log ϵ)	361 (3.74)
IR (neat) $\nu_{\text{cm}^{-1}}$	3443 (O-H stretching), 2926, 2856 (C-H stretching), 1742, 1640 (C=O stretching)

$^1\text{H NMR}$ (CDCl_3) (δ ppm)	13.09 (<i>s</i> , 1H), 7.53 (<i>d</i> , $J = 1.5$ Hz, 1H), 6.04 (<i>s</i> , 1H), 4.55 (<i>q</i> , $J = 6.5$ Hz, 1H), 4.36 (<i>md</i> , $J = 10.5$ Hz, 1H), 3.65 (<i>s</i> , 3H), 2.69 (<i>md</i> , $J = 14.5$ Hz, 1H), 2.61 (<i>d</i> , $J = 9.5$ Hz, 1H), 2.55 (<i>dd</i> , $J = 14.5$ and 10.5 Hz, 1H), 2.36 (<i>md</i> , $J = 13.0$ Hz, 1H), 1.72 (<i>s</i> , 3H), 1.67 (<i>dd</i> , $J = 13.0$ and 9.5 Hz, 1H), 1.50 (<i>s</i> , 3H), 1.42 (<i>s</i> , 3H), 1.38 (<i>brs</i> , 3H), 1.30 (<i>d</i> , $J = 6.5$ Hz, 3H), 1.29 (<i>s</i> , 3H), 1.07 (<i>brs</i> , 3H)
(500 MHz)	

Subfraction A5.11 showed one major UV-active spot on normal phase TLC using 15% ethyl acetate in petroleum ether as a mobile phase with the R_f value of 0.47. Further purification on precoated TLC with 5% ethyl acetate in petroleum ether (40 runs) was performed to afford two bands which were obtained in low quantity. Therefore, they were not further investigated.

Fraction A6 displayed four major UV-active spots on normal phase TLC using 15% ethyl acetate in petroleum ether as a mobile phase with the R_f values of 0.41, 0.32, 0.18 and 0.11. It was rechromatographed by flash column chromatography over silica gel. Elution was performed using a stepwise gradient system (ethyl acetate in petroleum ether and methanol in ethyl acetate) and finally with pure methanol. Fractions with the similar chromatogram were combined and evaporated to dryness under reduced pressure to give four subfractions, as shown in Table 9.

Table 9 Subfractions obtained from **A6** by flash column chromatography over silica gel

subfraction	weight (mg)	physical appearance
A6.1	42.1	pale yellow gum
A6.2	77.1	white solid mixed with yellow gum
A6.3	144.9	white solid mixed with yellow gum
A6.4	259.9	brown-yellow gum

Subfraction A6.1 showed no major components on normal phase TLC under UV-S using 30% ethyl acetate in petroleum ether as a mobile phase. Therefore, it was not further investigated.

Subfraction A6.2 displayed **DD1** as major component on normal phase TLC under UV-S using 30% ethyl acetate in petroleum ether as a mobile phase. Therefore, further separation was not performed.

Subfraction A6.3 showed one major component as **DD4**. Therefore, it was not investigated.

Subfraction A6.4 displayed unseparable spots on normal phase TLC under UV-S with 30% ethyl acetate in petroleum ether. Further investigation was not carried out.

Fraction A7 showed the similar chromatogram as that of **fraction A6**. Therefore, it was not investigation.

Fraction A8 displayed four major components on normal phase TLC under UV-S using 15% ethyl acetate in petroleum ether as a mobile phase (8 runs) with the R_f values of 0.36, 0.27, 0.18 and 0.11. Further separation by column chromatography over silica gel was introduced. Elution was conducted using a stepwise gradient

system (ethyl acetate in hexane and methanol in ethyl acetate) and finally with pure methanol. Fractions with the similar chromatogram were combined and evaporated to dryness under reduced pressure to give ten subfractions, as shown in Table 10.

Table 10 Subfractions obtained from A8 by column chromatography over silica gel

subfraction	weight (mg)	physical appearance
A8.1	372.7	green-yellow gum
A8.2	1,932.0	brown-yellow gum
A8.3	1,059.8	green-yellow gum
A8.4	1,124.8	green-yellow gum
A8.5	427.2	green-yellow gum
A8.6	177.5	green-yellow gum
A8.7	477.1	brown-yellow gum
A8.8	525.7	brown-yellow gum
A8.9	642.7	brown-yellow gum
A8.10	303.2	brown gum

Subfraction A8.1 showed no distinct UV-active spots on normal phase TLC using 15% ethyl acetate in petroleum ether as a mobile phase. After dipping the TLC plate in ASA reagent and subsequently heating, three additional spots were observed above UV-active spots. Attempted purification using various mobile phase systems was not successful.

Subfraction A8.2 displayed one major UV-active spot as **DD13** on normal phase TLC under UV-S using 25% ethyl acetate in petroleum ether as a mobile phase (2 runs) with the R_f value of 0.42. Thus, it was not purified further.

Subfraction A8.3 showed two major UV-active spots as **DD11** and **DD13** on normal phase TLC with 25% ethyl acetate in petroleum ether (2 runs). Therefore, further separation was not carried out.

Subfraction A8.4 displayed two major UV-active spots as **DD11** and **DD12** on normal phase TLC with 25% ethyl acetate in petroleum ether (2 runs). Therefore, it was not separated.

Subfraction A8.5 showed two major UV-active spots on normal phase TLC using 25% ethyl acetate in petroleum ether (2 runs) as a mobile phase with the R_f values of 0.25 and 0.23. Further separation by column chromatography over silica gel was performed. Elution was conducted with 0.5% methanol in chloroform with increasing amount of methanol up to pure methanol. Fractions with the similar chromatogram were combined and evaporated to dryness under reduced pressure to afford four subfractions, as shown in Table 11.

Table 11 Subfractions obtained from **A8.5** by column chromatography over silica gel

subfraction	weight (mg)	physical appearance
K1	194.4	white solid mixed with yellow gum
K2	138.2	yellow gum
K3	43.7	yellow gum
K4	55.2	yellow-brown gum

Subfraction K1 showed **DD12** as a major component on normal phase TLC with 25% ethyl acetate in petroleum ether (3 runs). Therefore, it was not purified.

Subfraction K2 displayed two major UV-active spots on normal phase TLC using 25% ethyl acetate in petroleum ether (2 runs) as a mobile phase with the R_f values of 0.25 and 0.23. It was then purified by flash column chromatography over silica gel. Elution was conducted using a stepwise gradient system (ethyl acetate in petroleum ether and methanol in ethyl acetate) and finally with pure methanol. Fractions with the similar chromatogram were combined and evaporated to dryness under reduced pressure to afford four subfractions, as shown in Table 12.

Table 12 Subfractions obtained from **K2** by flash column chromatography over silica gel

subfraction	weight (mg)	physical appearance
KB1	14.8	yellow gum
KB2	46.7	yellow gum
KB3	5.6	yellow gum
KB4	99.1	yellow gum

Subfraction KB1 displayed two major UV-active spots which were shown to be **DD13** and **DD11** by TLC. Thus, it was not further purified.

Subfraction KB2 showed three major UV-active spots on normal phase TLC using 25% ethyl acetate in petroleum ether (4 runs) as a mobile phase with the R_f values of 0.35, 0.31 and 0.25. It was then purified by flash column chromatography over silica gel. Elution was performed with 15% ethyl acetate in petroleum ether,

followed by increasing the polarity until 30% ethyl acetate in petroleum ether. Fractions with the similar chromatogram were combined and evaporated to dryness under reduced pressure to afford three subfractions, as shown in Table 13.

Table 13 Subfractions obtained from **KB2** by flash column chromatography over silica gel

subfraction	weight (mg)	physical appearance
KB2.1	6.9	yellow gum
KB2.2	15.0	yellow gum
KB2.3	27.0	yellow gum

Subfraction KB2.1 displayed **DD11**, **DD12** and **DD10** as major components on normal phase TLC under UV-S using 25% ethyl acetate in petroleum ether (4 runs) as a mobile phase. Therefore, it was not investigated.

Subfraction KB2.2 showed two major UV-active spots on normal phase TLC using 25% ethyl acetate in petroleum ether (4 runs) as a mobile phase with the R_f values of 0.31 and 0.25. Thus, it was purified on precoated TLC with 25% ethyl acetate in petroleum ether (11 runs) to afford two bands.

Band 1 (DD12) was a pale yellow gum (4.5 mg). Its chromatogram showed one UV-active spot on normal phase TLC using 25% ethyl acetate in petroleum ether (5 runs) as a mobile phase with the R_f value of 0.37.

$[\alpha]_D^{29}$ $+53^\circ$ ($c = 1.9 \times 10^{-2}$ g/100 cm³, MeOH)
 UV λ_{\max} nm (MeOH) (log ϵ) 305 (4.11)

IR (neat) $\nu_{\text{cm}^{-1}}$	3600-2500 (O-H stretching), 2959, 2927, 2856 (C-H stretching), 1746, 1683, 1634 (C=O stretching)
$^1\text{H NMR}$ (CDCl_3) (δ ppm) (500 MHz)	12.07 (<i>s</i> , 1H), 6.57 (<i>mt</i> , $J = 7.5$ Hz, 1H), 5.23 (<i>mt</i> , $J = 7.0$ Hz, 1H), 4.47 (<i>d</i> , $J = 0.5$ Hz, 1H), 4.41 (<i>q</i> , $J = 6.5$ Hz, 1H), 3.50 (<i>s</i> , 3H), 3.38 (<i>s</i> , 3H), 3.22-3.21 (<i>m</i> , 2H), 3.19 (<i>mdd</i> , $J = 17.0$ and 7.5 Hz, 1H), 3.16 (<i>d</i> , $J = 0.5$ Hz, 1H), 3.07 (<i>mdd</i> , $J = 17.0$ and 7.5 Hz, 1H), 2.71 (<i>d</i> , $J = 9.0$ Hz, 1H), 2.02 (<i>d</i> , $J = 14.0$ Hz, 1H), 1.98 (<i>d</i> , $J = 1.5$ Hz, 3H), 1.76 (<i>brs</i> , 3H), 1.69 (<i>d</i> , $J = 1.0$ Hz, 3H), 1.64 (<i>dd</i> , $J = 14.0$ and 9.0 Hz, 1H), 1.44 (<i>s</i> , 3H), 1.42 (<i>s</i> , 3H), 1.34 (<i>d</i> , $J = 6.5$ Hz, 3H), 1.21 (<i>s</i> , 3H), 1.12 (<i>s</i> , 3H)

Band 2 was a yellow gum (8.4 mg) which was shown to be **DD10** by TLC.

Subfraction KB2.3 showed **DD10**, as a major spot, on normal phase TLC. Further purification was not performed.

Subfraction KB3 displayed one major UV-active spot which was shown to be **DD10** by TLC. Thus, it was not separated.

Subfraction KB4 contained two major overlapping spots on normal phase TLC under UV-S using 25% ethyl acetate in petroleum ether as a mobile phase (4 runs). Because it was obtained in low quantity, it was not further investigated.

Subfraction K3 showed **DD10** as a major UV-active spot on normal phase TLC with 25% ethyl acetate in petroleum ether (3 runs). Therefore, it was not further purified.

Subfraction K4 displayed unseparable spots on normal phase TLC under UV-S using 25% ethyl acetate in petroleum ether as a mobile phase (3 runs). Thus, it was not investigated.

Subfraction A8.6 showed two major UV-active spots on normal phase TLC using 30% ethyl acetate in petroleum ether (2 runs) as a mobile phase with the R_f values of 0.25 and 0.09. It was then separated by column chromatography over silica gel. Elution was performed using a stepwise gradient system (ethyl acetate in petroleum ether and methanol in ethyl acetate) and finally with pure methanol. Fractions with the similar chromatogram were combined and evaporated to dryness under reduced pressure to afford three subfractions, as shown in Table 14.

Table 14 Subfractions obtained from **A8.6** by column chromatography over silica gel

subfraction	weight (mg)	physical appearance
A8.6/1	96.4	white solid mixed with yellow gum
A8.6/2	87.7	yellow gum
A8.6/3	32.4	white solid mixed with brown-yellow gum

Subfraction A8.6/1 contained no major UV-active spots on normal phase TLC with 30% ethyl acetate in petroleum ether (2 runs). Thus, it was not investigated.

Subfraction A8.6/2 showed one major UV-active spot on normal phase TLC using 30% ethyl acetate in petroleum ether (2 runs) with the R_f value of 0.25. It was

then purified by column chromatography over silica gel. Elution was performed with 1% methanol in chloroform with increasing amount of methanol up to pure methanol. Fractions with the similar chromatogram were combined and evaporated to dryness under reduced pressure to afford three subfractions, as shown in Table 15.

Table 15 Subfractions obtained from A8.6/2 by column chromatography over silica gel

subfraction	weight (mg)	physical appearance
C1	96.4	white solid mixed with yellow gum
C2	87.7	yellow gum
C3	32.4	white solid mixed with brown-yellow gum

Subfraction C1 showed no distinct spots on normal phase TLC under UV-S with 30% ethyl acetate in petroleum ether. Thus, further investigation was not carried out.

Subfraction C2 displayed one major UV-active spot as **DD10** on normal phase TLC with 30% ethyl acetate in petroleum ether. Therefore, it was not separated.

Subfraction C3 showed one major UV-active spot on normal phase TLC with 30% ethyl acetate in petroleum ether with the R_f value of 0.16. Further purification by column chromatography over silica gel was introduced. Elution was performed with 3% methanol in chloroform with increasing amount of methanol up to pure methanol. Fractions with the similar chromatogram were combined and evaporated to dryness under reduced pressure to afford three subfractions, as shown in Table 16.

Table 16 Subfractions obtained from C3 by column chromatography over silica gel

subfraction	weight (mg)	physical appearance
C3.1	4.9	yellow gum
C3.2	23.6	yellow gum
C3.3	33.1	white solid mixed with yellow gum

Subfraction C3.1 showed no major UV-active spots on normal phase TLC with 1% methanol in chloroform (3 runs). Thus, it was not investigated.

Subfraction C3.2 displayed one major UV-active spot on normal phase TLC using 1% methanol in chloroform as a mobile phase (3 runs) with the R_f value of 0.26. Further chromatographic separation by precoated TLC with 1% methanol in chloroform (10 runs) gave a yellow gum (**DD10**, 19.7 mg). Chromatogram on normal phase TLC using 1% methanol in chloroform (3 runs) as a mobile phase showed a single UV-active spot with the R_f value of 0.26.

$[\alpha]_D^{29}$	-353° ($c = 1.7 \times 10^{-2}$ g/100 cm ³ , MeOH)
UV λ_{\max} nm (MeOH) ($\log \epsilon$)	366 (4.10)
IR (neat) $\nu_{\text{cm}^{-1}}$	3600-2500 (O-H stretching), 2952, 2927, 2849 (C-H stretching), 1744, 1687, 1634 (C=O stretching)
¹ H NMR (CDCl ₃) (δ ppm) (500 MHz)	13.28 (<i>s</i> , 1H), 7.52 (<i>d</i> , $J = 1.0$ Hz, 1H), 5.39 (<i>md</i> , $J = 11.5$ Hz, 1H), 5.06 (<i>brs</i> , 1H), 4.89 (<i>brs</i> , 1H), 4.55 (<i>q</i> , $J = 6.5$ Hz, 1H), 4.51 (<i>dd</i> , $J = 11.0$ and 3.5 Hz, 1H), 3.64 (<i>s</i> , 3H), 3.56 (<i>dd</i> , $J = 15.5$ and

	11.5 Hz, 1H), 2.94 (<i>dd</i> , $J = 14.5$ and 11.0 Hz, 1H), 2.74 (<i>md</i> , $J = 15.5$ Hz, 1H), 2.69 (<i>dd</i> , $J = 14.5$ and 3.5 Hz, 1H), 2.64 (<i>d</i> , $J = 9.5$ Hz, 1H), 2.31 (<i>md</i> , $J = 12.5$ Hz, 1H), 1.85 (<i>s</i> , 3H), 1.72 (<i>s</i> , 3H), 1.71 (<i>dd</i> , $J = 12.5$ and 9.5 Hz, 1H), 1.67 (<i>dd</i> , $J = 2.0$ and 1.5 Hz, 3H), 1.48 (<i>s</i> , 3H), 1.40 (<i>s</i> , 3H), 1.38 (<i>d</i> , $J = 6.5$ Hz, 3H), 1.29 (<i>s</i> , 3H)
^{13}C NMR (CDCl_3) (δ ppm)	203.18, 177.80, 167.67, 167.35, 164.13, 155.02,
(125 MHz)	147.12, 135.64, 134.67, 132.52, 129.57, 112.75, 110.63, 102.30, 101.31, 92.12, 89.09, 85.12, 84.15, 83.51, 74.95, 53.83, 49.68, 43.49, 30.89, 30.45, 28.82, 28.70, 28.42, 27.99, 21.18, 19.63, 18.28, 16.27

Subfraction C3.3 showed one major UV-active spot on normal phase TLC using 1% methanol in chloroform as a mobile phase (3 runs) with the R_f value of 0.24. It was then separated on precoated TLC with 1% methanol in chloroform (16 runs) to give a white solid mixed with yellow gum (10.8 mg). Chromatogram on normal phase TLC using 2% methanol in chloroform as a mobile phase showed two UV-active spots with the R_f values of 0.26 and 0.24. Therefore, it was rechromatographed on precoated TLC with 2% methanol in chloroform (5 runs) to afford two bands.

Band 1 was a yellow gum (1.2 mg). It was shown to be **DD10** by TLC.

Band 2 was a yellow gum (3.5 mg). Chromatogram showed two UV-active spots on normal phase TLC with 2% methanol in chloroform. Because of low quantity, it was not carried out.

Subfraction A8.7 displayed three major UV-active spots on normal phase TLC using 25% ethyl acetate in petroleum ether (4 runs) as a mobile phase with the R_f values of 0.36, 0.27 and 0.13. Further purification by column chromatography over reverse-phase silica gel was carried out. Elution was performed initially with 50% methanol in water, followed by increasing amount of methanol and finally with pure methanol. Fractions with the similar chromatogram were combined and evaporated to dryness under reduced pressure to afford six subfractions, as shown in Table 17.

Table 17 Subfractions obtained from A8.7 by column chromatography over reverse-phase silica gel

subfraction	weight (mg)	physical appearance
L1	55.2	yellow gum
L2	91.9	yellow gum
L3	18.3	yellow gum
L4	32.6	white solid mixed with yellow gum
L5	36.3	white solid mixed with yellow gum
L6	216.9	brown- green gum

Subfraction L1 showed no distinct spots on normal phase TLC using 30% ethyl acetate in petroleum ether (3 runs) as a mobile phase. Thus, it was not investigated.

Subfraction L2 displayed three major UV-active spots on normal phase TLC using 30% ethyl acetate in petroleum ether (3 runs) as a mobile phase with the R_f values of 0.36, 0.27 and 0.15. Further separation by flash column chromatography over silica gel was performed. Elution was conducted using a stepwise gradient system (ethyl acetate in petroleum ether and methanol in ethyl acetate) and finally with pure methanol. Fractions with the similar chromatogram were combined and evaporated to dryness under reduced pressure to afford two subfractions, as shown in Table 18.

Table 18 Subfractions obtained from L2 by flash column chromatography over silica gel

subfraction	weight (mg)	physical appearance
LA1	32.2	yellow gum
LA2	37.7	white solid mixed with yellow gum

Subfraction LA1 showed DD10 as a major spot on normal phase TLC under UV-S using 30% ethyl acetate in petroleum ether (3 runs) as a mobile phase. Further purification was not performed.

Subfraction LA2 displayed one major UV-active spot on normal phase TLC using 30% ethyl acetate in petroleum ether (3 runs) as a mobile phase with the R_f value of 0.15. It was rechromatographed on precoated TLC with 30% ethyl acetate in petroleum ether (5 runs) to give a white solid mixed with yellow gum (9.5 mg). Chromatogram on normal phase TLC using 30% ethyl acetate in petroleum ether as a mobile phase showed three UV-active spots with the R_f values of 0.36, 0.29 and 0.15.

Further purification by column chromatography over reverse-phase silica gel was attempted. Elution was performed with 40% methanol in water, followed by increasing methanol up to 60% methanol in water. Fractions with the similar chromatogram were combined and evaporated to dryness under reduced pressure to afford four subfractions which were obtained in low quantity. Therefore, they were not further investigated.

Subfraction L3 displayed one major UV-active spot on normal phase TLC using 30% ethyl acetate in petroleum ether (3 runs) as a mobile phase with the R_f value of 0.21. Further separation by flash column chromatography over silica gel was carried out. Elution was conducted using a stepwise gradient system (ethyl acetate in petroleum ether and methanol in ethyl acetate) and finally with pure methanol. Fractions with the similar chromatogram were combined and evaporated to dryness under reduced pressure to afford twelve subfractions which were obtained in low quantity. Their chromatograms on normal phase TLC showed many UV-active spots using 30% ethyl acetate in petroleum ether (3 runs) as a mobile phase. Therefore, they were not further investigated.

Subfraction L4 displayed many UV-active spots on normal phase TLC without any major components. Therefore, it was not investigated.

Subfraction L5 showed the similar chromatogram to that of **subfraction D6**. Thus, they were combined.

Subfraction L6 displayed unseparable UV-active spots on normal phase TLC using 30% ethyl acetate in petroleum ether (3 runs) as a mobile phase. Further separation was not performed.

Subfraction A8.8 showed three major UV-active spots on normal phase TLC using 40% ethyl acetate in petroleum ether (3 runs) as a mobile phase with the R_f values of

0.80, 0.71 and 0.08. Further purification by column chromatography over reverse-phase silica gel was carried out. Elution was performed initially with 30% methanol in water, followed by increasing amount of methanol and finally with pure methanol. Fractions with the similar chromatogram were combined and evaporated to dryness under reduced pressure to afford five subfractions, as shown in Table 19.

Table 19 Subfractions obtained from A8.8 by column chromatography over reverse-phase silica gel

subfraction	weight (mg)	physical appearance
D1	417.5	pale yellow solid mixed with yellow gum
D2	102.1	yellow gum
D3	71.5	brown- yellow gum
D4	78.5	brown- yellow gum
D5	238.0	brown gum

Subfraction D1 displayed two major UV-active spots on normal phase TLC using 2% methanol in chloroform (2 runs) as a mobile phase with the R_f values of 0.18 and 0.07. Further purification by various mobile phase systems was not successful.

Subfraction D2 showed two major components on normal phase TLC using 2% methanol in chloroform (2 runs) as a mobile phase with the R_f values of 0.49 and 0.39. Further purification by column chromatography over silica gel was performed. Elution was conducted initially with 1% methanol in chloroform followed by increasing amount of methanol and finally with pure methanol. Fractions with the

similar chromatogram were combined and evaporated to dryness under reduced pressure to afford five subfractions, as shown in Table 20.

Table 20 Subfractions obtained from **D2** by column chromatography over silica gel

subfraction	weight (mg)	physical appearance
D2.1	5.2	pale yellow gum
D2.2	11.4	yellow gum
D2.3	39.5	yellow gum
D2.4	46.3	yellow gum
D2.5	5.9	yellow gum

Subfraction D2.1 showed many UV-active spots on normal phase TLC without any major components. Therefore, it was not investigated.

Subfraction D2.2 showed two major UV-active components on normal phase TLC using 2% methanol in chloroform as a mobile phase with the R_f values of 0.36 and 0.27. It was rechromatographed on precoated TLC with 2% methanol in chloroform (3 runs) to afford two bands.

Band 1 (DD11) was a yellow gum (4.9 mg) which showed only one UV-active spot on normal phase TLC using 2% methanol in chloroform as a mobile phase with the R_f values of 0.36.

$[\alpha]_D^{29}$ -222° (c = 9.0x10⁻³ g/100 cm³, MeOH)

UV λ_{\max} nm (MeOH) (log ϵ) 367 (4.01)

IR (neat) $\nu_{\text{cm}^{-1}}$	3600-2500 (O-H stretching), 2959, 2926, 2849 (C-H stretching), 1742, 1683, 1634 (C=O stretching)
^1H NMR (CDCl_3) (δ ppm) (500 MHz)	13.16 (<i>s</i> , 1H), 7.52 (<i>d</i> , $J = 1.0$ Hz, 1H), 5.20 (<i>md</i> , $J = 12.0$ Hz, 1H), 5.08-5.07 (<i>m</i> , 1H), 4.94-4.92 (<i>m</i> , 1H), 4.57 (<i>q</i> , $J = 6.5$ Hz, 1H), 4.32 (<i>brdd</i> , $J =$ 11.5 and 3.5 Hz, 1H), 3.82 (<i>dd</i> , $J = 15.5$ and 12.0 Hz, 1H), 3.66 (<i>s</i> , 3H), 2.99 (<i>dd</i> , $J = 14.5$ and 3.5 Hz, 1H), 2.72 (<i>md</i> , $J = 15.5$ Hz, 1H), 2.64 (<i>dd</i> , $J = 14.5$ and 11.5 Hz, 1H), 2.63 (<i>d</i> , $J =$ 9.5 Hz, 1H), 2.35 (<i>md</i> , $J = 13.0$ Hz, 1H), 1.87 (<i>brs</i> , 3H), 1.71 (<i>s</i> , 3H), 1.70 (<i>dd</i> , $J = 13.0$ and 9.5 Hz, 1H), 1.64 (<i>dd</i> , $J = 2.5$ and 1.5 Hz, 3H), 1.56 (<i>s</i> , 3H), 1.45 (<i>d</i> , $J = 6.5$ Hz, 3H), 1.38 (<i>s</i> , 3H), 1.29 (<i>s</i> , 3H)

Band 2 was a yellow gum (4.9 mg) which was indentified to be **DD10** by TLC.

Subfraction D2.3 showed one major UV-active component on normal phase TLC using 2% methanol in chloroform as a mobile phase with the R_f value 0.27. It was rechromatographed on precoated TLC with 2% methanol in chloroform (3 runs) to afford **DD10** (18.0 mg).

Subfraction D2.4 showed three major UV-active components on normal phase TLC using 2% methanol in chloroform as a mobile phase with the R_f values of 0.27, 0.25 and 0.06. It was further purified by column chromatography over silica gel.

Elution was conducted with 1% methanol in chloroform with increasing amount of methanol up to 30% methanol in chloroform. Fractions with the similar chromatogram were combined and evaporated to dryness under reduced pressure to afford three subfractions, as shown in Table 21.

Table 21 Subfractions obtained from **D2.4** by column chromatography over silica gel

subfraction	weight (mg)	physical appearance
DC1	3.7	yellow gum
DC2	26.7	yellow gum
DC3	22.2	yellow gum

Subfraction DC1 displayed **DD10** as a major UV-active component on normal phase TLC using 2% methanol in chloroform as a mobile phase with the R_f value of 0.27. Thus, it was not further purified.

Subfraction DC2 contained one major UV-active component on normal phase TLC using 2% methanol in chloroform as a mobile phase with the R_f value of 0.21. Further separation by column chromatography over silica gel was carried out. Elution was conducted with 2% methanol in chloroform with increasing amount of methanol up to 10% methanol in chloroform. Fractions with the similar chromatogram were combined and evaporated to dryness under reduced pressure to give three subfractions, as shown in Table 22.

Table 22 Subfractions obtained from DC2 by column chromatography over silica gel

subfraction	weight (mg)	physical appearance
DC2.1	5.2	pale yellow gum
DC2.2	17.9	yellow gum
DC2.3	9.2	yellow gum

Subfraction DC2.1 showed many UV-active spots on normal phase TLC. Because of low quantity, it was not carried out.

Subfraction DC2.2 contained one major UV-active component on normal phase TLC using 2% methanol in chloroform as a mobile phase with the R_f value of 0.21. Further chromatographic separation by precoated TLC on silica gel plate using 2% methanol in chloroform as a mobile phase (7 runs) afforded a yellow gum (13.1 mg). Its chromatogram showed three UV-active spots on normal phase TLC using 2% methanol in chloroform as a mobile phase with the R_f value of 0.40, 0.27 and 0.21. It was rechromatographed on precoated TLC using 2% methanol in chloroform as a mobile phase to give a yellow gum (9.8 mg) which displayed three spots on normal phase TLC under UV-S using 2% methanol in chloroform as a mobile phase with the R_f values of 0.40, 0.27 and 0.21. It was then separation on precoated TLC using 2% methanol in chloroform as a mobile phase (2 runs) afford a yellow gum (**DD14**, 6.5 mg). Its chromatogram showed one UV-active spot on normal phase TLC using 2% methanol in chloroform as a mobile phase with the R_f values of 0.21.

$[\alpha]_D^{29}$ -43° ($c = 2.3 \times 10^{-2}$ g/100 cm³, MeOH)
 UV λ_{\max} nm (MeOH) (log ϵ) 305 (4.26)

IR (neat) $\nu_{\text{cm}^{-1}}$	3600-2500 (O-H stretching), 2967, 2929, 2856 (C-H stretching), 1744, 1687, 1634 (C=O stretching)
^1H NMR (CDCl_3) (δ ppm) (500 MHz)	12.26 (<i>s</i> , 1H), 6.63 (<i>mt</i> , $J = 7.0$ Hz, 1H), 4.99 (<i>brs</i> , 1H), 4.84 (<i>brs</i> , 1H), 4.47 (<i>d</i> , $J = 1.5$ Hz, 1H), 4.42 (<i>q</i> , $J = 6.5$ Hz, 1H), 4.29 (<i>dd</i> , $J = 8.5$ and 4.0 Hz, 1H), 3.51 (<i>s</i> , 3H), 3.38 (<i>s</i> , 3H), 3.23 (<i>mdd</i> , $J = 15.5$ and 7.0 Hz, 1H), 3.20 (<i>d</i> , $J = 1.5$ Hz, 1H), 3.15 (<i>mdd</i> , $J = 15.5$ and 7.0 Hz, 1H), 2.88 (<i>dd</i> , $J = 14.5$ and 4.0 Hz, 1H), 2.77 (<i>dd</i> , $J = 14.5$ and 8.5 Hz, 1H), 2.70 (<i>d</i> , $J = 8.5$ Hz, 1H), 2.03 (<i>d</i> , $J = 14.5$ Hz, 1H), 1.97 (<i>d</i> , $J = 1.5$ Hz, 3H), 1.84 (<i>s</i> , 3H), 1.64 (<i>dd</i> , $J = 14.5$ and 8.5 Hz, 1H), 1.44 (<i>s</i> , 3H), 1.43 (<i>s</i> , 3H), 1.34 (<i>d</i> , $J = 6.5$ Hz, 3H), 1.22 (<i>s</i> , 3H), 1.12 (<i>s</i> , 3H)
^{13}C NMR (CDCl_3) (δ ppm) (125 MHz)	205.47, 192.23, 171.10, 167.40, 162.00, 152.69, 147.33, 138.06, 128.02, 113.80, 110.40, 102.51, 102.37, 90.50, 87.13, 86.41, 82.64, 81.40, 75.34, 75.11, 57.43, 52.41, 48.91, 45.29, 44.00, 30.48, 29.26, 28.46, 27.17, 26.07, 23.93, 22.08, 20.85, 18.06, 13.85
DEPT (135°) (CDCl_3)	CH_3 : 57.43, 52.41, 30.48, 27.17, 26.07, 22.08, 20.85, 18.06, 13.85 CH_2 : 110.40, 29.26, 28.46, 23.93 CH : 138.06, 90.50, 75.34, 75.11, 48.91, 45.29

Subfraction DC2.3 showed no major UV-active spots on normal phase TLC. Thus, it was not investigated.

Subfraction DC3 displayed one major UV-active spot on normal phase TLC using 2% methanol in chloroform as a mobile phase with the R_f value of 0.06. It was rechromatographed on precoated TLC using 40% ethyl acetate in petroleum ether as a mobile phase (5 runs) to afford a white solid (1.4 mg). Its chromatogram showed one UV-active spot on normal phase TLC using 2% methanol in chloroform as a mobile phase with the R_f value of 0.06. Its ^1H NMR spectrum indicated that it contained some impurities.

Subfraction D2.5 displayed unseparable UV-active spots on normal phase TLC with 2% methanol in chloroform (2 runs). Thus, it was not carried out.

Subfraction D3 contained **DD10** as a major component on normal phase TLC with 2% methanol in chloroform (2 runs). Thus, it was not further separation.

Subfraction D4 showed two major UV-active spots on normal phase TLC using 2% methanol in chloroform as a mobile phase (4 runs) with the R_f values of 0.16 and 0.09. Because its chromatogram was similar to that of **subfraction L5**, they were combined and further purified by flash column chromatography over silica gel. Elution was conducted using a stepwise gradient system (ethyl acetate in petroleum ether and methanol in ethyl acetate) and finally with 50% methanol in ethyl acetate. Fractions with the similar chromatogram were combined and evaporated to dryness under reduced pressure to afford six subfractions, as shown in Table 23.

Table 23 Subfractions obtained from **D4** by flash column chromatograph over silica gel

subfraction	weight (mg)	physical appearance
LC1	7.2	pale yellow gum
LC2	4.7	yellow gum
LC3	5.5	yellow gum
LC4	11.3	pale yellow gum
LC5	6.7	yellow gum
LC6	66.9	brown-yellow gum

Subfraction LC1 showed many spots on normal phase TLC under UV-S without any major components. Therefore, it was not investigated.

Subfraction LC2 (DD13) displayed a single UV-active spot on normal phase TLC using 30% ethyl acetate in petroleum ether as a mobile phase (6 runs) with the R_f values of 0.65. It melted at 158-159°C.

$[\alpha]_D^{29}$	-222° (c = 1.8x10 ⁻² g/100 cm ³ , MeOH)
UV λ_{max} nm (MeOH) (log ϵ)	367 (4.03)
IR (neat) $\nu_{cm^{-1}}$	3600-2500 (O-H stretching), 2974, 2928 (C-H stretching), 1742, 1683, 1635 (C=O stretching)
¹ H NMR (CDCl ₃) (δ ppm) (500 MHz)	13.11 (<i>s</i> , 1H), 7.57 (<i>d</i> , <i>J</i> = 1.0 Hz, 1H), 5.66 (<i>mdd</i> , <i>J</i> = 10.0 and 4.5 Hz, 1H), 5.21 (<i>mt</i> , <i>J</i> = 7.0 Hz, 1H), 4.47 (<i>q</i> , <i>J</i> = 6.5 Hz, 1H), 3.63 (<i>s</i> , 3H), 3.30 (<i>brdd</i> , <i>J</i> = 16.0 and 10.0 Hz, 1H), 3.17

(*brdd*, $J = 14.5$ and 7.0 Hz, 1H), 3.12 (*brdd*, $J = 14.5$ and 7.0 Hz, 1H), 2.84 (*mdd*, $J = 16.0$ and 4.5 Hz, 1H), 2.61 (*d*, $J = 9.0$ Hz, 1H), 2.33 (*d*, $J = 13.5$ Hz, 1H), 1.73 (*brs*, 9H), 1.70 (*dd*, $J = 13.5$ and 9.0 Hz, 1H), 1.67 (*s*, 3H), 1.38 (*s*, 6H), 1.29 (*s*, 3H), 1.23 (*d*, $J = 6.5$ Hz, 3H)

Subfraction LC3 contained **DD13**, **DD11** and **DD12** as major UV-active spots on normal phase TLC using 30% ethyl acetate in petroleum ether as a mobile phase (6 runs) with the R_f values of 0.65, 0.55 and 0.53, respectively. Thus, it was not separated further.

Subfraction LC4 showed **DD12** as a major UV-active component on normal phase TLC using 30% ethyl acetate in petroleum ether as a mobile phase (6 runs) with the R_f value of 0.53. Therefore, purification was then not performed.

Subfraction LC5 contained **DD12** and **DD10** as major components on normal phase TLC under UV-S using 30% ethyl acetate in petroleum ether as a mobile phase (6 runs) with the R_f value of 0.53 and 0.47, respectively. Thus, further separation was not introduced.

Subfraction LC6 displayed no major UV-active spots on normal phase TLC. Therefore, it was not carried out.

Subfraction D5 showed unseparable spots on normal phase TLC under UV-S. Thus, it was not investigated further.

Subfraction A8.9 displayed two major components on normal TLC under UV-S using 40% ethyl acetate in petroleum ether as a mobile phase (3 runs) with the R_f values of 0.71 and 0.08. Further separation by column chromatography over reverse-phase silica

gel was carried out. Elution was performed with 35% methanol in water, followed by decreasing the polarity until pure methanol. Fractions with the similar chromatogram were combined and evaporated to dryness under reduced pressure to afford four subfractions, as shown in Table 24.

Table 24 Subfractions obtained from A8.9 by column chromatography over reverse-phase silica gel

subfraction	weight (mg)	physical appearance
M1	96.5	yellow solid
M2	197.5	yellow gum
M3	72.0	white solid mixed with yellow gum
M4	290.7	brown-yellow gum

Subfraction M1 showed unseparable UV-active spots on normal phase TLC. Thus, it was not further investigated.

Subfraction M2 displayed two UV-active spots on normal phase TLC using 50% ethyl acetate in petroleum ether as a mobile phase (5 runs) with the R_f values of 0.19 and 0.13. It was further purified by column chromatography over reverse-phase silica gel. Elution was performed with 35% methanol in water, followed by decreasing the polarity until pure methanol. Fractions with the similar chromatogram were combined and evaporated to dryness under reduced pressure to afford three subfractions, as shown in Table 25.

Table 25 Subfractions obtained from M2 by column chromatography over reverse-phase silica gel

subfraction	weight (mg)	physical appearance
M2.1	63.2	yellow solid
M2.2	65.3	yellow gum
M2.3	74.4	orange-yellow gum

Subfraction M2.1 showed unseparable UV-active spots on normal phase TLC with 5% methanol in chloroform (6 runs). Thus, it was not further investigated.

Subfraction M2.2 displayed three major UV-active spots on normal phase TLC using 5% methanol in chloroform as a mobile phase (6 runs) with the R_f values of 0.33, 0.29 and 0.27. Further chromatographic separation by flash column chromatography over silica gel was carried out. Elution was performed with 1% methanol in chloroform. Fractions with the similar chromatogram were combined and evaporated to dryness under reduced pressure to afford three subfractions, as shown in Table 26.

Table 26 Subfractions obtained from M2.2 by flash column chromatography over silica gel

subfraction	weight (mg)	physical appearance
M2.2/1	9.3	yellow solid
M2.2/2	19.4	yellow gum
M2.2/3	7.3	orange-yellow gum

Subfraction M2.2/1 contained no major UV-active components on normal phase TLC with 5% methanol in chloroform (6 runs). Thus, it was not investigated.

Subfraction M2.2/2 displayed two overlapping UV-active spots on normal phase TLC using 5% methanol in chloroform as a mobile phase (6 runs). It was rechromatographed on precoated TLC with 5% methanol in chloroform (8 runs) to afford two bands.

Band 1 was a pale yellow gum (6.7 mg). Its chromatogram showed three UV-active spots on normal phase TLC using 5% methanol in chloroform as a mobile phase (8 runs) with the R_f values of 0.44, 0.40 and 0.31. Because of low quantity, it was not further purified.

Band 2 was a pale yellow gum (3.5 mg) which showed a single UV-active spot on normal phase TLC using 5% methanol in chloroform as a mobile phase (8 runs) with the R_f value of 0.37. Its ^1H NMR spectrum indicated that it contained some impurities.

Subfraction M2.2/3 displayed many UV-active spots on normal phase TLC without any major components. Further investigation was not attempted.

Subfraction M2.3 contained no major components on normal phase TLC. Thus, it was not investigated.

Subfraction M3 showed two major UV-active components on normal phase TLC using 5% methanol in chloroform as a mobile phase (2 runs) with the R_f values of 0.42 and 0.31. It was then separated by column chromatography over silica gel. Elution was conducted with 2% methanol in chloroform with increasing amount of methanol up to 50% methanol in chloroform. Fractions with the similar chromatogram

were combined and evaporated to dryness under reduced pressure to afford three subfractions, as shown in Table 27.

Table 27 Subfractions obtained from M3 by column chromatography over silica gel

subfraction	weight (mg)	physical appearance
M3.1	15.7	yellow solid
M3.2	6.5	yellow gum
M3.3	20.6	orange-yellow gum

Subfraction M3.1 contained no major UV-active components on normal phase TLC with 3% methanol in chloroform (2 runs). Thus, it was not investigated.

Subfraction M3.2 showed one major UV-active spot on normal phase TLC using 3% methanol in chloroform (2 runs) as a mobile phase with the R_f value of 0.27. Further chromatographic separation by precoated TLC with 3% methanol in chloroform (8 runs) was introduced to give a yellow gum (**DD15**, 1.5 mg). Chromatogram on normal phase TLC using 3% methanol in chloroform (2 runs) as a mobile phase showed a single UV-active spot with the R_f value of 0.27.

$[\alpha]_D^{29}$	-300° ($c = 1.0 \times 10^{-2}$ g/100 cm ³ , MeOH)
UV λ_{\max} nm (MeOH) (log ϵ)	367 (4.19)
IR (neat) $\nu_{\text{cm}^{-1}}$	3500-2500 (O-H stretching), 2959, 2927, 2849 (C-H stretching), 1742, 1631 (C=O stretching)
¹ H NMR (CDCl ₃) (δ ppm)	13.16 (<i>s</i> , 1H), 7.51 (<i>d</i> , $J = 1.5$ Hz, 1H), 5.20
(400 MHz)	(<i>mdd</i> , $J = 11.6$ and 1.5 Hz, 1H), 4.56 (<i>q</i> , $J = 6.4$

	Hz, 1H), 3.77 (<i>dd</i> , $J = 15.2$ and 11.6 Hz, 1H), 3.72 (<i>dd</i> , $J = 11.2$ and 3.2 Hz, 1H), 3.64 (<i>s</i> , 3H), 2.87 (<i>dd</i> , $J = 14.0$ and 3.2 Hz, 1H), 2.71 (<i>md</i> , $J =$ 15.2 Hz, 1H), 2.65 (<i>dd</i> , $J = 14.0$ and 11.2 Hz, 1H), 2.64 (<i>d</i> , $J = 9.6$ Hz, 1H), 2.34 (<i>dd</i> , $J = 12.8$ and 1.5 Hz, 1H), 1.72 (<i>dd</i> , $J = 12.8$ and 9.6 Hz, 1H), 1.71 (<i>s</i> , 3H), 1.62 (<i>dd</i> , $J = 2.5$ and 1.5 Hz, 3H), 1.53 (<i>s</i> , 3H), 1.43 (<i>d</i> , $J = 6.4$ Hz, 3H), 1.37 (<i>s</i> , 3H), 1.33 (<i>s</i> , 3H), 1.31 (<i>s</i> , 3H), 1.29 (<i>s</i> , 3H)
^{13}C NMR (CDCl_3) (δ ppm) (100 MHz)	203.00, 178.14, 167.68, 166.98, 163.76, 154.70, 135.60, 134.78, 132.51, 129.55, 112.53, 101.79, 101.31, 92.34, 89.04, 85.11, 84.31, 83.45, 76.44, 72.90, 53.80, 49.70, 43.85, 30.80, 30.34, 29.10, 28.85, 28.53, 26.44, 24.53, 24.23, 21.12, 19.29, 16.63
DEPT (135°) (CDCl_3)	CH_3 : 53.80, 30.80, 28.85, 28.53, 26.44, 24.53, 21.12, 19.29, 16.63 CH_2 : 30.34, 29.10, 24.23 CH : 135.60, 134.78, 92.34, 76.44, 49.70
EIMS (m/z) (% rel. int.)	626 (2.5), 598 (100), 508 (36), 472 (22), 413 (22), 381 (45), 277 (22), 233 (24), 177 (21)

Subfraction M4 displayed **DD11** and **DD10** as major UV-active components on normal phase TLC with 5% methanol in chloroform (2 runs). Thus, it was not further investigated.

Subfraction A8.10 contained unseparable components on normal phase TLC under UV-S using 40% ethyl acetate in petroleum ether as a mobile phase (3 runs). Therefore, it was not carried out.

Fraction A9 displayed three major UV-active spots on normal phase TLC using 40% ethyl acetate in petroleum ether as a mobile phase with the R_f values of 0.38, 0.21 and 0.07. It was further purified by column chromatography over reverse-phase silica gel. Elution was performed with 30% methanol in water, followed by decreasing the polarity until pure methanol. Fractions with the similar chromatogram were combined and evaporated to dryness under reduced pressure to afford six subfractions, as shown in Table 28.

Table 28 Subfractions obtained from A9 by column chromatography over reverse-phase silica gel

subfraction	weight (mg)	physical appearance
A9.1	294.4	brown solid mixed with brown gum
A9.2	89.5	yellow gum
A9.3	84.7	yellow gum
A9.4	94.0	yellow gum
A9.5	94.9	yellow gum
A9.6	187.8	brown solid mixed with brown gum

Subfraction A9.1 showed unseparable UV-active spots on normal phase TLC with 5% methanol in chloroform (5 runs). Thus, it was not further separated.

Subfraction A9.2 contained four major UV-active spots on normal phase TLC using 5% methanol in chloroform as a mobile phase (5 runs) with the R_f values of 0.57, 0.47, 0.30 and 0.19. Further chromatographic separation by flash column chromatography over silica gel was carried out. Elution was performed with 0.5% methanol in chloroform with increasing amount of methanol up to 3% methanol in chloroform. Fractions with the similar chromatogram were combined and evaporated to dryness under reduced pressure to afford eight subfractions, as shown in Table 29.

Table 29 Subfractions obtained from A9.2 by flash column chromatography over silica gel

subfraction	weight (mg)	physical appearance
A9.2/1	1.6	yellow gum
A9.2/2	4.3	yellow gum
A9.2/3	15.1	yellow gum
A9.2/4	10.7	yellow gum
A9.2/5	17.2	yellow gum
A9.2/6	13.5	yellow gum
A9.2/7	9.6	yellow gum
A9.2/8	8.5	yellow gum

Subfraction A9.2/1 contained no major component on normal phase TLC under UV-S with 3% methanol in chloroform. Further investigation was not carried out.

Subfraction A9.2/2 showed DD11 as a major component on normal phase TLC under UV-S with 3% methanol in chloroform. Thus, it was not separated.

Subfraction A9.2/3 displayed DD12 and DD10 as major UV-active components on normal phase TLC with 3% methanol in chloroform. Therefore, it was not purified.

Subfraction A9.2/4 showed DD10 as a major component on normal phase TLC under UV-S with 3% methanol in chloroform. Thus, it was not investigated.

Subfraction A9.2/5 contained DD10 and DD14 as major components on normal phase TLC under UV-S with 3% methanol in chloroform. Further separation was not performed.

Subfraction A9.2/6 displayed DD14 as a major component on normal phase TLC under UV-S with 3% methanol in chloroform. Thus, it was not purified.

Subfraction A9.2/7 showed one major UV-active spot on normal phase TLC using 3% methanol in chloroform as a mobile phase with the R_f value of 0.19. Further chromatographic separation by precoated TLC with 3% methanol in chloroform (8 runs) was introduced to give a yellow gum (2.1 mg). Chromatogram on normal phase TLC using 3% methanol in chloroform (2 runs) as a mobile phase showed a single UV-active spot with the R_f value of 0.25. Its ^1H NMR spectrum indicated the presence of impurities. It was not further investigated.

Subfraction A9.2/8 contained unseparable UV-active spots on normal phase TLC using 3% methanol in chloroform as a mobile phase. Therefore, it was not investigated.

Subfraction A9.3 showed two major UV-active spots on normal phase TLC using 3% methanol in chloroform as a mobile phase with the R_f values of 0.20 and 0.10. Attempted purification using various mobile phase systems was not successful.

Subfraction A9.4 displayed four major UV-active spots on normal phase TLC using 3% methanol in chloroform as a mobile phase with the R_f values of 0.57, 0.43, 0.20 and 0.15. It was then separated by flash column chromatography over silica gel. Elution was performed with 0.5% methanol in chloroform with increasing amount of methanol up to 5% methanol in chloroform. Fractions with the similar chromatogram were combined and evaporated to dryness under reduced pressure to afford four subfractions, as shown in Table 30.

Table 30 Subfractions obtained from A9.4 by flash column chromatography over silica gel

subfraction	weight (mg)	physical appearance
A9.4/1	10.0	yellow gum
A9.4/2	23.1	yellow gum
A9.4/3	28.2	yellow gum
A9.4/4	16.3	yellow gum

Subfraction A9.4/1 contained **DD13** as a major component on normal phase TLC with 3% methanol in chloroform. Further separation was not carried out.

Subfraction A9.4/2 showed one UV-active spot as **DD13** on normal phase TLC with 3% methanol in chloroform.

Subfraction A9.4/3 displayed one major UV-active spot on normal phase TLC using 3% methanol in chloroform as a mobile phase with the R_f value of 0.24. It was rechromatographed on precoated TLC with 15% ethyl acetate in petroleum ether (33 runs) to give a yellow gum (**DD2**, 5.2 mg). Its chromatogram showed a single UV-

active spot on normal phase TLC with the R_f value of 0.57 using 2% methanol in chloroform (2 runs) as a mobile phase.

$[\alpha]_D^{29}$	-200° ($c = 5.0 \times 10^{-3}$ g/100 cm ³ , MeOH)
UV λ_{\max} nm (MeOH) ($\log \epsilon$)	364 (4.02)
IR (neat) $\nu_{\text{cm}^{-1}}$	3600-2500 (O-H stretching), 2926, 2849 (C-H stretching), 1742, 1633 (C=O stretching)
¹ H NMR (CDCl ₃) (δ ppm) (400 MHz)	13.09 (<i>s</i> , 1H), 7.60 (<i>s</i> , 1H), 6.40 (<i>dd</i> , $J = 10.0$ and 5.6 Hz, 1H), 5.22 (<i>brt</i> , $J = 6.8$ Hz, 1H), 4.54 (<i>q</i> , $J = 6.8$ Hz, 1H), 3.63 (<i>s</i> , 3H), 3.20 (<i>d</i> , $J = 6.8$ Hz, 2H), 2.80 (<i>brdd</i> , $J = 14.8$ and 5.6 Hz, 1H), 2.61 (<i>d</i> , $J = 9.6$ Hz, 1H), 2.56 (<i>dd</i> , $J = 14.8$ and 10.0 Hz, 1H), 2.34 (<i>d</i> , $J = 12.8$ Hz, 1H), 1.74 (<i>s</i> , 3H), 1.73 (<i>s</i> , 3H), 1.68 (<i>dd</i> , $J = 12.8$ and 9.6 Hz, 1H), 1.68 (<i>s</i> , 3H), 1.47 (<i>s</i> , 3H), 1.41 (<i>s</i> , 3H), 1.39 (<i>s</i> , 3H), 1.29 (<i>d</i> , $J = 6.8$ Hz, 3H), 1.29 (<i>s</i> , 3H)

Subfraction A9.4/4 contained many UV-active spots on normal phase TLC without any major components. Thus, it was not investigated.

Subfraction A9.5 showed **DD12** as major component on normal phase TLC with 3% methanol in chloroform. Further separation was not carried out.

Subfraction A9.6 contained many UV-active spots on normal phase TLC without any major components. Thus, it was not investigated.

Fraction A10 displayed three major UV-active spots on normal phase TLC using 40% ethyl acetate in petroleum ether as a mobile phase with the R_f values of 0.16, 0.08 and

0.04. Further chromatography by column chromatography over reverse-phase silica gel was carried out. Elution was performed initially with 30% methanol in water, follow by increasing amount of methanol and finally with pure methanol. Fractions with the similar chromatogram were combined and evaporated to dryness under reduced pressure to afford seven subfractions, as shown in Table 31.

Table 31 Subfractions obtained from A10 by column chromatography over reverse-phase silica gel

subfraction	weight (mg)	physical appearance
A10.1	214.6	brown gum
A10.2	23.7	brown gum
A10.3	124.8	brown gum
A10.4	161.4	brown gum
A10.5	127.2	brown gum
A10.6	250.5	brown gum
A10.7	512.0	brown gum

Subfraction A10.1 contained three major components on normal phase TLC using 4% methanol in chloroform as a mobile phase with the R_f values of 0.48, 0.23 and 0.16. Further purification by flash column chromatography over silica gel was performed. Elution was conducted with 1% methanol in chloroform with increasing amount of methanol up to 50% methanol in chloroform. Fractions with the similar chromatogram were combined and evaporated to dryness under reduced pressure to afford five subfractions, as shown in Table 32.

Table 32 Subfractions obtained from **A10.1** by flash column chromatography over silica gel

subfraction	weight (mg)	physical appearance
A10.1/1	6.5	pale yellow gum
A10.1/2	2.7	colorless gum
A10.1/3	15.6	yellow gum
A10.1/4	11.5	yellow gum
A10.1/5	62.5	pale yellow gum

Subfraction A10.1/1 showed no major UV-active spots on normal phase TLC using 5% methanol in chloroform (4 runs) as a mobile phase. Therefore, it was not investigated further.

Subfraction A10.1/2 displayed one UV-active spot on normal phase TLC using 5% methanol in chloroform (4 runs) as a mobile phase with the R_f value of 0.46. Its ^1H NMR spectrum indicated the presence of impurities. It was not further investigated.

Subfraction A10.1/3 contained one major UV-active spot on normal phase TLC using 5% methanol in chloroform (4 runs) as a mobile phase with the R_f value of 0.54. Further chromatographic separation by precoated TLC with 5% methanol in chloroform (10 runs) was performed to give three bands of which their chromatograms contained many spots. Further purification was not carried out.

Subfraction A10.1/4 showed no major UV-active spots on normal phase TLC using 5% methanol in chloroform (4 runs) as a mobile phase. Therefore, it was not investigated further.

Subfraction A10.1/5 displayed two major UV-active spots on normal phase TLC using 5% methanol in chloroform (4 runs) as a mobile phase with the R_f values of 0.29 and 0.19. Attempted purification using various mobile phase systems was not successful.

Subfraction A10.2 showed no distinct spots on normal phase TLC using 4% methanol in chloroform as a mobile phase. Therefore, further separation was not performed.

Subfraction A10.3 contained one major UV-active spot on reverse-phase TLC using 60% methanol in water (4 runs) as a mobile phase with the R_f values of 0.34. Further purification by column chromatography over reverse-phase silica gel was performed. Elution was conducted with 60% methanol in water with decreasing polarity up to 65% methanol in water. Fractions with the similar chromatogram were combined and evaporated to dryness under reduced pressure to afford three subfractions, as shown in Table 33.

Table 33 Subfractions obtained from A10.3 by column chromatography over reverse-phase silica gel

subfraction	weight (mg)	physical appearance
A10.3/1	25.2	brown-yellow gum
A10.3/2	52.0	brown-yellow gum
A10.3/3	40.6	brown-yellow gum

Subfraction A10.3/1 showed no major UV-active components on normal phase TLC using 8% methanol in chloroform as a mobile phase. Therefore, it was not investigated further.

Subfraction A10.3/2 displayed one major UV-active components on normal phase TLC using 8% methanol in chloroform (3 runs) as a mobile phase with the R_f value of 0.16. Further chromatographic separation by column chromatography over reverse-phase silica gel was introduced. Elution was conducted with 50% methanol in water with increasing amount of methanol up to 70% methanol in water. Fractions with the similar chromatogram were combined and evaporated to dryness under reduced pressure to afford two subfractions, as shown in Table 34.

Table 34 Subfractions obtained from A10.3/2 by column chromatography over reverse-phase silica gel

subfraction	weight (mg)	physical appearance
U1	21.1	brown-yellow gum
U2	29.5	brown-yellow gum

Subfraction U1 showed the same major UV-active component with that of **subfraction U2**.

Subfraction U2 contained one major UV-active components on normal phase TLC using 8% methanol in chloroform (3 runs) as a mobile phase with the R_f value of 0.15. It was rechromatographed by column chromatography over reverse-phase silica gel. Elution was performed with 55% methanol in water with increasing amount of methanol up to 70% methanol in water. Fractions with the similar chromatogram were

combined and evaporated to dryness under reduced pressure to afford a brown-yellow gum in 17.8 mg. Further separation by column chromatography over reverse-phase silica gel. Elution was performed with 30% methanol in water with increasing amount of methanol up to pure methanol. Fractions with the similar chromatogram were combined and evaporated to dryness under reduced pressure to afford three subfractions, as shown in Table 35.

Table 35 Subfractions obtained from U2 by column chromatography over reverse-phase silica gel

subfraction	weight (mg)	physical appearance
U2/1	6.5	pale brown-yellow solid
U2/2	13.2	brown-yellow solid
U2/3	10.2	brown-yellow solid

Subfraction U2/1 contained no major UV-active component on normal phase TLC using 8% methanol in chloroform (3 runs). Thus, it was not investigated.

Subfraction U2/2 (DD16) displayed one UV-active component on normal phase TLC using 8% methanol in chloroform (3 runs) with the R_f value of 0.15. It decomposed at 210°C.

$[\alpha]_D^{29}$	+40° (c = 2.5 × 10 ⁻² g/100 cm ³ , MeOH)
UV λ_{max} nm (MeOH) (log ϵ)	228 (4.15), 273 (3.97), 290 (3.99), 343 (3.81)
IR (neat) $\nu_{cm^{-1}}$	3419 (O-H stretching), 1634 (C=O stretching)

$^1\text{H NMR}$ (CD_3OD) (δ ppm) (500 MHz)	7.36 (<i>d</i> , $J = 2.0$ Hz, 1H), 7.31 (<i>dd</i> , $J = 8.5$ and 2.0 Hz, 1H), 7.25-7.23 (<i>m</i> , 0.5H), 7.11 (<i>d</i> , $J = 8.5$ Hz, 2H), 7.06 (<i>d</i> , $J = 8.5$ Hz, 1.5H), 6.94 (<i>d</i> , $J = 8.5$ Hz, 1H), 6.64 (<i>d</i> , $J = 8.5$ Hz, 1.3H), 6.56 (<i>d</i> , $J = 8.5$ Hz, 0.5H), 6.54 (<i>s</i> , 0.5H), 6.44 (<i>s</i> , 1H), 6.43 (<i>d</i> , $J = 8.5$ Hz, 2H), 6.28 (<i>s</i> , 1H), 6.08 (<i>brs</i> , 0.5H), 6.06-6.05 (<i>m</i> , 0.5H), 6.02-6.01 (<i>m</i> , 0.5H), 5.99 (<i>d</i> , $J = 1.5$ Hz, 1H), 5.98 (<i>d</i> , $J = 1.5$ Hz, 1H), 5.75 (<i>d</i> , $J = 12.0$ Hz, 1H), 5.62 (<i>d</i> , $J = 12.0$ Hz, 0.5H)
--	---

Subfraction A10.3/3 showed many UV-active spots on normal phase TLC without any major components. Therefore, it was not investigated.

Subfraction A10.4 showed four major UV-active components on normal phase TLC using 4% methanol in chloroform (4 runs) as a mobile phase with the R_f values of 0.55, 0.45, 0.23 and 0.15. Attempted purification using various mobile phase systems was not successful.

Subfraction A10.5 displayed two major UV-active components on normal phase TLC using 4% methanol in chloroform (4 runs) as a mobile phase with the R_f values of 0.22 and 0.14. It was separated by flash column chromatography over silica gel. Elution was introduced with 1% methanol in chloroform with increasing amount of methanol up to 50% methanol in chloroform. Fractions with the similar chromatogram were combined and evaporated to dryness under reduced pressure to afford three subfractions. Attempted purification of each subfraction was unsuccessful.

Subfraction A10.6 showed three major UV-active components on normal phase TLC using 4% methanol in chloroform (4 runs) as a mobile phase with the R_f values of 0.52, 0.19 and 0.11. Attempted purification using various mobile phase systems was not successful.

Subfraction A10.7 contained many UV-active spots on normal phase TLC using 4% methanol in chloroform (4 runs) as a mobile phase. Further separation by column chromatography over reverse-phase silica gel was carried out. Elution was introduced with 70% methanol in water with increasing amount of methanol up to pure methanol. Fractions with the similar chromatogram were combined and evaporated to dryness under reduced pressure to afford three subfractions of which chromatograms contained unseparable spots. Further purification was then not performed.

Fraction A11 showed no major UV-active components on normal phase TLC using 40% ethyl acetate in petroleum ether as a mobile phase. Therefore, it was not investigated further.

Chapter 3

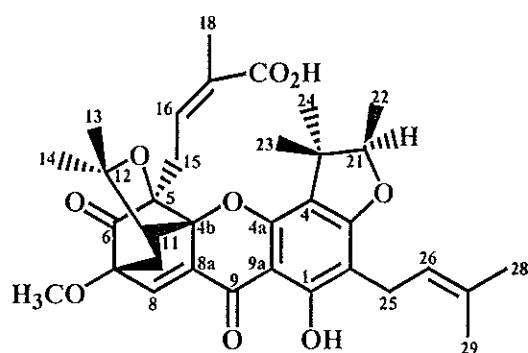
RESULTS AND DISCUSSION

The methanol extract of the twigs of *G. merguensis* was separated into two parts. The dichloromethane soluble part, upon repeated chromatography, afforded four new caged-polyprenylated xanthenes (**DD3**, **DD5**, **DD14** and **DD15**) together with twelve known compounds : eight caged-polyprenylated xanthenes (**DD1**, **DD2**, **DD8**, **DD9**, **DD10**, **DD11**, **DD12** and **DD13**), one steroid [stigmasterol (**DD4**)], one triterpene [friedelin (**DD6**)], one sesquiterpene [germacra-4(15), 5*E*, 10(14)-trien-1-ol (**DD7**)] and one biflavone [I-5, II-5, I-7, II-7, I-3', I-4', II-4'-heptahydroxy-[I-3,II-8]-flavanonylflavone (**DD16**)]. All structures were determined by 1D and/or 2D NMR spectroscopic data and/or comparison of ¹H and/or ¹³C spectral data from those reported in the literature. The ¹³C NMR signals were assigned from DEPT, HMQC and HMBC spectra.

3.1 Compound DD13

Compound **DD13** was isolated as a yellow solid, melting at 158-159°C. The IR spectrum (**Figure 2**) exhibited absorption bands at 3600-2500, 1742, 1683 and 1635 cm⁻¹ for hydroxyl, unconjugated carbonyl, α,β -unsaturated carbonyl and chelated *ortho*-hydroxyl carbonyl functionalities, respectively (Rukachaisirikul, 2000a). In the UV spectrum (**Figure 1**), the long wavelength absorption band at λ_{\max} 367 nm was similar to that of caged-polyprenylated xanthenes recently isolated from *Garcinia scortechinii*

(Rukachaisirikul, 2000a), indicating that **DD13** had a caged-polyprenylated xanthone chromophore. The ^1H NMR spectrum (**Figure 3**) (**Table 36**) revealed the presence of one chelated hydroxy proton [δ_{H} 13.11 (1-OH, *s*)], three olefinic protons [δ_{H} 7.57 (1H, *d*, $J = 1.0$ Hz) ; δ_{H} 5.66 (1H, *mdd*, $J = 10.0$ and 4.5 Hz) and δ_{H} 5.21 (1H, *mt*, $J = 7.0$ Hz), one methoxy group [δ_{H} 3.63 (3H, *s*)], one oxymethine proton [δ_{H} 4.47 (1H, *q*, $J = 6.5$ Hz)], one methine proton [δ_{H} 2.61 (1H, *d*, $J = 9.0$ Hz)], three methylene groups [δ_{H} 3.30 (1H, *brdd*, $J = 16.0$ and 10.0 Hz) and δ_{H} 2.84 (1H, *mdd*, $J = 16.0$ and 4.5 Hz) ; δ_{H} 3.17 and 3.12 (1H each, *brdd*, $J = 14.5$ and 7.0 Hz) and δ_{H} 2.33 (1H, *d*, $J = 13.5$ Hz) and δ_{H} 1.70 (1H, *dd*, $J = 13.5$ and 9.0 Hz)], one secondary methyl group [δ_{H} 1.23 (3H, *d*, $J = 6.5$ Hz)] and seven tertiary methyl groups [δ_{H} 1.73 (9H, *brs*) ; δ_{H} 1.67 (3H, *s*) ; δ_{H} 1.38 (6H, *s*) and δ_{H} 1.29 (3H, *s*)]. Direct comparison of its ^1H NMR spectrum with the previously reported data of **scortechinone B** (Rukachaisirikul, 2000a) indicated that **DD13** gave identical spectral data to **scortechinone B**. It was therefore identified as **scortechinone B (1)**.



(1)

Table 36 The ^1H NMR data of compounds DD13 and scortechinone B

Position	DD13	scortechinone B
	δ_{H} (mult., J_{Hz})	δ_{H} (mult., J_{Hz})
1-OH	13.11 (s)	13.10 (s)
8	7.57 (d, 1.0)	7.56 (d, 1.2)
10	2.33 (d, 13.5)	2.33 (dd, 13.2, 1.2)
	1.70 (dd, 13.5, 9.0)	1.68 (dd, 13.2, 9.2)
11	2.61 (d, 9.0)	2.60 (d, 9.2)
13	1.73 (brs)	1.72 (s)
14	1.29 (s)	1.28 (s)
15	3.30 (brdd, 16.0, 10.0)	3.27 (brdd, 16.0, 9.6)
	2.84 (mdd, 16.0, 4.5)	2.83 (ddq, 16.0, 4.5, 2.0)
16	5.66 (mdd, 10.0, 4.5)	5.67 (ddq, 9.6, 4.5, 1.5)
18	1.73 (brs)	1.72 (s)
21	4.47 (q, 6.5)	4.46 (q, 6.6)
22	1.23 (d, 6.5)	1.23 (d, 6.6)
23	1.38 (s)	1.37 (s)
24	1.38 (s)	1.37 (s)
25	3.17 (brdd, 14.5, 7.0)	3.17 (mdd, 14.4, 7.2)
	3.12 (brdd, 14.5, 7.0)	3.11 (mdd, 14.4, 7.2)
26	5.21 (mt, 7.0)	5.20 (ht, 7.2, 1.5)
28	1.67 (s)	1.65 (q, 1.5)
29	1.73 (brs)	1.72 (brs)
OMe	3.63 (s)	3.52 (s)

3.2 Compound DD15

Compound **DD15** was obtained as a yellow gum. It exhibited similar UV (Figure 4) and IR (Figure 5) spectra to those of **DD13** (**scortechinone B**). The mass spectrum (Figure 15) showed the molecular ion peak at m/z 626 for a molecular formula of $C_{34}H_{42}O_{11}$. The 1H NMR spectrum (Figure 6) (Table 37) suggested the presence of a chelated hydroxy proton [δ_H 13.16 (1-OH, *s*)], a 3-carboxybut-2-enyl group [δ_H 5.20 (1H, *mdd*, $J = 11.6$ and 1.5 Hz), δ_H 3.77 (1H, *dd*, $J = 15.2$ and 11.6 Hz), δ_H 2.71 (1H, *md*, $J = 15.2$ Hz) and δ_H 1.62 (3H, *dd*, $J = 2.5$ and 1.5 Hz)], a 2,3,3-trimethylhydrofuran unit [δ_H 4.56 (1H, *q*, $J = 6.4$ Hz), δ_H 1.53 (3H, *s*), δ_H 1.43 (3H, *d*, $J = 6.4$ Hz) and δ_H 1.37 (3H, *s*)] and one unit of $-C(Me_2)-CHCH_2-C(OMe)-CH=C-$ [δ_H 7.51 (1H, *d*, $J = 1.5$ Hz), δ_H 3.64 (3H, *s*), δ_H 2.64 (1H, *d*, $J = 9.6$ Hz), δ_H 2.34 (1H, *dd*, $J = 12.8$ and 1.5 Hz), δ_H 1.72 (1H, *dd*, $J = 12.8$ and 9.6 Hz), δ_H 1.71 and 1.29 (3H each, *s*)]. These signals were similar to those of **scortechinone B**. The minor difference between **DD15** and **scortechinone B** was as follows. The olefinic-proton signal [δ_H 5.20 (1H, *ht*, $J = 7.2$ and 1.5 Hz)] of the 3-methylbut-2-enyl group of **scortechinone B** was replaced by an oxymethine proton signal [δ_H 3.72 (1H, *dd*, $J = 11.2$ and 3.2 Hz)], indicating that the double-bond of the 3-methylbut-2-enyl group of **scortechinone B** was saturated by two hydroxyl groups to form 2,3-dihydroxy-3-methylbutyl unit [δ_H 3.72 (1H, *dd*, $J = 11.2$ and 3.2 Hz), δ_H 2.87 (1H, *dd*, $J = 14.0$ and 3.2 Hz), δ_H 2.65 (1H, *dd*, $J = 14.0$ and 11.2 Hz), δ_H 1.33 and 1.31 (3H each, *s*)] in **DD15**. The ^{13}C NMR (Figure 7) (Table 37), DEPT (Figure 8) and HMQC (Figure 13) spectra showed resonances for three carbonyl carbons (δ_C 203.00, 178.14 and 166.98), fourteen quarternary carbons (sp^2C : δ_C 167.68, 163.76, 154.70, 132.51, 129.55, 112.53, 101.79 and 101.31 ; sp^3C : δ_C 89.04, 85.11, 84.31, 83.45, 72.90 and

43.85), five methine carbons (sp^2C : δ_C 135.60 and 134.78; sp^3C : δ_C 92.34, 76.44 and 49.70), three methylene carbons (δ_C 30.34, 29.10 and 24.23) and nine methyl carbons (δ_C 53.80, 30.80, 28.85, 28.53, 26.44, 24.53, 21.12, 19.29 and 16.63). Comparison of their ^{13}C NMR spectrum showed that two signals of olefinic carbons in **scortechinone B** were substituted by two oxycarbon signals (δ_C 76.44 and 72.90). These confirmed that **DD15** had the 2,3-dihydroxy-3-methylbutyl unit instead of the 3-methylbut-2-enyl group. In the HMBC spectrum (Figure 14) (Table 37), the olefinic-proton H-8 (δ_H 7.51/ δ_C 134.78) showed 2J correlation with C-8a (δ_C 132.51) and 3J correlations with C-4b (δ_C 89.04), C-6 (δ_C 203.00) and C-9 (δ_C 178.14). The methylene proton H_a-10 (δ_H 2.34/ δ_C 30.34) caused 2J cross peaks with C-7 (δ_C 85.11) and C-11 (δ_C 49.70) and 3J cross peaks with C-4b, C-8 and C-12 (δ_C 83.45) while the methine proton H-11 (δ_H 2.64/ δ_C 49.70) gave 2J correlations with C-4b and C-10 and 3J correlations with C-5 (δ_C 84.31) and C-7. Data from the above HMBC correlations together with the value of ^{13}C chemical shift of C-4b established a bicyclo[2.2.2]octane ring bearing carbonyl and ether functionalities at C-8a and C-4b, respectively. Further HMBC correlations of two methyl groups (δ_H 1.71/ δ_C 30.80, Me-13 and δ_H 1.29/ δ_C 28.85, Me-14) to C-11 and C-12 suggested that a 2,2-dimethyltetrahydrofuran ring was fused to positions C-5 and C-11 of the bicyclooctane ring to form a tricyclodecane system. According to the chemical-shift values of C-5 and C-11, the oxygen atom of the tetrahydrofuran ring was located at C-5 rather than C-11. The methylene proton H_a-15 (δ_H 3.77/ δ_C 29.10) exhibited 2J correlations with C-5 and C-16 (δ_C 135.60) and 3J correlations with C-4b, C-6 and C-17 (δ_C 129.55), indicating the attachment of a 3-carboxybut-2-enyl group at C-5. The methoxy group (δ_H 3.64/ δ_C 53.80) was placed at C-7 according to a correlation between its protons with C-7; C-7 had correlations also with H_{ab}-10 and H-11. The structure of the left-hand part was thus determined as shown, which was

identical to that of **scortechinone B**. The 3J correlations of the chelated hydroxy proton (δ_{H} 13.16, 1-OH) with C-2 (δ_{C} 101.79) and C-9a (δ_{C} 101.31), the methylene protons $\text{H}_{\text{ab}}-25$ (δ_{H} 2.87 and 2.65/ δ_{C} 24.23) of the 2,3-dihydroxy-3-methylbutyl group with C-1 (δ_{C} 163.76) and C-3 (δ_{C} 167.68) and methyl protons [Me-23 (δ_{H} 1.37/ δ_{C} 28.53) and Me-24 (δ_{H} 1.53/ δ_{C} 19.29)] of the 2,3,3-trimethylhydrofuran ring with C-4 (δ_{C} 112.53) suggested that the right-hand part contained a phloroglucinol-type aromatic ring with a chelated hydroxyl group at C-1, a carbonyl group *peri* to the chelated hydroxy group, the 2,3-dihydroxy-3-methylbutyl group at C-2 and the 2,3,3-trimethylhydrofuran ring at C-3 and C-4. The chemical-shift values of C-3 and C-4 confirmed that the hydrofuran ring was fused to the aromatic ring by linkage of its *gem*-dimethyl carbon and ring oxygen atom with C-4 and C-3, respectively. The relative stereochemistry of **DD15** was established by the NOE difference results. Firstly, the signal of Me-18 (δ_{H} 1.62) was enhanced when the olefinic H-16 (δ_{H} 5.20) was irradiated (**Figure 12**), indicating that the double-bond configuration was *Z*. Secondly, the selective enhancement of $\text{H}_{\text{a}}-15$ and Me-22 (δ_{H} 1.43) signals by the irradiation of Me-24 (**Figure 10**) indicated that the C-5 carboxybutenyl group was located on the same side of the molecule as Me-24 and Me-22 ; the α -side in **DD15**. Finally, Me-13 showed selective NOE with H-11 and Me-14 (**Figure 11**) whereas Me-14 gave correlations with 7-OMe, $\text{H}_{\text{a}}-10$ and Me-13 (**Figure 9**). The structure of **DD15** was thus assigned to be **2**, a new caged-tetraprenylated xanthone with the 2,3-dihydroxy-3-methylbutyl group at C-2.

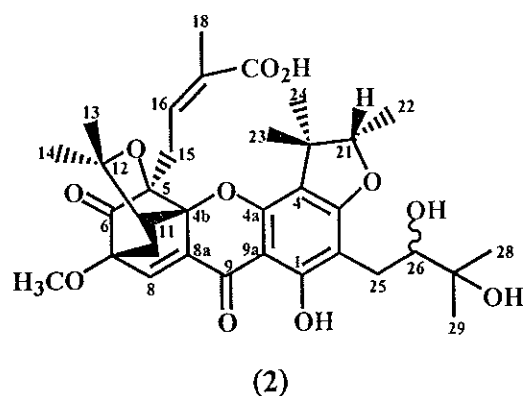


Table 37 The NMR data of compounds **DD15** and **scortechinone B**

Position	DD15		HMBC correlation	scortechinone B	
	$\delta_{\text{H}}(\text{mult.}, J_{\text{Hz}})$	$\delta_{\text{C}}(\text{C-Type})$		$\delta_{\text{H}}(\text{mult.}, J_{\text{Hz}})$	$\delta_{\text{C}}(\text{C-Type})$
1-OH	13.16 (<i>s</i>)	163.76 (C)	C-1, C-2, C-9a	13.10 (<i>s</i>)	163.46 (C)
2		101.79 (C)			105.81 (C)
3		167.68 (C)			167.08 (C)
4		112.53 (C)			112.30 (C)
4a		154.70 (C)			154.07 (C)
4b		89.04 (C)			89.38 (C)
5		84.31 (C)			83.77 (C)
6		203.00 (C=O)			202.30 (C=O)
7		85.11 (C)			84.93 (C)
8	7.51 (<i>d</i> , 1.5)	134.78 (CH)	C-4b, C-5, C-6, C-8a, C-9, C-11	7.56 (<i>d</i> , 1.2)	135.09 (CH)
8a		132.51 (C)			132.38 (C)
9		178.14 (C=O)			177.60 (C=O)
9a		101.31 (C)			101.27 (C)

Table 37 (Continued)

Position	DD15		HMBC correlation	scortechinone B	
	$\delta_{\text{H}}(\text{mult.}, J_{\text{Hz}})$	$\delta_{\text{C}}(\text{C-Type})$		$\delta_{\text{H}}(\text{mult.}, J_{\text{Hz}})$	$\delta_{\text{C}}(\text{C-Type})$
10	H _a : 2.34 (<i>dd</i> , 12.8, 1.5)	30.34 (CH ₂)	C-4b, C-7, C-8, C-11, C-12	2.33 (<i>dd</i> , 13.2, 1.2)	30.54 (CH ₂)
	H _b : 1.72 (<i>dd</i> , 12.8, 9.6)		C-6, C-7, C-8, C-12	1.68 (<i>dd</i> , 13.2, 9.2)	
11	2.64 (<i>d</i> , 9.6)	49.70 (CH)	C-4b, C-5, C-7, C-10	2.60 (<i>d</i> , 9.2)	49.75 (CH)
12		83.45 (C)			83.71 (C)
13	1.71 (<i>s</i>)	30.80 (CH ₃)	C-11, C-12, C-14	1.72 (<i>s</i>)	28.79 (CH ₃)
14	1.29 (<i>s</i>)	28.85 (CH ₃)	C-11, C-12, C-13	1.28 (<i>s</i>)	30.93 (CH ₃)
15	H _a : 3.77 (<i>dd</i> , 15.2, 11.6)	29.10 (CH ₂)	C-4b, C-5, C-6, C-16, C-17	3.27 (<i>brdd</i> , 16.0, 9.6)	29.91 (CH ₂)
	H _b : 2.71 (<i>md</i> , 15.2)			2.83 (<i>ddq</i> , 16.0, 4.5, 2.0)	
16	5.20 (<i>mdd</i> , 11.6, 1.5)	135.60 (CH)	C-18	5.67 (<i>ddq</i> , 9.6, 4.5, 1.5)	136.99 (CH)
17		129.55 (C)			128.68 (C)
18	1.62 (<i>dd</i> , 2.5, 1.5)	21.12 (CH ₃)	C-16, C-17, C-19	1.72 (<i>s</i>)	20.57 (CH ₃)
19		166.98 (C=O)			170.67 (C=O)
20		43.85 (C)			43.51 (C)
21	4.56 (<i>q</i> , 6.4)	92.34 (CH)	C-3, C-4, C-23, C-24	4.46 (<i>q</i> , 6.6)	91.40 (CH)
22	1.43 (<i>d</i> , 6.4)	16.63 (CH ₃)	C-20, C-21	1.23 (<i>d</i> , 6.6)	15.81 (CH ₃)

Table 37 (Continued)

Position	DD15		HMBC correlation	scortechinone B	
	$\delta_{\text{H}}(\text{mult.}, J_{\text{Hz}})$	$\delta_{\text{C}}(\text{C-Type})$		$\delta_{\text{H}}(\text{mult.}, J_{\text{Hz}})$	$\delta_{\text{C}}(\text{C-Type})$
23	1.37 (s)	28.53 (CH ₃)	C-4, C-20, C-21, C-24	1.37 (s)	28.53 (CH ₃)*
24	1.53 (s)	19.29 (CH ₃)	C-4, C-20, C-21, C-23	1.37 (s)	19.29 (CH ₃)*
25	H _a : 2.87 (dd, 14.0, 3.2) H _b : 2.65 (dd, 14.0, 11.2)	24.23 (CH ₂)	C-1, C-2, C-3, C-26 C-1, C-2, C-3	3.17 (mdd, 14.4, 7.2) 3.11 (mdd, 14.4, 7.2)	21.35 (CH ₂)
26	3.72 (dd, 11.2, 3.2)	76.44 (CH)	C-2, C-28, C-29	5.20 (ht, 7.2, 1.5)	121.69 (CH)
27		72.90 (C)			132.05 (C)
28	1.33 (s)	26.44 (CH ₃)	C-26, C-27, C-29	1.65 (q, 1.5)	25.66 (CH ₃)
29	1.31 (s)	24.53 (CH ₃)	C-26, C-27, C-28	1.72 (brs)	17.72 (CH ₃)
OMe	3.64 (s)	53.80 (CH ₃)	C-7	3.52 (s)	53.88 (CH ₃)

* interchangeable

3.3 Compound DD2

Compound DD2 was isolated as a yellow gum. It exhibited similar UV (Figure 16) and IR (Figure 17) spectra to those of DD13 (scortechinone B). The ¹H NMR spectrum (Figure 18) (Table 38) was similar to that of scortechinone B (a chelated hydroxy proton, a 3-methylbut-2-enyl group, a 2,3,3-trimethylhydrofuran unit and one

unit of $-\text{C}(\text{Me}_2)\text{-CHCH}_2\text{-C}(\text{OMe})\text{-CH}=\text{C}-$) except for the fact that the olefinic-proton H-16 [δ_{H} 6.40 (1H, *dd*, $J = 10.0$ and 5.6 Hz)] of the 3-carboxybut-2-enyl group attached to the tricyclodecane ring was shifted to lower field, suggesting that the H-16 and carboxyl group were *cis*. These was confirmed by direct comparison of the ^1H NMR spectrum of **DD2** and **PP9** previously isolated from latex of *Garcinia scortechinii* (Phainuphong, 2002). It was found that **DD2** gave identical spectral data to **PP9**. Therefore, **DD2** was identified as **PP9** (3).

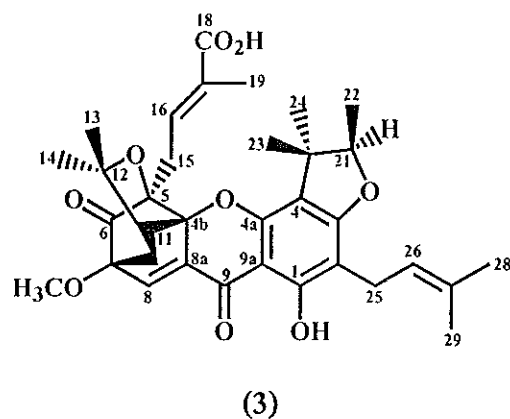


Table 38 The ^1H NMR data of compounds **DD2**, **PP9** and **scortechinone B**

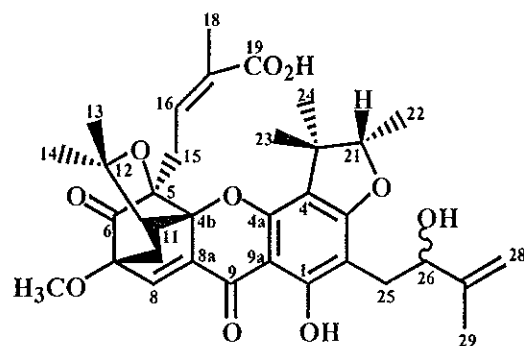
Position	DD2	PP9	scortechinone B
	δ_{H} (<i>mult.</i> , J_{Hz})	δ_{H} (<i>mult.</i> , J_{Hz})	δ_{H} (<i>mult.</i> , J_{Hz})
1-OH	13.09 (<i>s</i>)	13.10 (<i>s</i>)	13.10 (<i>s</i>)
8	7.60 (<i>s</i>)	7.61 (<i>d</i> , 1.0)	7.56 (<i>d</i> , 1.2)
10	2.34 (<i>d</i> , 12.8)	2.33 (<i>d</i> , 13.0)	2.33 (<i>dd</i> , 13.2, 1.2)
	1.68 (<i>dd</i> , 12.8, 9.6)	1.69 (<i>dd</i> , 13.0, 9.5)	1.68 (<i>dd</i> , 13.2, 9.2)
11	2.61 (<i>d</i> , 9.0)	2.61 (<i>d</i> , 9.5)	2.60 (<i>d</i> , 9.2)
13	1.73 (<i>s</i>)	1.72 (<i>s</i>)	1.72 (<i>s</i>)

Table 38 (Continued)

Position	DD2	PP9	scortechinone B
	δ_{H} (mult., J_{Hz})	δ_{H} (mult., J_{Hz})	δ_{H} (mult., J_{Hz})
14	1.29 (s)	1.29 (s)	1.28 (s)
15	2.80 (brdd, 14.8, 5.6)	2.79 (mdd, 15.0, 5.5)	3.27 (brdd, 16.0, 9.6)
	2.56 (dd, 14.8, 10.0)	2.56 (dd, 15.0, 10.0)	2.83 (ddq, 16.0, 4.5, 2.0)
16	6.40 (dd, 10.0, 5.6)	6.41 (ddq, 10.0, 5.5, 1.5)	5.67 (ddq, 9.6, 4.5, 1.5)
18			1.72 (s)
19	1.39 (s)	1.38 (s)	
21	4.54 (q, 6.8)	4.54 (q, 6.5)	4.46 (q, 6.6)
22	1.29 (d, 6.8)	1.29 (d, 6.5)	1.23 (d, 6.6)
23	1.41 (s)	1.41 (s)	1.37 (s)
24	1.47 (s)	1.46 (s)	1.37 (s)
25	3.20 (d, 6.8)	3.20 (d, 7.0)	3.17 (mdd, 14.4, 7.2)
			3.11 (mdd, 14.4, 7.2)
26	5.22 (brt, 6.8)	5.22 (mt, 7.0)	5.20 (ht, 7.2, 1.5)
28	1.68 (s)	1.67 (s)	1.65 (q, 1.5)
29	1.74 (s)	1.74 (s)	1.72 (brs)
OMe	3.63 (s)	3.63 (s)	3.52 (s)

3.4 Compound DD11

Compound **DD11** was obtained as a yellow gum. The caged-polyprenylated xanthone chromophore was evident by its UV (**Figure 19**) absorption bands at λ_{\max} 367 nm. The hydroxyl, unconjugated carbonyl, α,β -unsaturated carboxyl and chelated *ortho*-hydroxyl carbonyl stretching frequencies were found in the region of 3600-2500, 1742, 1683 and 1634 cm^{-1} , respectively in the IR spectrum (**Figure 20**). Its ^1H NMR spectrum (**Figure 21**) (**Table 39**) was very similar to that of **scortechinone B**. However, a substituent at C-2 on the phloroglucinol-type aromatic ring was different from that of **scortechinone B**. The characteristic signals of the olefinic methylene protons of a terminal double-bond [δ_{H} 5.08-5.07 and 4.94-4.92 (1H each, *m*)] instead of a signal for an olefinic proton of a 3-methylbut-2-enyl group and the hydroxymethine proton [δ_{H} 4.32 (1H, *brdd*, $J = 11.5$ and 3.5 Hz)] established the substituent to be a 2-hydroxy-3-methylbut-3-enyl group. Furthermore, the ^1H NMR data of **DD11** was compared with the previously reported data of **scortechinone C** (Rukachaisirikul, 2000a), indicating that **DD11** was **scortechinone C** (**4**).



(4)

Table 39 The ^1H NMR data of compounds **DD11**, **scortechinone C** and **scortechinone B**

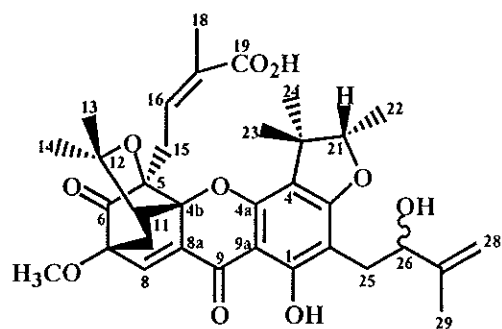
Position	DD11	scortechinone C	scortechinone B
	δ_{H} (mult., J_{Hz})	δ_{H} (mult., J_{Hz})	δ_{H} (mult., J_{Hz})
1-OH	13.16 (s)	13.15 (s)	13.10 (s)
8	7.52 (d, 1.0)	7.51 (d, 1.4)	7.56 (d, 1.2)
10	2.35 (md, 13.0)	2.35 (dd, 13.0, 1.4)	2.33 (dd, 13.2, 1.2)
	1.70 (dd, 13.0, 9.5)	1.70 (dd, 13.0, 9.3)	1.68 (dd, 13.2, 9.2)
11	2.63 (d, 9.5)	2.63 (d, 9.3)	2.60 (d, 9.2)
13	1.71 (s)	1.71 (s)	1.72 (s)
14	1.29 (s)	1.29 (s)	1.28 (s)
15	3.82 (dd, 15.5, 12.0)	3.81 (dd, 15.2, 11.8)	3.27 (brdd, 16.0, 9.6)
	2.72 (md, 15.5)	2.73 (ddq, 15.2, 3.4, 2.5)	2.83 (ddq, 16.0, 4.5, 2.0)
16	5.20 (md, 12.0)	5.20 (ddq, 11.4, 3.4, 1.4)	5.67 (ddq, 9.6, 4.5, 1.5)
18	1.64 (dd, 2.5, 1.5)	1.65 (dd, 2.5, 1.4)	1.72 (s)
21	4.57 (q, 6.5)	4.56 (q, 6.6)	4.46 (q, 6.6)
22	1.45 (d, 6.5)	1.45 (d, 6.6)	1.23 (d, 6.6)
23	1.38 (s)	1.37 (s)	1.37 (s)
24	1.56 (s)	1.56 (s)	1.37 (s)
25	2.99 (dd, 14.5, 3.5)	2.98 (dd, 14.0, 3.4)	3.17 (mdd, 14.4, 7.2)
	2.64 (dd, 14.5, 11.5)	2.64 (dd, 14.0, 11.1)	3.11 (mdd, 14.4, 7.2)
26	4.32 (brdd, 11.5, 3.5)	4.32 (brdd, 11.1, 3.4)	5.20 (ht, 7.2, 1.5)
28	5.08-5.07 (m)	5.08-5.07 (m)	1.65 (q, 1.5)
	4.94-4.92 (m)	4.93-4.92 (m)	

Table 39 (Continued)

Position	DD11	scortechinone C	scortechinone B
	δ_{H} (mult., $J_{\text{H:}}$)	δ_{H} (mult., $J_{\text{H:}}$)	δ_{H} (mult., $J_{\text{H:}}$)
29	1.87 (brs)	1.87-1.86 (m)	1.72 (brs)
OMe	3.66 (s)	3.65 (s)	3.52 (s)

3.5 Compound DD10

Compound **DD10** was isolated as a yellow gum. Its UV spectrum (**Figure 22**) (λ_{max} 366 nm) showed the presence of a caged-polyprenylated xanthone nucleus. Its IR spectrum (**Figure 23**) showed absorption bands at 3600-2500 (a hydroxyl group), 1744 (an unconjugated carbonyl group), 1687 (an α,β -unsaturated carbonyl group) and 1634 cm^{-1} (a chelated *ortho*-hydroxyl carbonyl group). The ^1H NMR (**Figure 24**) (**Table 40**) and ^{13}C NMR (**Figure 25**) (**Table 40**) spectra of **DD10** were almost (but not exactly) identical to those of **DD11** (**scortechinone C**), albeit for some minor differences in the 2-hydroxy-3-methylbut-3-enyl group. The oxymethine proton H-26 [δ_{H} 4.51 (1H, *dd*, $J = 11.0$ and 3.5 Hz)] was shift to upper field, indicating that **DD10** was the C-26 epimer of **scortechinone C**. This conclusion was confirmed by direct comparison of its ^1H and ^{13}C NMR data with those of **PP14** previously isolated from stem bark of *Garcinia scortechinii* (Phainuphong, 2002).



(5)

Table 40 The NMR data of compounds DD10, PP14 and scortechinone C

Position	DD10		PP14		scortechinone C	
	δ_{H} (mult., J_{Hz})	δ_{C}	δ_{H} (mult., J_{Hz})	δ_{C}	δ_{H} (mult., J_{Hz})	δ_{C}
1-OH	13.28 (s)	164.13		164.12	13.15 (s)	163.83
2		102.30		102.36		101.66
3		167.67		167.68		167.71
4		112.75		112.72		112.50
4a		155.02		155.00		155.49
4b		89.09		89.18		89.20
5		84.15		84.08		84.35
6		203.18		203.08		203.20
7		85.12		85.10		85.15
8	7.52 (d, 1.0)	134.67	7.52 (d, 1.3)	134.80	7.51 (d, 1.4)	134.79
8a		132.52		132.50		132.50
9		177.80		177.82		179.00
9a		101.31		101.32		101.38

Table 40 (Continued)

Position	DD10		PP14		scortechinone C	
	δ_{H} (mult., J_{Hz})	δ_{C}	δ_{H} (mult., J_{Hz})	δ_{C}	δ_{H} (mult., J_{Hz})	δ_{C}
10	2.31 (<i>md</i> , 12.5)	30.45	2.32 (<i>d</i> , 13.6)	30.44	2.35 (<i>dd</i> , 13.0, 1.4)	30.42
	1.71 (<i>dd</i> , 12.5, 9.5)		1.72 (<i>dd</i> , 13.6, 9.5)		1.70 (<i>dd</i> , 13.0, 9.3)	
11	2.64 (<i>d</i> , 9.5)	49.68	2.64 (<i>d</i> , 9.5)	49.69	2.64 (<i>d</i> , 9.3)	49.74
12		83.51		83.56		83.46
13	1.72 (<i>s</i>)	30.89	1.72 (<i>s</i>)	30.91	1.71 (<i>s</i>)	28.88
14	1.29 (<i>s</i>)	28.70	1.28 (<i>s</i>)	28.69	1.29 (<i>s</i>)	30.81
15	3.56 (<i>dd</i> , 15.5, 11.5)	28.82	3.51 (<i>dd</i> , 15.6, 10.4)	29.00	3.81 (<i>dd</i> , 15.2, 11.8)	29.07
	2.74 (<i>md</i> , 15.5)		2.75 (<i>md</i> , 15.6)		2.73 (<i>ddq</i> , 15.2, 3.4, 2.5)	
16	5.39 (<i>md</i> , 11.5)	135.64	5.43 (<i>md</i> , 10.4)	135.81	5.20 (<i>ddq</i> , 11.4, 3.4, 1.4)	135.65
17		129.64		129.45		129.58
18	1.67 (<i>dd</i> , 2.0, 1.5)	21.18	1.67 (<i>brs</i>)	21.09	1.65 (<i>dd</i> , 2.5, 1.4)	21.11
19		167.35		167.90		166.65
20		43.49		43.49		43.94
21	4.55 (<i>q</i> , 6.5)	92.12	4.55 (<i>q</i> , 6.6)	92.07	4.56 (<i>q</i> , 6.6)	92.43
22	1.38 (<i>d</i> , 6.5)	16.27	1.37 (<i>d</i> , 6.6)	16.19	1.45 (<i>d</i> , 6.6)	16.77
23	1.40 (<i>s</i>)	27.99	1.39 (<i>s</i>)	27.98	1.37 (<i>s</i>)	28.66
24	1.48 (<i>s</i>)	19.63	1.46 (<i>s</i>)	19.68	1.56 (<i>s</i>)	19.28
25	2.94 (<i>dd</i> , 14.5, 11.0)	28.42	2.92 (<i>dd</i> , 14.3, 10.8)	28.50	2.98 (<i>dd</i> , 14.0, 3.4)	28.80
	2.69 (<i>dd</i> , 14.5, 3.5)		2.68 (<i>dd</i> , 14.3, 3.0)		2.64 (<i>dd</i> , 14.0, 11.1)	

Table 40 (Continued)

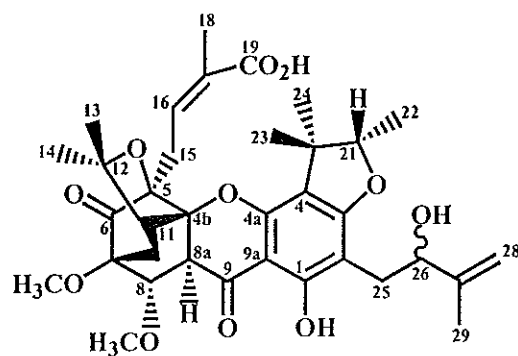
Position	DD10		PP14		scortechinone C	
	δ_{H} (mult., J_{Hz})	δ_{C}	δ_{H} (mult., J_{Hz})	δ_{C}	δ_{H} (mult., J_{Hz})	δ_{C}
26	4.51 (<i>dd</i> , 11.0, 3.5)	74.95	4.50 (<i>dd</i> , 10.8, 3.0)	74.88	4.32 (<i>brdd</i> , 11.1, 3.4)	73.72
27		147.12		147.13		146.84
28	5.06 (<i>brs</i>) 4.89(<i>brs</i>)	110.63	5.03 (<i>brs</i>) 4.88 (<i>brs</i>)	110.58	5.08-5.07 (<i>m</i>) 4.93- 4.92 (<i>m</i>)	110.32
29	1.85 (<i>s</i>)	18.28	1.84 (<i>brs</i>)	18.25	1.87 (<i>m</i>)	18.66
OMe	3.64 (<i>s</i>)	53.83	3.63 (<i>s</i>)	53.84	3.65 (<i>s</i>)	53.82

3.6 Compound DD14

Compound **DD14** was isolated as a yellow gum. The caged-polyprenylated xanthone chromophore was evident by its UV (**Figure 26**) absorption bands at λ_{max} 305 nm. The IR spectrum (**Figure 27**) showed absorption bands of a hydroxyl group at 3600-2500 cm^{-1} , an unconjugated carbonyl group at 1744 cm^{-1} , an α,β -unsaturated carboxyl group at 1687 cm^{-1} and a chelated *ortho*-hydroxyl carbonyl group at 1634 cm^{-1} . The ^1H NMR spectrum (**Figure 28**) (**Table 41**) was similar to that of **scortechinone C**, but a lowest-field signal for an olefinic proton [δ_{H} 7.51 (1H, *d*, $J = 1.4$ Hz)] was replaced by one methine proton [δ_{H} 3.20 (1H, *d*, $J = 1.5$ Hz)], one oxymethine proton [δ_{H} 4.47 (1H, *d*, $J = 1.5$ Hz)] and one methoxy group [δ_{H} 3.38 (3H, *s*)]. These data revealed that the C-8/C-8a double-bond of **scortechinone C** was saturated by addition of methanol. The methoxy group was attached to C-8 due to a

HMBC correlation (**Figure 37**) (**Table 41**) between the methoxy protons and C-8 (δ_C 75.11). The methine protons at δ_H 3.20 and 4.47 were attributed to H-8 and H-8a as the methine proton at δ_H 3.20 caused 2J cross peaks with C-4b (δ_C 87.13), C-8 and C-9 (δ_C 192.23) and 3J cross peaks with C-7 (δ_C 81.40) and C-11 (δ_C 45.29) whereas the methine proton at δ_H 4.47 showed 2J correlations with C-7 and C-8a (δ_C 48.91) and 3J correlations with C-4b, C-6 (δ_C 205.47), C-9 (δ_C 192.23) and C-10 (δ_C 30.34). H-8 (δ_H 4.47) showed selective NOE only with 7-OMe (δ_H 3.51) and H_b-10 (δ_H 1.64) (**Figure 34**), indicating that the H-8 was located on the same side as H_b-10, the β side, and *trans* to H-8a (δ_H 3.20). The HMBC data indicated that a 3-carboxybut-2-enyl group [δ_H 6.63 (1H, *mt*, $J = 7.0$ Hz), δ_H 3.23 and 3.15 (1H each, *mdd*, $J = 15.5$ and 7.0 Hz) and δ_H 1.97 (3H, *d*, $J = 1.5$ Hz)], a 2,3,3-trimethylhydrofuran unit [δ_H 4.42 (1H, *q*, $J = 6.5$ Hz), δ_H 1.44 and 1.12 (3H each, *s*) and δ_H 1.34 (3H, *d*, $J = 6.5$ Hz)], a 2-hydroxy-3-methylbut-3-enyl group [δ_H 4.99 and 4.84 (1H each, *brs*), δ_H 4.29 (1H, *dd*, $J = 8.5$ and 4.0 Hz), δ_H 2.88 (1H, *dd*, $J = 14.5$ and 4.0 Hz), δ_H 2.77 (1H, *dd*, $J = 14.5$ and 8.5 Hz) and δ_H 1.84 (3H, *s*)] and a methoxy group [δ_H 3.51 (3H, *s*)] were located at the same positions as those of **scortechinone C**. The relative stereochemistry of **DD14** was established by the NOE different results. Firstly, the signal of Me-18 (δ_H 1.97) was enhanced when the H-16 (δ_H 6.63) was irradiated (**Figure 35**), indicating that the double-bond configuration was *Z*. Secondly, the selective enhancement of the H_{ab}-15 (δ_H 3.22 and 3.15), Me-18 (δ_H 1.97), Me-22 (δ_H 1.34) and Me-23 (δ_H 1.44) signals by the irradiation at δ_H 1.12 (Me-24) (**Figure 31**) suggested that the C-5 carboxybutenyl group was located on the same side of the molecule as Me-22 and Me-24-the α -side in **DD14**. Thirdly, Me-13 (δ_H 1.43) showed selective NOE with Me-11 (δ_H 2.70) and Me-24 (δ_H 1.12) (**Figure 33**) whereas Me-14 (δ_H 1.22) gave correlation with 7-OMe (δ_H

3.51) and H_a -10 (δ_H 2.03) (Figure 32). The structure of **DD14** was thus assigned to be **6**, a new caged-tetraprenylated xanthone.



(6)

Table 41 The NMR data of compounds **DD14** and **scortechinone C**

Position	DD14		HMBC correlation	scortechinone C	
	δ_H (mult., J_H)	δ_C (C-Type)		δ_H (mult., J_H)	δ_C (C-Type)
1-OH	12.26 (<i>s</i>)	162.00 (C)	C-1, C-2, C-3	13.15 (<i>s</i>)	163.83 (C)
2		102.37 (C)			101.66 (C)
3		167.40 (C)			167.71 (C)
4		113.80 (C)			112.50 (C)
4a		152.69 (C)			155.49 (C)
4b		87.13 (C)			89.20 (C)
5		86.41 (C)			84.35 (C)
6		205.47 (C=O)			202.20 (C=O)
7		81.40 (C)			85.15 (C)
8	4.47 (<i>d</i> , 1.5)	75.11 (CH)	C-4b, C-6, C-7, C-8a, C-9, C-10, 8-OMe	7.51 (<i>d</i> , 1.4)	134.79 (CH)

Table 41 (Continued)

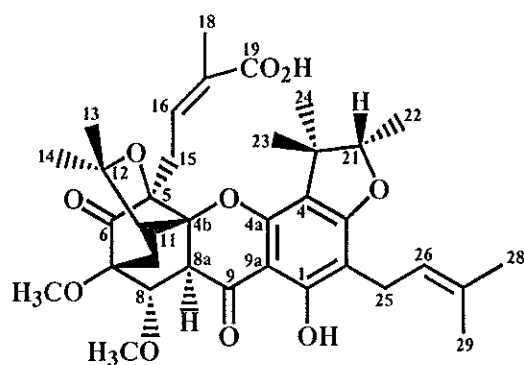
Position	DD14		HMBC correlation	scortechinone C	
	δ_{H} (mult., J_{H})	δ_{C} (C-Type)		δ_{H} (mult., J_{H})	δ_{C} (C-Type)
8a	3.20 (<i>d</i> , 1.5)	48.91 (CH)	C-4b, C-7, C-8, C-9, C-11		132.50 (C)
9		192.23 (C=O)			179.00 (C=O)
9a		102.51 (C)			101.38 (C)
10	H _a : 2.03 (<i>d</i> , 14.5)	23.93 (CH ₂)	C-4b, C-7, C-8, C-11, C-12	2.35 (<i>dd</i> , 13.0, 1.4)	30.42 (CH ₂)
	H _b : 1.64 (<i>dd</i> , 14.5, 8.5)		C-6, C-7, C-8, C-11, C-12	1.70 (<i>dd</i> , 13.0, 9.3)	
11	2.70 (<i>d</i> , 8.5)	45.29 (CH)	C-4b, C-7, C-10, C-13	2.64 (<i>d</i> , 9.3)	49.74 (CH)
12		82.64 (C)			83.46 (C)
13	1.43 (<i>s</i>)	30.48 (CH ₃)	C-11, C-12, C-14	1.71 (<i>s</i>)	28.88 (CH ₃)
14	1.22 (<i>s</i>)	27.17 (CH ₃)	C-10, C-11, C-12, C- 13	1.29 (<i>s</i>)	30.81 (CH ₃)
15	H _a : 3.23 (<i>mdd</i> , 15.5, 7.0)	28.46 (CH ₂)	C-5, C-6, C-16, C-17	3.81 (<i>dd</i> , 15.2, 11.8)	29.07 (CH ₂)
	H _b : 3.15 (<i>mdd</i> , 15.5, 7.0)		C-5, C-6, C-16, C-17	2.73 (<i>ddq</i> , 15.2, 3.4, 2.5)	
16	6.63 (<i>mt</i> , 7.0)	138.06 (CH)	C-5, C-18, C-19	5.20 (<i>ddq</i> , 11.4, 3.4, 1.4)	135.65 (CH)
17		128.02 (C)			129.58 (C)
18	1.97 (<i>d</i> , 1.5)	20.85 (CH ₃)	C-16, C-17, C-19	1.65 (<i>dd</i> , 2.5, 1.4)	21.11 (CH ₃)

Table 41 (Continued)

Position	DD14		HMBC correlation	scortechinone C	
	δ_{H} (mult., J_{H})	δ_{C} (C-Type)		δ_{H} (mult., J_{H})	δ_{C} (C-Type)
19		171.10 (C=O)			166.65 (C=O)
20		44.00 (C)			43.94 (C)
21	4.42 (<i>q</i> , 6.5)	90.50 (CH)	C-23, C-24	4.56 (<i>q</i> , 6.6)	92.43 (CH)
22	1.34 (<i>d</i> , 6.5)	13.85 (CH ₃)	C-20, C-21	1.45 (<i>d</i> , 6.6)	16.77 (CH ₃)
23	1.44 (<i>s</i>)	26.07 (CH ₃)	C-4, C-20, C-21, C-24	1.37 (<i>s</i>)	28.66 (CH ₃)
24	1.12 (<i>s</i>)	22.08 (CH ₃)	C-4, C-20, C-21, C-23	1.56 (<i>s</i>)	19.28 (CH ₃)
25	H _a : 2.88 (<i>dd</i> , 14.5, 4.0) H _b : 2.77 (<i>dd</i> , 14.5, 8.5)	29.26 (CH ₂)	C-1, C-2, C-3, C-26, C-27 C-1, C-2, C-3, C-26, C-27	2.98 (<i>mdd</i> , 14.0, 3.4) 2.64 (<i>mdd</i> , 14.0, 11.1)	28.80 (CH ₂)
26	4.29 (<i>dd</i> , 8.5, 4.0)	75.34 (CH)	C-25	4.32 (<i>brdd</i> , 11.1, 3.4)	73.72 (CH)
27		147.33 (C)			146.84 (C)
28	4.99 (<i>brs</i>) 4.84 (<i>brs</i>)	110.40 (CH ₂)	C-26, C-27, C-29 C-26, C-27, C-29	5.08-5.07 (<i>m</i>) 4.93-4.92 (<i>m</i>)	110.32 (CH ₂)
29	1.84 (<i>s</i>)	18.06 (CH ₃)	C-26, C-27, C-28	1.87 (<i>m</i>)	18.66 (CH ₃)
OMe	3.51 (<i>s</i>)	52.41 (CH ₃)	C-7	3.65 (<i>s</i>)	53.82 (CH ₃)
OMe	3.38 (<i>s</i>)	57.43 (CH ₃)	C-8		

3.7 Compound DD12

Compound **DD12** was obtained as a yellow gum. It exhibited similar UV (Figure 38) and IR (Figure 39) spectra to those of **DD14**. From the ^1H NMR data (Figure 40) (Table 42) indicated that the left-hand part was identical to that of **DD14**, but the substituent at C-2 on the phloroglucinol-type aromatic ring was different from that of **DD14**. The characteristic signals of olefinic methylene protons of a terminal double-bond [δ_{H} 4.99 and 4.84 (1H each, *brs*)] and an oxymethine proton [δ_{H} 4.29 (1H each, *dd*, $J = 8.5$ and 4.0 Hz)] were absent in **DD12** whereas the olefinic proton [δ_{H} 5.23 (1H, *mt*, $J = 7.0$ Hz)] and one additional methyl group were present. These revealed that the substituent at C-2 of **DD12** was a 3-methylbut-2-enyl group. Direct comparison of its ^1H NMR data with those of **PP8** previously isolated from latex of *Garcinia scortechinii* (Phainuphong, 2002) suggested that **DD12** had the same structure as **PP8** (7).



(7)

Table 42 The ^1H NMR data of compounds **DD12**, **PP8** and **DD14**

Position	DD12	PP8	DD14
	δ_{H} (mult., J_{Hz})	δ_{H} (mult., J_{Hz})	δ_{H} (mult., J_{Hz})
1-OH	12.07 (<i>s</i>)	12.08 (<i>s</i>)	12.26 (<i>s</i>)
8	4.47 (<i>d</i> , 0.5)	4.46 (<i>s</i>)	4.47 (<i>d</i> , 1.5)
8a	3.16 (<i>d</i> , 0.5)	3.16 (<i>s</i>)	3.20 (<i>d</i> , 1.5)
10	2.02 (<i>d</i> , 14.0)	2.02 (<i>d</i> , 14.2)	2.03 (<i>d</i> , 14.5)
	1.64 (<i>dd</i> , 14.0, 9.0)	1.63 (<i>dd</i> , 14.2, 8.8)	1.64 (<i>dd</i> , 14.5, 8.5)
11	2.71 (<i>d</i> , 9.0)	2.70 (<i>d</i> , 8.8)	2.70 (<i>d</i> , 8.5)
13	1.42 (<i>s</i>)	1.41 (<i>s</i>)	1.43 (<i>s</i>)
14	1.21 (<i>s</i>)	1.20 (<i>s</i>)	1.22 (<i>s</i>)
15	3.19 (<i>mdd</i> , 17.0, 7.5)	3.29-3.17 (<i>m</i>)	3.23 (<i>mdd</i> , 15.5, 7.0)
	3.07 (<i>mdd</i> , 17.0, 7.5)		3.15 (<i>mdd</i> , 15.5, 7.0)
16	6.57 (<i>mt</i> , 7.5)	6.62 (<i>qt</i> , 6.8, 1.5)	6.63 (<i>mt</i> , 7.0)
18	1.98 (<i>d</i> , 1.5)	1.98 (<i>d</i> , 1.5)	1.97 (<i>d</i> , 1.5)
21	4.41 (<i>q</i> , 6.5)	4.40 (<i>q</i> , 6.8)	4.42 (<i>q</i> , 6.5)
22	1.34 (<i>d</i> , 6.5)	1.34 (<i>d</i> , 6.8)	1.34 (<i>d</i> , 6.5)
23	1.44 (<i>s</i>)	1.43 (<i>s</i>)	1.44 (<i>s</i>)
24	1.12 (<i>s</i>)	1.10 (<i>s</i>)	1.12 (<i>s</i>)
25	3.22-3.21 (<i>m</i>)	3.26-3.17 (<i>m</i>)	2.88 (<i>dd</i> , 14.5, 4.0)
			2.77 (<i>dd</i> , 14.5, 8.5)
26	5.23 (<i>mt</i> , 7.0)	5.25 (<i>mt</i> , 7.0)	4.29 (<i>dd</i> , 8.5, 4.0)
28	1.69 (<i>d</i> , 1.0)	1.69 (<i>s</i>)	4.99 (<i>brs</i>)
			4.84 (<i>brs</i>)

Table 42 (Continued)

Position	DD12	PP8	DD14
	δ_{H} (mult., J_{Hz})	δ_{H} (mult., J_{Hz})	δ_{H} (mult., J_{Hz})
29	1.76 (brs)	1.76 (s)	1.84 (s)
OMe	3.50 (s)	3.50 (s)	3.51 (s)
OMe	3.38 (s)	3.36 (s)	3.38 (s)

3.8 Compound DD1

Compound **DD1** was isolated as a yellow gum. In the UV spectrum (**Figure 41**), the long wavelength absorption band at λ_{max} 362 nm indicated the presence of a caged-polyprenylated xanthone nucleus. The IR spectrum (**Figure 42**) exhibited absorption bands at 3432, 1742, 1635 cm^{-1} for hydroxyl, unconjugated carbonyl and chelated *ortho*-hydroxyl carbonyl functionalities, respectively. These indicated the absence of carboxyl group in **DD1**. Its ^1H NMR spectrum (**Figure 43**) (**Table 43**) was similar to that of **DD13** (**scortechinone B**) except for the presence of one additional methyl group. These suggested that the carboxyl group in **DD13** was replaced with the methyl group in **DD1**. The ^{13}C NMR spectrum (**Figure 44**) (**Table 43**) confirmed the above conclusion by the absence of one carbonyl carbon and the presence of one additional methyl carbon. Comparison of its ^1H NMR data with those of **scortechinone A** (Rukachaisirikul, 2000a) indicated that **DD1** had the same structure as **scortechinone A** (**8**).

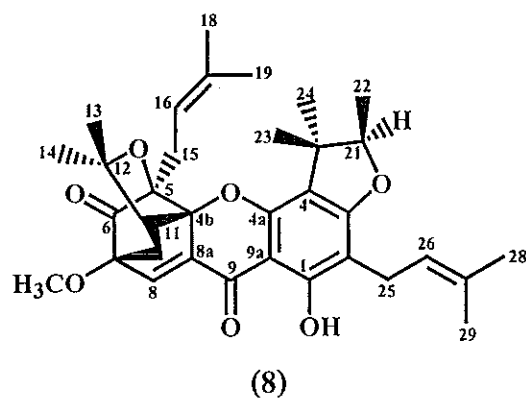


Table 43 The NMR data of compounds DD1, scortechinone A and scortechinone B

Position	DD1		scortechinone A		scortechinone B	
	δ_{H} (mult., J_{H_2})	δ_{C}	δ_{H} (mult., J_{H_2})	δ_{C}	δ_{H} (mult., J_{H_2})	δ_{C}
1-OH	13.19 (<i>s</i>)	163.25	13.15 (<i>s</i>)	163.26	13.10 (<i>s</i>)	163.46
2		105.75		105.77		105.81
3		166.82		166.87		167.08
4		113.04		113.03		112.30
4a		153.81		153.82		154.07
4b		89.27		89.30		89.38
5		84.17		84.19		83.77
6		202.31		202.26		202.30
7		84.89		84.90		84.93
8	7.51 (<i>d</i> , 1.5)	133.93	7.49 (<i>d</i> , 1.4)	133.96	7.56 (<i>d</i> , 1.2)	135.09
8a		132.38		132.38		132.38
9		178.23		178.23		179.60
9a		101.38		101.39		101.27

Table 43 (Continued)

Position	DD1		scortechinone A		scortechinone B	
	δ_{H} (mult., J_{Hz})	δ_{C}	δ_{H} (mult., J_{Hz})	δ_{C}	δ_{H} (mult., J_{Hz})	δ_{C}
10	2.33 (<i>brd</i> , 13.0)	30.84	2.33 (<i>dd</i> , 12.8, 1.4)	30.85	2.33 (<i>dd</i> , 13.2, 1.2)	30.54
	1.65 (<i>dd</i> , 13.0, 9.5)		1.65 (<i>dd</i> , 12.8, 9.6)		1.68 (<i>dd</i> , 13.2, 9.2)	
11	2.55 (<i>d</i> , 9.5)	49.91	2.55 (<i>d</i> , 9.6)	49.94	2.60 (<i>d</i> , 9.2)	49.75
12		83.26		83.23		83.71
13	1.71 (<i>s</i>)	29.00	1.71 (<i>s</i>)	28.97	1.72 (<i>s</i>)	28.79
14	1.29 (<i>s</i>)	30.78	1.29 (<i>s</i>)	30.78	1.28 (<i>s</i>)	30.93
15	2.69 (<i>md</i> , 14.5)	28.93	2.69 (<i>ddh</i> , 14.4, 4.5, 1.5)	28.93	3.27 (<i>brdd</i> , 16.0, 9.6)	29.91
	2.56 (<i>dd</i> , 14.5, 10.5)		2.55 (<i>dd</i> , 14.4, 10.5)		2.83 (<i>ddq</i> , 16.0, 4.5, 2.0)	
16	4.41-4.37 (<i>m</i>)	117.16	4.41-4.37 (<i>m</i>)	117.17	5.67 (<i>ddq</i> , 9.6, 4.5, 1.5)	136.99
		135.64		135.55	128.68	
18	1.06 (<i>brs</i>)	25.51	1.07 (<i>bri</i> , 1.4)	25.47	1.72 (<i>s</i>)	20.57
19	1.36 (<i>brs</i>)	16.87	1.36 (<i>bri</i> , 1.5)	16.87		170.67
20		43.47		43.47		43.50
21	4.37 (<i>q</i> , 6.5)	90.61	4.37 (<i>q</i> , 6.4)	90.61	4.46 (<i>q</i> , 6.6)	91.40
22	1.41 (<i>d</i> , 6.5)	13.59	1.41 (<i>d</i> , 6.4)	13.57	1.23 (<i>q</i> , 6.6)	15.81
23	1.16 (<i>s</i>)	21.09	1.16 (<i>s</i>)	21.07	1.37 (<i>s</i>)	19.95*
24	1.58 (<i>s</i>)	24.05	1.58 (<i>s</i>)	24.06	1.37 (<i>s</i>)	28.09*

Table 43 (Continued)

Position	DD1		scortechinone A		scortechinone B	
	δ_{H} (mult., J_{Hz})	δ_{C}	δ_{H} (mult., J_{Hz})	δ_{C}	δ_{H} (mult., J_{Hz})	δ_{C}
25	3.22 (<i>bri</i> , 7.0)	21.42	3.22 (<i>md</i> , 7.2)	21.42	2.98 (<i>mdd</i> , 14.4, 7.2) 3.11 (<i>mdd</i> , 14.4, 7.2)	21.35
26	5.22 (<i>mt</i> , 7.0)	121.74	5.22 (<i>ht</i> , 7.2, 1.4)	121.75	5.20 (<i>ht</i> , 7.2, 1.5)	121.69
27		132.05		131.98		132.05
28	1.68 (<i>brd</i> , 1.0)	25.74	1.68 (<i>brq</i> , 1.2)	25.70	1.65 (<i>q</i> , 1.5)	25.66
29	1.75 (<i>s</i>)	17.76	1.75 (<i>brd</i> , 1.2)	17.73	1.72 (<i>s</i>)	17.72
OMe	3.63 (<i>s</i>)	53.97	3.63 (<i>s</i>)	53.94	3.52 (<i>s</i>)	53.88

* interchangeable

3.9 Compound DD3

Compound **DD3** was obtained as a yellow gum. The UV spectrum (**Figure 45**) (λ_{max} 360 nm) indicated the presence of a caged-polyprenylated xanthone nucleus while its IR spectrum (**Figure 46**) exhibited absorption bands at 3453 (a hydroxyl group), 1741 (an unconjugated carbonyl group) and 1646 (a chelated *ortho*-hydroxyl carbonyl group) cm^{-1} . The mass spectrum (**Figure 57**) showed the molecular ion peak at m/z 562 for a molecular formula of $\text{C}_{34}\text{H}_{42}\text{O}_7$. Its ^1H NMR spectrum (**Figure 47**) (**Table 44**) was similar to that of **scortechinone A**, containing typical signals of a chelated hydroxy proton [δ_{H} 12.65 (1-OH, *s*)], 9 tertiary methyl groups and four

proton-coupled systems : two units belonging to 3-methylbut-2-enyl groups [δ_{H} 5.32 (1H, *mt*, $J = 6.5$ Hz), δ_{H} 3.29 (1H, *ddd*, $J = 15.0$ and 6.5 Hz), δ_{H} 3.21 (1H, *ddd*, $J = 15.0$ and 6.5 Hz), δ_{H} 1.71 and 1.68 (3H each, *s*) ; δ_{H} 4.40 (1H, *mt*, $J = 7.5$ Hz), δ_{H} 2.59 (2H, *d*, $J = 7.5$ Hz), δ_{H} 1.36 and 0.96 (3H each, *brs*)], one unit of 2,3,3-trimethylhydrofuran ring [δ_{H} 4.46 (1H, *q*, $J = 6.5$ Hz), δ_{H} 1.45 (3H, *s*), δ_{H} 1.37 (3H, *d*, $J = 6.5$ Hz) and δ_{H} 1.21 (3H, *s*)] and one unit of $-\text{C}(\text{Me})_2\text{-CHCH}_2\text{-C}(\text{OMe})\text{-CH}=\text{C}$ [δ_{H} 7.47 (1H, *d*, $J = 1.5$ Hz), δ_{H} 3.64 (3H, *s*), δ_{H} 2.53 (1H, *d*, $J = 9.5$ Hz), δ_{H} 2.34 (1H, *d*, $J = 14.0$ Hz), δ_{H} 1.68 (3H, *s*), δ_{H} 1.63 (1H, *dd*, $J = 14.0$ and 9.5 Hz) and δ_{H} 1.30 (3H, *s*)]. The difference was found in the phoroglucinol-type aromatic ring. One of the 3-methylbut-2-enyl groups was located at C-4 (δ_{C} 103.72), due to the methylene protons H_{ab}-25 (δ_{H} 3.29 and 3.21) showed cross peaks with the C-3 (δ_{C} 166.61), C-4 and C-4a (δ_{C} 158.40) in the HMBC spectrum (Figure 56) (Table 44). These indicated that the 2,3,3-trimethylhydrofuran ring was located at C-2 (δ_{C} 114.58) and C-3. The correlations between Me-23 (δ_{H} 1.45) and Me-24 (δ_{H} 1.21) with C-2 confirmed the position of the furan ring. The chemical shifts of C-2 and C-3 indicated the furan ring formed an ether linkage with C-3, not C-2. In addition, other substituted groups were attached to the same position as found in scortechinone A by the HMBC data. The relative stereochemistry of **DD3** was established by the NOE different results. Firstly, Me-18 (δ_{H} 1.36) and Me-28 (δ_{H} 1.68) were assigned since they gave selective enhancement with H-16 (δ_{H} 4.40) (Figure 53) and H-26 (δ_{H} 5.32) (Figure 54), respectively. Secondly, Me-22 (δ_{H} 1.37) showed selective NOE with H-16 (δ_{H} 4.40), Me-19 (δ_{H} 0.96) and Me-24 (δ_{H} 1.68) (Figure 51), suggesting that the C-5 isoprenyl group was located on the same side of the molecule as Me-22 and Me-24-the α -side in **DD3**. Finally, Me-13 (δ_{H} 1.68) showed selective NOE with H-11 (δ_{H} 2.53) and Me-14 (δ_{H} 1.30) (Figure 52) whereas Me-14 (δ_{H} 1.30) gave correlations with Me-13 (δ_{H}

1.68), H_a-10 (δ_{H} 2.34) and 7-OMe (δ_{H} 3.64) (Figure 50). The structure of DD3 was thus assigned to be **9**, a new caged-tetraprenylated xanthone.

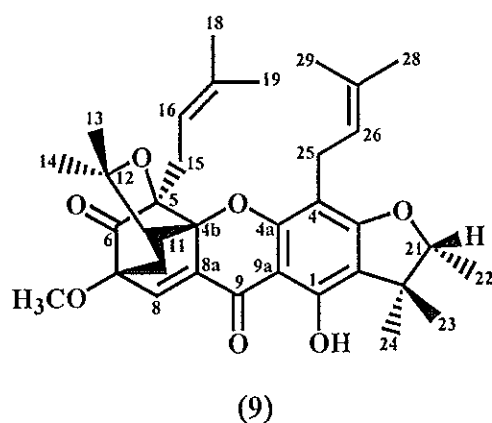


Table 44 The NMR data of compounds DD3 and scortechinone A

Position	DD3		HMBC correlation	scortechinone A	
	δ_{H} (mult., J_{Hz})	δ_{C} (C-Type)		δ_{H} (mult., J_{Hz})	δ_{C} (C-Type)
1-OH	12.65 (<i>s</i>)	158.24 (C)	C-1, C-2, C-9a	13.15 (<i>s</i>)	163.26 (C)
2		114.58 (C)			105.77 (C)
3		166.61 (C)			166.87 (C)
4		103.72 (C)			113.03 (C)
4a		158.40 (C)			153.82 (C)
4b		84.27 (C)			89.30 (C)
5		89.09 (C)			84.19 (C)
6		202.08 (C=O)			202.26 (C=O)
7		84.80 (C)			84.90 (C)
8	7.47 (<i>d</i> , 1.5)	133.52 (CH)	C-5, C-6, C-9	7.49 (<i>d</i> , 1.4)	133.96 (CH)
8a		132.67 (C)			132.38 (C)

Table 44 (Continued)

Position	DD3		HMBC correlation	scortechinone A	
	δ_{H} (mult., J_{H})	δ_{C} (C-Type)		δ_{H} (mult., J_{H})	δ_{C} (C-Type)
9		178.93 (C=O)			178.23 (C=O)
9a		101.53 (C)			101.39 (C)
10	H_a : 2.34 (<i>brd</i> , 14.0) H_b : 1.63 (<i>dd</i> , 14.0, 9.5)	30.20 (CH ₂)	C-5, C-6, C-7, C-8, C- 11, C-12	2.33 (<i>dd</i> , 12.8, 1.4) 1.65 (<i>dd</i> , 12.8, 9.6)	30.85 (CH ₂)
11	2.53 (<i>d</i> , 9.5)	49.72 (CH)	C-4b, C-5, C-10	2.55 (<i>d</i> , 9.6)	49.94 (CH)
12		83.57 (C)			83.23 (C)
13	1.68 (<i>s</i>)	30.09 (CH ₃)	C-11, C-12, C-14	1.71 (<i>s</i>)	28.97 (CH ₃)
14	1.30 (<i>s</i>)	29.03 (CH ₃)	C-11, C-12, C-13	1.29 (<i>s</i>)	30.78 (CH ₃)
15	2.59 (<i>d</i> , 7.5)	28.89 (CH ₂)	C-4b, C-5, C-6, C-16, C-17	2.69 (<i>ddh</i> , 14.4, 4.5, 1.5) 2.55 (<i>dd</i> , 14.4, 10.5)	28.93 (CH ₂)
16	4.40 (<i>mt</i> , 7.5)	117.59 (CH)	C-19	4.41-4.37 (<i>m</i>)	117.17 (CH)
17		135.28 (C)			135.55 (C)
18	1.36 (<i>s</i>)	14.38 (CH ₃)	C-16, C-17, C-19	1.07 (<i>brt</i> , 1.4)	25.47 (CH ₃)
19	0.96 (<i>s</i>)	16.53 (CH ₃)	C-16, C-17	1.36 (<i>brt</i> , 1.5)	16.87 (CH ₃)
20		43.51 (C)			43.47 (C)
21	4.46 (<i>q</i> , 6.5)	90.77 (CH)	C-23, C-24	4.37 (<i>q</i> , 6.4)	90.61 (CH)

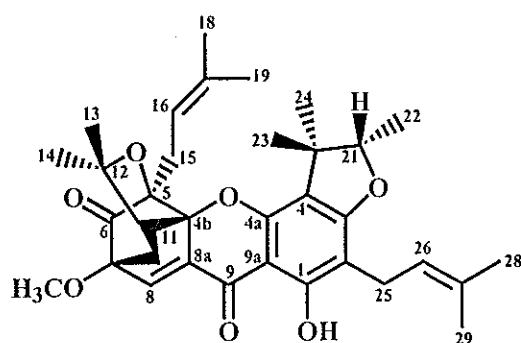
Table 44 (Continued)

Position	DD3		HMBC correlation	scortechinone A	
	δ_{H} (mult., J_{H})	δ_{C} (C-Type)		δ_{H} (mult., J_{H})	δ_{C} (C-Type)
22	1.37 (<i>d</i> , 6.5)	25.55 (CH ₃)	C-20, C-21	1.41 (<i>d</i> , 6.4)	13.57 (CH ₃)
23	1.45 (<i>s</i>)	25.26 (CH ₃)	C-2, C-20, C-21, C-24	1.16 (<i>s</i>)	21.07 (CH ₃)
24	1.21 (<i>s</i>)	20.64 (CH ₃)	C-2, C-20, C-21, C-23	1.58 (<i>s</i>)	24.06 (CH ₃)
25	3.29 (<i>mdd</i> , 15.0, 6.5)	22.10 (CH ₂)	C-3, C-4, C-4a, C-26, C-27	3.22 (<i>md</i> , 7.2)	21.42 (CH ₂)
	3.21 (<i>mdd</i> , 15.0, 6.5)		C-3, C-4, C-4a, C-26, C-27		
26	5.32 (<i>mt</i> , 6.5)	121.76 (CH)	C-28, C-29	5.22 (<i>ht</i> , 7.2, 1.4)	121.75 (CH)
27		132.37 (C)			131.98 (C)
28	1.68 (<i>brs</i>)	25.71 (CH ₃)	C-26, C-27, C-29	1.68 (<i>brq</i> , 1.2)	25.70 (CH ₃)
29	1.71 (<i>brs</i>)	17.96 (CH ₃)	C-26, C-27, C-28	1.75 (<i>brd</i> , 1.2)	17.73 (CH ₃)
OMe	3.64 (<i>s</i>)	53.94 (CH ₃)	C-7	3.63 (<i>s</i>)	53.94 (CH ₃)

3.10 Compound DD5

Compound **DD5** was isolated as a yellow gum. Its UV spectrum (**Figure 58**) (λ_{max} 364 nm) showed the presence of a caged-polyprenylated xanthone nucleus. Its IR spectrum (**Figure 59**) exhibited absorption bands at 3444 (a hydroxyl group), 1745 (an unconjugated carbonyl group) and 1635 cm^{-1} (a chelated *ortho*-hydroxyl carbonyl group). The ^1H NMR spectrum (**Figure 60**) (**Table 45**) of **DD5** was almost (but not exactly) identical to that of **scortechinone A**, albeit for some minor differences in the

2,3,3-trimethylhydrofuran ring. The methine proton H-21 [δ_{H} 4.54 (1H, *q*, $J = 6.5$ Hz)] was shifted to lower field, indicating that **DD5** was the C-21 epimer of **scortechinone A**. The same coupled systems found in **scortechinone A**, viz. the 2,3,3-trimethylhydrofuran ring, two 3-methylbut-2-enyl groups and $-\text{C}(\text{Me})_2-\text{CHCH}_2-\text{C}(\text{OMe})-\text{CH}=\text{C}-$ system were also present in **DD5**. To confirm the conclusion, the ^1H NMR data of **DD5** was compared with those of **GF3** which was previously isolated from the fruits of *Garcinia scortechinii* (Sukpondma, 2002), indicating that **DD5** had the same structure as **GF3** (**10**), a new caged-tetraprenylated xanthone.



(10)

Table 45 The ^1H NMR data of compounds **DD5**, **GF3** and **scortechinone A**

Position	DD5	GF3	scortechinone A
	δ_{H} (<i>mult.</i> , J_{Hz})	δ_{H} (<i>mult.</i> , J_{Hz})	δ_{H} (<i>mult.</i> , J_{Hz})
1-OH	13.24 (<i>s</i>)	13.24 (<i>s</i>)	13.15 (<i>s</i>)
8	7.51 (<i>d</i> , 1.5)	7.51 (<i>d</i> , 1.5)	7.49 (<i>d</i> , 1.4)
10	2.34 (<i>brd</i> , 12.5)	2.34 (<i>d</i> , 13.5)	2.33 (<i>dd</i> , 12.8, 1.4)
	1.66 (<i>dd</i> , 12.5, 9.5)	1.67 (<i>dd</i> , 13.5, 9.5)	1.65 (<i>dd</i> , 12.8, 9.6)
11	2.58 (<i>d</i> , 9.5)	2.57 (<i>d</i> , 9.5)	2.55 (<i>d</i> , 9.6)

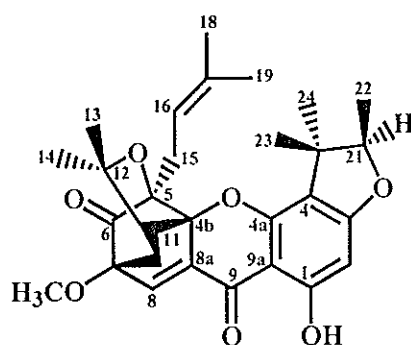
Table 45 (Continued)

Position	DD5	GF3	scortechinone A
	δ_{H} (mult., J_{Hz})	δ_{H} (mult., J_{Hz})	δ_{H} (mult., J_{Hz})
13	1.71 (s)	1.72 (s)	1.71 (s)
14	1.29 (s)	1.29 (s)	1.29 (s)
15	2.67 (md, 14.0)	2.67 (md, 14.5)	2.69 (ddh, 14.4, 4.5, 1.5)
	2.54 (dd, 14.0, 10.5)	2.54 (dd, 14.5, 10.5)	2.55 (dd, 14.4, 10.5)
16	4.36 (md, 10.5)	4.36 (md, 10.5)	4.41-4.37 (m)
18	1.36 (s)	1.36 (s)	1.07 (brt, 1.4)
19	1.02 (s)	1.02 (s)	1.36 (brt, 1.5)
21	4.54 (q, 6.5)	4.55 (q, 6.5)	4.37 (q, 6.4)
22	1.29 (d, 6.5)	1.30 (d, 6.5)	1.41 (d, 6.4)
23	1.41 (s)	1.42 (s)	1.16 (s)
24	1.49 (s)	1.49 (s)	1.58 (s)
25	3.22 (d, 7.0)	3.22 (d, 7.0)	3.22 (md, 7.2)
26	5.22 (mt, 7.0)	5.23 (mt, 7.0)	5.22 (ht, 7.2, 1.4)
28	1.68 (d, 1.0)	1.68 (d, 1.0)	1.68 (brq, 1.2)
29	1.75 (s)	1.76 (s)	1.75 (brd, 1.2)
OMe	3.64 (s)	3.64 (s)	3.63 (s)

3.11 Compound DD8

Compound DD8 was obtained as a yellow solid, melting at 180-181°C. The UV spectrum (Figure 61) (λ_{max} 360 nm) showed the presence of a caged-polyprenylated

xanthone chromophore. Its IR spectrum (Figure 62) exhibited absorption bands at 3422, 1742 and 1640 cm^{-1} for hydroxyl, unconjugated carbonyl, chelated *ortho*-hydroxyl carbonyl functionalities, respectively. The ^1H NMR spectrum (Figure 63) (Table 46) was similar to that of DD1 (scortechinone A) except for the replacement of signals of a 3-methylbut-2-enyl group with a signal of an aromatic proton [δ_{H} 6.04 (1H, *s*)] in DD8. Comparison of the ^1H NMR data of DD8 with those of PP3 previously isolated from latex of *Garcinia scortechinii* (Phainuphong, 2002) indicated that DD8 was PP3 (11).



(11)

Table 46 The ^1H NMR data of compounds DD8, PP3 and scortechinone A

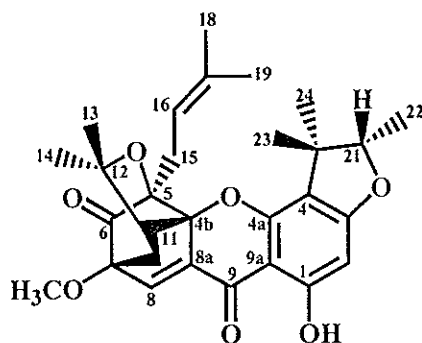
Position	DD8	PP3	scortechinone A
	δ_{H} (<i>mult.</i> , J_{Hz})	δ_{H} (<i>mult.</i> , J_{Hz})	δ_{H} (<i>mult.</i> , J_{Hz})
1-OH	13.03 (<i>s</i>)	13.03 (<i>s</i>)	13.15 (<i>s</i>)
2	6.04 (<i>s</i>)	6.04 (<i>s</i>)	
8	7.52 (<i>d</i> , 1.5)	7.52 (<i>d</i> , 1.5)	7.49 (<i>d</i> , 1.4)
10	2.36 (<i>d</i> , 13.0)	2.36 (<i>d</i> , 13.0)	2.33 (<i>dd</i> , 12.8, 1.4)
	1.66 (<i>dd</i> , 13.0, 9.5)	1.66 (<i>dd</i> , 13.0, 9.5)	1.65 (<i>dd</i> , 12.8, 9.6)

Table 46 (Continued)

Position	DD8	PP3	scortechinone A
	δ_{H} (mult., J_{Hz})	δ_{H} (mult., J_{Hz})	δ_{H} (mult., J_{Hz})
11	2.59 (<i>d</i> , 9.5)	2.59 (<i>d</i> , 9.5)	2.55 (<i>d</i> , 9.6)
13	1.72 (<i>s</i>)	1.72 (<i>s</i>)	1.71 (<i>s</i>)
14	1.30 (<i>s</i>)	1.30 (<i>s</i>)	1.29 (<i>s</i>)
15	2.70 (<i>md</i> , 14.5)	2.71 (<i>md</i> , 14.5)	2.69 (<i>ddh</i> , 14.4, 4.5, 1.5)
	2.58 (<i>dd</i> , 14.5, 11.0)	2.58 (<i>dd</i> , 14.5, 10.5)	2.55 (<i>dd</i> , 14.4, 10.5)
16	4.30-4.37 (<i>m</i>)	4.42-4.36 (<i>m</i>)	4.41-4.37 (<i>m</i>)
18	1.38 (<i>brs</i>)	1.38 (<i>s</i>)	1.07 (<i>brt</i> , 1.4)
19	1.09 (<i>s</i>)	1.09 (<i>s</i>)	1.36 (<i>brt</i> , 1.5)
21	4.40 (<i>q</i> , 6.5)	4.40 (<i>q</i> , 6.5)	4.37 (<i>q</i> , 6.4)
22	1.41 (<i>d</i> , 6.5)	1.41 (<i>d</i> , 6.5)	1.41 (<i>d</i> , 6.4)
23	1.17 (<i>s</i>)	1.17 (<i>s</i>)	1.16 (<i>s</i>)
24	1.59 (<i>s</i>)	1.59 (<i>s</i>)	1.58 (<i>s</i>)
25			3.22 (<i>md</i> , 7.2)
26			5.22 (<i>ht</i> , 7.2, 1.4)
28			1.68 (<i>brq</i> , 1.2)
29			1.75 (<i>brd</i> , 1.2)
OMe	3.64 (<i>s</i>)	3.64 (<i>s</i>)	3.63 (<i>s</i>)

3.12 Compound DD9

Compound **DD9** was isolated as a yellow solid, melting at 186-187°C. Its UV spectrum (**Figure 64**) (λ_{max} 361 nm) indicated the presence of a caged-polyprenylated xanthone nucleus while the IR spectrum (**Figure 65**) showed absorption bands at 3443 (a hydroxyl group), 1742 (an unconjugated carbonyl group) and 1640 (a chelated *ortho*-hydroxyl carbonyl group) cm^{-1} . Its ^1H NMR spectrum (**Figure 66**) (**Table 47**) was almost (but not exactly) identical to that of **DD8** (**PP3**), albeit for some minor differences in the 2,3,3-trimethylhydrofuran ring. The methine proton H-21 [δ_{H} 4.55 (1H, *q*, $J = 6.5$ Hz)] was shifted to lower field, indicating that **DD9** was the C-21 epimer of **DD8**. The same coupled systems found in **DD8**, *viz.* the 2,3,3-trimethylhydrofuran ring, 3-methylbut-2-enyl groups and $-\text{C}(\text{Me})_2-\text{CHCH}_2-\text{C}(\text{OMe})-\text{CH}=\text{C}-$ system were also present in **DD9**. To confirm the conclusion, the ^1H NMR data of **DD9** was compared with those of **PP4** which was previously isolated from latex of *Garcinia scortechinii* (Phainuphong, 2002), indicating that **DD9** had the same structure as **PP4** (**12**).

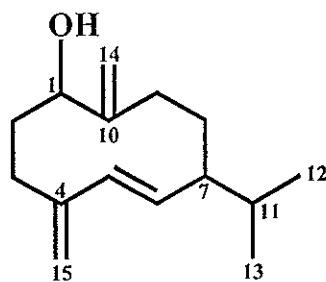


(12)

Table 47 The ^1H NMR data of compounds DD9, PP4 and DD8

Position	DD9	PP4	DD8
	δ_{H} (mult., J_{Hz})	δ_{H} (mult., J_{Hz})	δ_{H} (mult., J_{Hz})
1-OH	13.09 (s)	13.09 (s)	13.03 (s)
2	6.04 (s)	6.03 (s)	6.04 (s)
8	7.53 (d, 1.5)	7.52 (d, 1.0)	7.52 (d, 1.5)
10	2.36 (md, 13.0)	2.36 (dd, 13.0, 1.0)	2.36 (d, 13.0)
	1.67 (dd, 13.0, 9.5)	1.67 (dd, 13.0, 9.5)	1.66 (dd, 13.0, 9.5)
11	2.61 (d, 9.5)	2.61 (d, 9.5)	2.59 (d, 9.5)
13	1.72 (s)	1.72 (s)	1.72 (s)
14	1.29 (s)	1.29 (s)	1.30 (s)
15	2.69 (md, 14.5)	2.68 (md, 14.5)	2.70 (md, 14.5)
	2.55 (dd, 14.5, 10.5)	2.55 (dd, 14.5, 11.0)	2.58 (dd, 14.5, 11.0)
16	4.36 (md, 10.5)	4.36 (md, 11.0)	4.30-4.37 (m)
18	1.38 (brs)	1.38 (s)	1.38 (s)
19	1.07 (brs)	1.07 (s)	1.09 (s)
21	4.55 (q, 6.5)	4.55 (q, 6.5)	4.40 (q, 6.5)
22	1.30 (d, 6.5)	1.30 (d, 6.5)	1.41 (d, 6.5)
23	1.42 (s)	1.42 (s)	1.17 (s)
24	1.50 (s)	1.49 (s)	1.59 (s)
OMe	3.65 (s)	3.64 (s)	3.64 (s)

The HMBC correlations (Table 48) as shown supported the proposed substructure. Furthermore, the selected HMBC correlations (Figure 73) (Table 48) of the oxymethine proton H-1 and the methylene protons H_{ab}-9 with C-10 (δ_{H} 153.49) and C-14 (δ_{H} 110.57) suggested that C-10 linked C-1 with C-9 to form as 10-membered ring. The correlations of H-11 (δ_{H} 1.53-1.46) with Me-12 (δ_{H} 0.89) and Me-13 (δ_{H} 0.82), in the ^1H - ^1H COSY spectrum, indicated the presence of isopropyl group [δ_{H} 1.53-1.46 (1H, *m*), δ_{H} 0.89 and 0.82 (1H each, *d*, $J = 6.5$ Hz)]. Both Me-12 and Me-13 showed correlations with C-7 (δ_{C} 52.50) and C-11 (δ_{C} 31.82), in the HMBC spectrum, indicating that the isopropyl group was located at C-7. Since none of other proton signals was observed in the ^1H NMR spectrum, the oxysubstituted group at C-1 was a hydroxyl group. Comparison of its ^1H NMR data with those of **germacra-4(15), 5*E*, 10(14)-trien-1-ol (13)** previously isolated from leaves of *Glycosmis petelotii* (Cuòng, 1999) indicated that **DD7** had the same structure as **13**.



(13)

Table 48 The NMR data of compound DD7

Position	δ_{H} (mult., J_{Hz})	δ_{C} (C-Type)	HMBC correlation	^1H - ^1H COSY correlation
1	3.78 (<i>dd</i> , 12.0, 4.0)	76.03 (CH)	C-10, C-14	H _{ab} -2
2	2.08-2.05 (<i>m</i>)	36.27 (CH ₂)	C-1, C-10	H-1, H _{ab} -3
	1.73-1.58 (<i>m</i>)		C-1, C-3, C-10	H-1, H _{ab} -3
3	H _a : 2.44 (<i>dt</i> , 13.0, 5.0)	29.93 (CH ₂)	C-2, C-4, C-5, C-15	H _{ab} -2, H _b -3, H _a -15
	H _b : 2.20 (<i>ddd</i> , 13.0, 5.0, 2.5)		C-1, C-2, C-4, C-5	H _{ab} -2, H _a -3
4		146.72 (C)		
5	6.00 (<i>d</i> , 16.5)	129.61 (CH)	C-3, C-4, C-7, C-15	H-6, H _{ab} -15
6	5.44 (<i>dd</i> , 16.5, 10.5)	137.97 (CH)	C-4, C-7, C-8, C-11	H-5, H-7
7	1.83-1.77 (<i>m</i>)	52.50 (CH)		H-6, H _a -8
8	H _a : 2.03-2.01 (<i>m</i>)	36.17 (CH ₂)	C-1, C-6, C-10	H-7, H _b -8, H _{ab} -9
	H _b : 1.73-1.58 (<i>m</i>)		C-1, C-10	H _a -8
9	H _a : 2.65-2.61 (<i>m</i>)	34.52 (CH ₂)	C-10, C-14	H-7, H _a -8, H _b -9
	H _b : 1.68-1.60 (<i>m</i>)		C-1, C-7, C-10, C-14	H-7, H _a -8, H _a -9
10		153.49 (C)		
11	1.53-1.46 (<i>m</i>)	31.82 (CH)	C-13	H-12, H-13
12	0.89 (<i>d</i> , 6.5)	20.75 (CH ₃)	C-7, C-11, C-13	H-11
13	0.82 (<i>d</i> , 6.5)	20.49 (CH ₃)	C-7, C-11, C-12	H-11
14	H _a : 5.28 (<i>s</i>)	110.57 (CH ₂)	C-1, C-9	
	H _b : 5.00 (<i>d</i> , 2.0)		C-1, C-9, C-10	

Table 48 (Continued)

Position	δ_{H} (mult., J_{Hz})	δ_{C} (C-Type)	HMBC correlation	^1H - ^1H COSY correlation
15	H _a : 4.93 (<i>d</i> , 1.0)	112.91 (CH ₂)	C-3, C-5	H _a -3, H-5
	H _b : 4.85 (<i>s</i>)		C-3, C-5	H-5

Table 49 The NMR data of compounds DD7 and germacra-4(15), 5*E*, 10(14)-trien-1-ol

Position	DD7		germacra-4(15), 5 <i>E</i> , 10(14)-trien-1-ol	
	δ_{H} (mult., J_{Hz})	δ_{C} (C-Type)	δ_{H} (mult., J_{Hz})	δ_{C} (C-Type)
1	3.78 (<i>dd</i> , 12.0, 4.0)	76.03 (CH)	3.77 (<i>dd</i> , 11.8, 3.9)	76.0 (CH)
2	2.08-2.05 (<i>m</i>)	36.27 (CH ₂)	2.04 (<i>m</i>)	36.2 (CH ₂)
	1.73-1.58 (<i>m</i>)		1.73-1.58 (<i>m</i>)	
3	2.44 (<i>dt</i> , 13.0, 5.0)	29.93 (CH ₂)	2.43 (<i>td</i> , 13.0, 4.8)	29.9 (CH ₂)
	2.20 (<i>ddd</i> , 13.0, 5.0, 2.5)		2.19 (<i>m</i>)	
4		147.72 (C)		153.5 (C)
5	6.00 (<i>d</i> , 16.5)	129.61 (CH)	6.00 (<i>d</i> , 15.8)	129.6 (CH)
6	5.44 (<i>dd</i> , 16.5, 10.5)	137.97 (CH)	5.43 (<i>dd</i> , 15.8, 10.3)	137.9 (CH)
7	1.83-1.77 (<i>m</i>)	52.50 (CH)	1.78 (<i>m</i>)	52.5 (CH)
8	2.03-2.01 (<i>m</i>)	36.17 (CH ₂)	2.04 (<i>m</i>)	36.2 (CH ₂)
	1.73-1.58 (<i>m</i>)		1.67 (<i>m</i>)	
9	2.65-2.61 (<i>m</i>)	34.52 (CH ₂)	2.62 (<i>ddt</i> , 9.3, 3.2, 2.0)	34.5 (CH ₂)
	1.68-1.60 (<i>m</i>)		1.67 (<i>m</i>)	

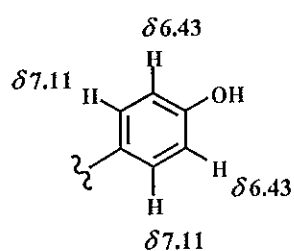
Table 49 (Continued)

Position	DD7		germacra-4(15), 5E, 10(14)-trien-1-ol	
	δ_{H} (mult., J_{Hz})	δ_{C} (C-Type)	δ_{H} (mult., J_{Hz})	δ_{C} (C-Type)
10		153.49 (C)		146.7 (C)
11	1.53-1.46 (m)	31.82 (CH)	1.49 (sextet, 6.6)	31.8 (CH)
12	0.89 (d, 6.5)	20.75 (CH ₃)	0.90 (d, 6.6)	20.7 (CH ₃)
13	0.82 (d, 6.5)	20.49 (CH ₃)	0.82 (d, 6.6)	20.5 (CH ₃)
14	5.28 (s)	110.57 (CH ₂)	5.27 (m)	110.5 (CH ₂)
	5.00 (d, 2.0)		5.00 (m)	
15	4.93 (d, 1.0)	112.91 (CH ₂)	4.92 (m)	112.8 (CH ₂)
	4.85 (s)		4.84 (m)	

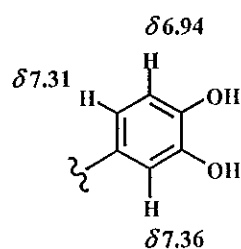
3.14 Compound DD16

Compound **DD16** was obtained as a yellow solid, decomposed at 210°C. In the UV spectrum (Figure 75), the absorption bands at λ_{max} 228, 273, 290 and 343 nm were similar to those of biflavones isolated from *Garcinia livingstonii* (Pelter, 1971). Its IR spectrum (Figure 76) exhibited absorptions band at 3419 and 1634 cm^{-1} for hydroxyl and chelated *ortho*-hydroxyl carbonyl functionalities, respectively. The ¹H NMR spectrum (Figure 77) (Table 50) revealed the presence of 1,4-disubstituted benzene [δ_{H} 7.11 and 6.34 (2H each, *d*, $J = 8.5$ Hz)] (unit A), 1,3,4-trisubstituted benzene [δ_{H} 7.36 (1H, *d*, $J = 2.0$ Hz), δ_{H} 7.31 (1H, *dd*, $J = 8.5$ and 2.0 Hz) and δ_{H} 6.94 (1H, *d*, $J = 8.5$ Hz)] (unit B), the flavanone derivative with a 1,2,3,5-tetrasubstituted benzene ring of unit C [δ_{H} 5.99 and 5.98 (1H each, *d*, $J = 1.5$ Hz), δ_{H} 5.75 (1H, *d*, $J = 12.0$ Hz,

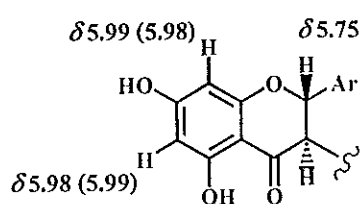
showing *trans*-coupling with the vicinal proton which appeared underneath a water peak at δ_{H} 4.85] and the flavone derivative [δ_{H} 6.44 and 6.28 (1H each, *s*)] (**unit D**).



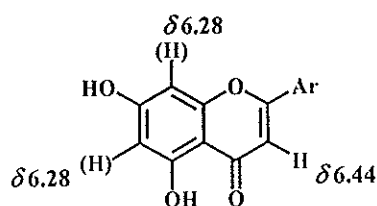
(unit A)



(unit B)

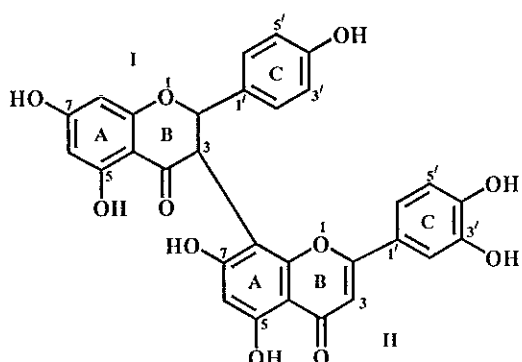


(unit C)

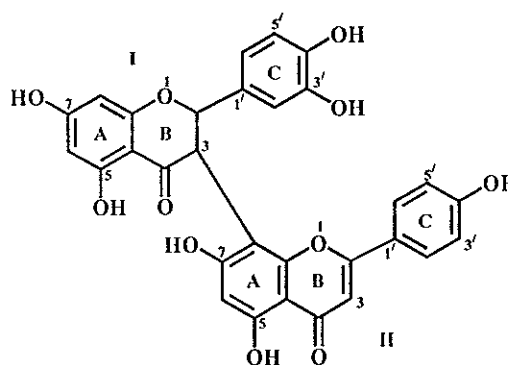


(unit D)

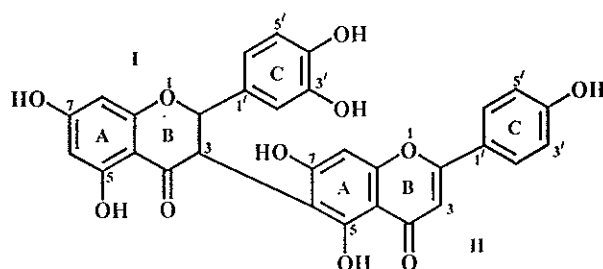
Since the aromatic protons of **unit A**, **B**, **C** and **D** were observed at high field, the benzene rings were substituted by hydroxyl groups. Comparison of its ^1H NMR data with those of **morelloflavone** (**14**) (Waterman and Cricnton, 1980) and **I-5**, **II-5**, **I-7**, **II-7**, **I-3'**, **I-4'**, **II-4'**-heptahydroxy-[**I-3,II-8**]-flavanonylflavone (**15**) (Babu, 1988) revealed that the chemical shift values of *ortho*-aromatic protons (δ_{H} 7.11 and 6.43) on *p*-hydroxylated benzene (**unit A**) and *meta*-aromatic protons (δ_{H} 7.36 and 7.31) on 3,4-dihydroxylated benzene (**unit B**) were more similar to that of **15** than that of **14**. These indicated that the structures of **DD16** were either **15** or **16** of which their structure is different in the position of attachment between the flavone and flavanone units.



(14)



(15)



(16)

Additionally, the comparison of its TLC chromatogram with that of **15** obtained from the twigs of *Garcinia scortechinii* (Kaewnok, 1999) indicated that **DD16** had the structure **15** with *trans* relative stereochemistry at C-2 and C-3 of the ring B of flavanone unit because of the large coupling constant value ($J_{H2-H3} = 12.0$ Hz) between H-2 and H-3.

Table 50 The ^1H NMR data of compounds **DD16**, morelloflavone (**14**) and **I-5**, **II-5**, **I-7**, **II-7**, **I-3'**, **I-4'**, **II-4'**-heptahydroxy-[**I-3**,**II-8**]-flavanonylflavone (**15**)

Position	DD16	Position	14	Position	15
	δ_{H} (mult., J_{Hz}) ^a		δ_{H} (mult., J_{Hz}) ^b		δ_{H} (mult., J_{Hz}) ^c
I-2	5.75 (<i>d</i> , 12.0)	I-2	5.73 (<i>d</i> , 12.0)	I-2	5.64 (<i>d</i> , 12.0)
I-3		I-3	4.86 (<i>d</i> , 12.0)	I-3	4.83 (<i>d</i> , 12.0)
I-6	5.98 (<i>d</i> , 1.5) [*]	I-6	5.97 (<i>s</i>)	I-6	5.91 (<i>s</i>)
I-8	5.99 (<i>d</i> , 1.5) [*]	I-8	5.97 (<i>s</i>)	I-8	5.91 (<i>s</i>)
I-2'	7.36 (<i>d</i> , 2.0)	I-2', I-6'	7.08 (<i>d</i> , 9.0)	I-2', I-6'	7.37 (<i>m</i>)
I-5'	6.94 (<i>d</i> , 8.5)	I-3', I-5'	6.50 (<i>d</i> , 9.0)	I-5'	6.84 (<i>d</i> , 8.0)
I-6'	7.31 (<i>dd</i> , 8.5, 2.0)				
II-3	6.44 (<i>s</i>)	II-3	6.43 (<i>s</i>)	II-3	6.53 (<i>s</i>)
II-6	6.28 (<i>s</i>)	II-6	6.20 (<i>s</i>)	II-6	6.17 (<i>s</i>)
II-2', II-6'	7.11 (<i>d</i> , 8.5)	II-2'	7.72 (<i>d</i> , 2.0)	II-2', II-6'	7.08 (<i>d</i> , 8.0)
II-3', II-5'	6.43 (<i>d</i> , 8.5)	II-5'	6.80 (<i>d</i> , 9.0)	II-3', II-5'	6.32 (<i>d</i> , 8.0)
		II-6'	7.19 (<i>dd</i> , 9.0, 2.0)		

^a ^1H NMR data of DD16 in CD_3OD .

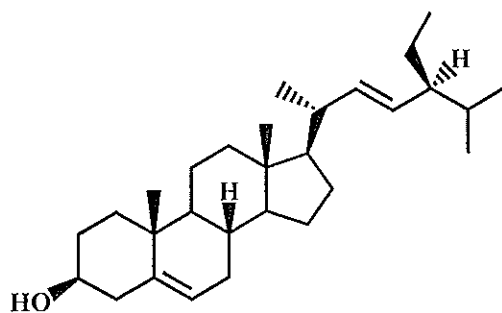
^b ^1H NMR data of morelloflavone in d_6 -DMSO.

^c ^1H NMR data of **I-5**, **II-5**, **I-7**, **II-7**, **I-3'**, **I-4'**, **II-4'**-heptahydroxy-[**I-3**,**II-8**]-flavanonylflavone in d_6 -DMSO.

^{*} interchangeable

3.15 Compound DD4

Compound **DD4** was obtained as a white solid, melting at 162-163°C. The IR spectrum (**Figure 78**) exhibited absorption band at 3443 cm^{-1} for a hydroxyl group. The ^1H NMR spectrum (**Figure 79**) (**Table 51**) indicated the presence of one primary methyl group [δ_{H} 0.80 (3H, *t*, $J = 7.5$ Hz)], three secondary methyl groups [δ_{H} 1.01 (3H, *d*, $J = 7.5$ Hz), δ_{H} 0.84 (3H, *d*, $J = 7.0$ Hz) and δ_{H} 0.79 (3H, *d*, $J = 7.5$ Hz)], two tertiary methyl groups [δ_{H} 1.00 and 0.69 (3H each, *s*)] and one oxymethine proton [δ_{H} 3.54-3.50 (1H, *m*)]. Additionally, the presence of three olefinic protons [δ_{H} 5.36-5.33 (1H, *m*), δ_{H} 5.15 (1H, *dd*, $J = 15.0$ and 8.5 Hz) and δ_{H} 5.02 (1H, *dd*, $J = 15.0$ and 8.5 Hz)] indicated that it contained one *trans*-disubstituted double-bond and one trisubstituted double-bond. The ^1H NMR data were compared with the previously reported data of **stigmasterol** (Kaewnok, 1999). It was found that **DD4** gave identical spectral data as **stigmasterol**. It was therefore identified as **stigmasterol** (17).



(17)

Table 51 The ^1H NMR data of compound **DD4** and stigmasterol

DD4	stigmasterol
δ_{H} (mult., J_{H_2})	δ_{H} (mult., J_{H_2})
5.36-5.33 (<i>m</i> , 1H)	5.36-5.33 (<i>m</i> , 1H)
5.15 (<i>dd</i> , $J = 15.0$ and 8.5 , 1H)	5.15 (<i>dd</i> , $J = 12.3$ and 6.7 , 1H)
5.02 (<i>dd</i> , $J = 15.0$ and 8.5 , 1H)	5.03 (<i>dd</i> , $J = 12.3$ and 6.7 , 1H)
3.54-3.50 (<i>m</i> , 1H)	3.56-3.48 (<i>m</i> , 1H)
2.28 (<i>ddd</i> , $J = 13.0$, 5.0 and 1.5 , 1H)	2.29 (<i>ddd</i> , $J = 12.3$, 6.0 and 2.1 , 1H)
2.24 (<i>qd</i> , $J = 11.0$ and 2.0 , 1H)	2.24 (<i>qd</i> , $J = 10.8$ and 2.1 , 1H)
2.07-1.93 (<i>m</i> , 3H)	2.09-1.94 (<i>m</i> , 3H)
1.86-1.80 (<i>m</i> , 2H)	1.88-1.80 (<i>m</i> , 2H)
1.74-1.66 (<i>m</i> , 1H)	1.75-1.66 (<i>m</i> , 1H)
1.56-1.39 (<i>m</i> , 11H)	1.60-1.39 (<i>m</i> , 11H)
1.30-1.04 (<i>m</i> , 5H)	1.31-1.04 (<i>m</i> , 5H)
1.01 (<i>d</i> , $J = 7.0$, 3H)	1.02 (<i>d</i> , $J = 6.7$, 3H)
1.00 (<i>s</i> , 3H)	1.01 (<i>s</i> , 3H)
0.98-0.90 (<i>m</i> , 2H)	1.00-0.90 (<i>m</i> , 2H)
0.84 (<i>d</i> , $J = 7.0$, 3H)	0.85 (<i>d</i> , $J = 6.7$, 3H)
0.80 (<i>t</i> , $J = 7.5$, 3H)	0.81 (<i>t</i> , $J = 7.1$, 3H)
0.79 (<i>d</i> , $J = 7.5$, 3H)	0.80 (<i>d</i> , $J = 6.5$, 3H)
0.69 (<i>s</i> , 3H)	0.70 (<i>s</i> , 3H)

3.16 Compound DD6

Compound **DD6** was obtained as a white solid, melting at 240-241 °C. The IR spectrum (**Figure 80**) exhibited absorption band at 1713 cm^{-1} for a carbonyl group. Its ^1H NMR data (**Figure 81**) (**Table 52**) were compared with the previously reported data of **friedelin** (Kaewnok, 1999). It was found that **DD6** gave identical spectral data as **friedelin**. It was therefore identified as **friedelin** (**18**).

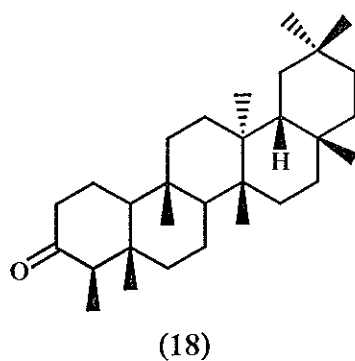


Table 52 The ^1H NMR data of compound **DD6** and **friedelin**

DD6	friedelin
δ_{H} (<i>mult.</i> , J_{Hz})	δ_{H} (<i>mult.</i> , J_{Hz})
2.40 (<i>ddd</i> , $J = 14.0, 5.0$ and 2.0 , 1H)	2.40 (<i>ddd</i> , $J = 13.6, 4.8$ and 1.6 , 1H)
2.31 (<i>ddd</i> , $J = 13.0, 7.0$ and 1.5 , 1H)	2.30 (<i>dd</i> , $J = 12.8$ and 6.4 , 1H)
2.25 (<i>q</i> , $J = 7.0$, 1H)	2.25 (<i>q</i> , $J = 7.2$, 1H)
2.00-1.94 (<i>m</i> , 1H)	2.00-1.94 (<i>m</i> , 1H)
1.76 (<i>md</i> , $J = 13.0$, 1H)	1.78 (<i>md</i> , $J = 12.8$, 1H)
1.69 (<i>dq</i> , $J = 13.0$ and 5.0 , 1H)	1.69 (<i>dq</i> , $J = 12.8$ and 1.6 , 1H)
1.60-1.20 (<i>m</i> , 20H)	1.60-1.20 (<i>m</i> , 20H)

Table 52 (Continued)

DD6	friedelin
δ_{H} (mult., J_{Hz})	δ_{H} (mult., J_{Hz})
1.18 (s, 3H)	1.18 (s, 3H)
1.05 (s, 3H)	1.06 (s, 3H)
1.01 (s, 3H)	1.02 (s, 3H)
1.00 (s, 3H)	1.01 (s, 3H)
0.95 (s, 3H)	0.96 (s, 3H)
0.89 (d, $J = 6.5$, 3H)	0.89 (d, $J = 7.2$, 3H)
0.87 (s, 3H)	0.87 (s, 3H)
0.73 (s, 3H)	0.73 (s, 3H)

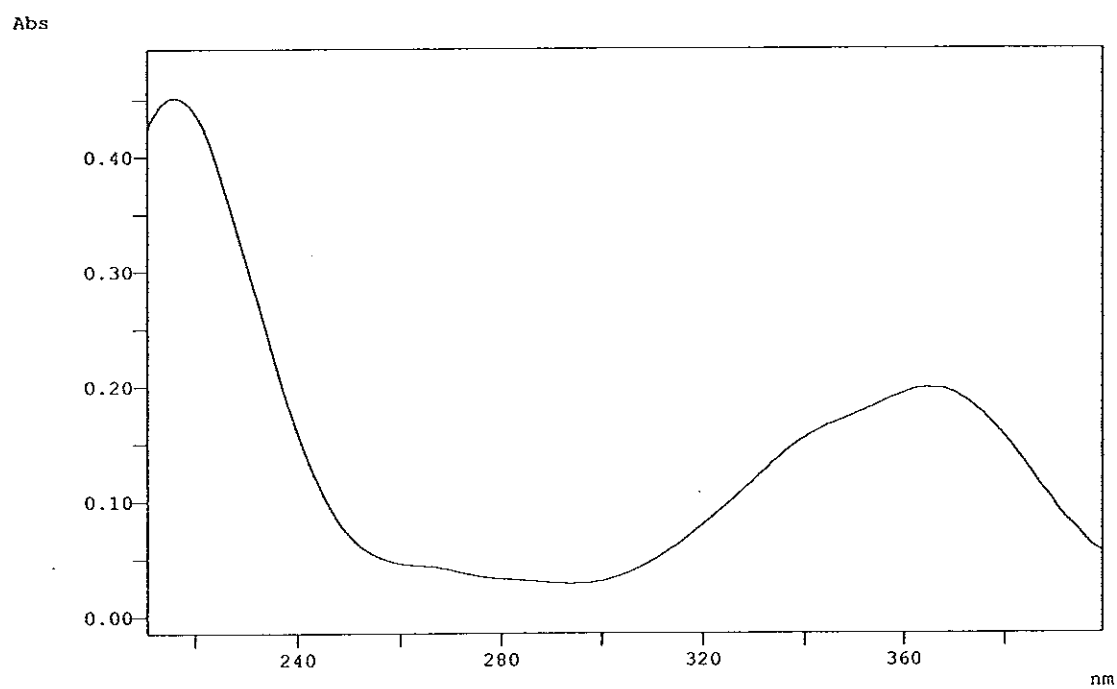


Figure 1 UV (MeOH) spectrum of DD13

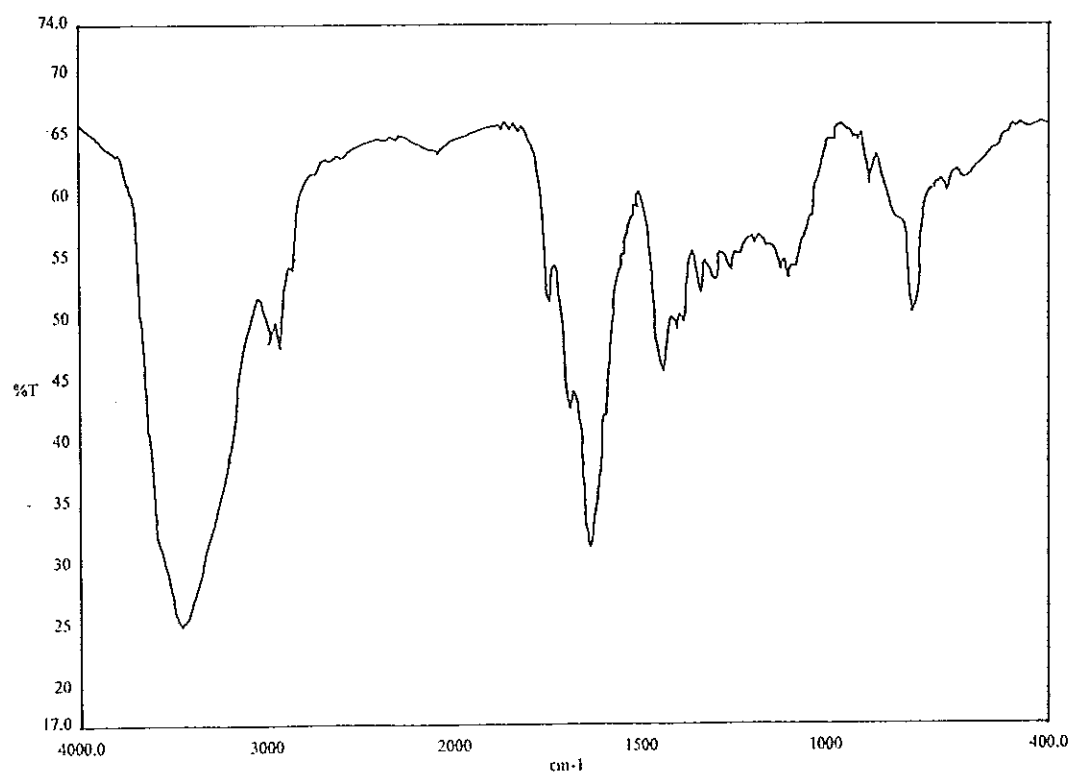


Figure 2 FT-IR (neat) spectrum of DD13

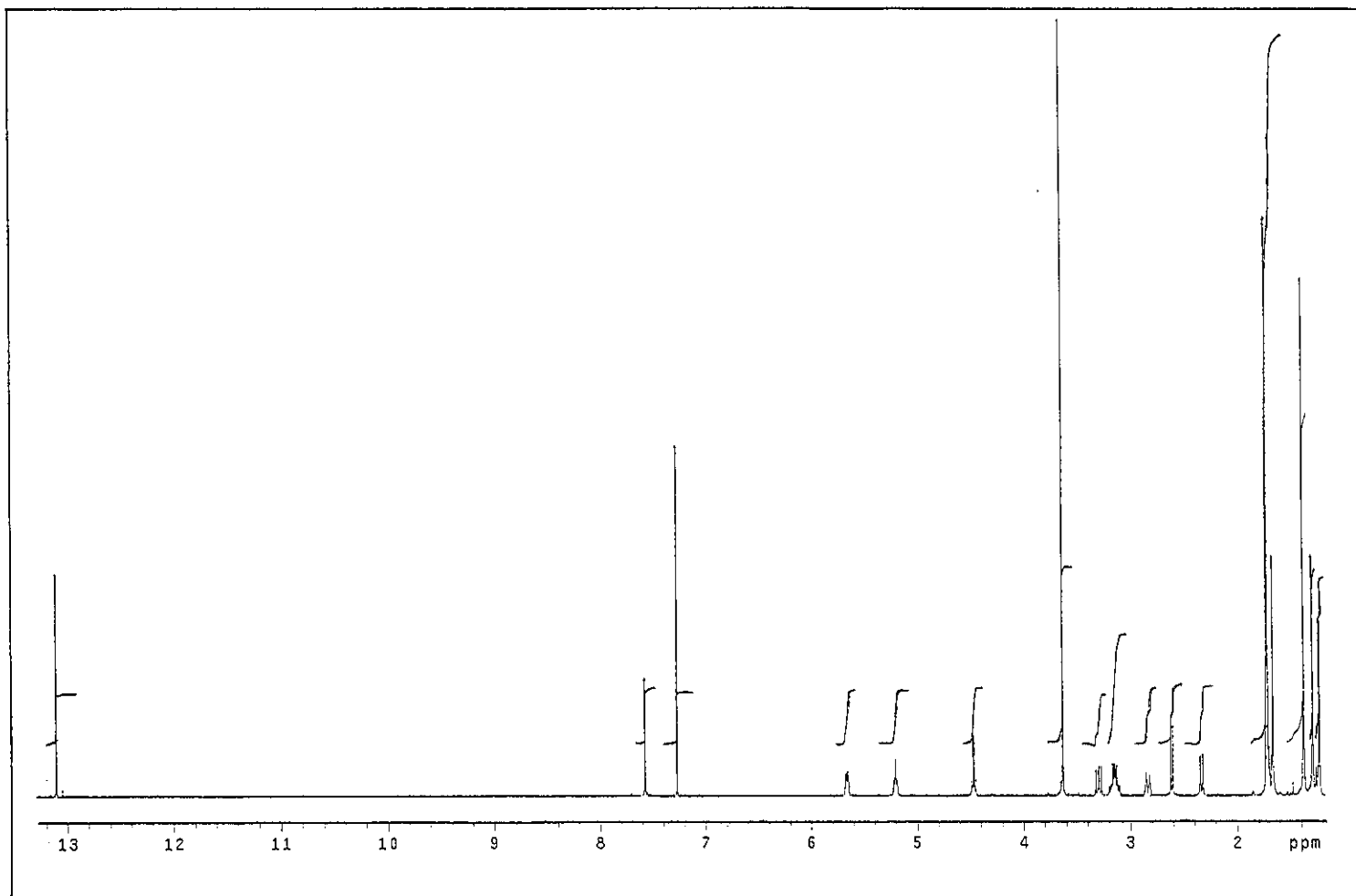
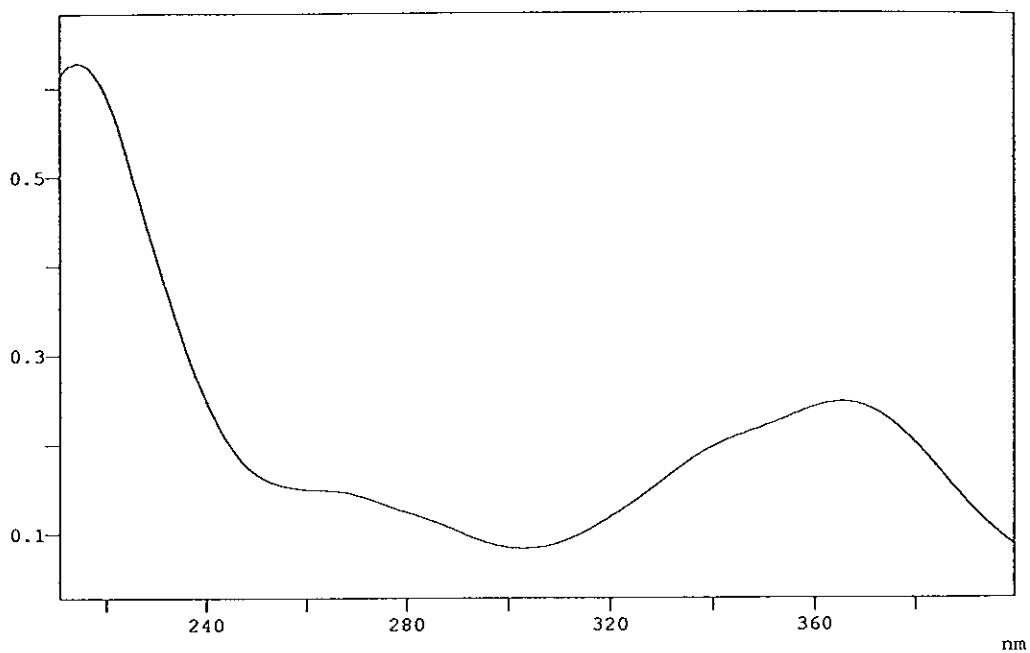
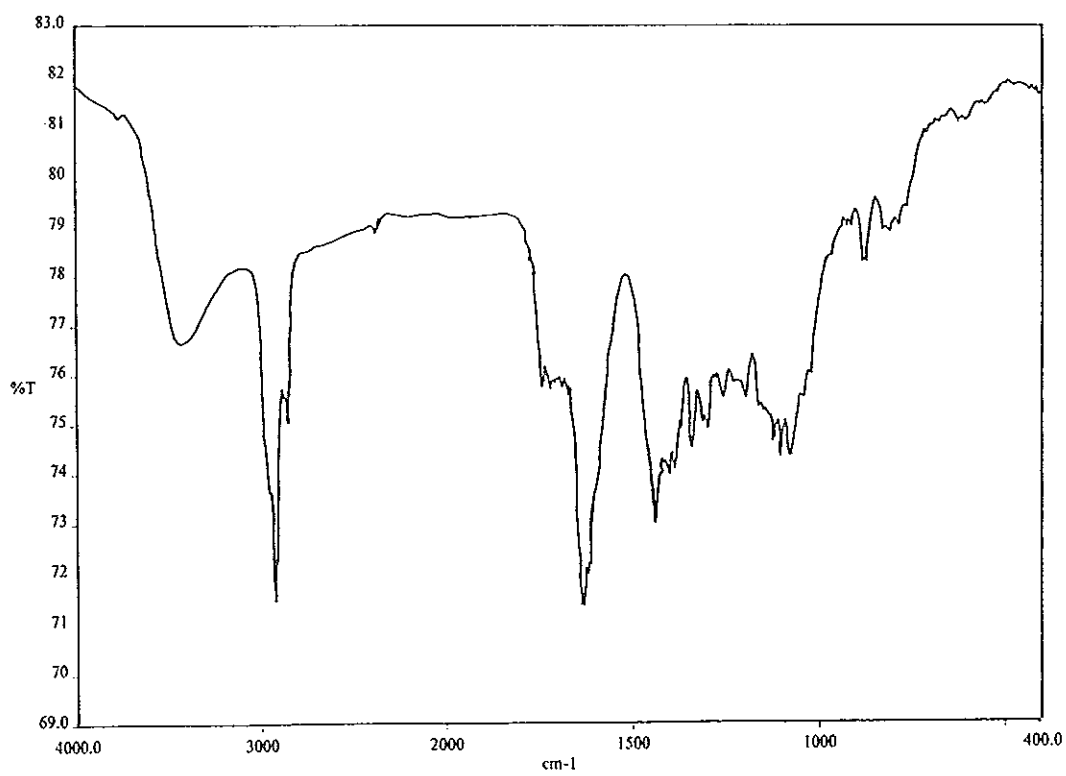


Figure 3 ^1H NMR (500 MHz) (CDCl_3) spectrum of DD13

Abs

**Figure 4 UV (MeOH) spectrum of DD15****Figure 5 FT-IR (neat) spectrum of DD15**

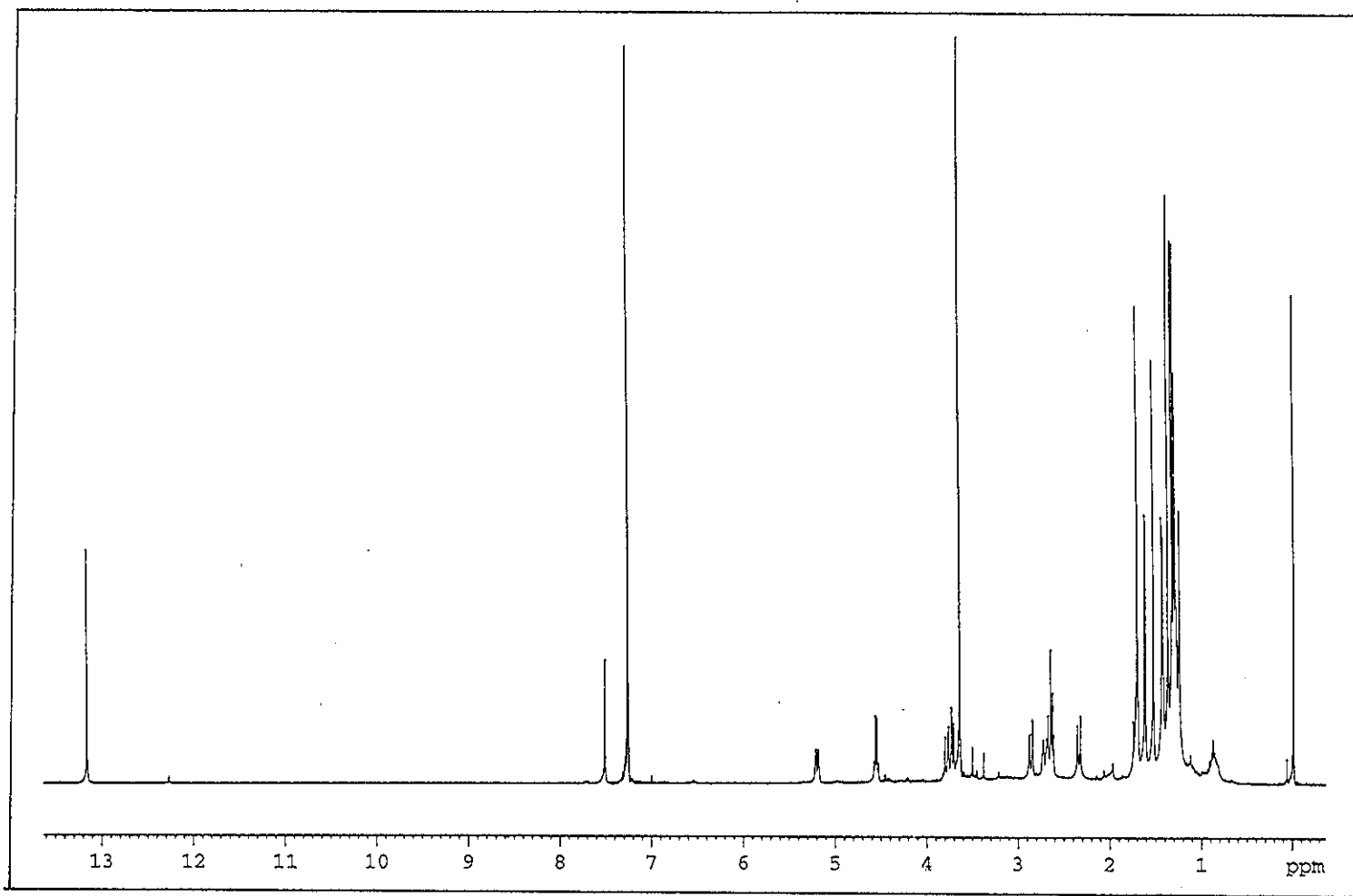


Figure 6 ^1H NMR (400 MHz) (CDCl_3) spectrum of DD15

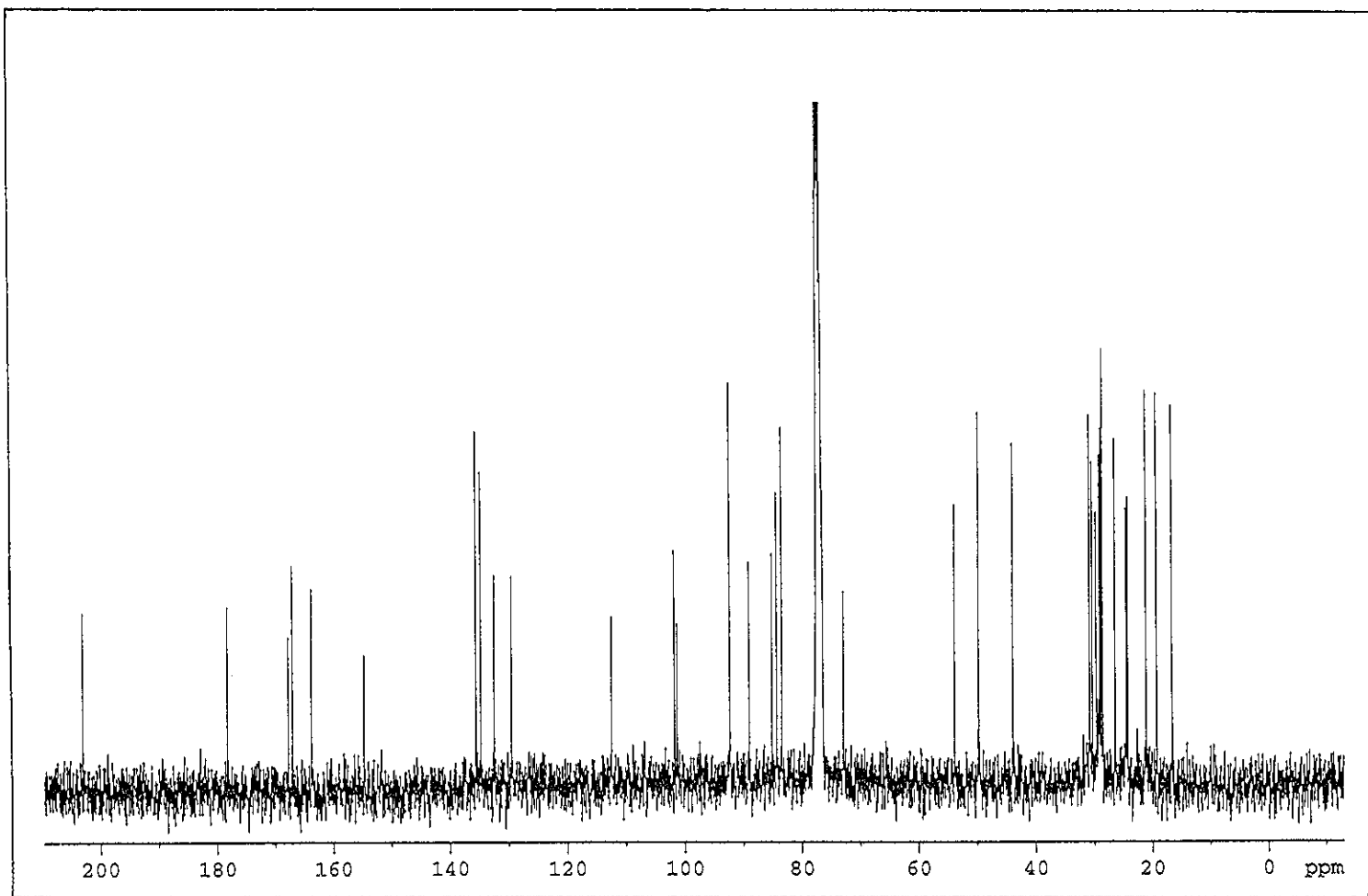


Figure 7 ^{13}C NMR (100 MHz) (CDCl_3) spectrum of DD15

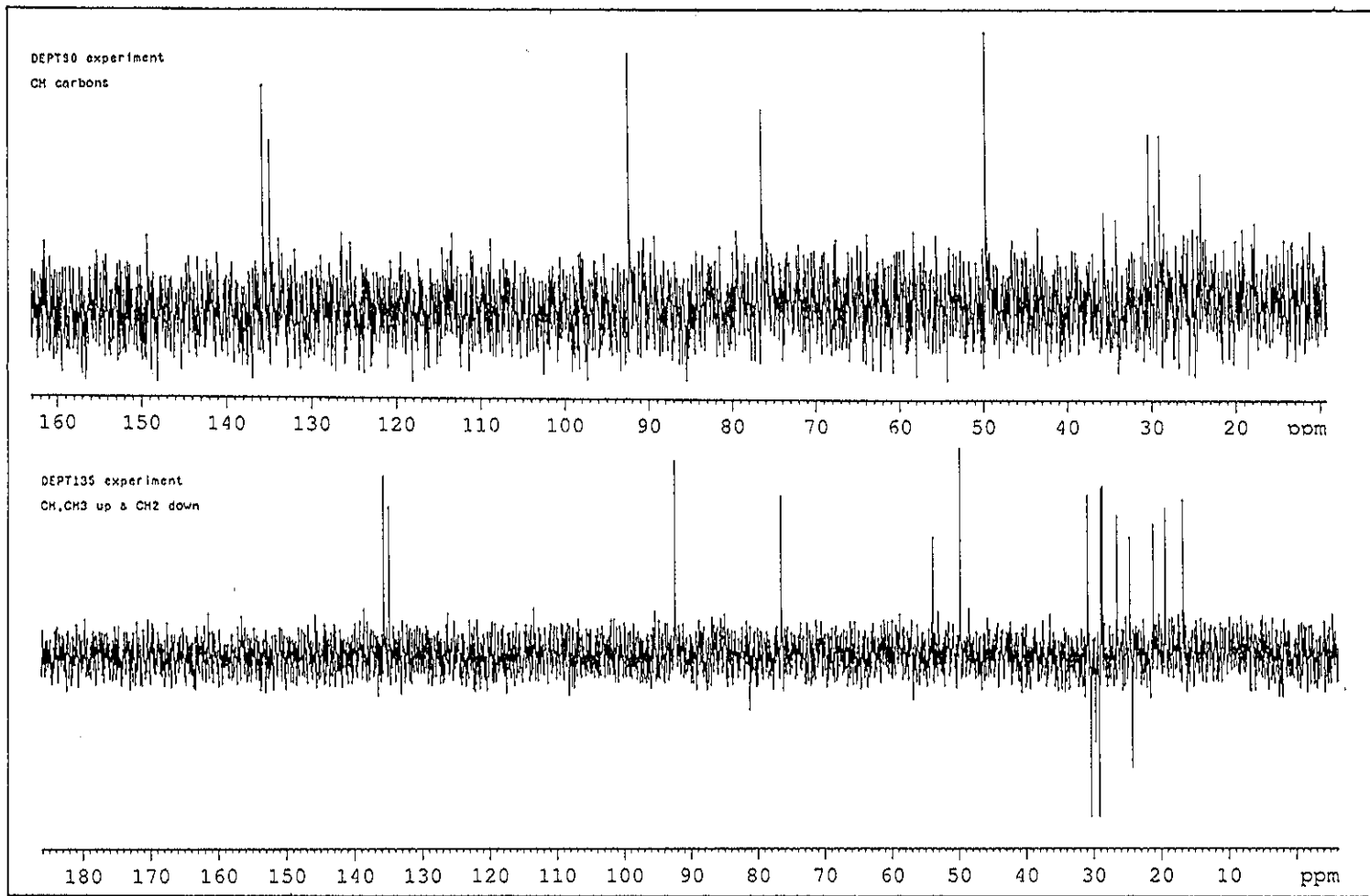


Figure 8 DEPT spectrum of DD15

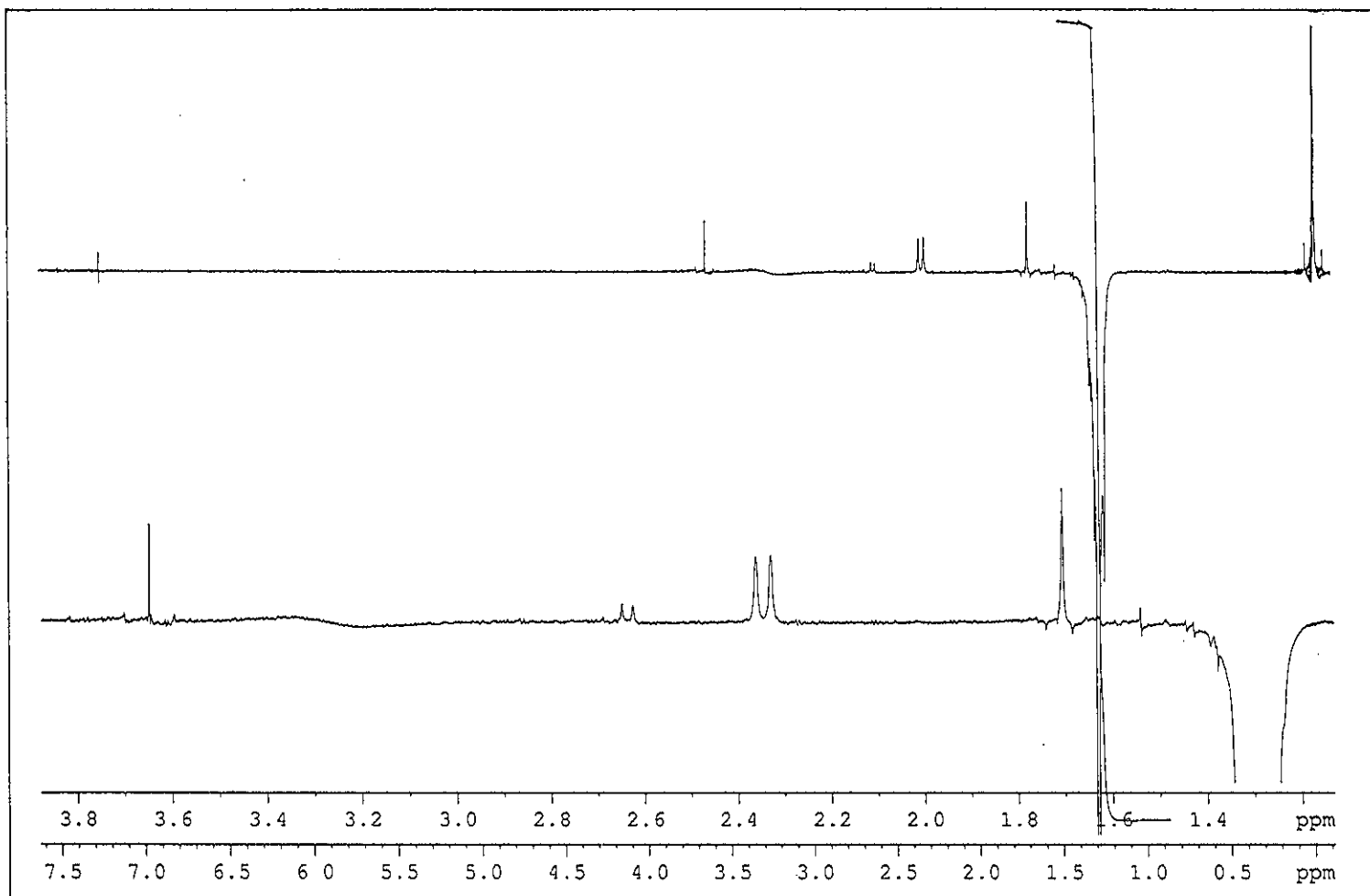


Figure 9 NOEDIFF spectrum of DD15 after irradiation at $\delta_{\text{H}}^- 1.29$

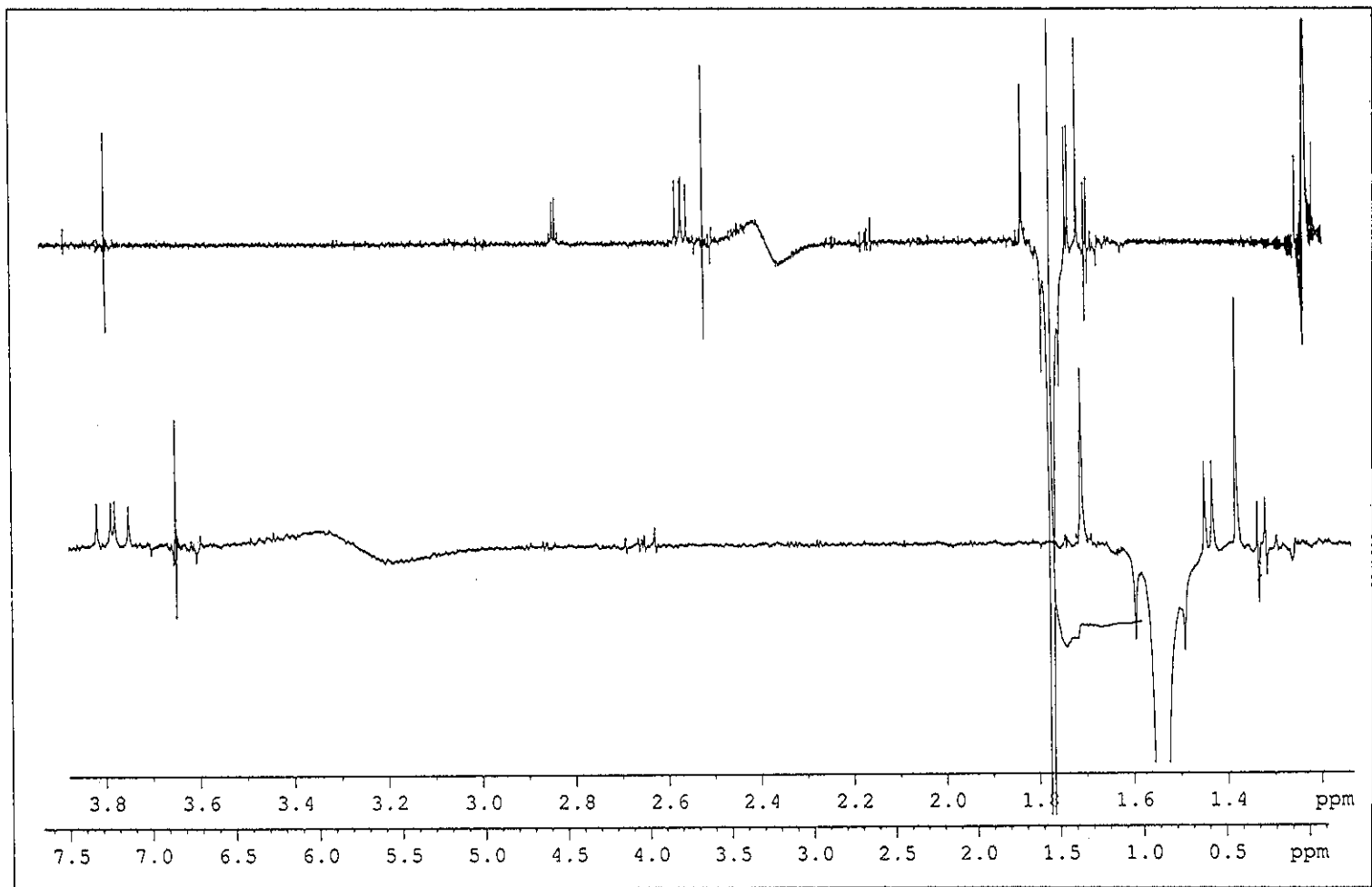


Figure 10 NOEDIFF spectrum of DD15 after irradiation at δ_H 1.53

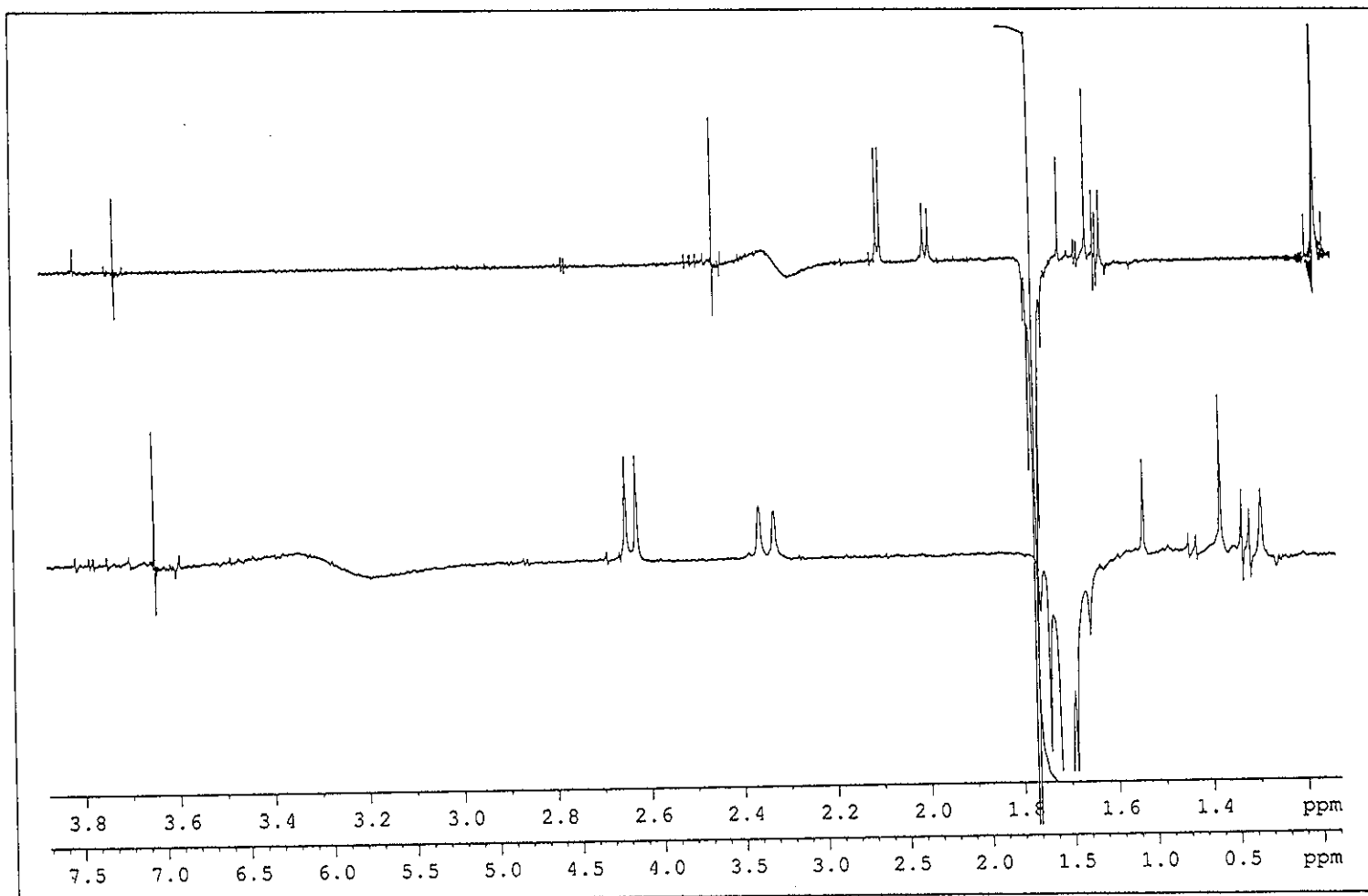


Figure 11 NOEDIFF spectrum of DD15 after irradiation at δ_H 1.71

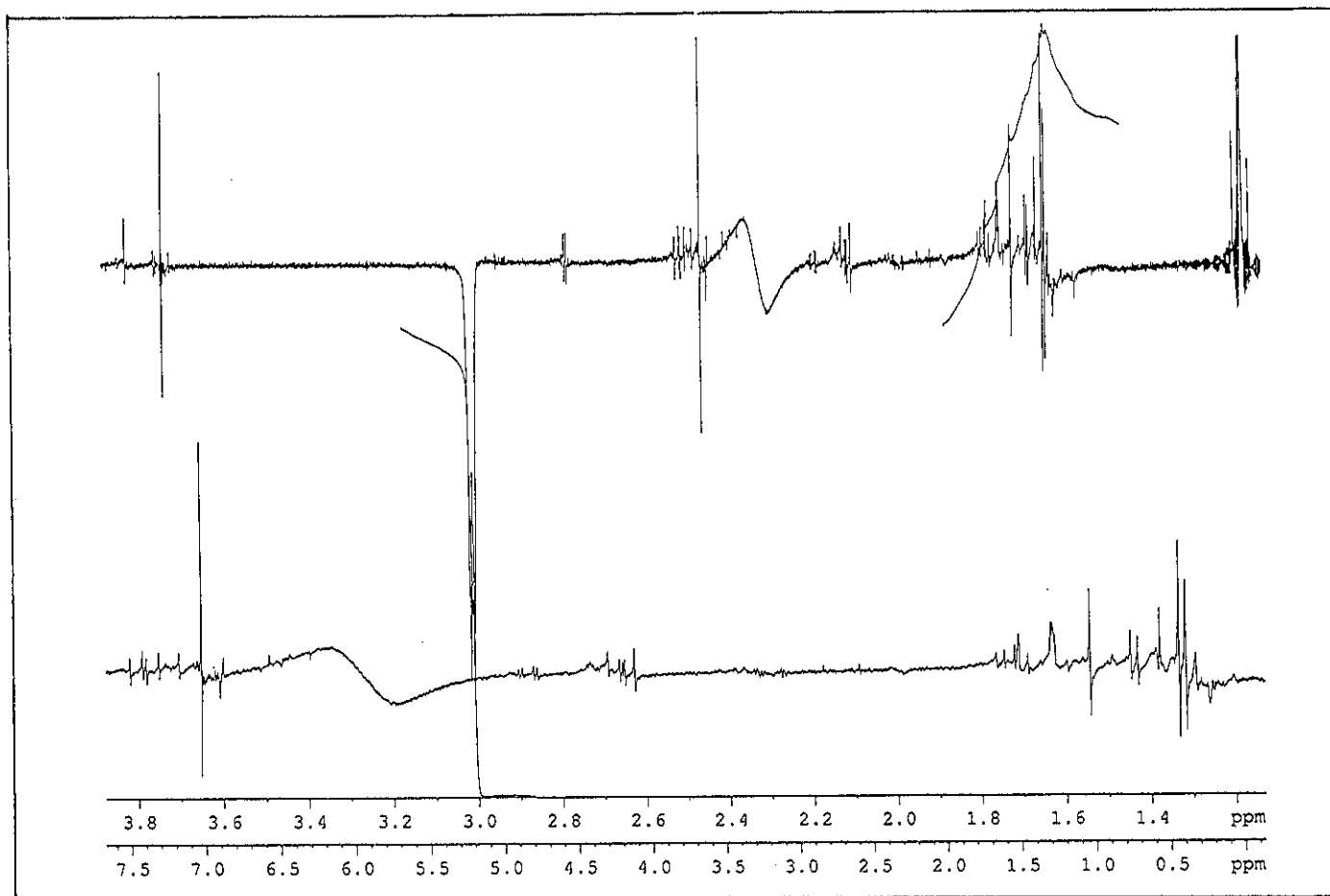


Figure 12 NOEDIFF spectrum of DD15 after irradiation at δ_H 5.20

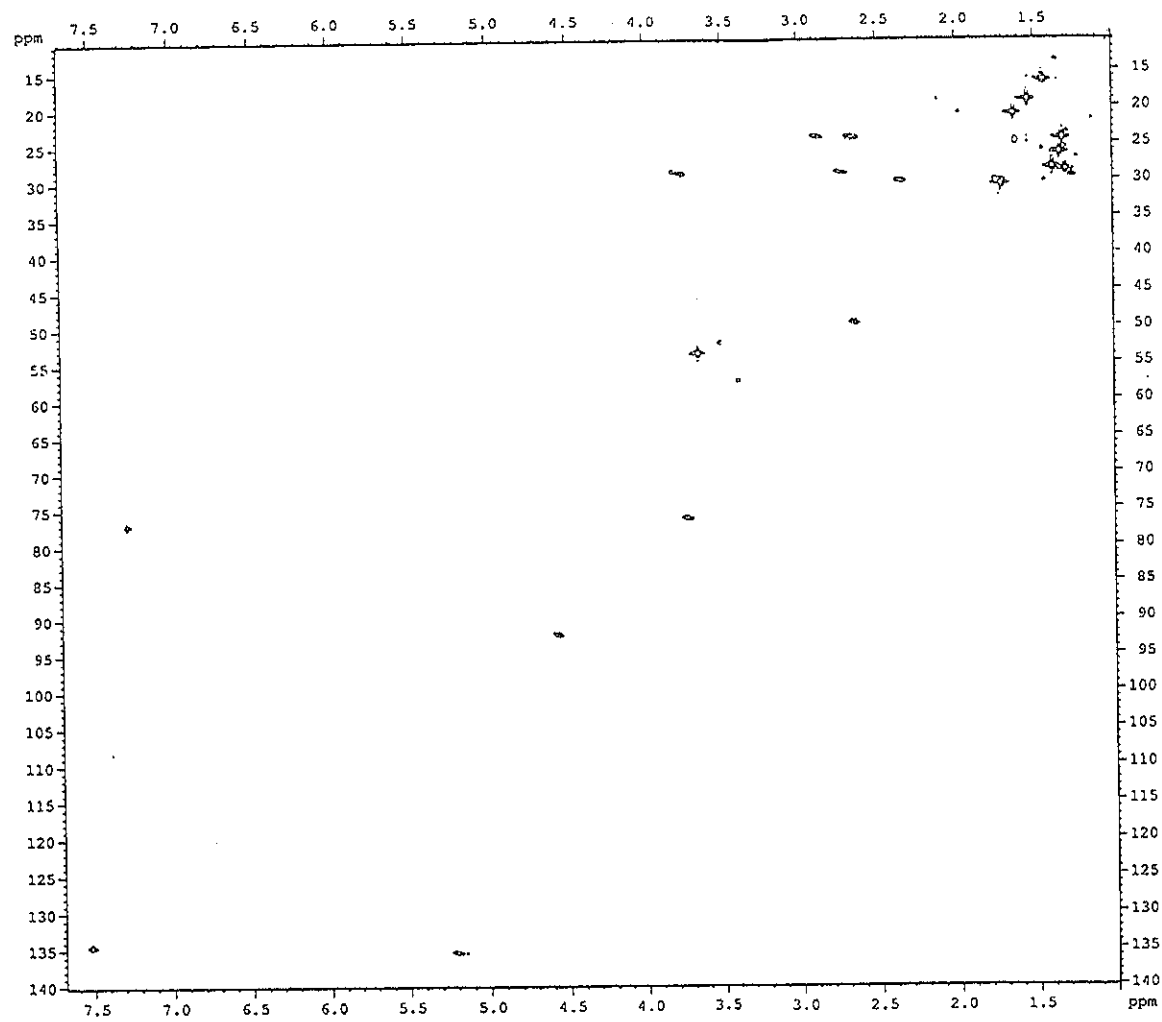


Figure 13 2D HMQC spectrum of DD15

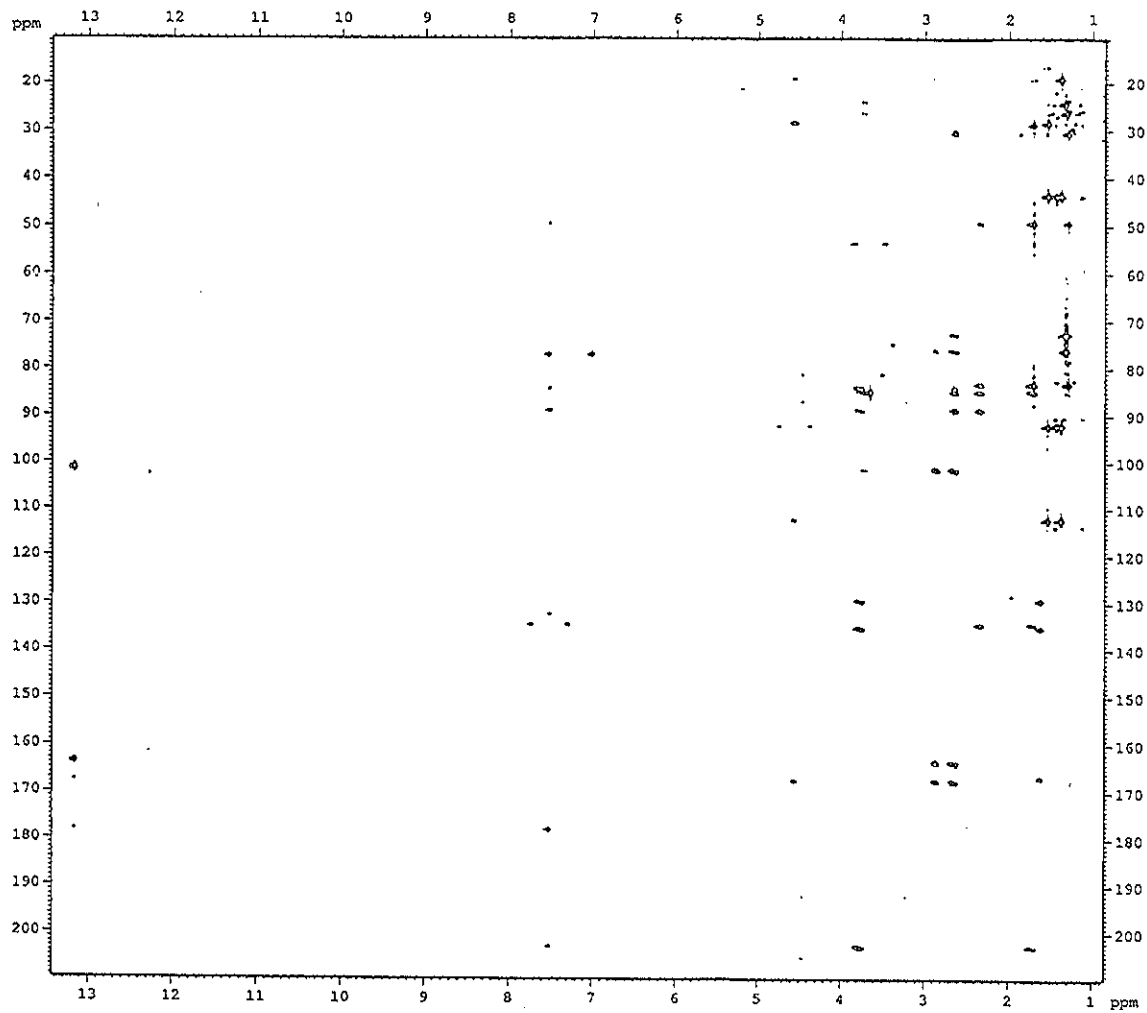


Figure 14 2D HMBC spectrum of DD15

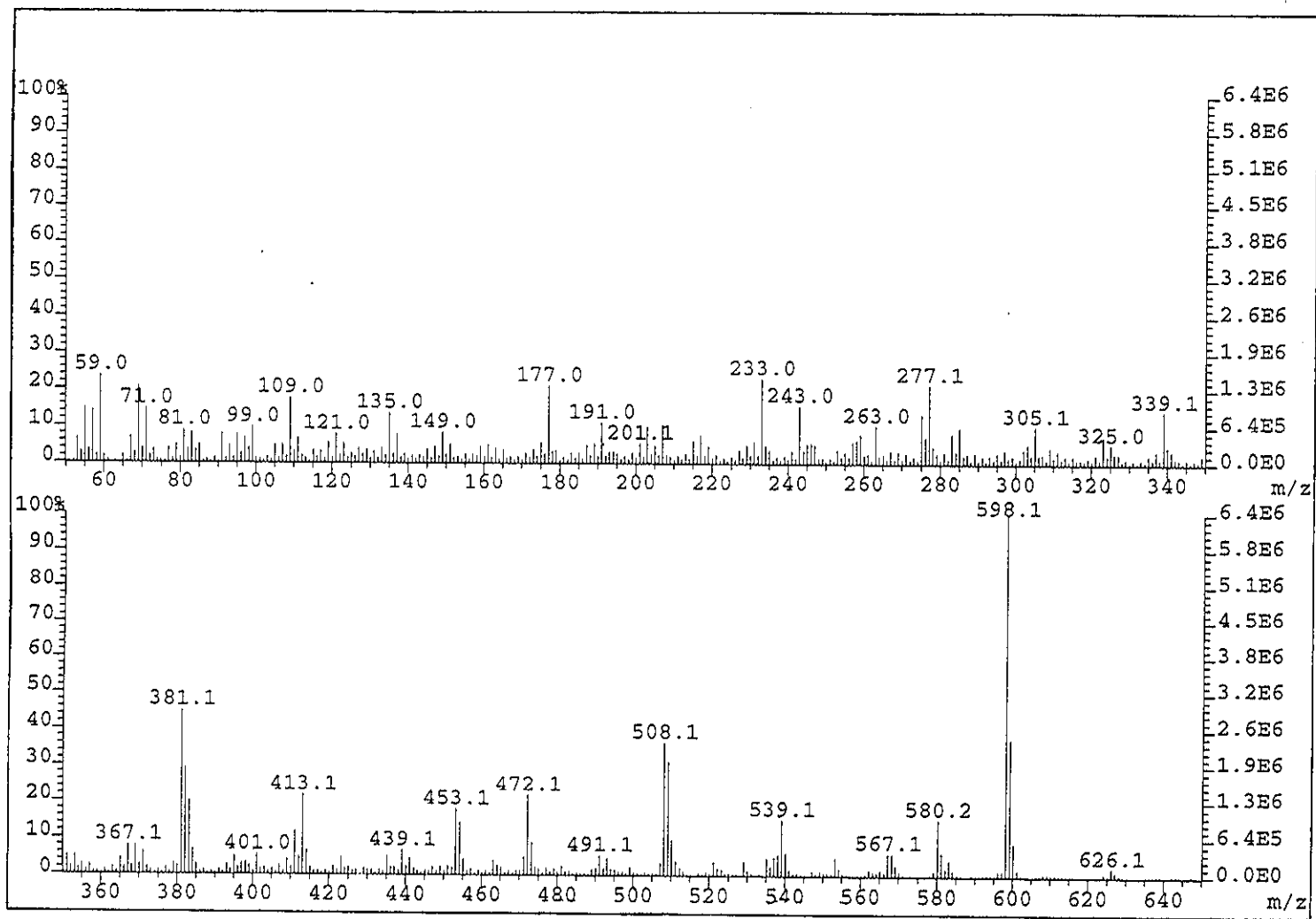


Figure 15 Mass spectrum of DD15

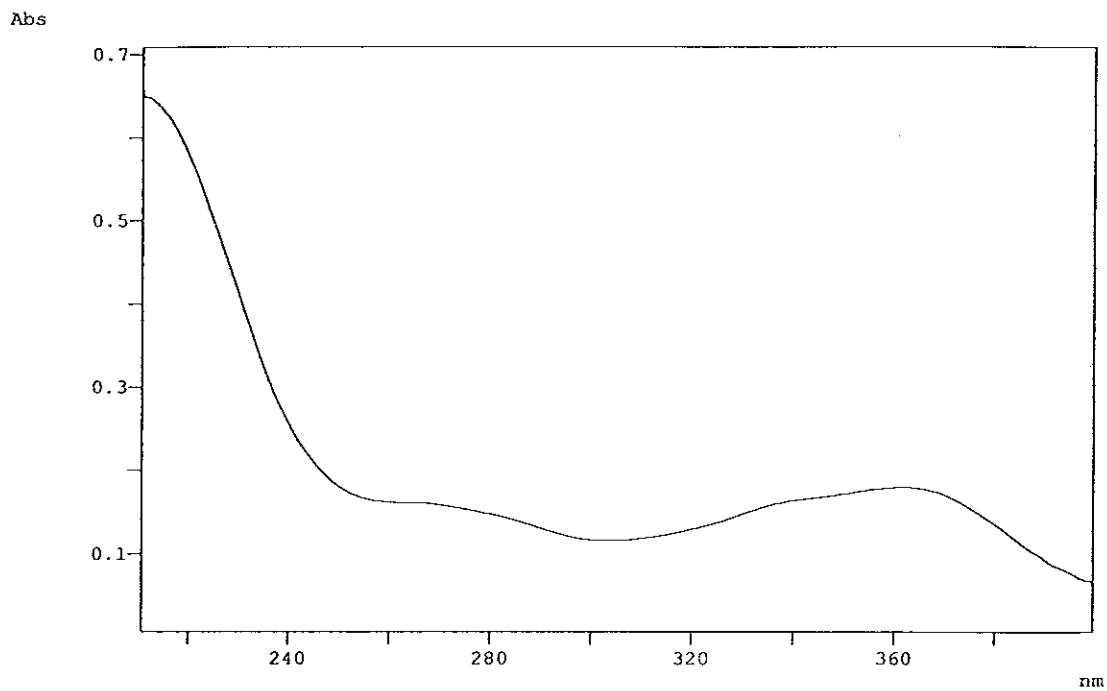


Figure 16 UV (MeOH) spectrum of DD2

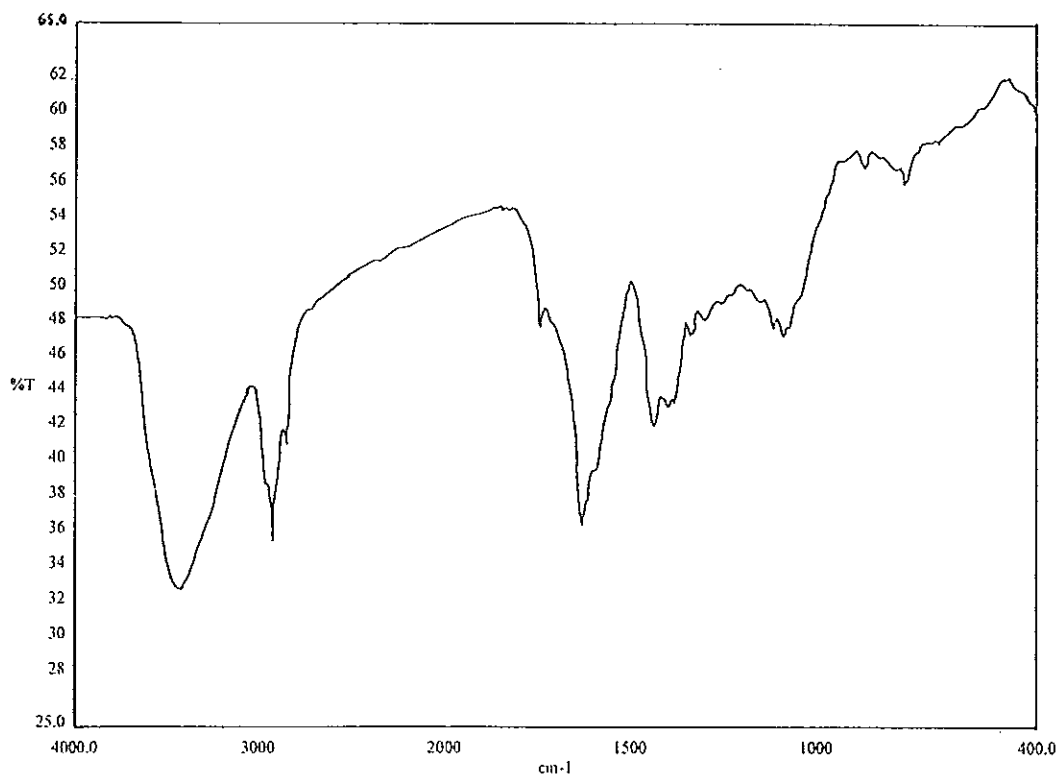


Figure 17 FT-IR (neat) spectrum of DD2

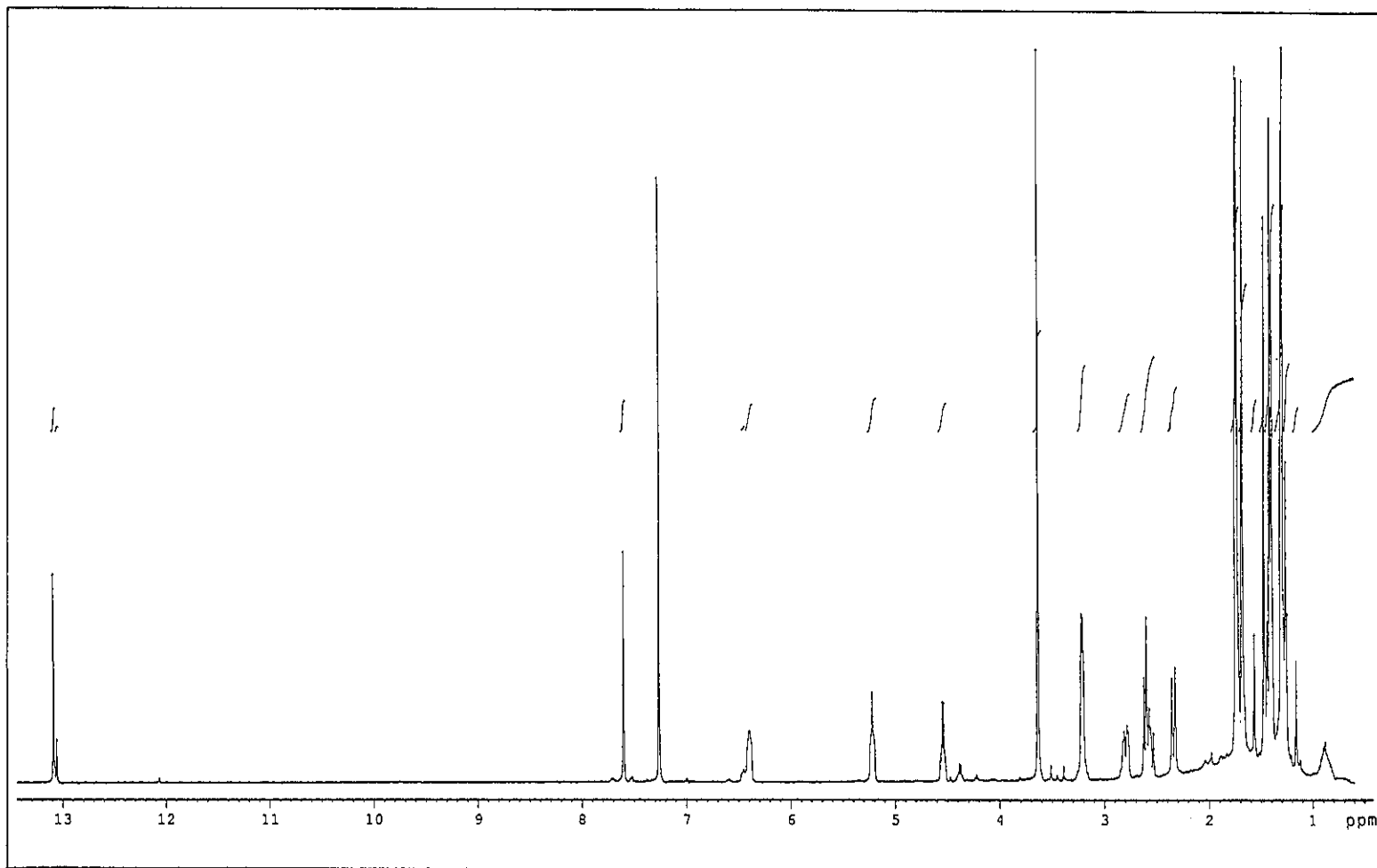


Figure 18 ^1H NMR (400 MHz) (CDCl_3) spectrum of DD2

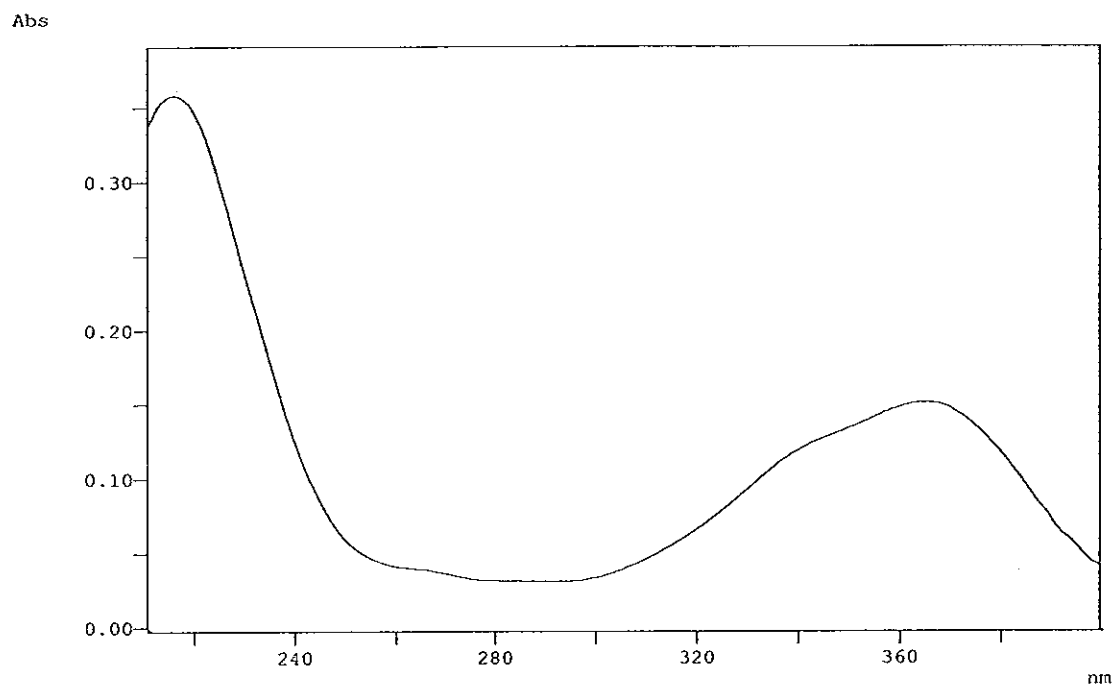


Figure 19 UV (MeOH) spectrum of DD11

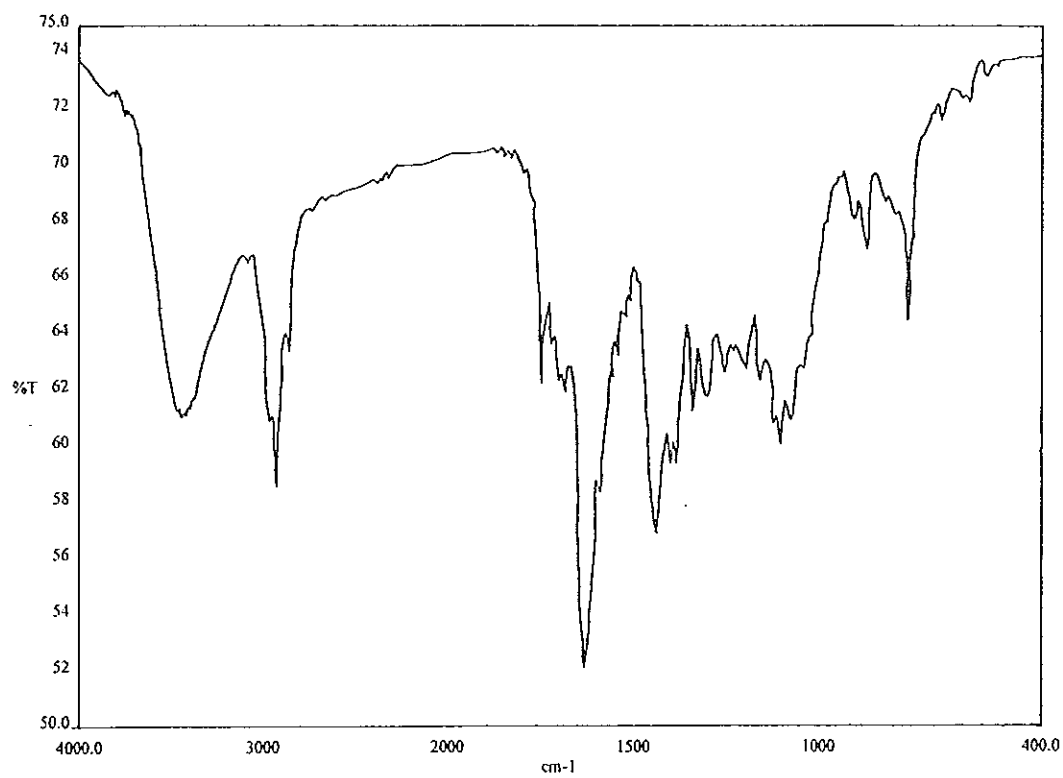


Figure 20 FT-IR (neat) spectrum of DD11

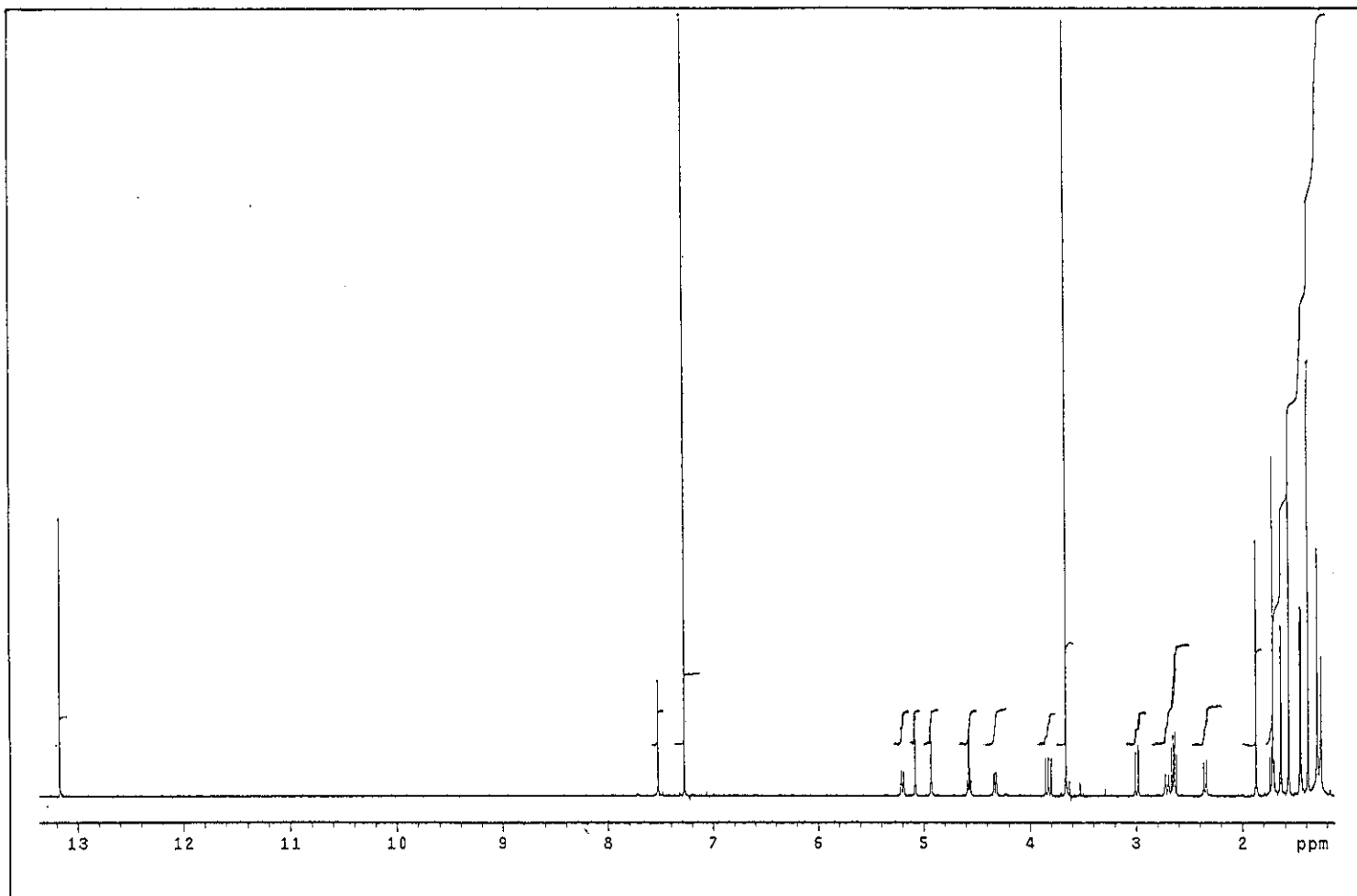


Figure 21 ^1H NMR (500 MHz) (CDCl_3) spectrum of DD11

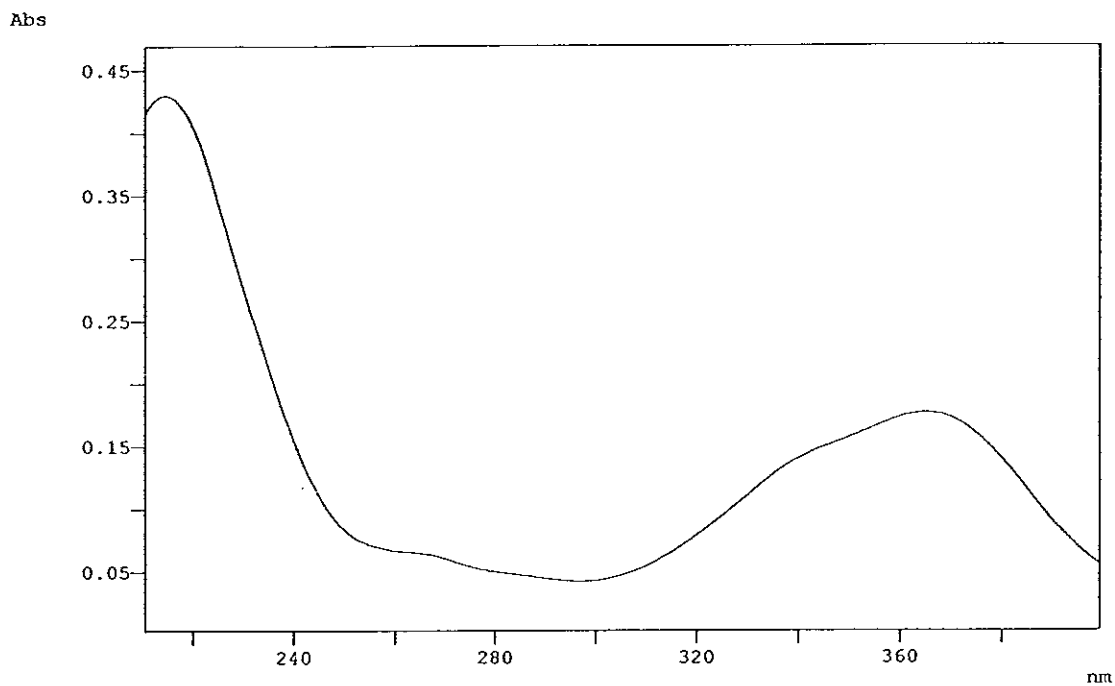


Figure 22 UV (MeOH) spectrum of DD10

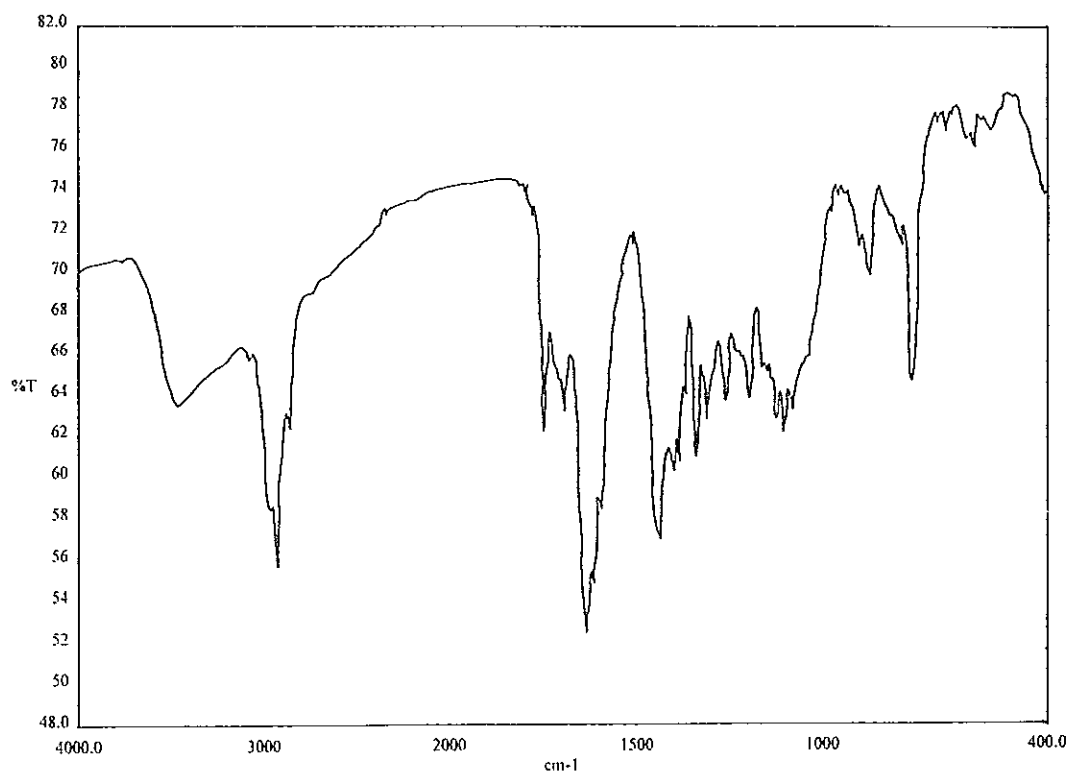


Figure 23 FT-IR (neat) spectrum of DD10

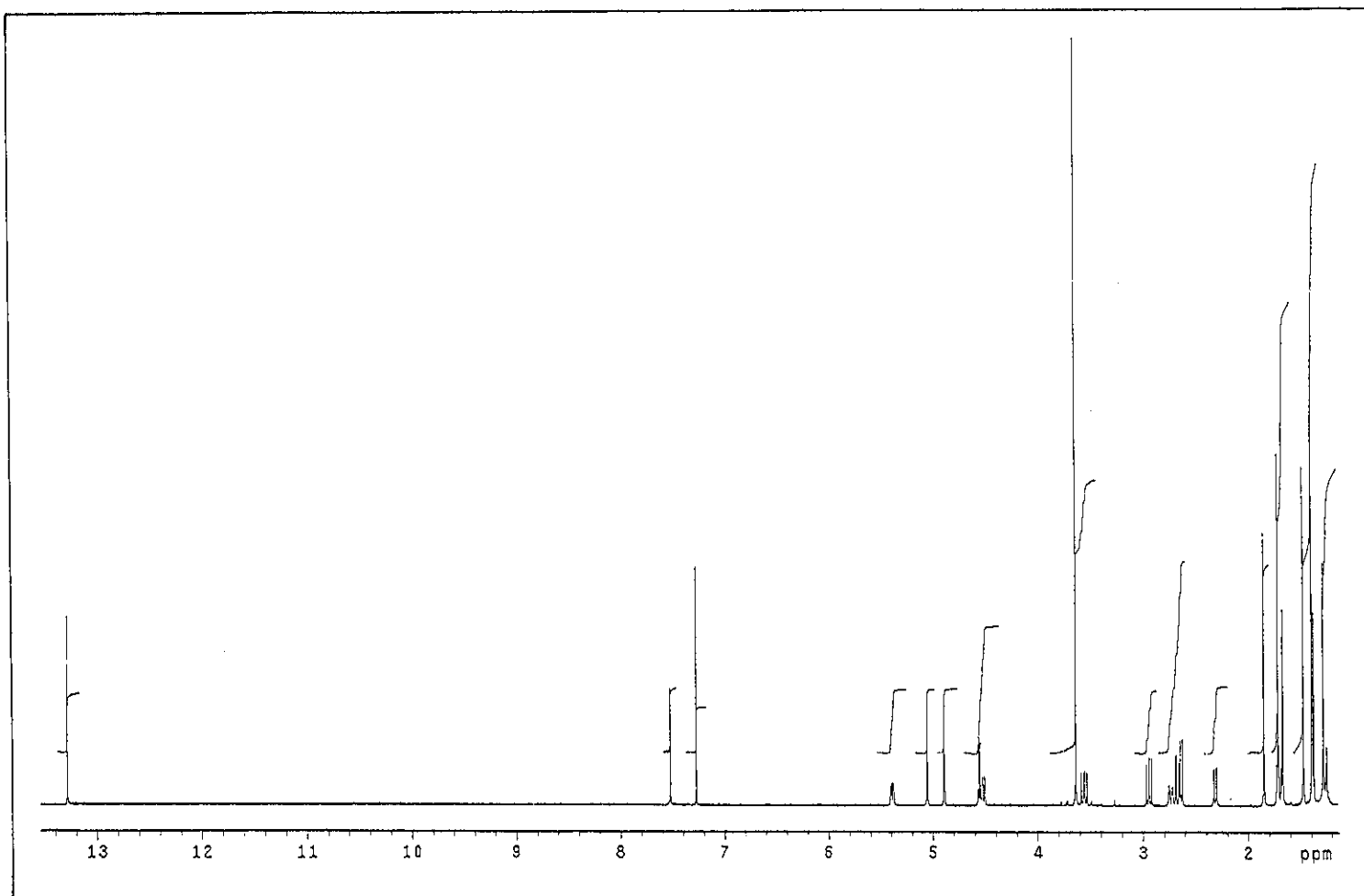


Figure 24 ^1H NMR (500 MHz) (CDCl_3) spectrum of DD10

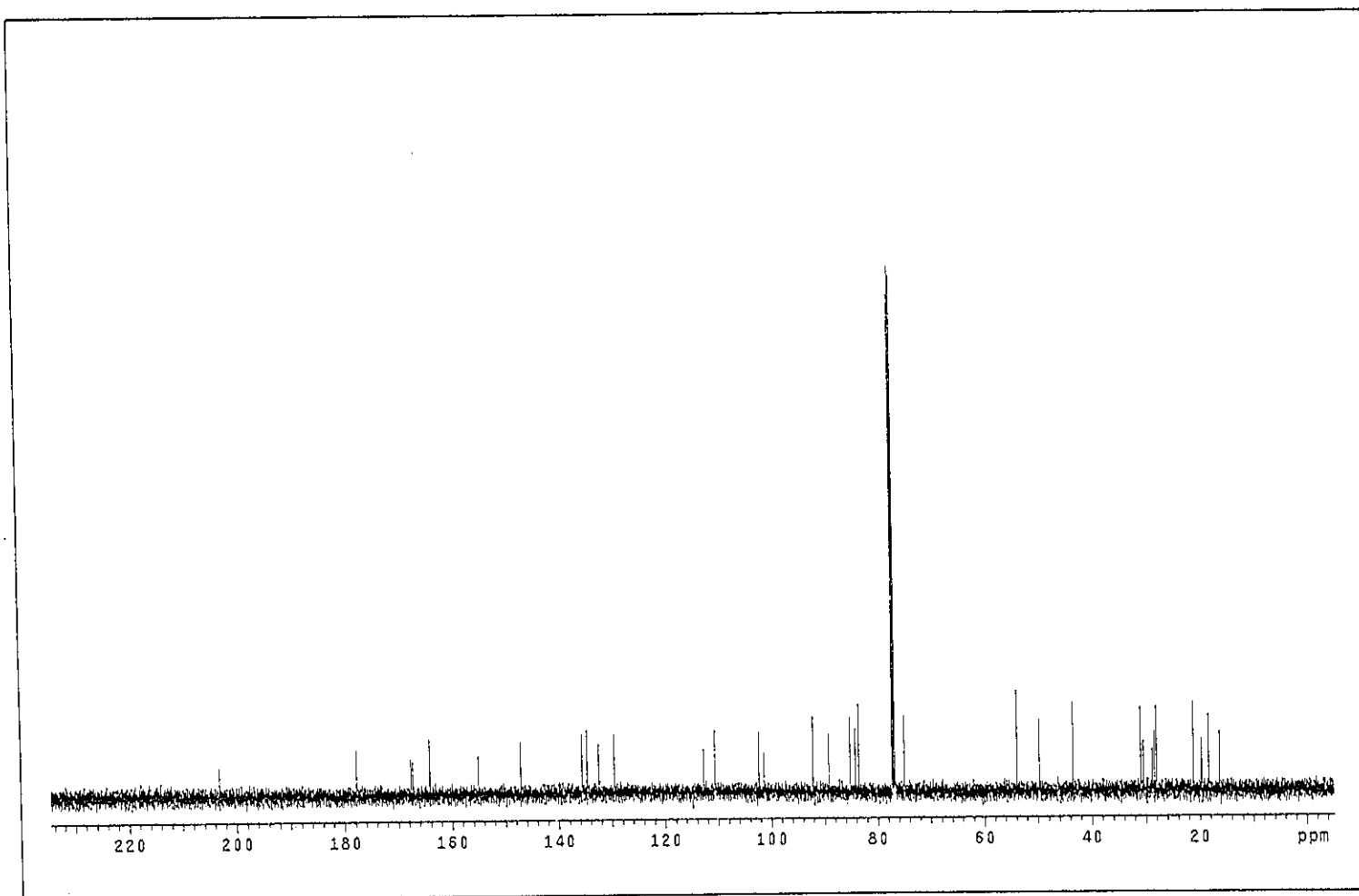


Figure 25 ^{13}C NMR (125 MHz) (CDCl_3) spectrum of DD10

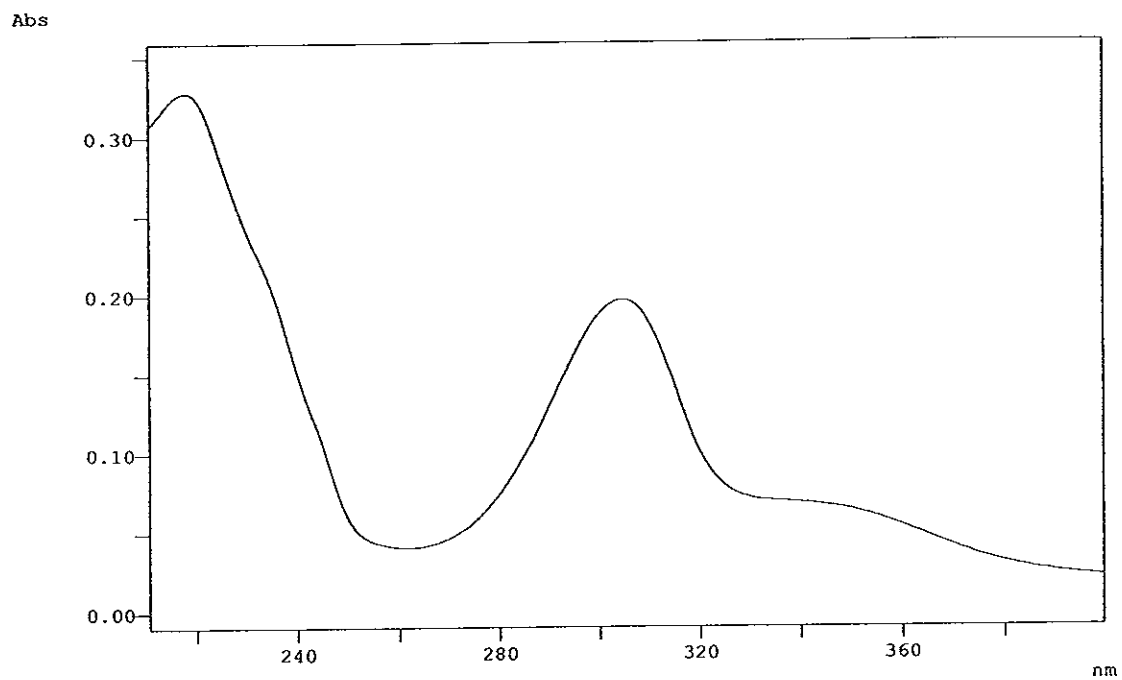


Figure 26 UV (MeOH) spectrum of DD14

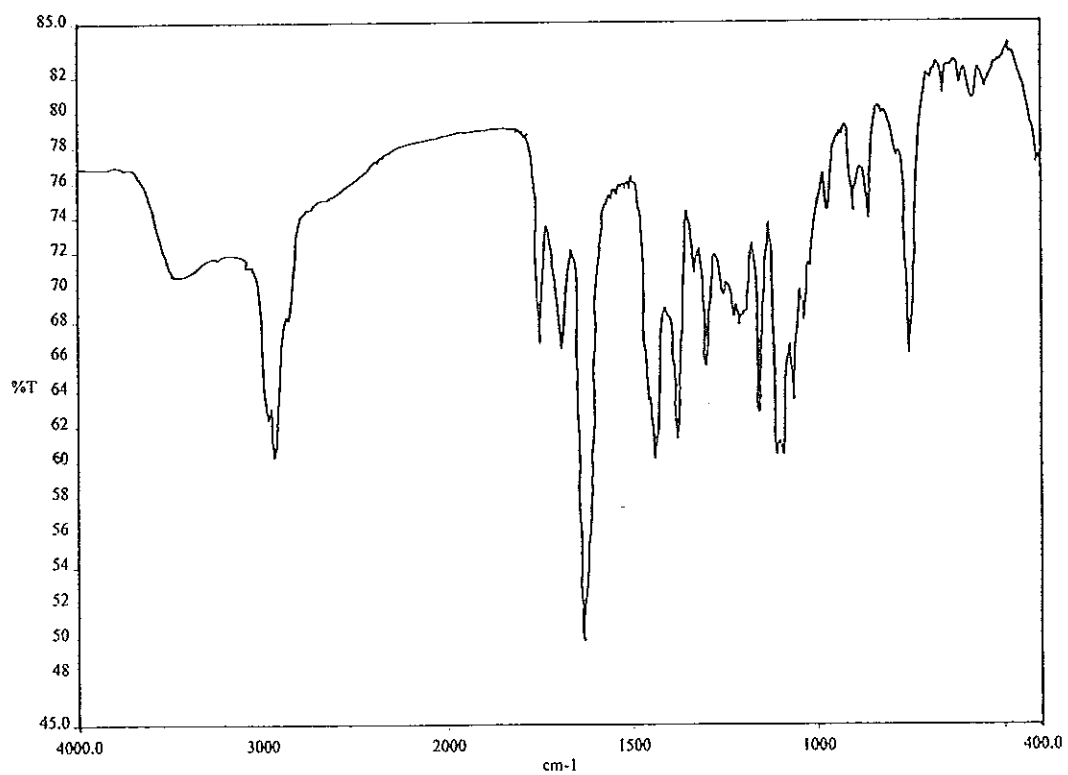


Figure 27 FT-IR (neat) spectrum of DD14

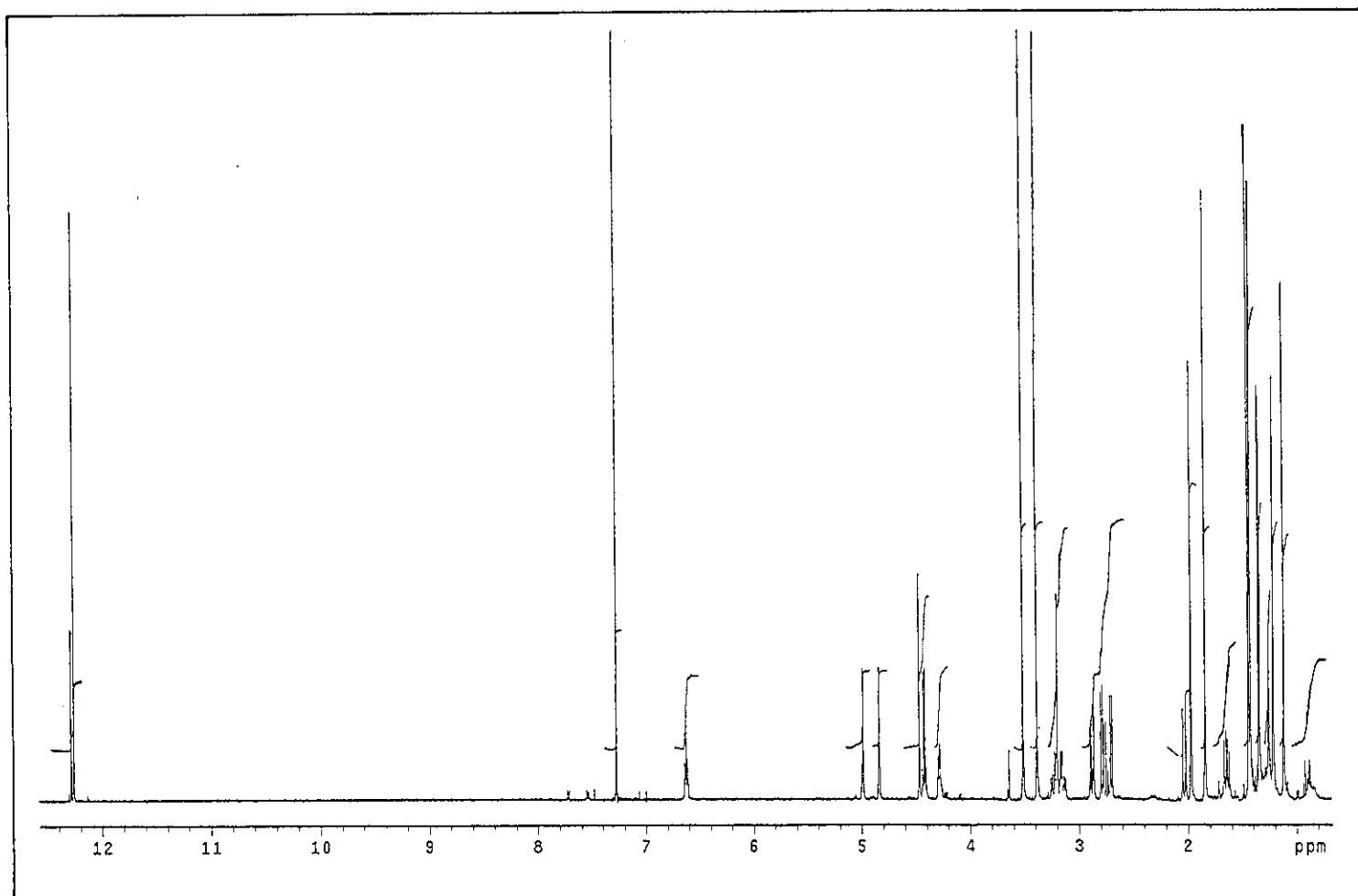


Figure 28 ^1H NMR (500 MHz) (CDCl_3) spectrum of DD14

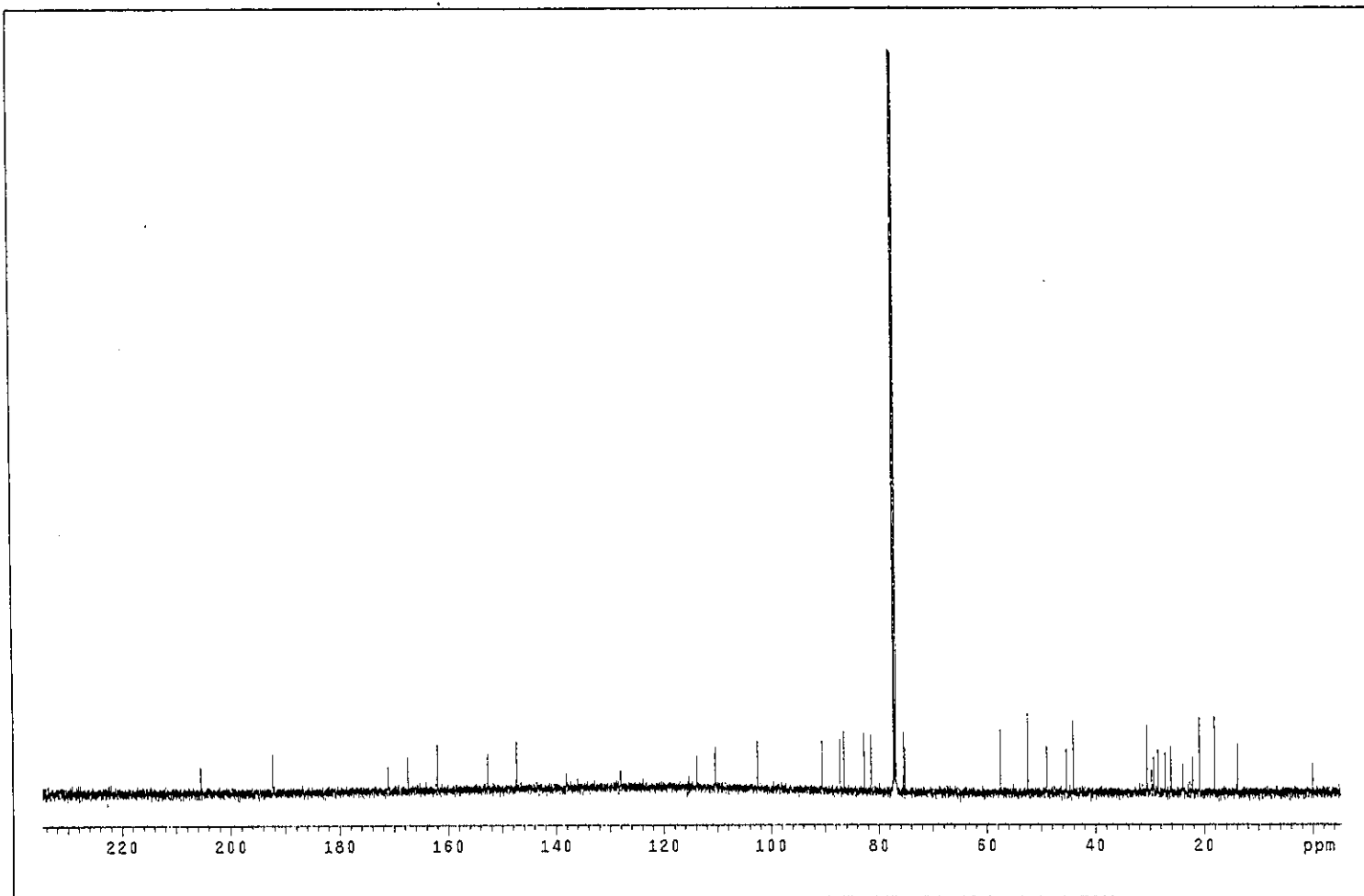


Figure 29 ^{13}C NMR (125 MHz) (CDCl_3) spectrum of DD14

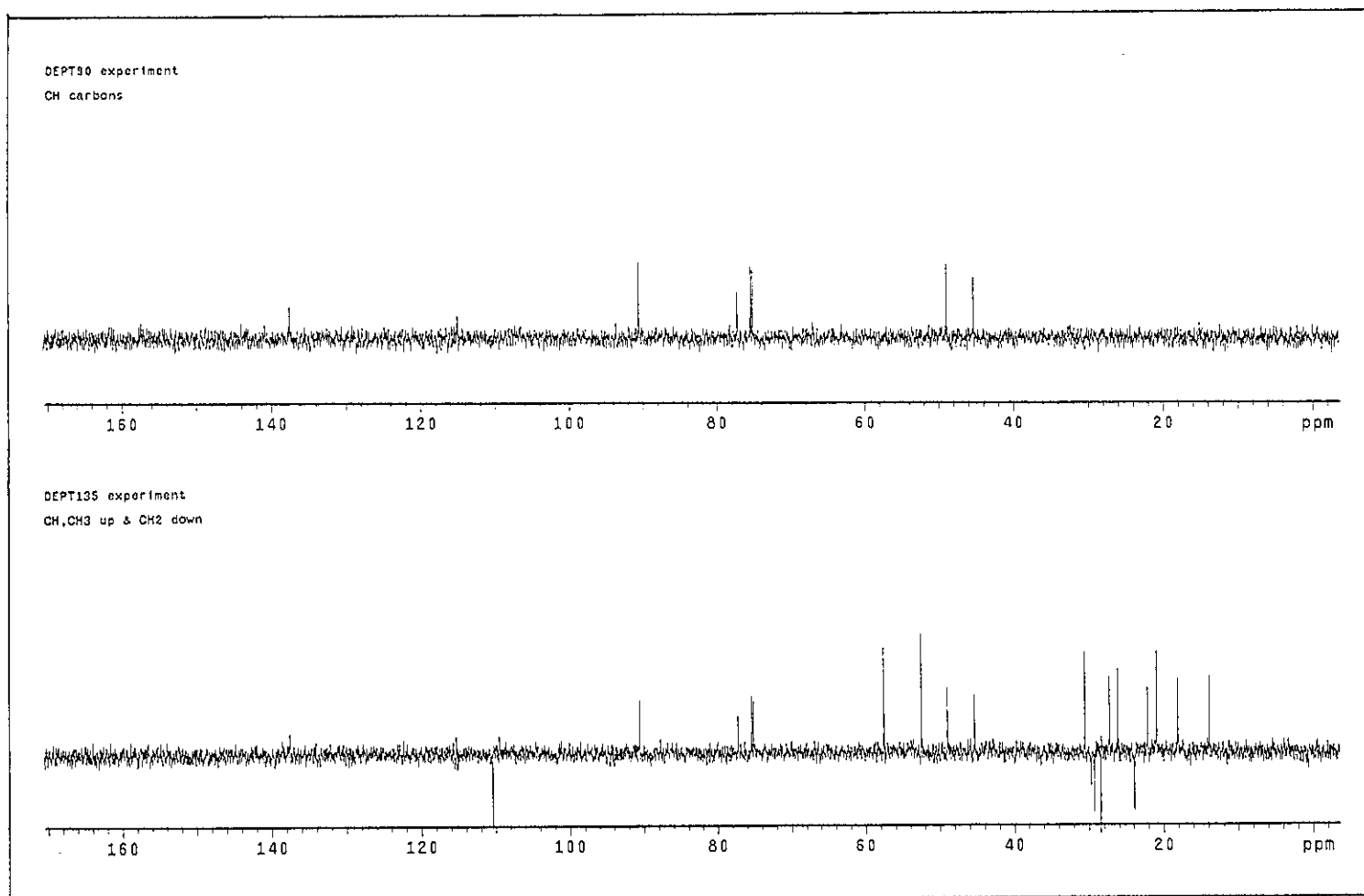


Figure 30 DEPT spectrum of DD14

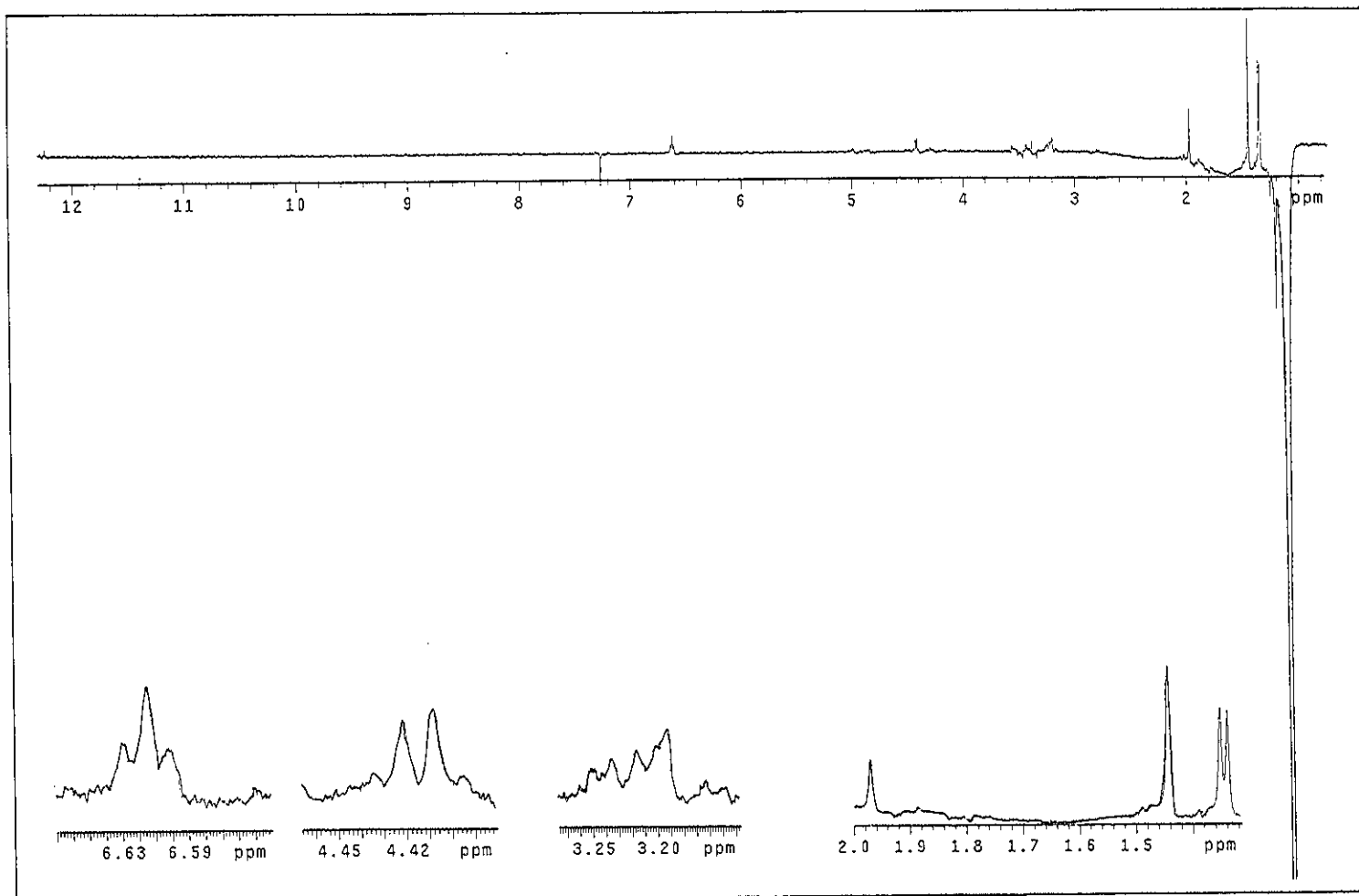


Figure 31 NOEDIFF spectrum of DD14 after irradiation at δ_H 1.12

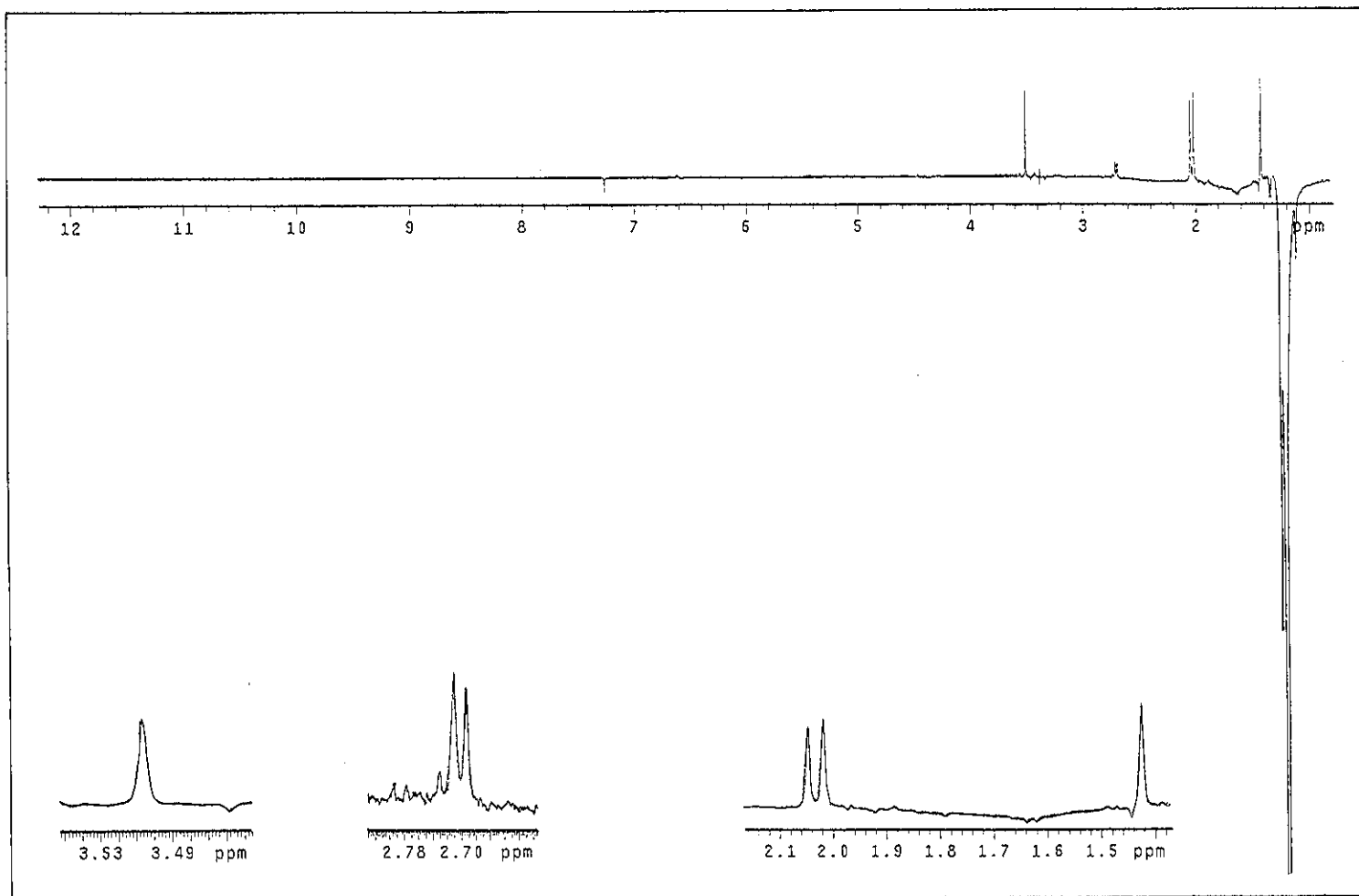


Figure 32 NOEDIFF spectrum of DD14 after irradiation at δ_H 1.22

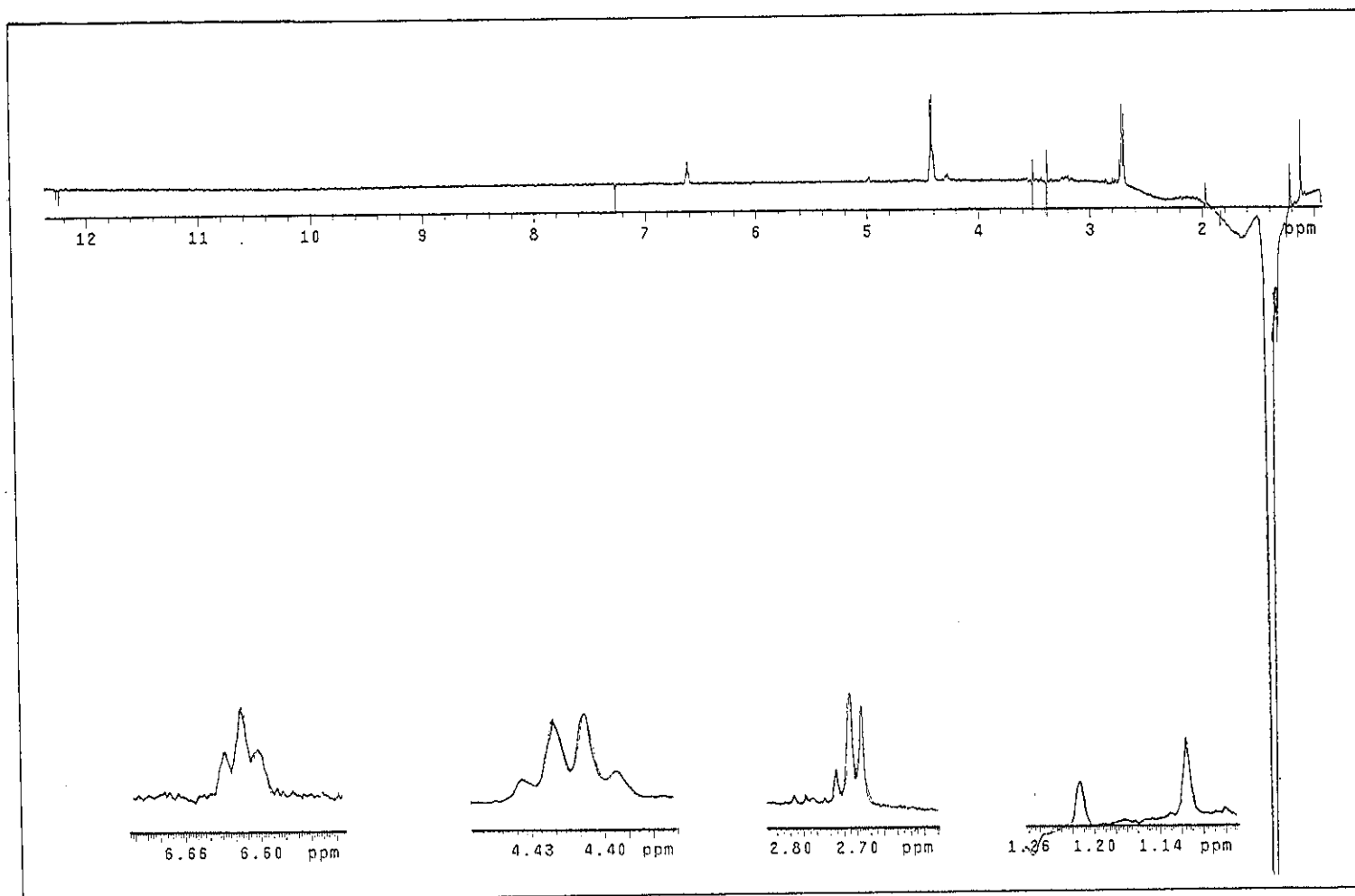


Figure 33 NOEDIFF spectrum of DD14 after irradiation at δ_H 1.43

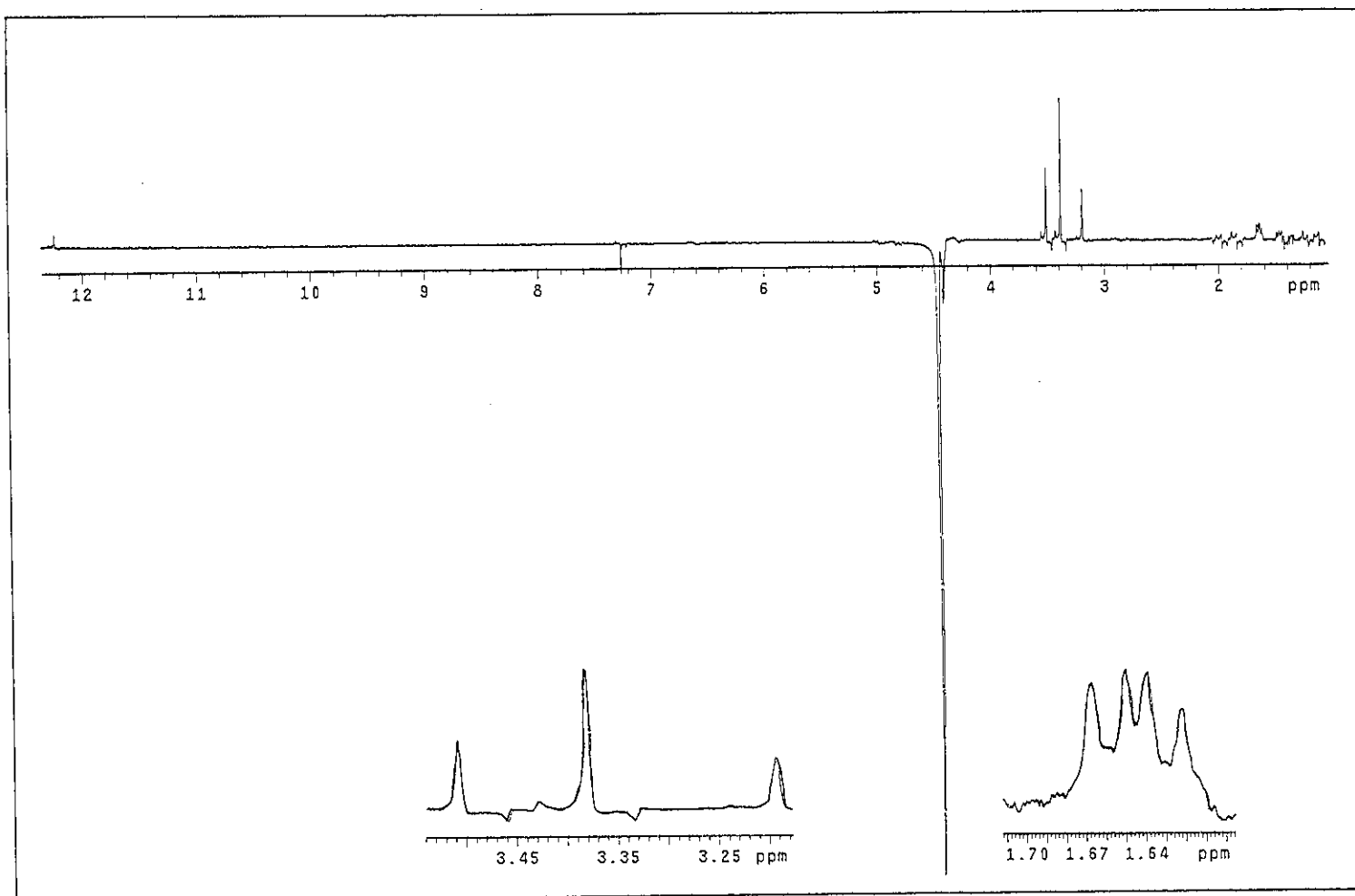


Figure 34 NOEDIFF spectrum of DD14 after irradiation at δ_H 4.47

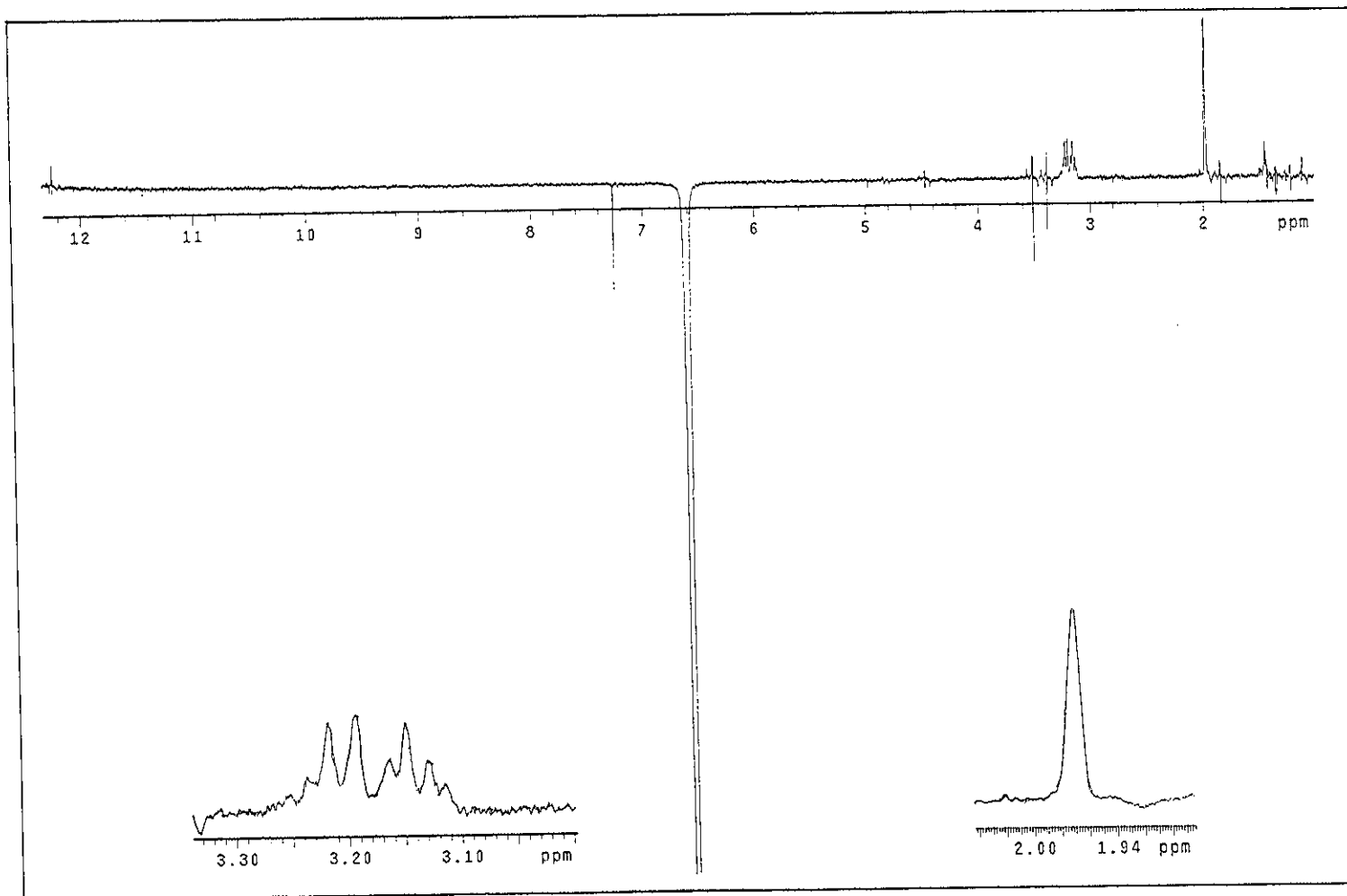


Figure 35 NOEDIFF spectrum of DD14 after irradiation at δ_H 6.63

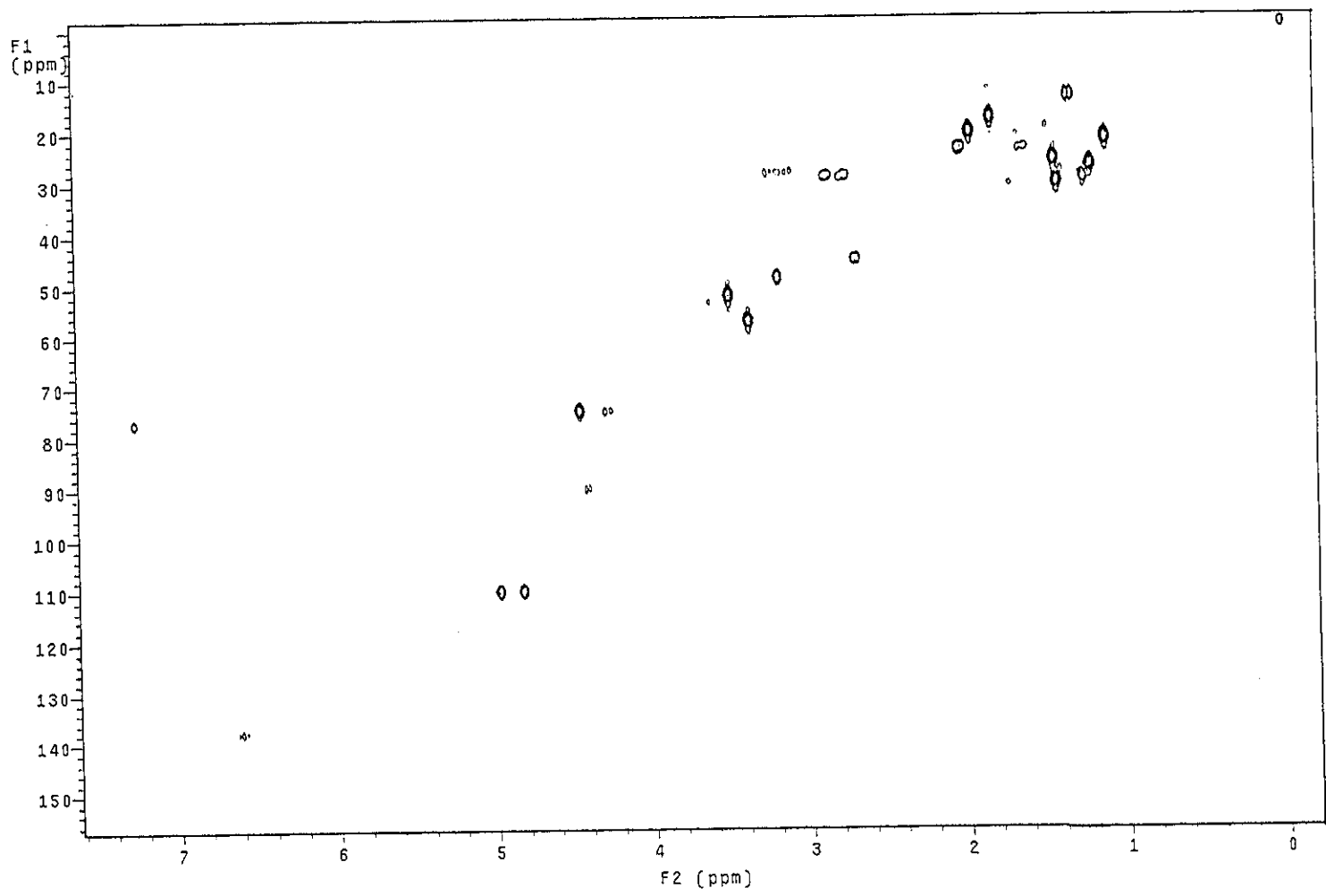


Figure 36 2D HMQC spectrum of DD14

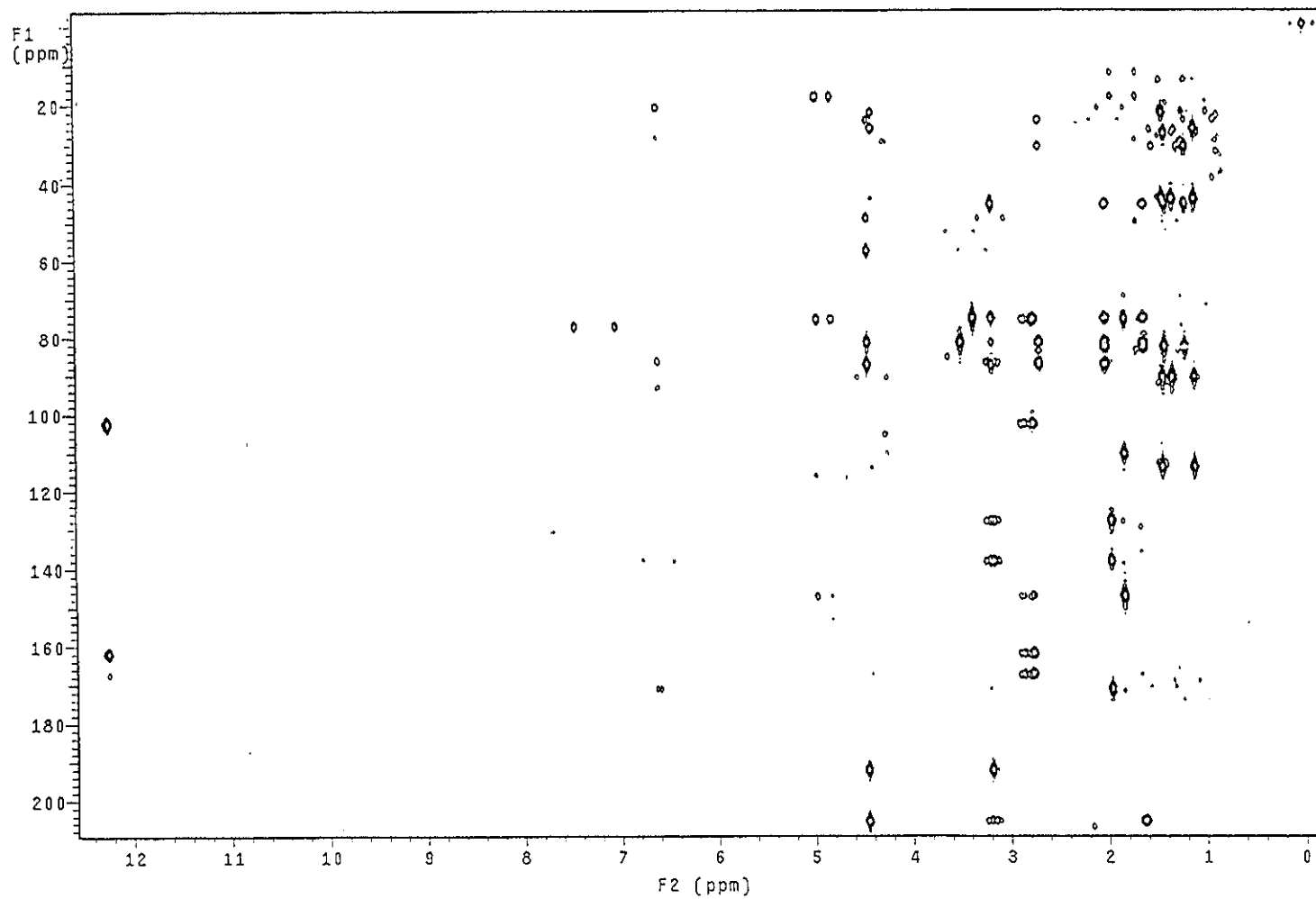


Figure 37 2D HMBC spectrum of DD14

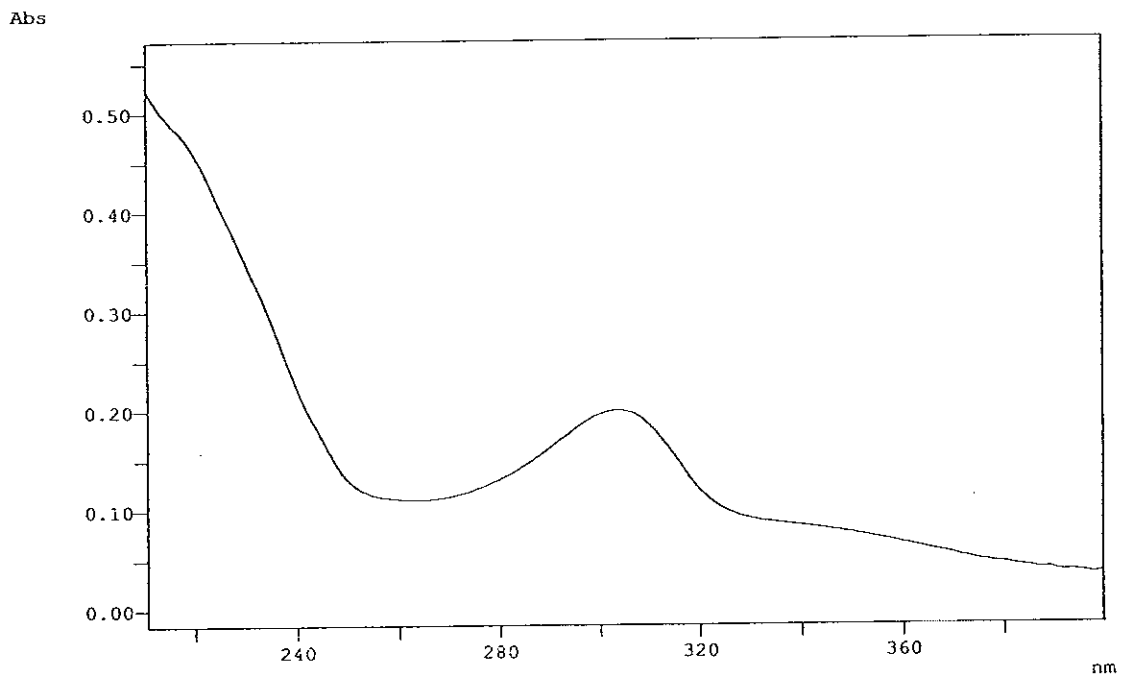


Figure 38 UV (MeOH) spectrum of DD12

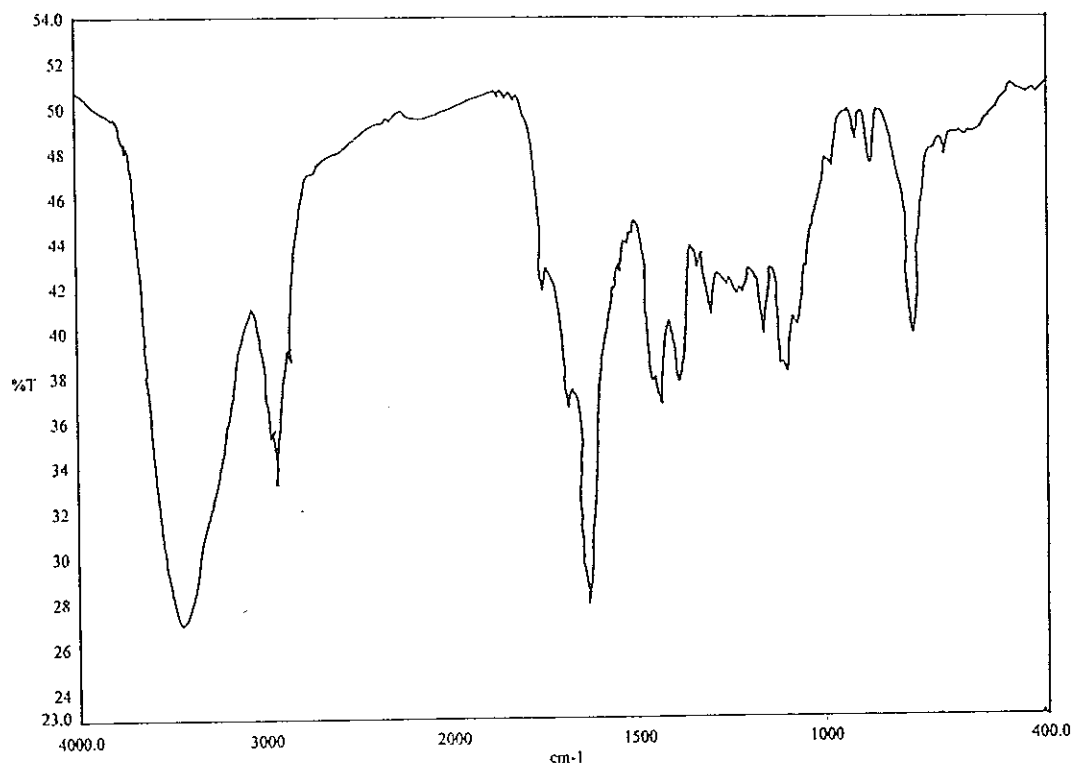


Figure 39 FT-IR (neat) spectrum of DD12

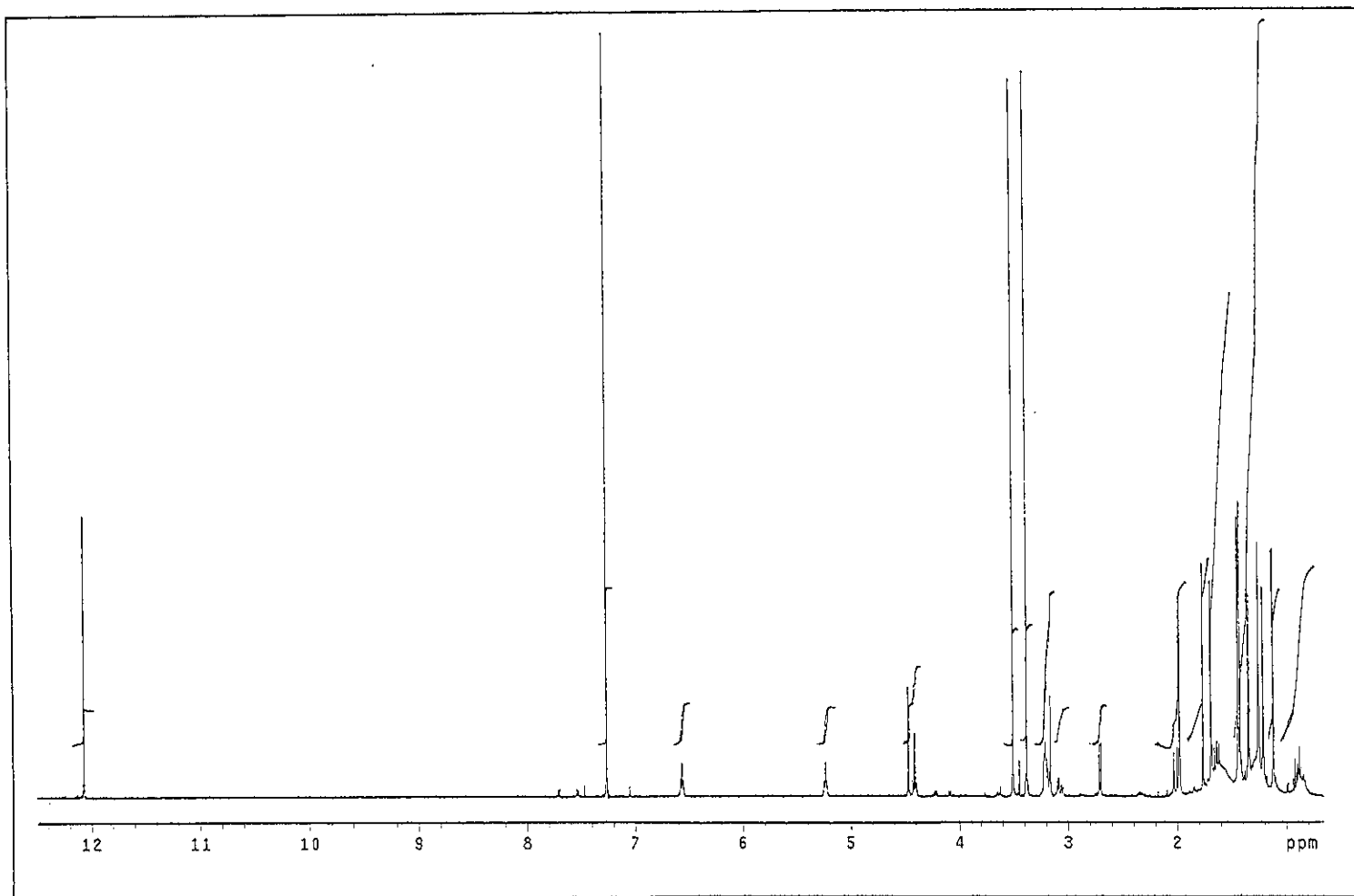
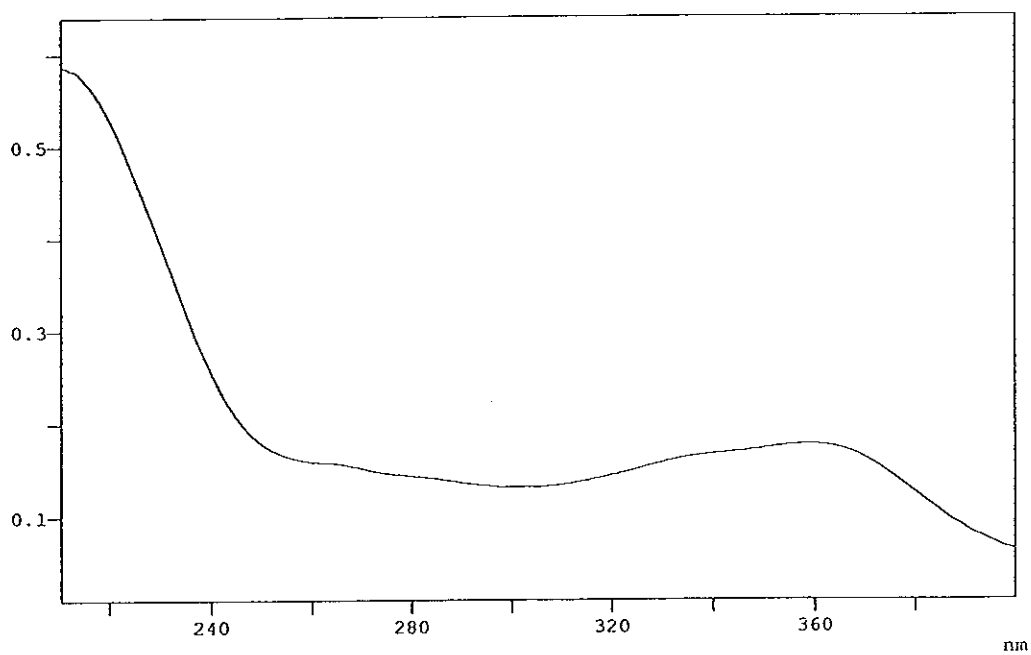
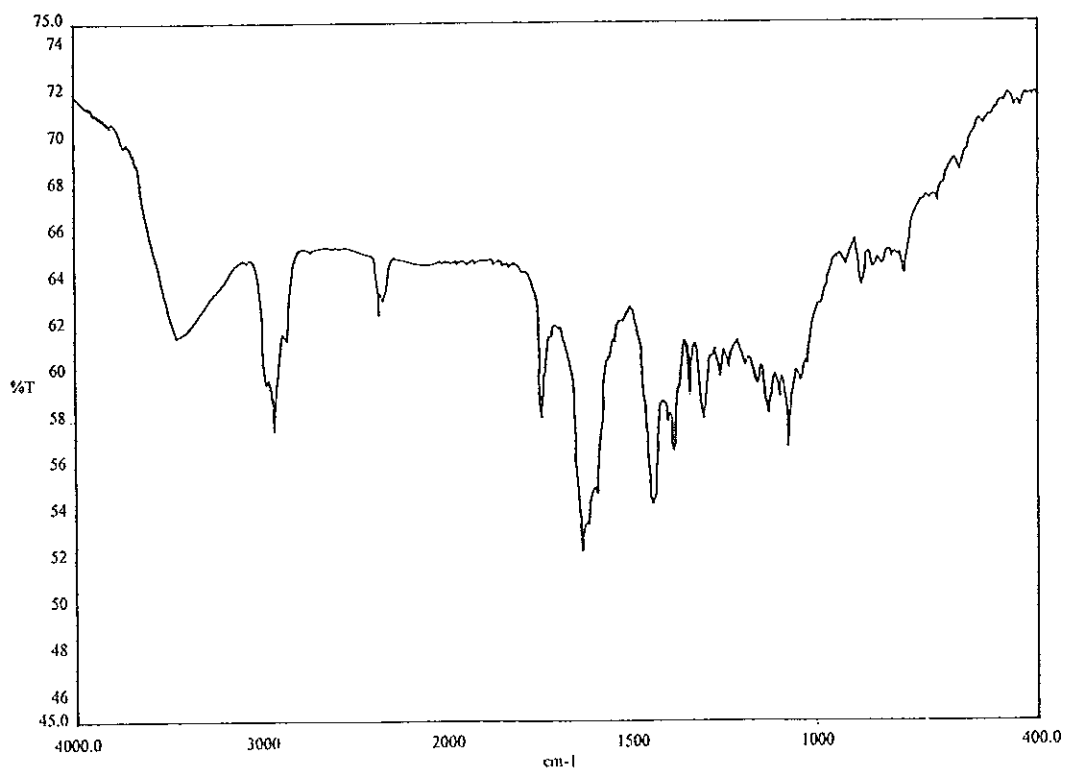


Figure 40 ^1H NMR (500 MHz) (CDCl_3) spectrum of DD12

Abs

**Figure 41 UV (MeOH) spectrum of DD1****Figure 42 FT-IR (neat) spectrum of DD1**

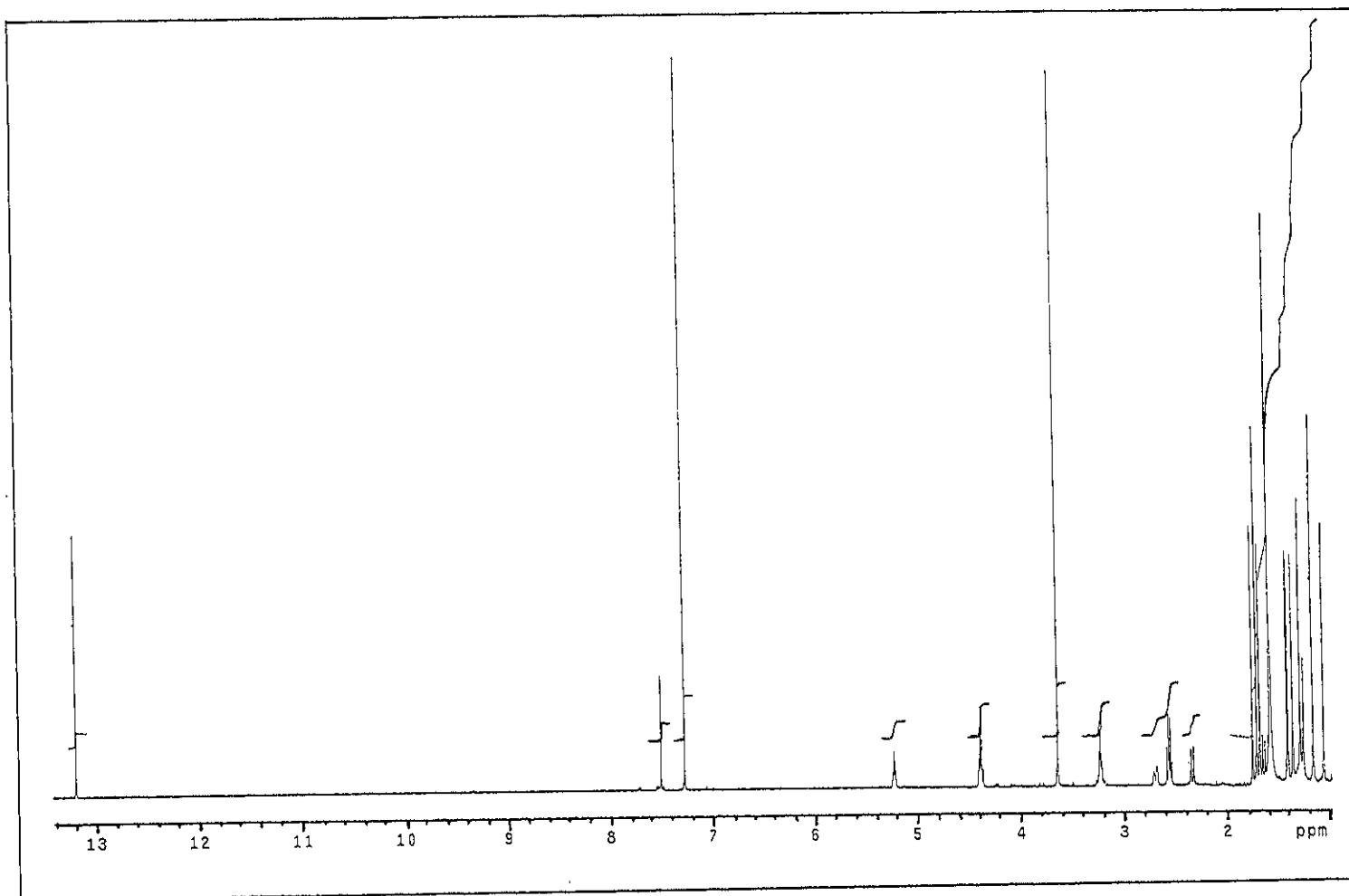


Figure 43 ^1H NMR (500 MHz) (CDCl_3) spectrum of DD1

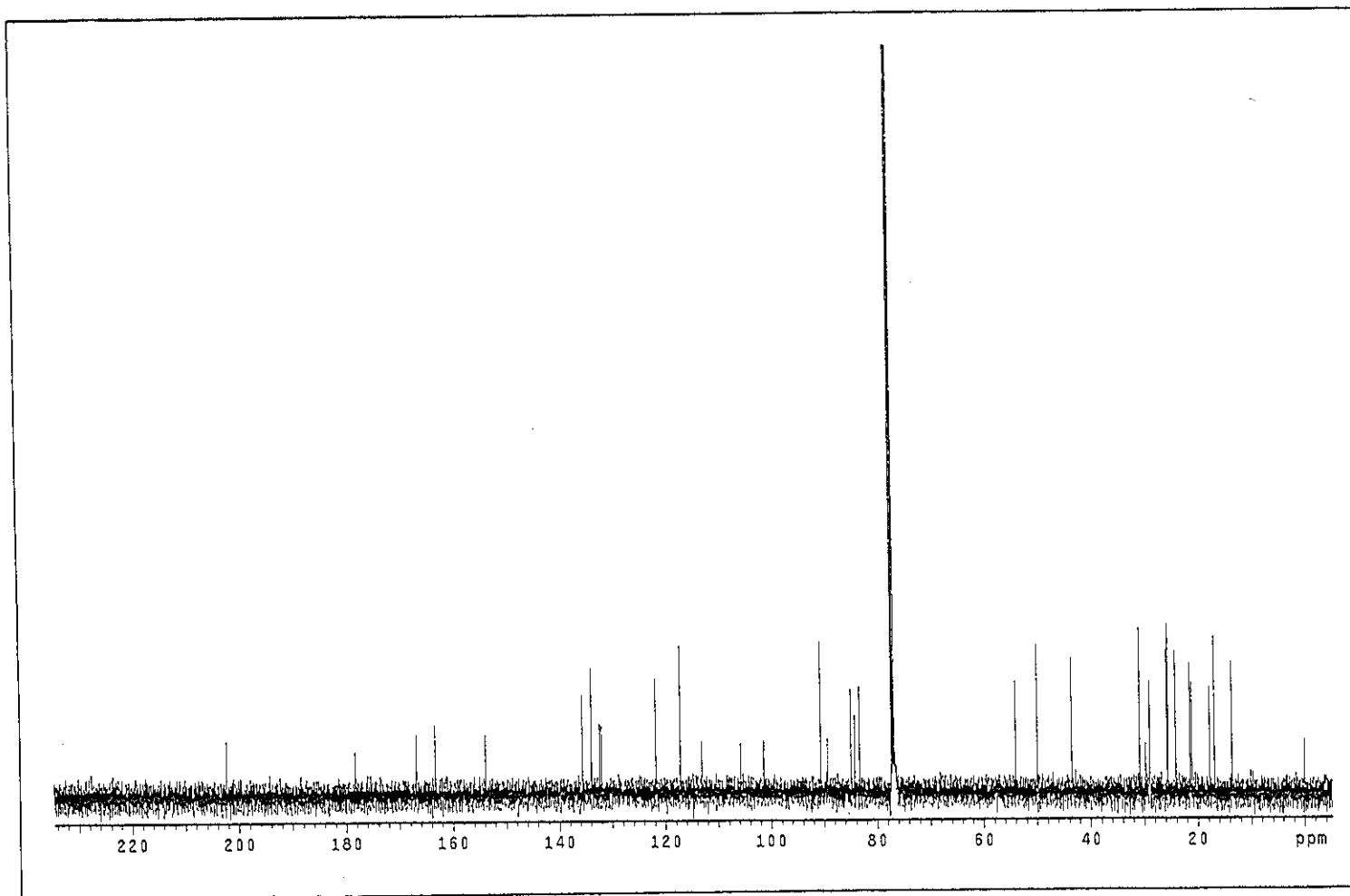
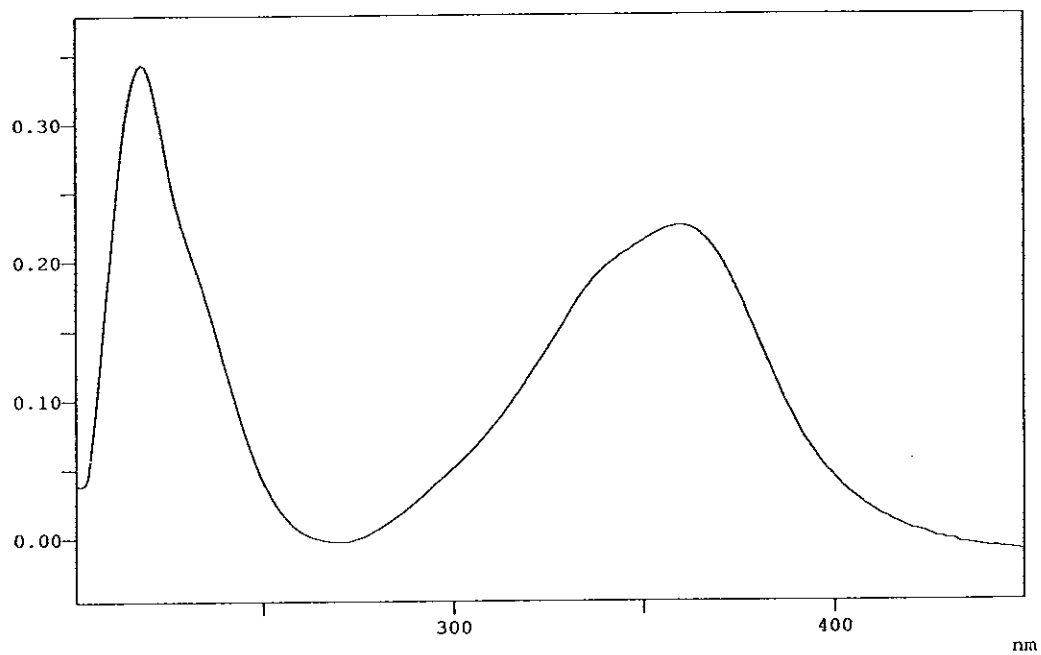
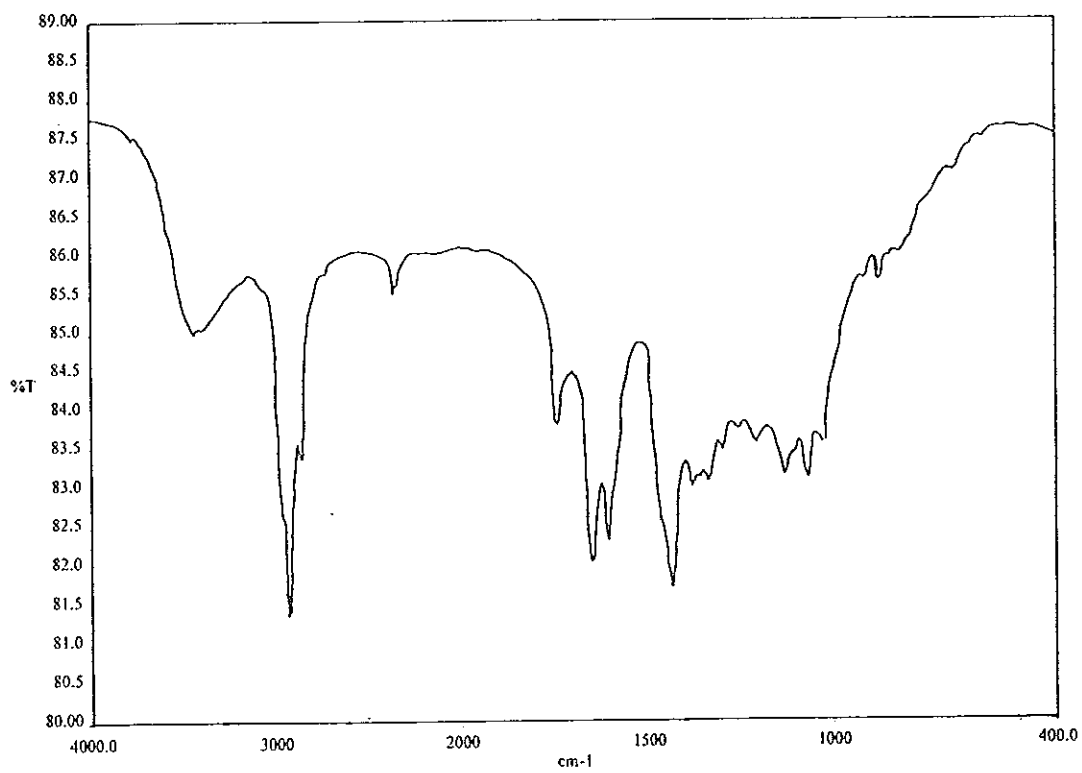


Figure 44 ^{13}C NMR (125 MHz) (CDCl_3) spectrum of DD1

Abs

**Figure 45 UV (MeOH) spectrum of DD3****Figure 46 FT-IR (neat) spectrum of DD3**

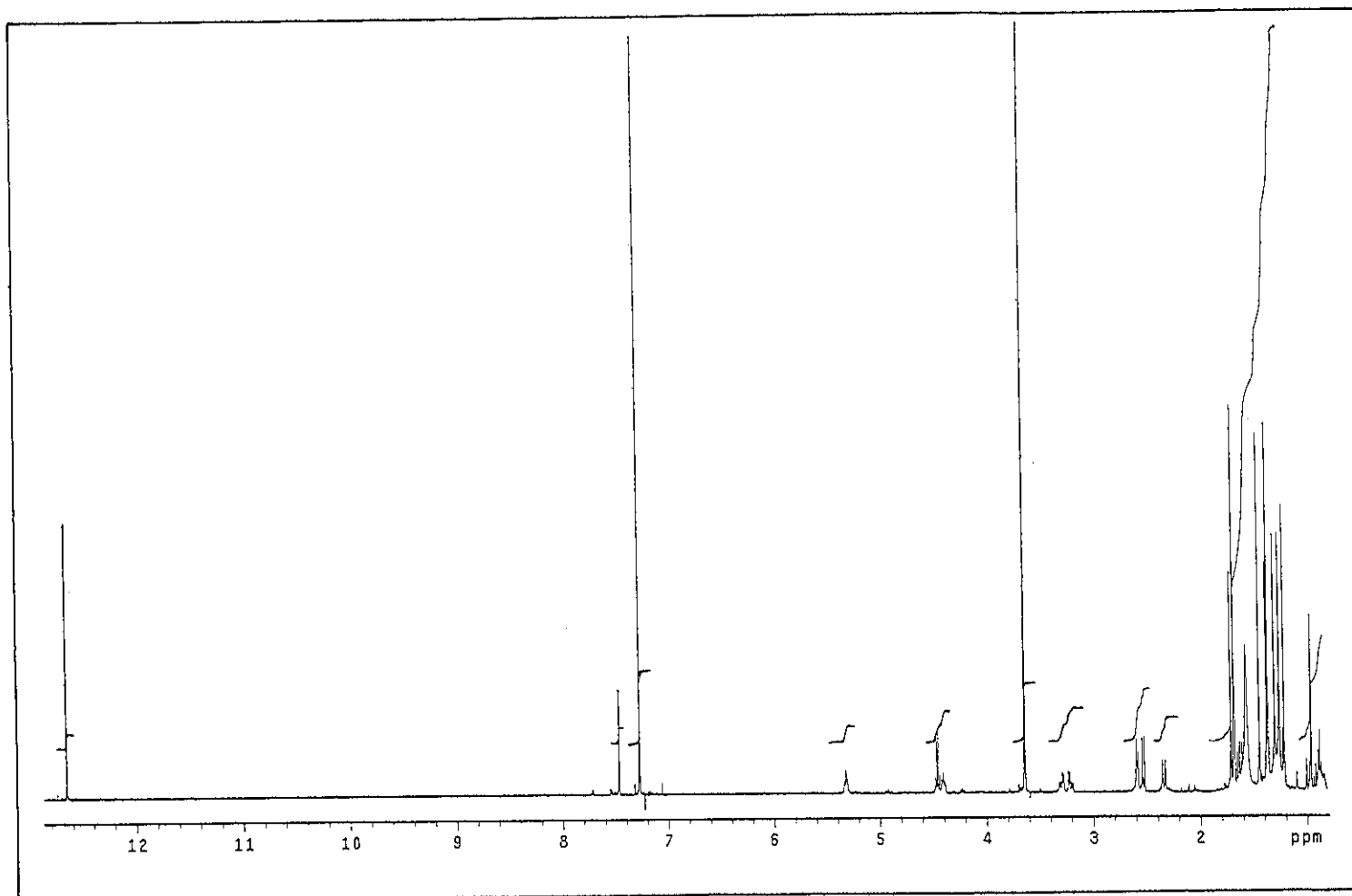


Figure 47 ^1H NMR (500 MHz) (CDCl_3) spectrum of DD3

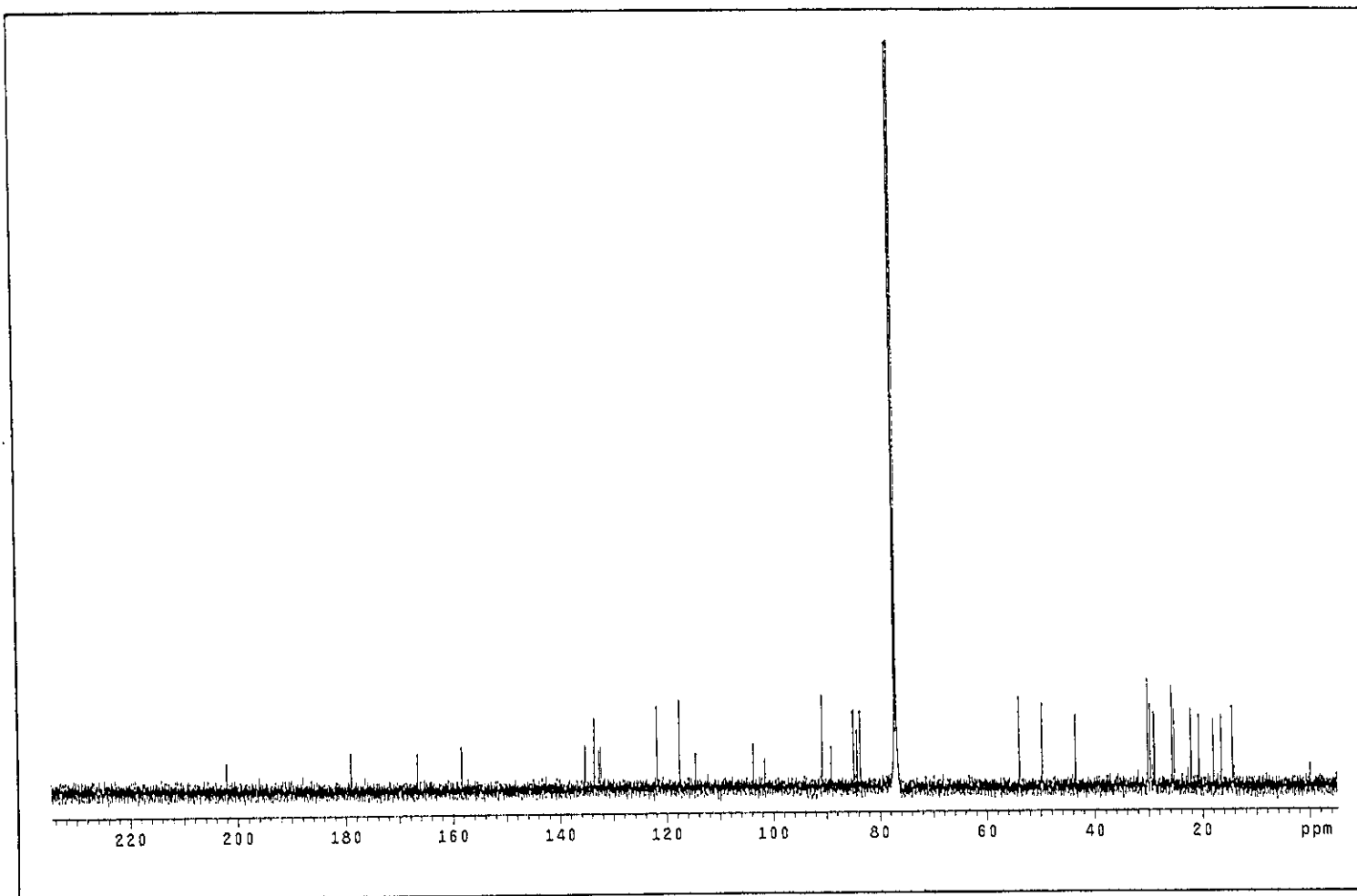


Figure 48 ^{13}C NMR (125 MHz) (CDCl_3) spectrum of DD3

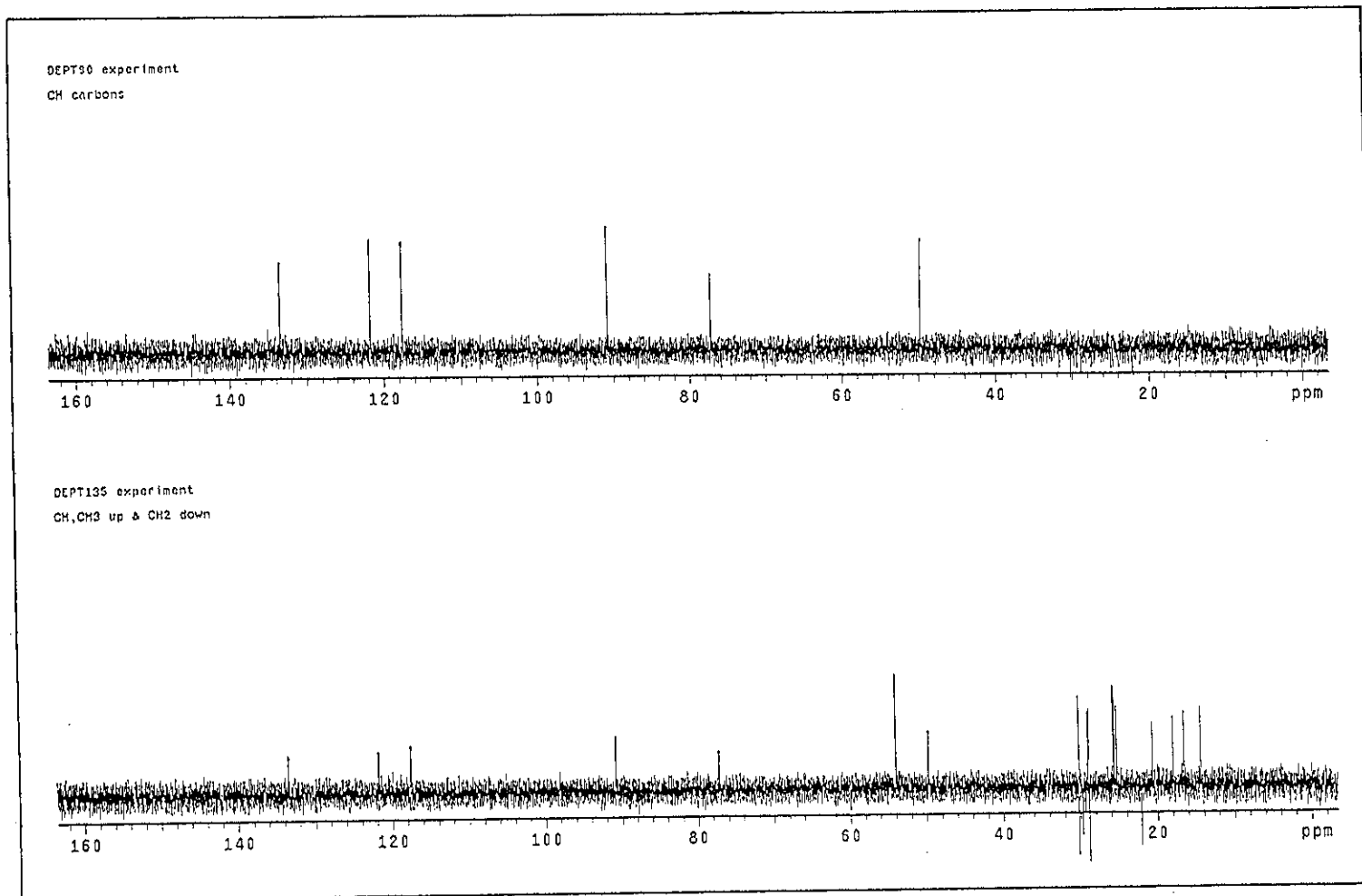


Figure 49 DEPT spectrum of DD3

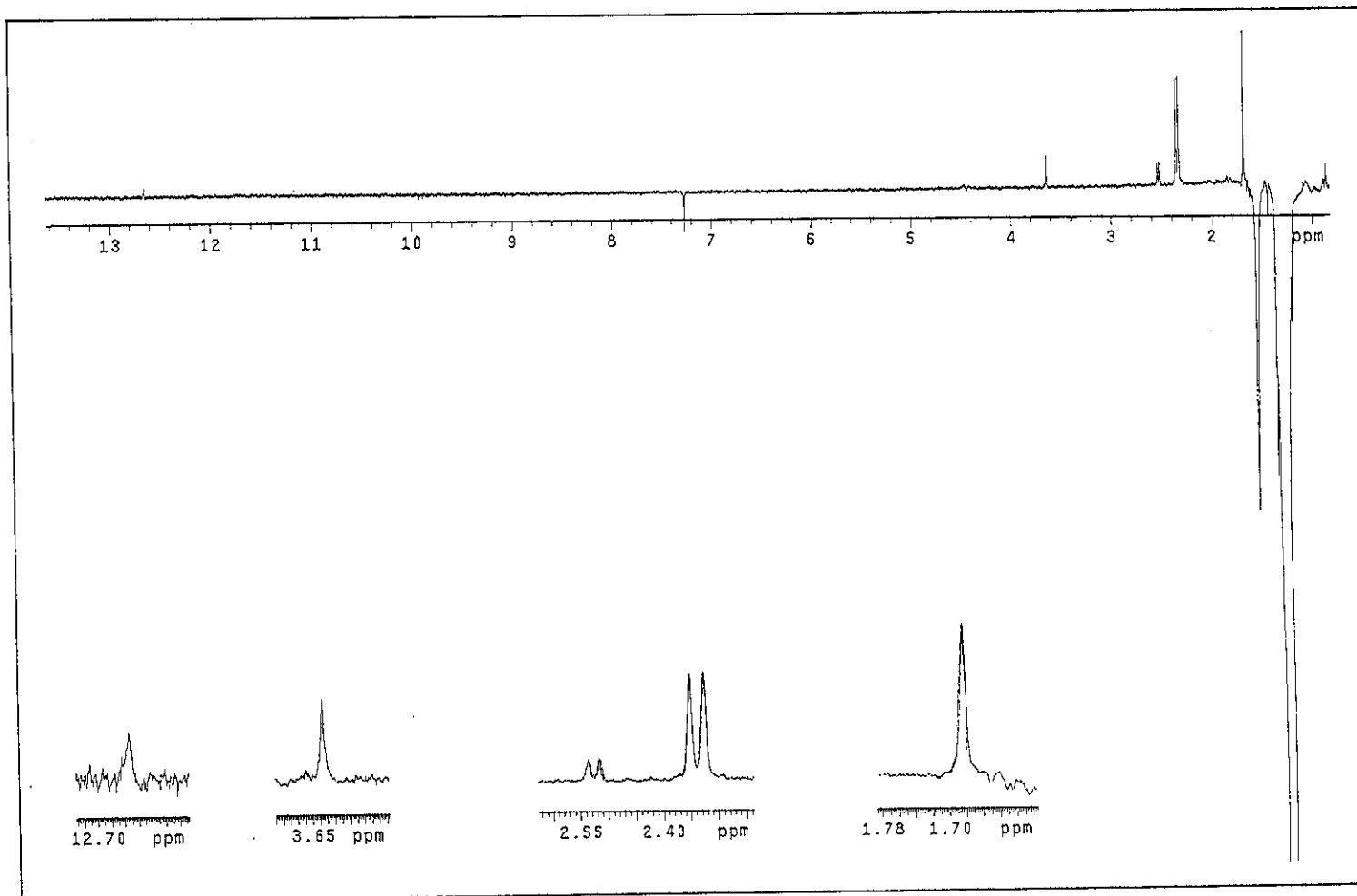


Figure 50 NOEDIFF spectrum of DD3 after irradiation at δ_H 1.30

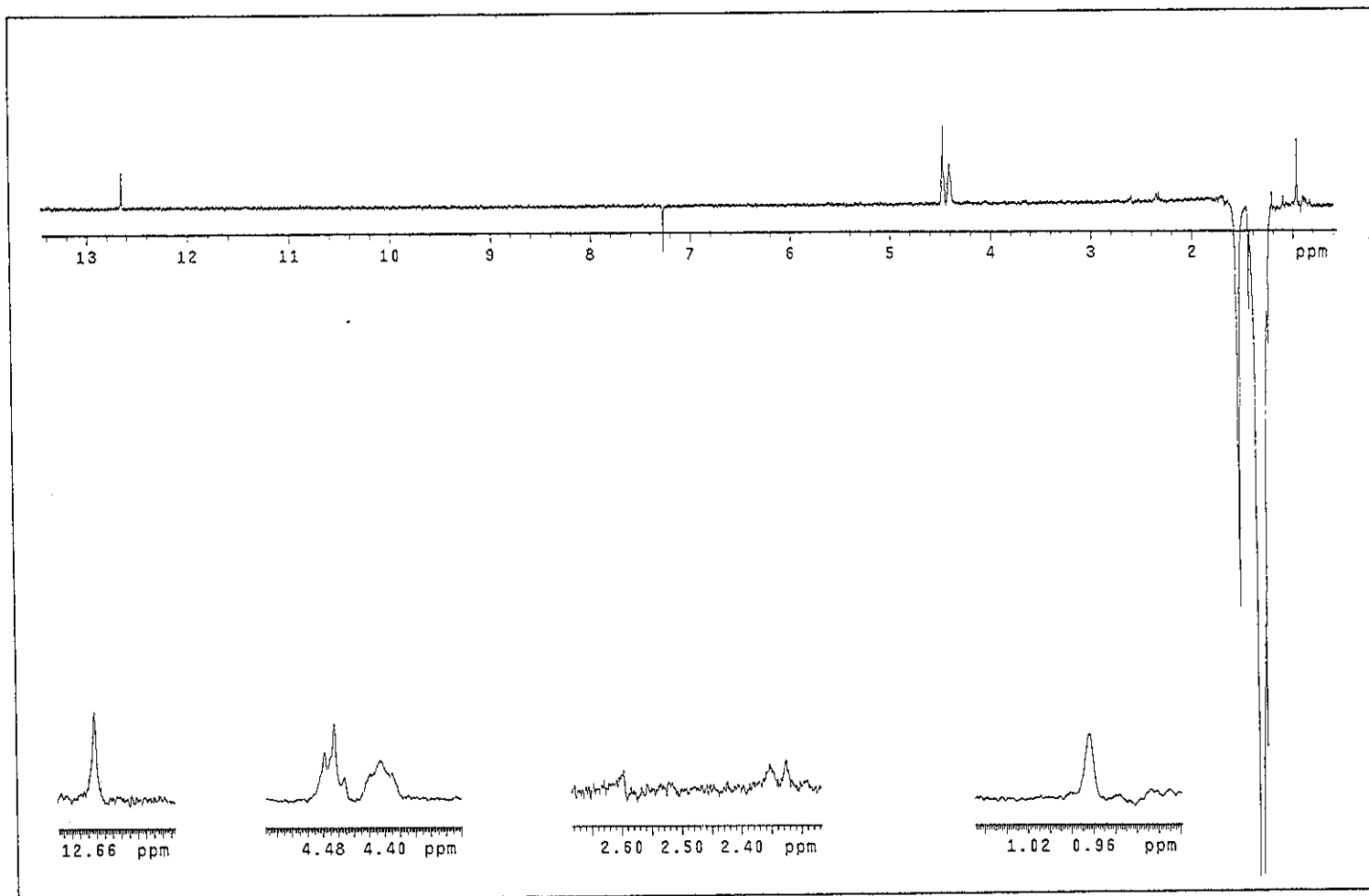


Figure 51 NOEDIFF spectrum of DD3 after irradiation at δ_H 1.37

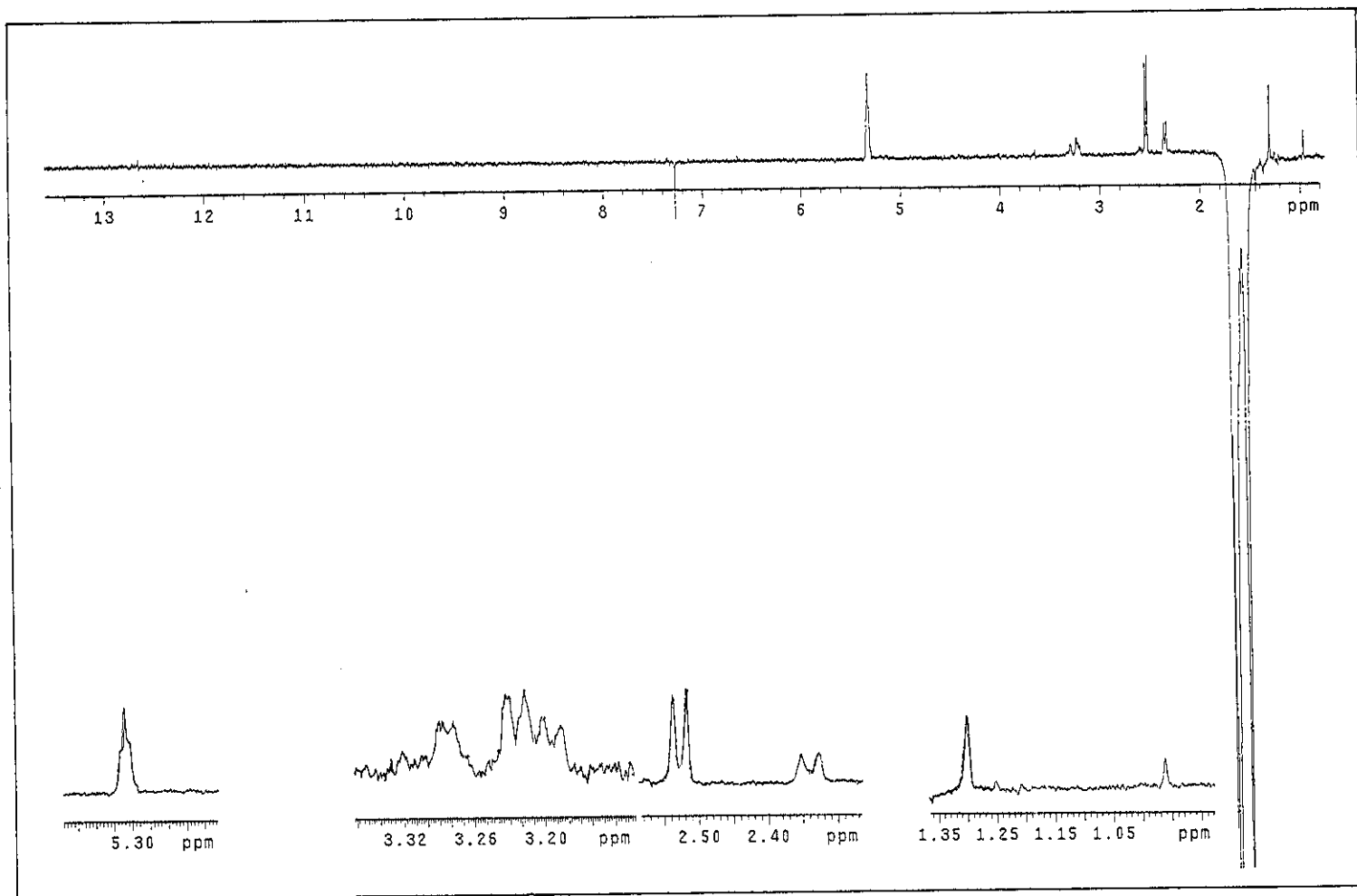


Figure 52 NOEDIFF spectrum of DD3 after irradiation at δ_H 1.68

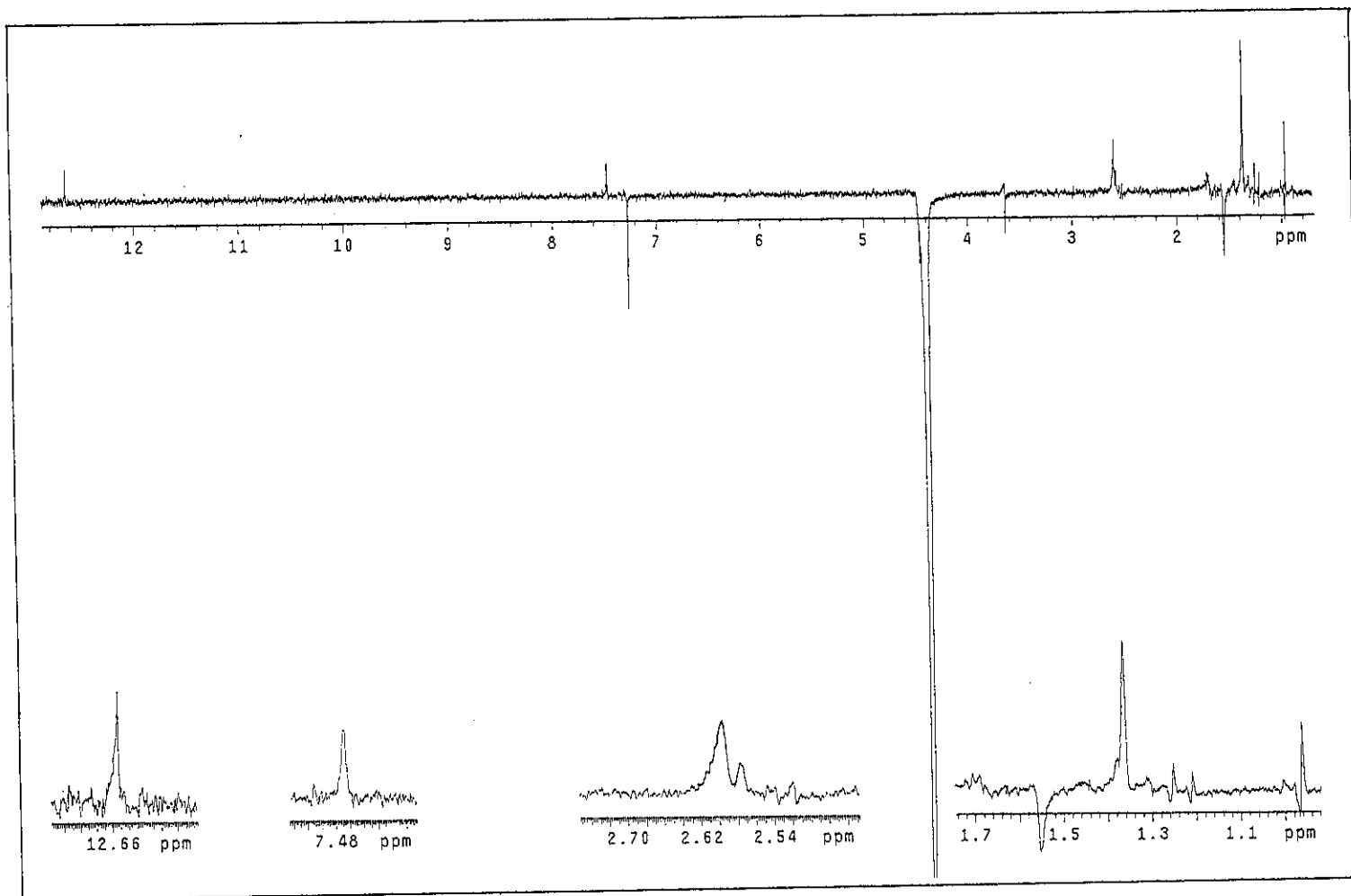


Figure 53 NOEDIFF spectrum of DD3 after irradiation at δ_H 4.40

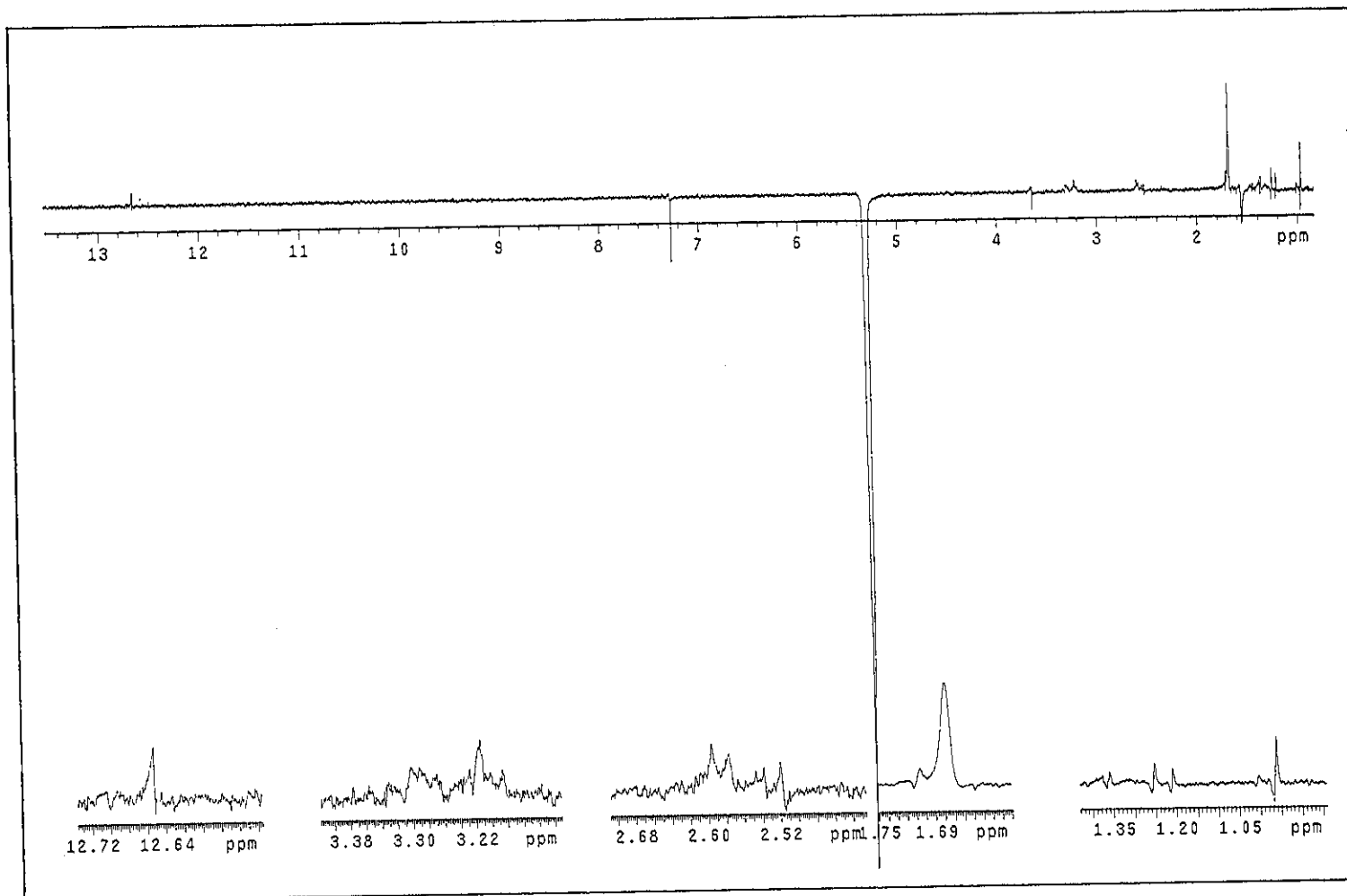


Figure 54 NOEDIFF spectrum of DD3 after irradiation at δ_H 5.32

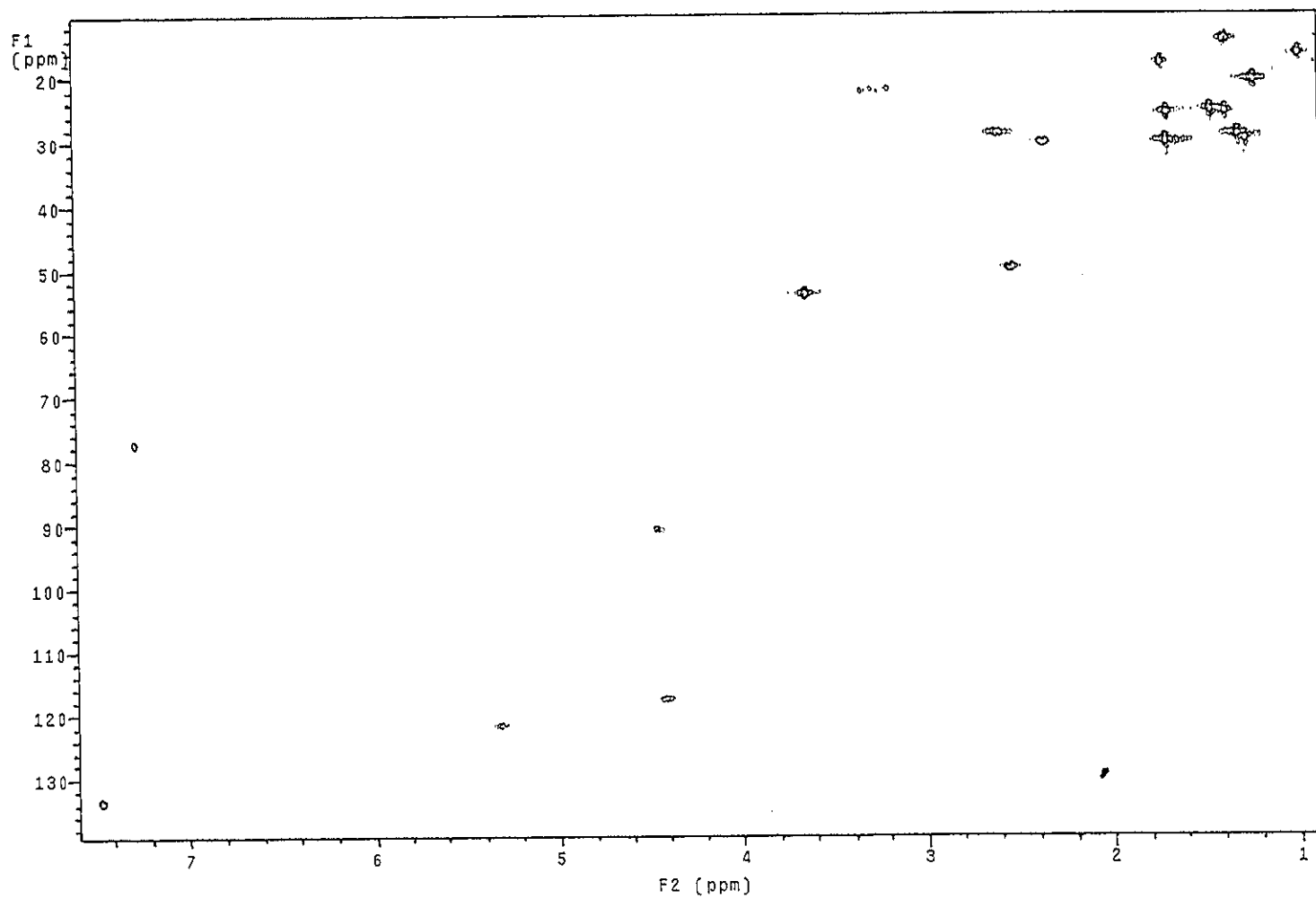


Figure 55 2D HMQC spectrum of DD3

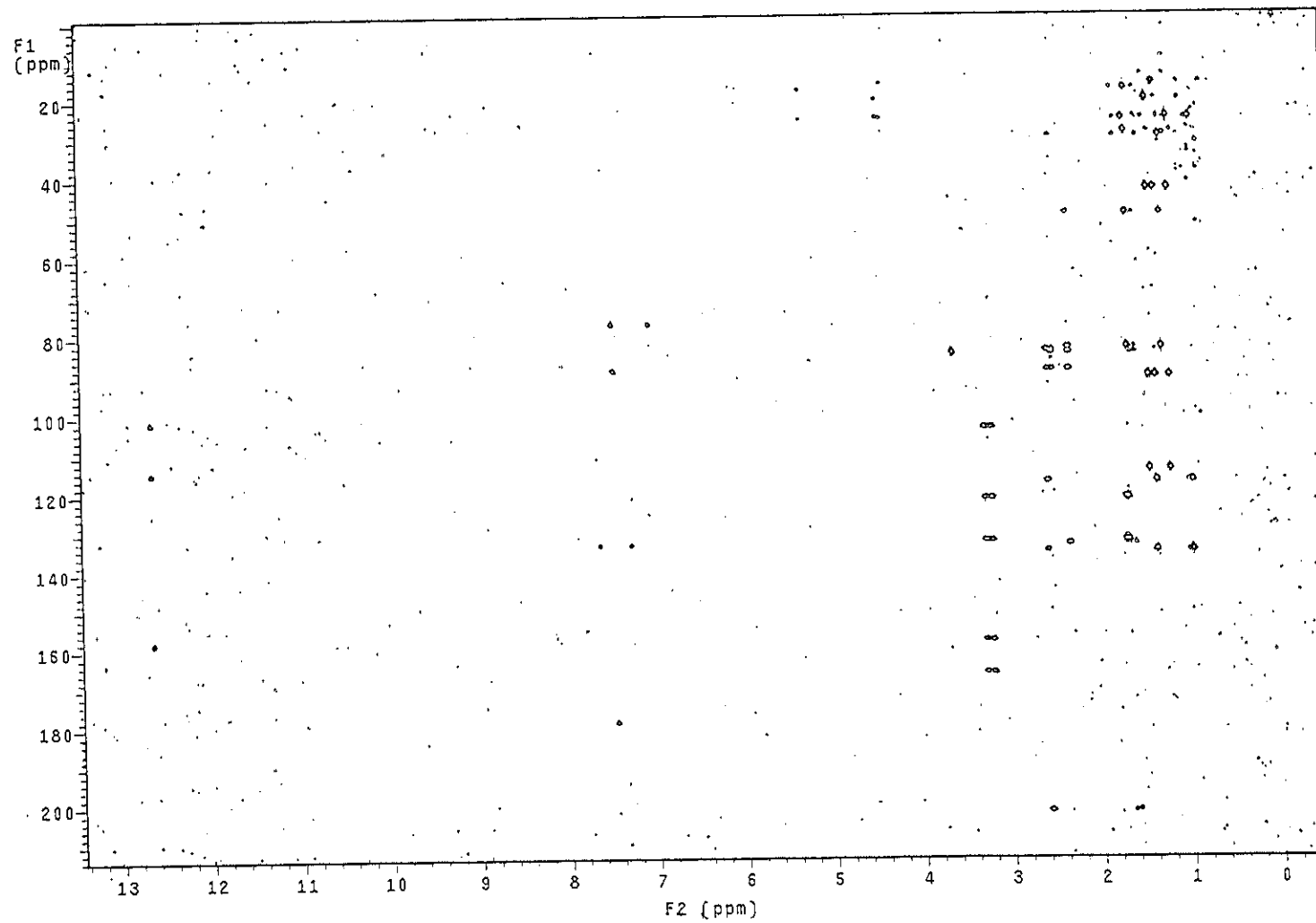


Figure 56 2D HMBC spectrum of DD3

Scan # : (9 - 58)
Mass Peak # : 571 Ret. Time : (0.401 - 3.396)
Base Peak : 85.05 (1729079)

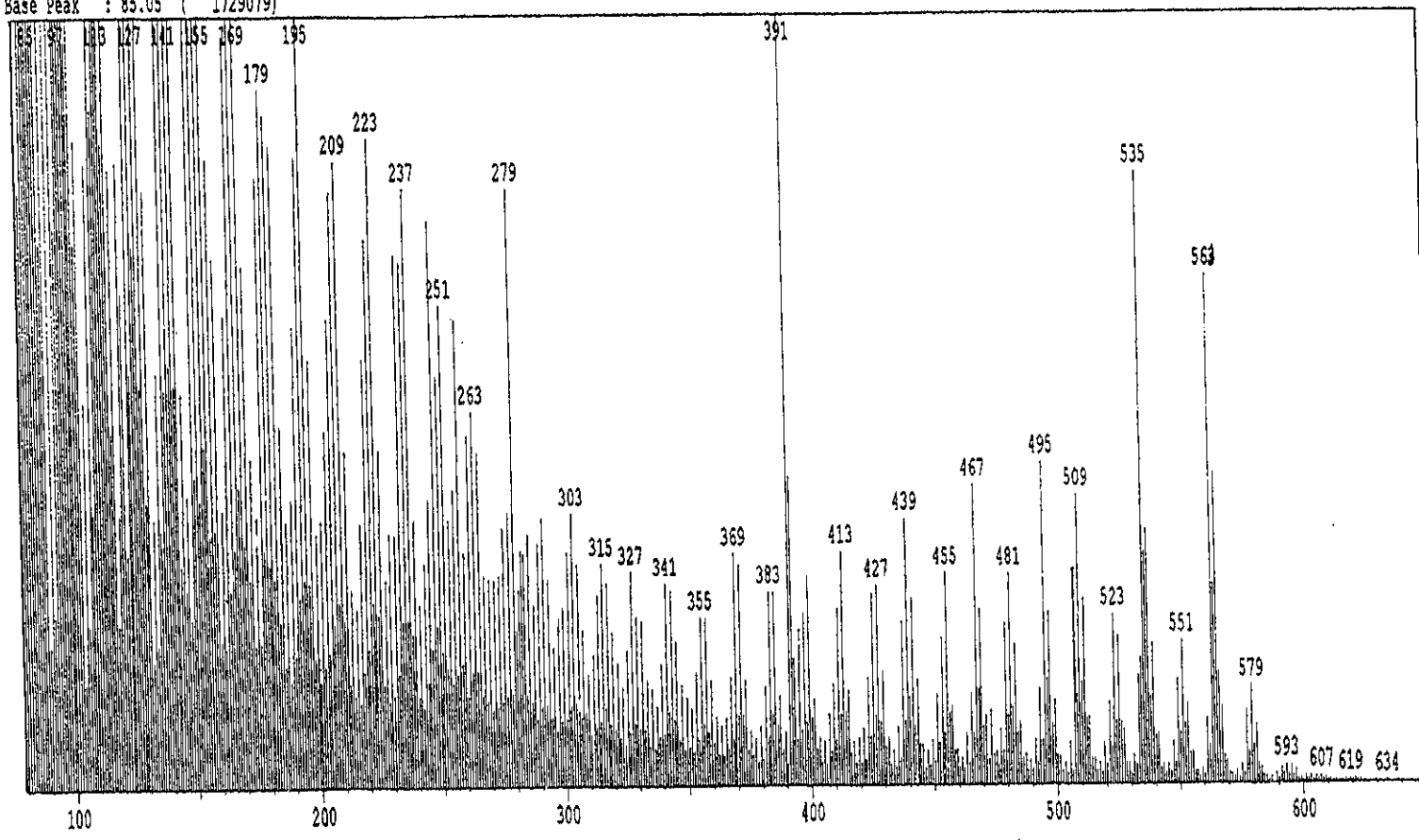


Figure 57 Mass spectrum of DD3

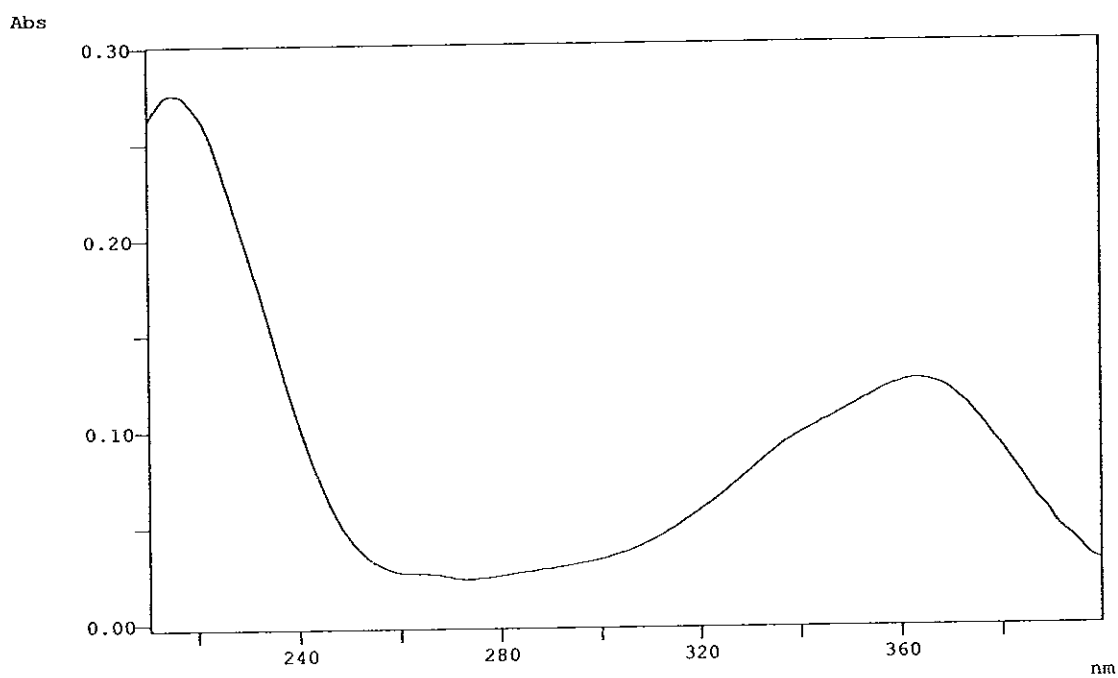


Figure 58 UV (MeOH) spectrum of DD5

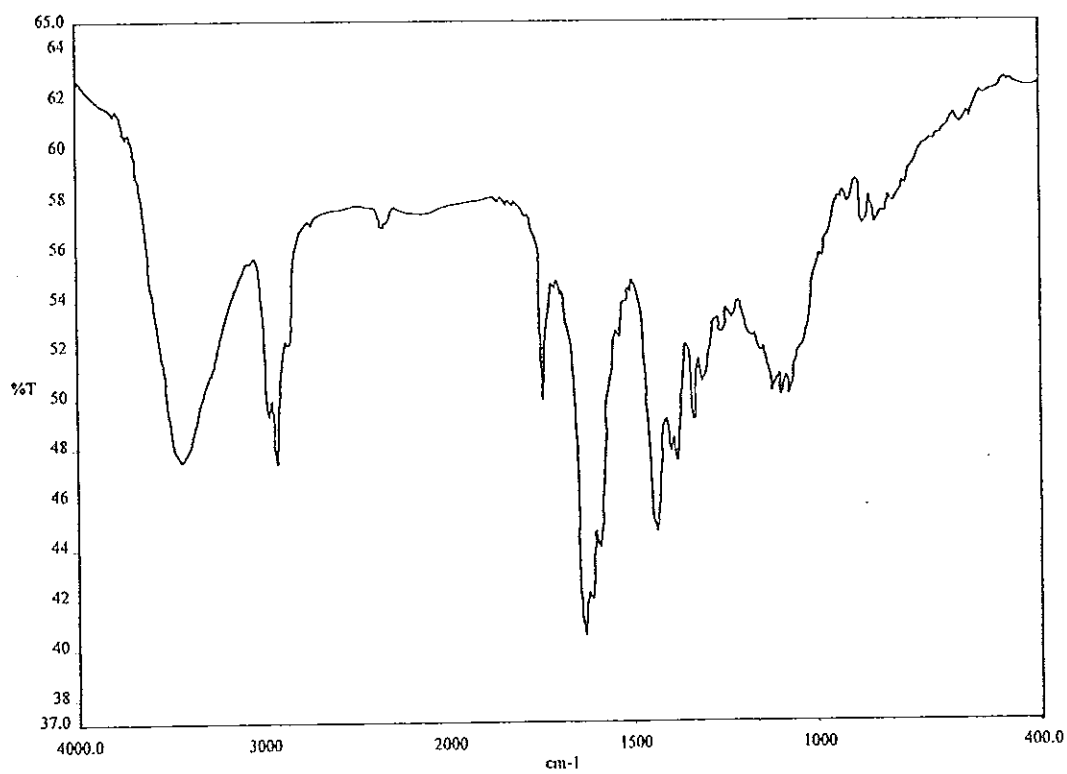


Figure 59 FT-IR (neat) spectrum of DD5

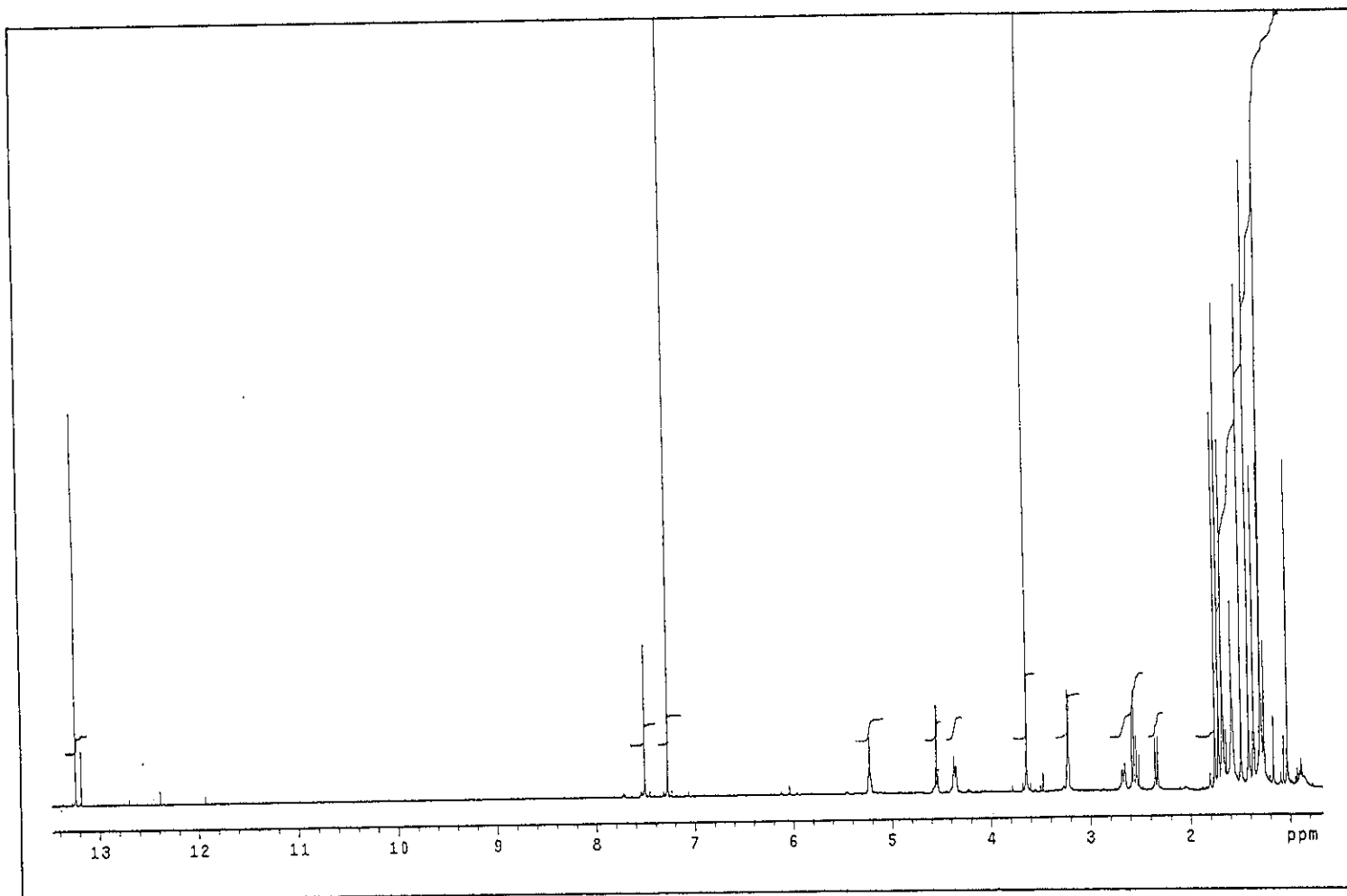


Figure 60 ^1H NMR (500 MHz) (CDCl_3) spectrum of DD5

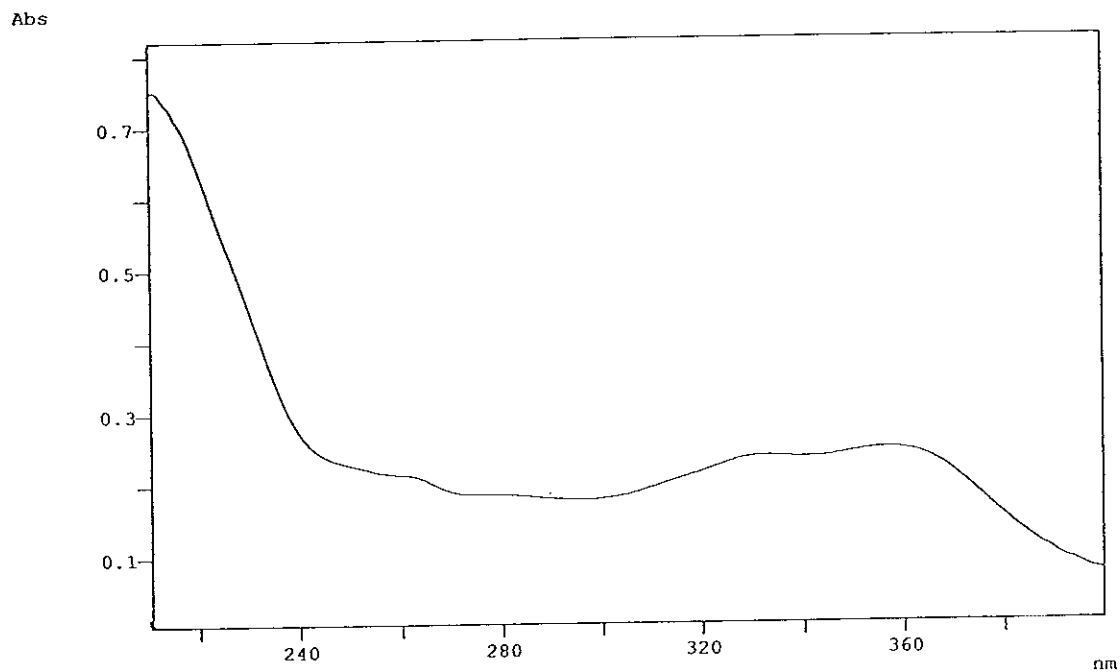


Figure 61 UV (MeOH) spectrum of DD8

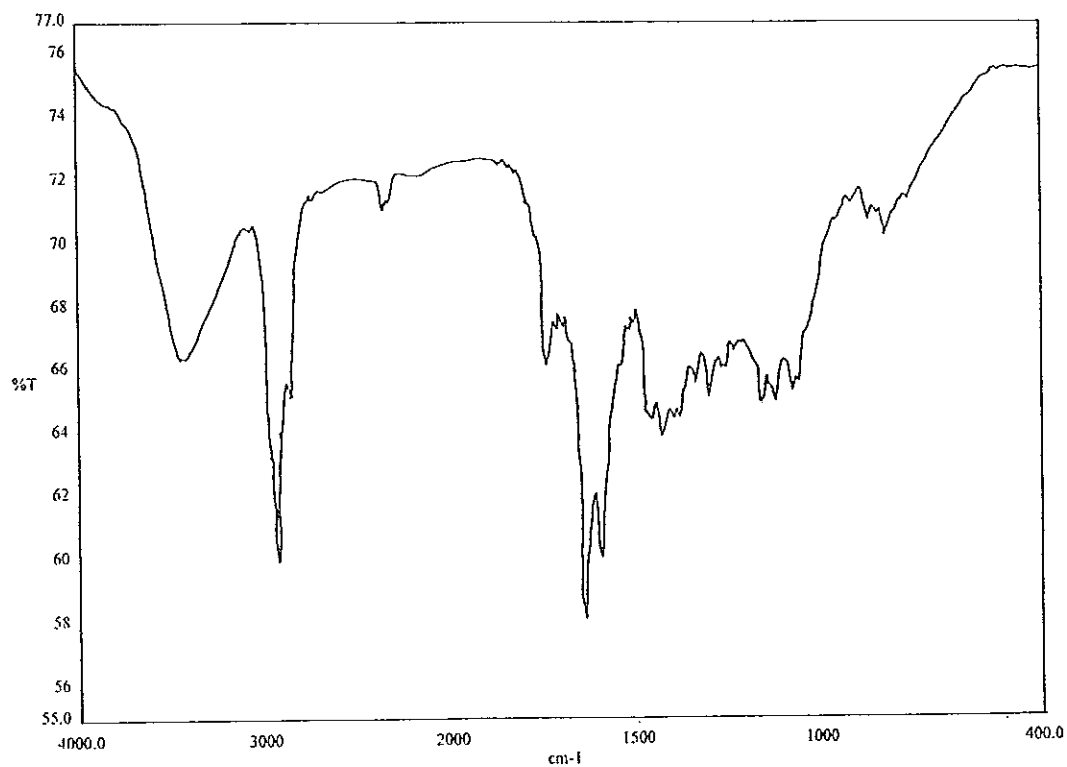


Figure 62 FT-IR (neat) spectrum of DD8

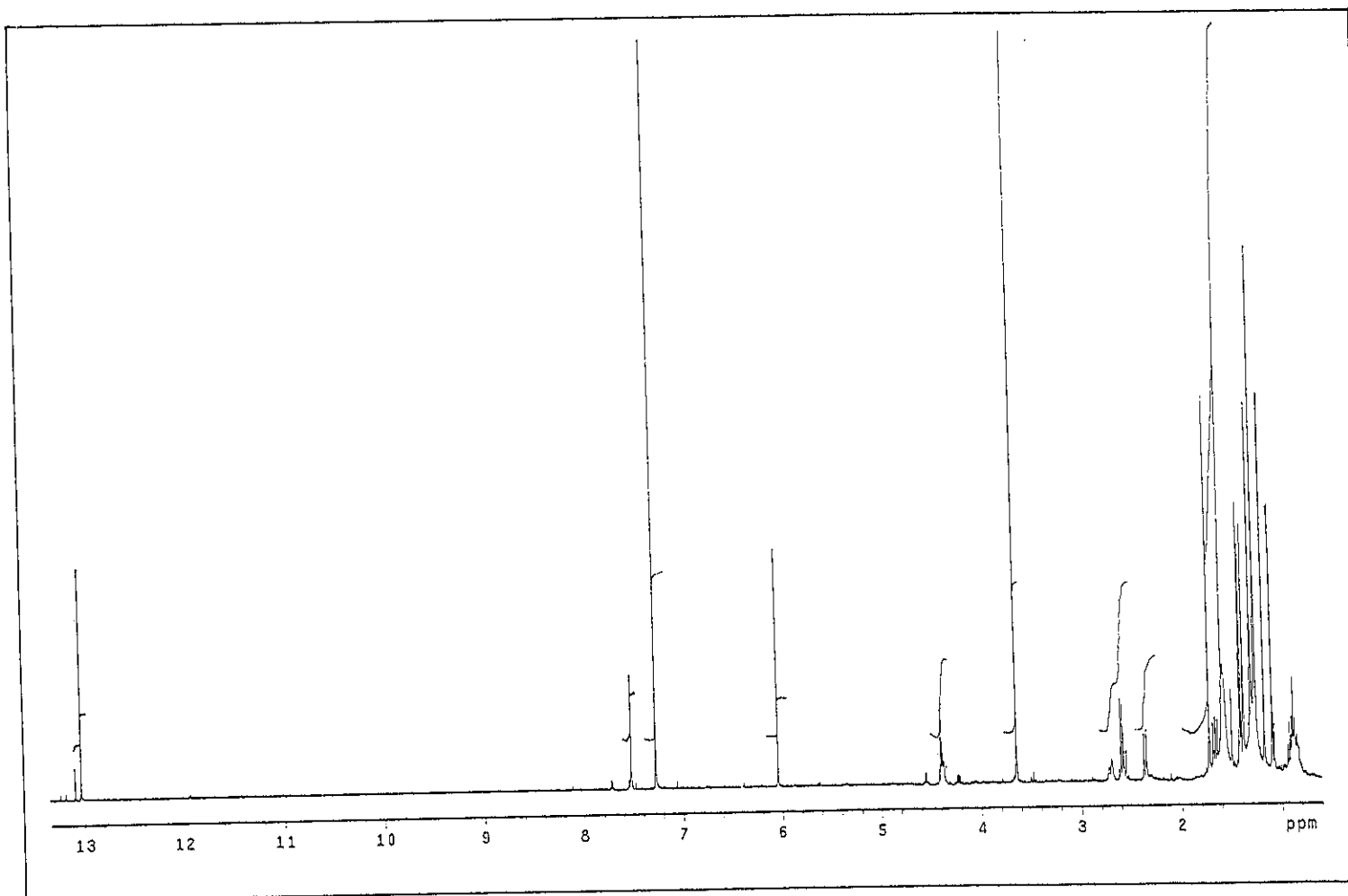


Figure 63 ^1H NMR (500 MHz) (CDCl_3) spectrum of DD8

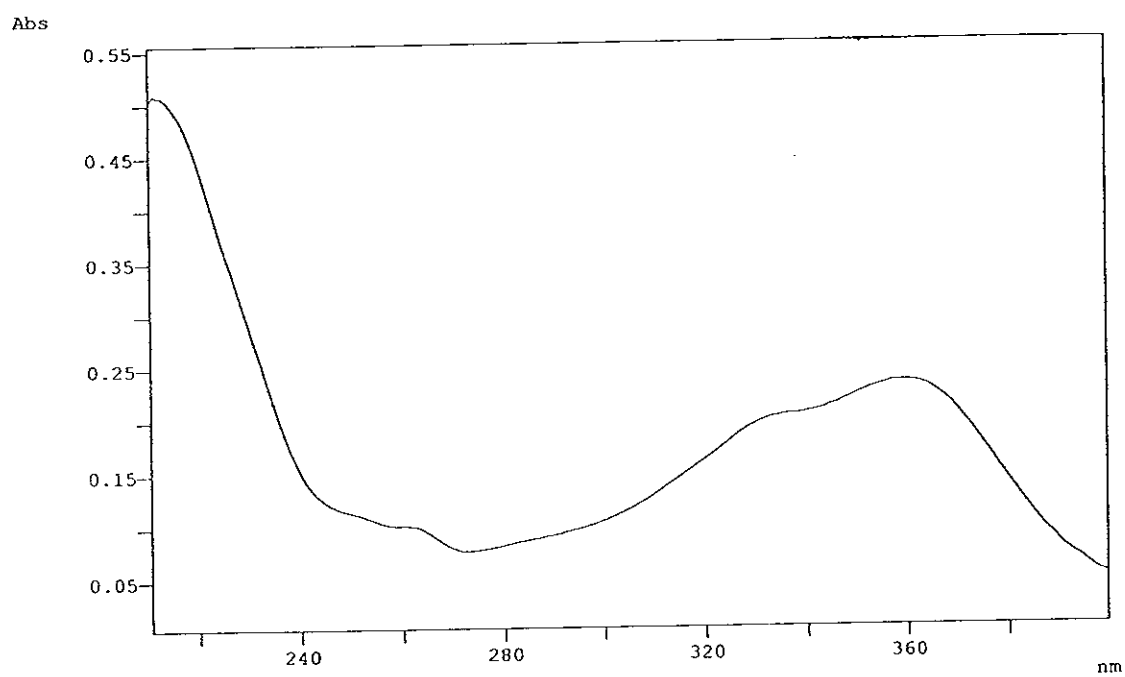


Figure 64 UV (MeOH) spectrum of DD9

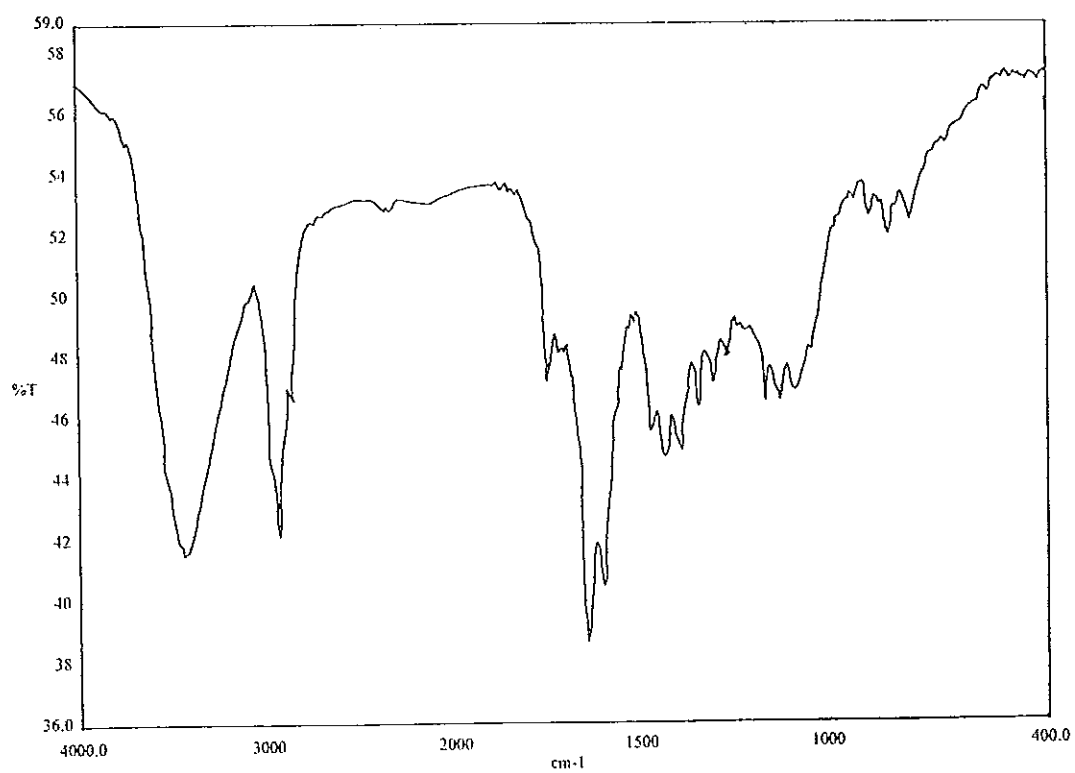


Figure 65 FT-IR (neat) spectrum of DD9

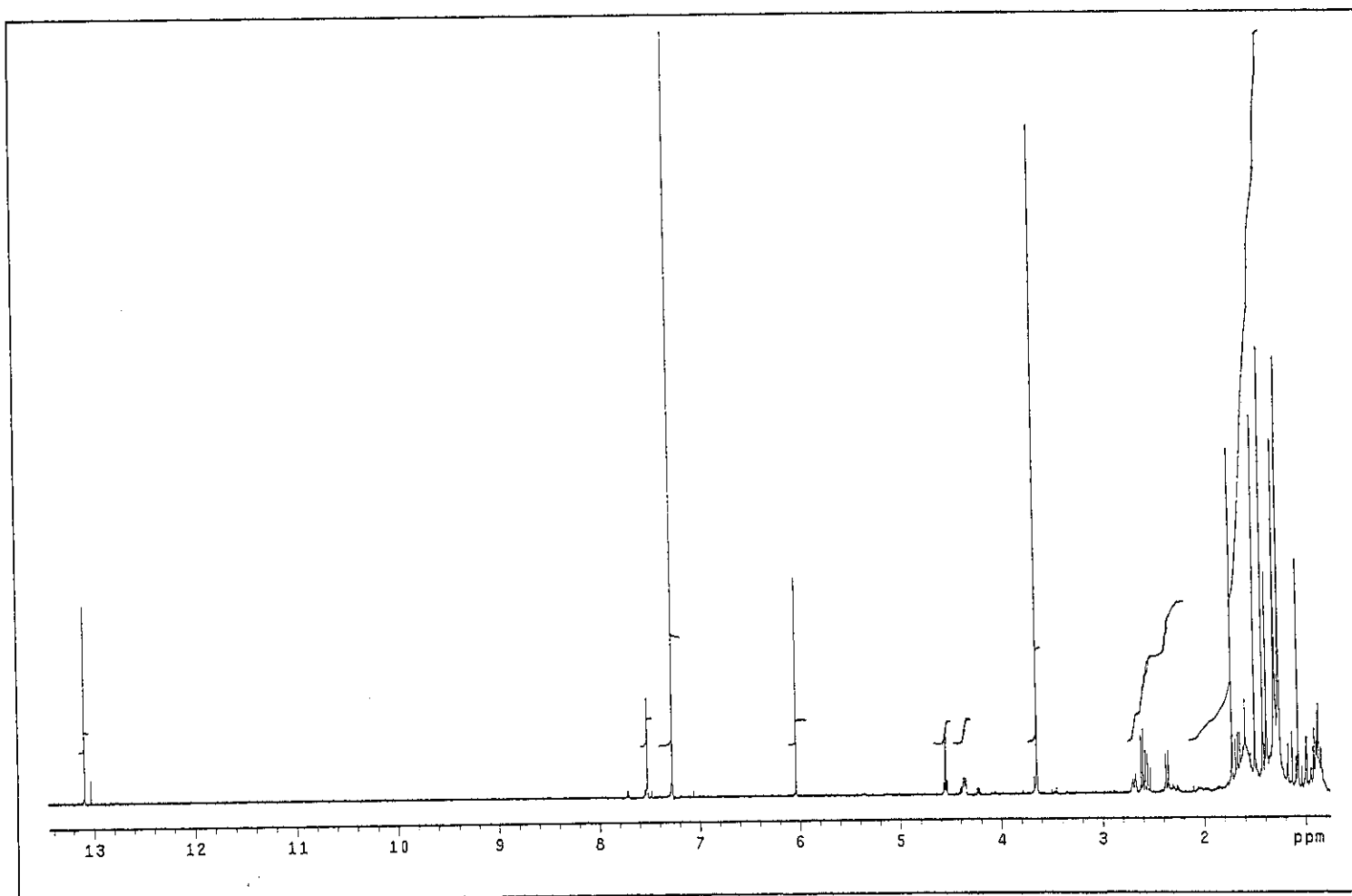


Figure 66 ^1H NMR (500 MHz) (CDCl_3) spectrum of DD9

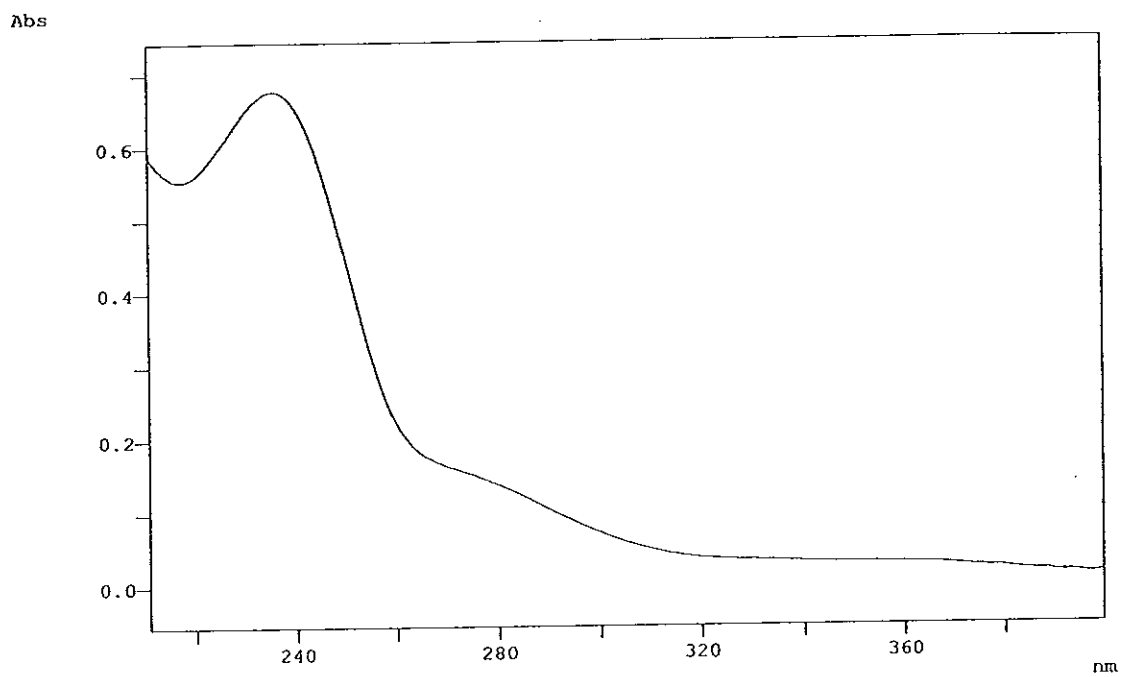


Figure 67 UV (MeOH) spectrum of DD7

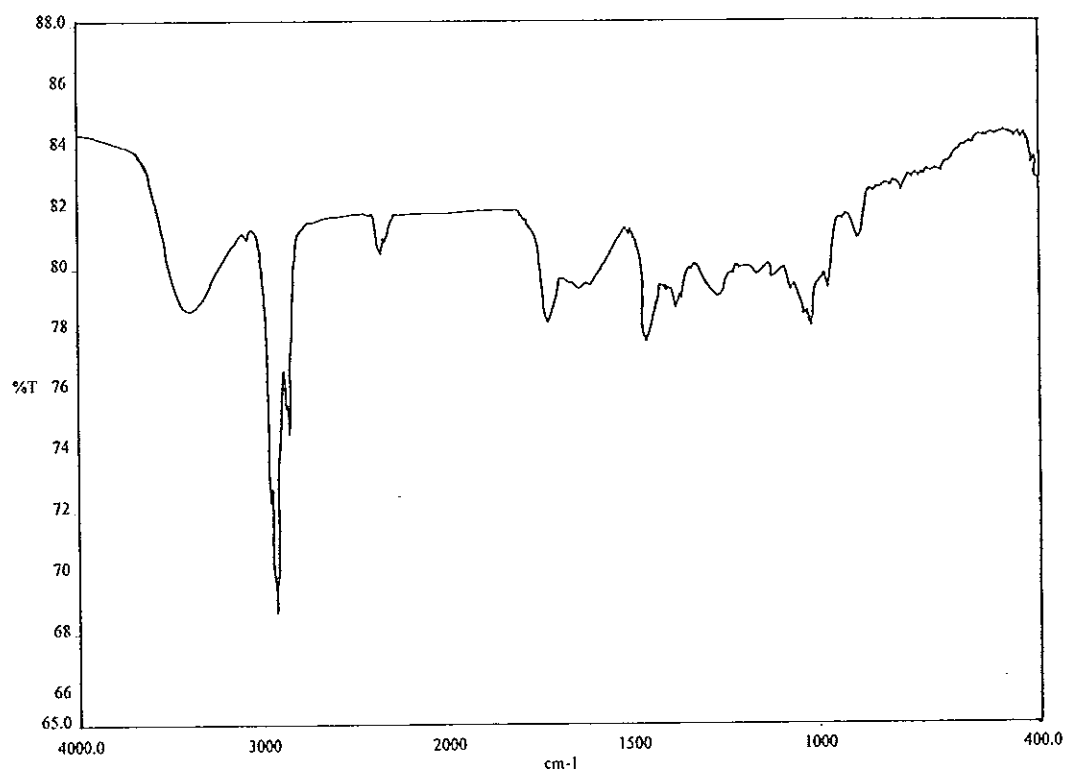


Figure 68 FT-IR (neat) spectrum of DD7

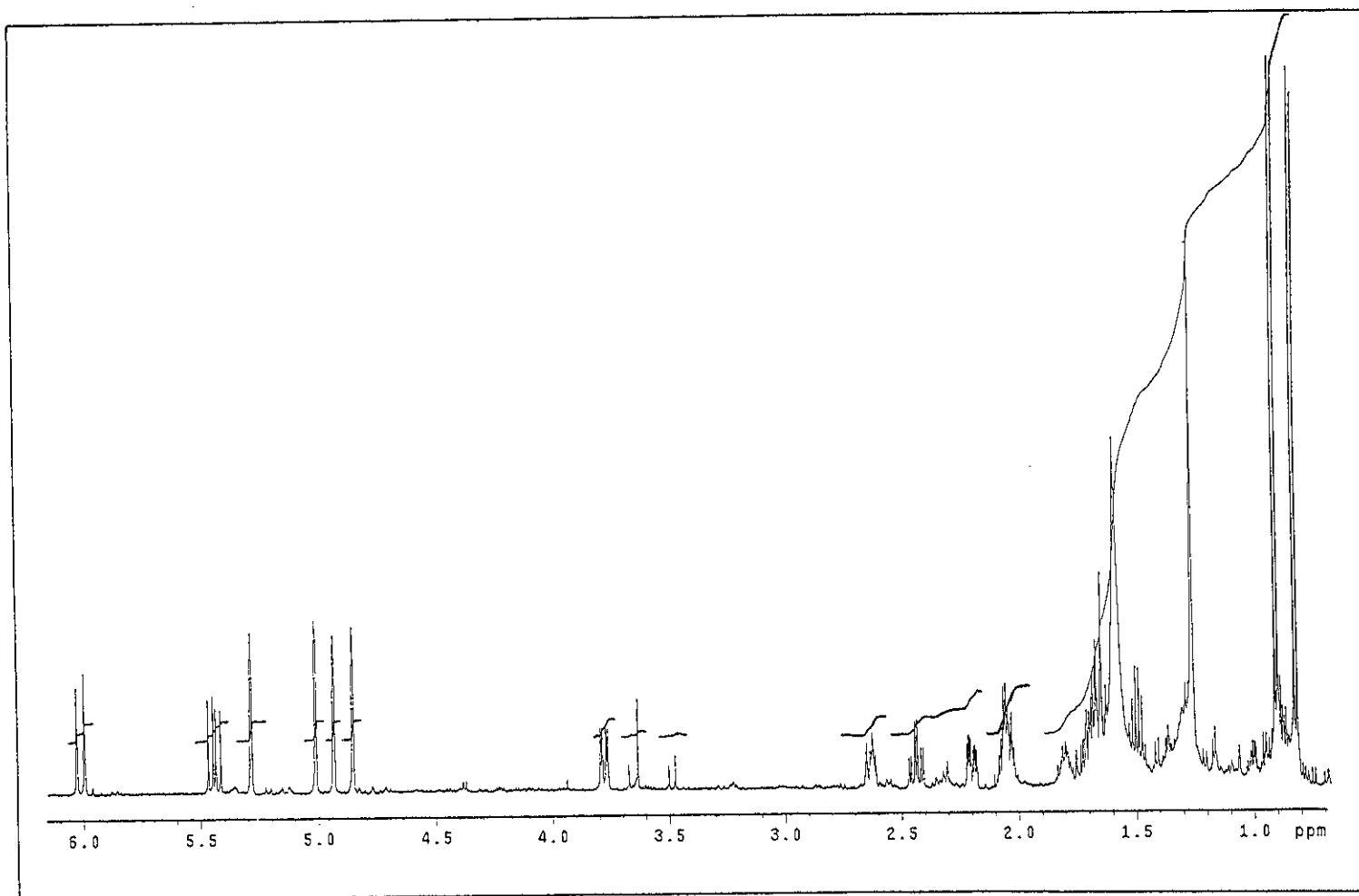


Figure 69 ^1H NMR (500 MHz) (CDCl_3) spectrum of DD7

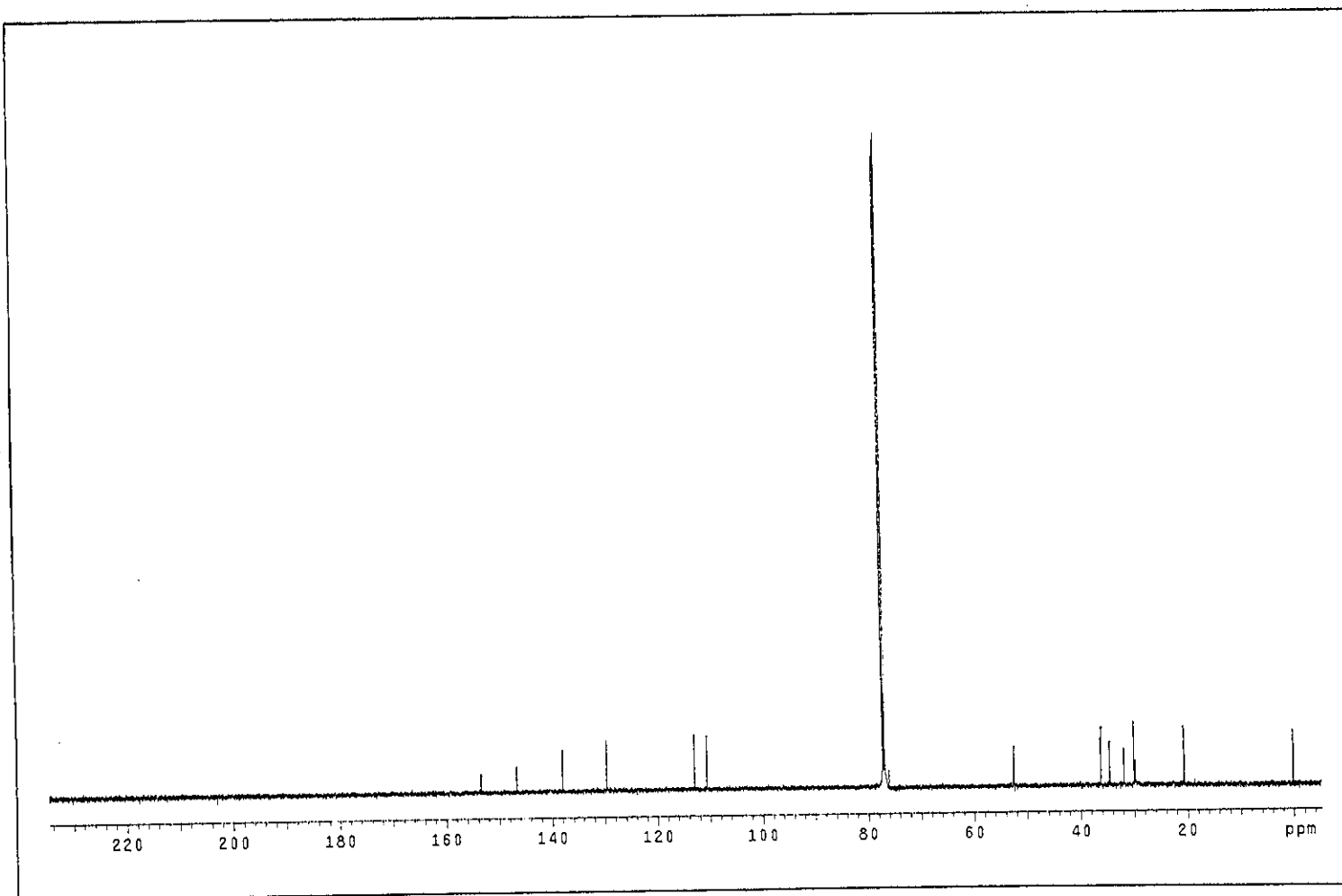


Figure 70 ^{13}C NMR (125 MHz) (CDCl_3) spectrum of DD7

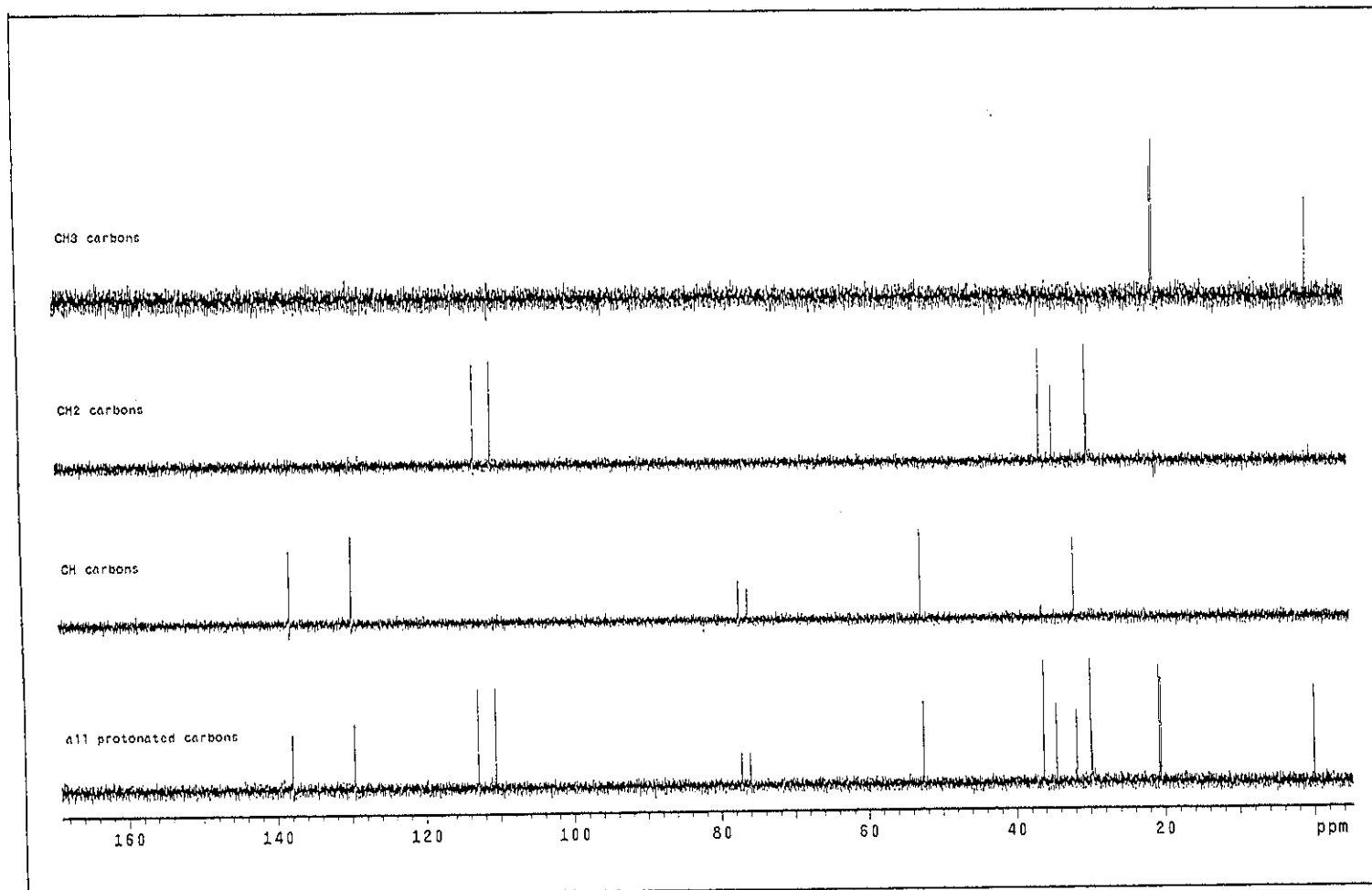


Figure 71 DEPT spectrum of DD7

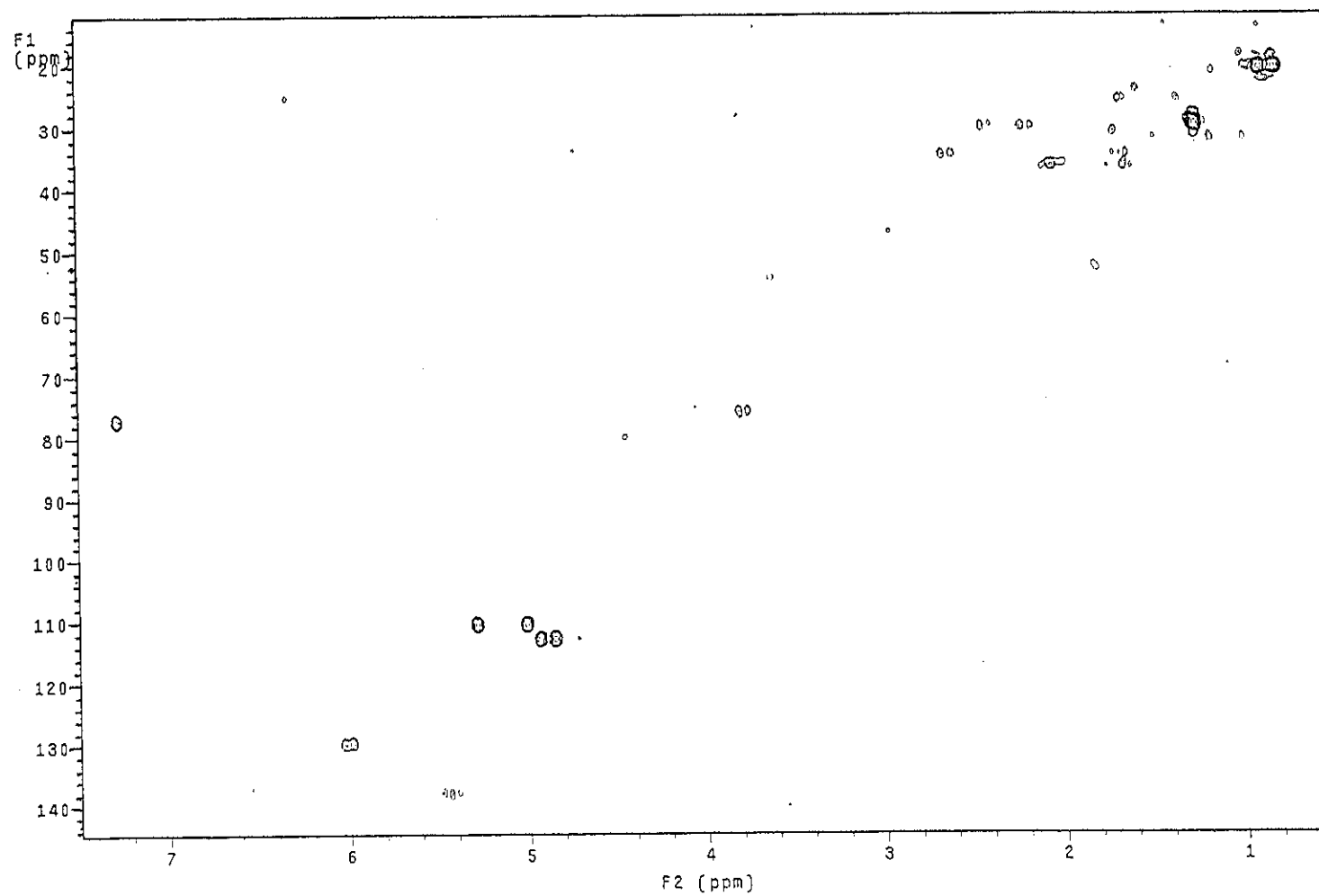


Figure 72 2D HMQC spectrum of DD7

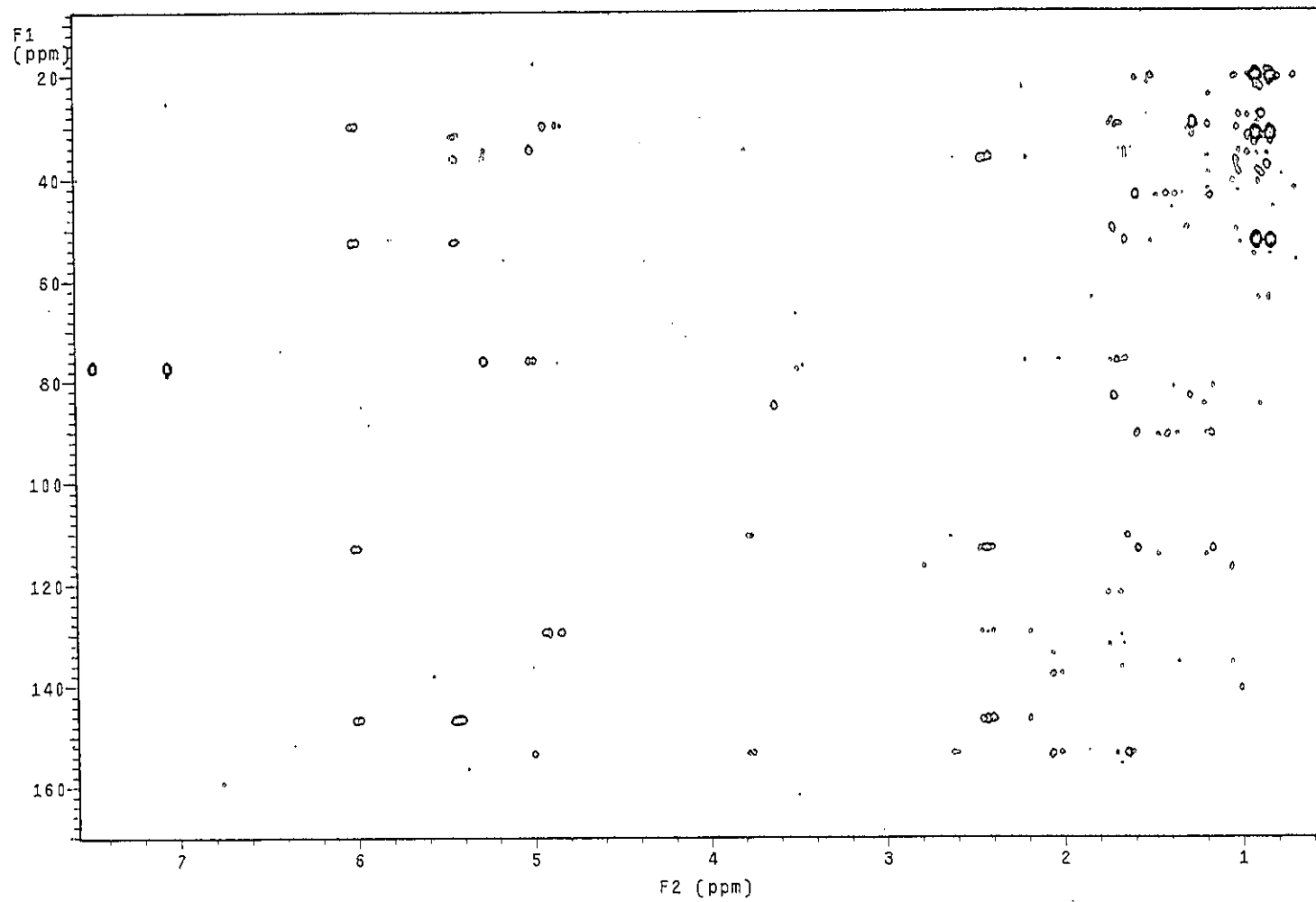


Figure 73 2D HMBC spectrum of DD7

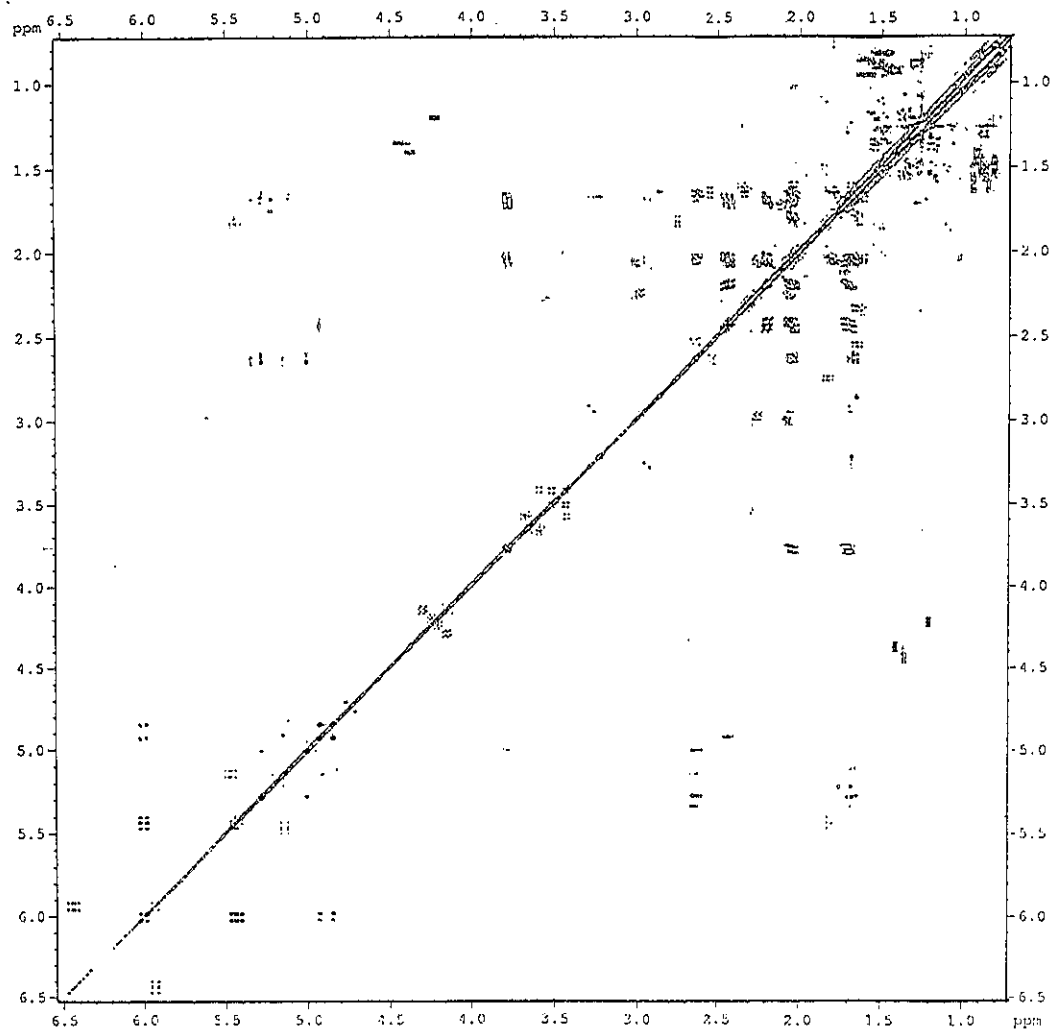


Figure 74 ^1H - ^1H cosy spectrum of DD7

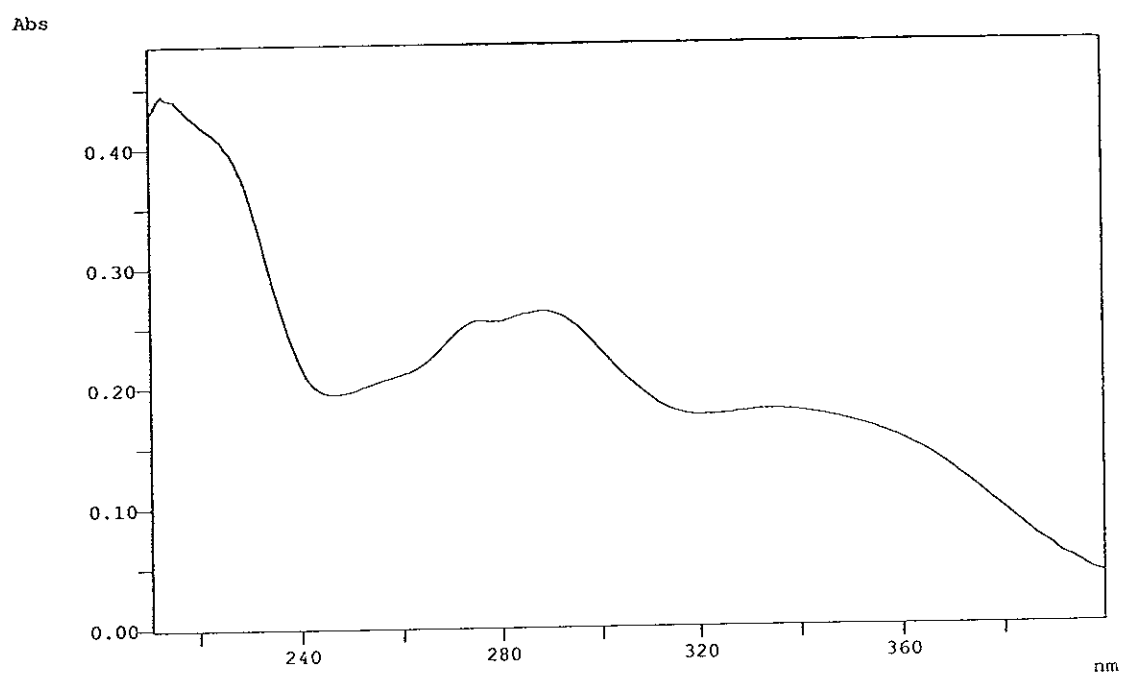


Figure 75 UV (MeOH) spectrum of DD16

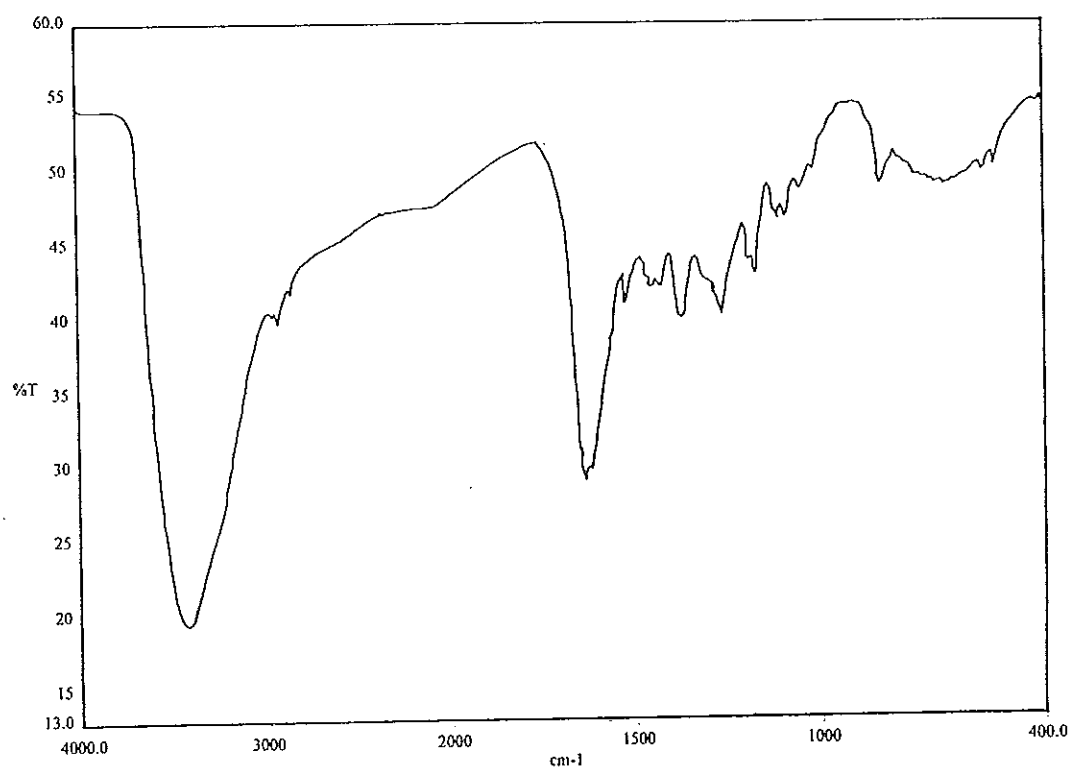


Figure 76 FT-IR (neat) spectrum of DD16

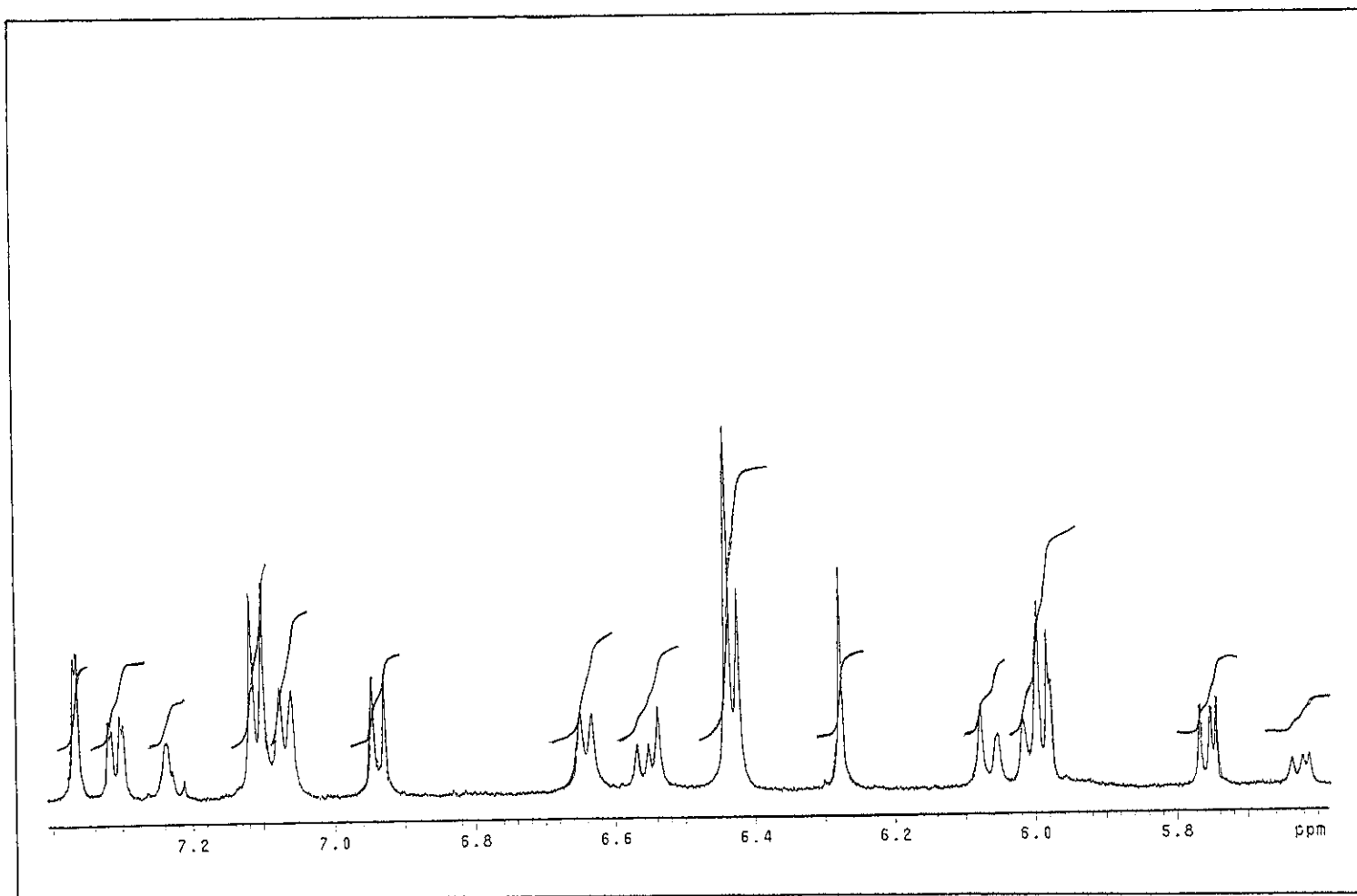


Figure 77 ¹H NMR (500 MHz) (CD₃OD) spectrum of DD16

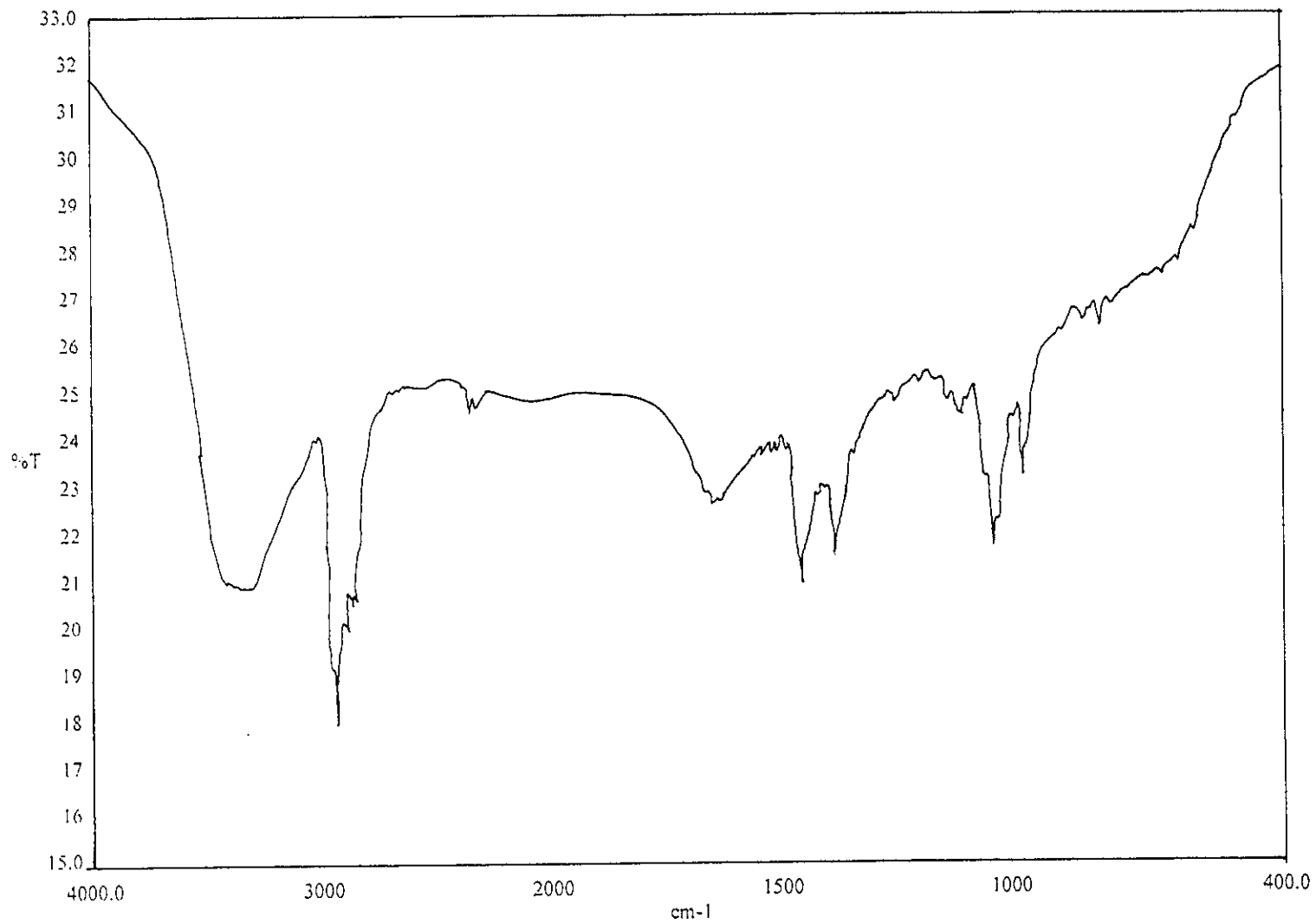


Figure 78 FT-IR (neat) spectrum of DD4

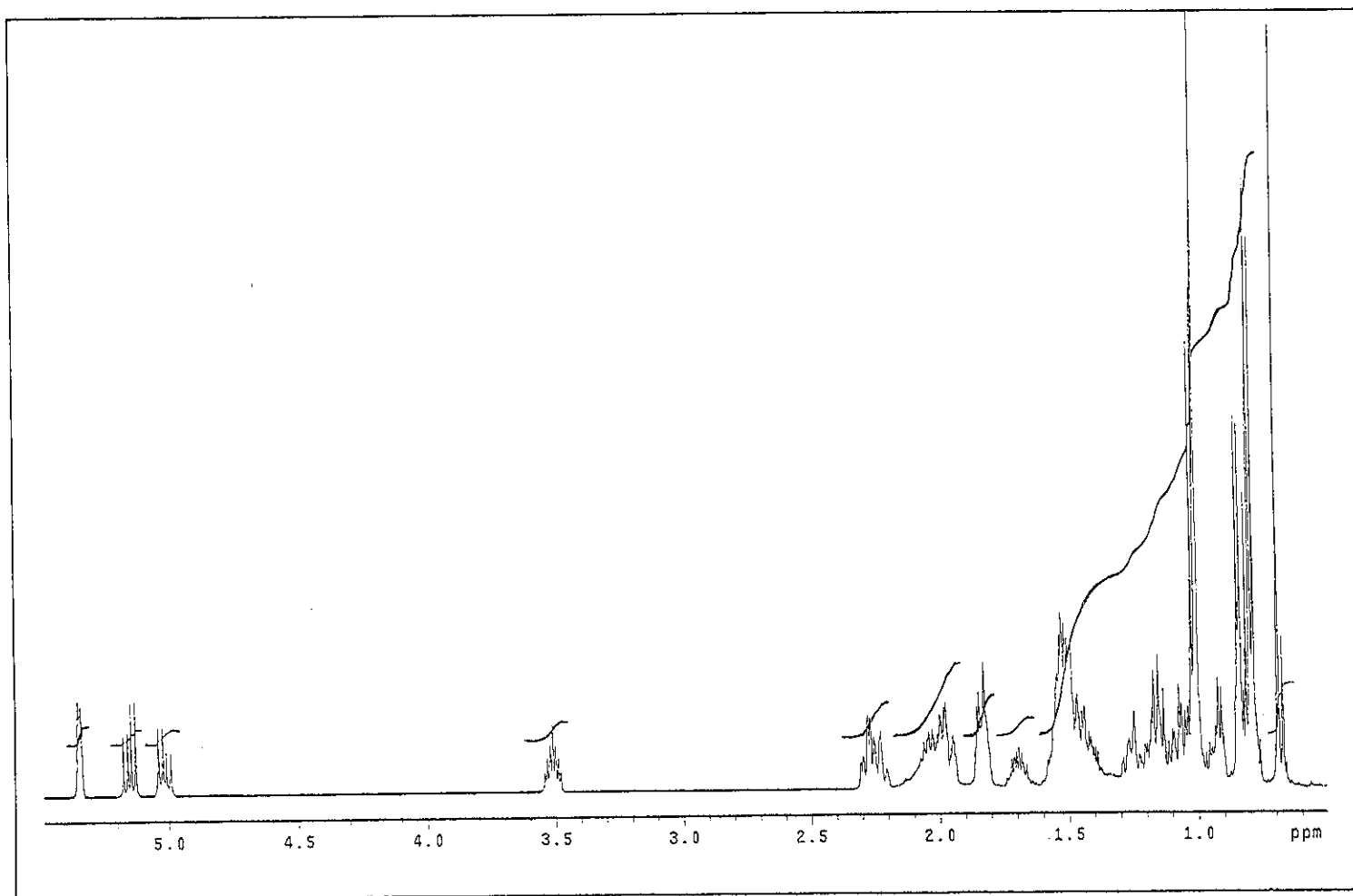


Figure 79 ^1H NMR (500 MHz) (CDCl_3) spectrum of DD4

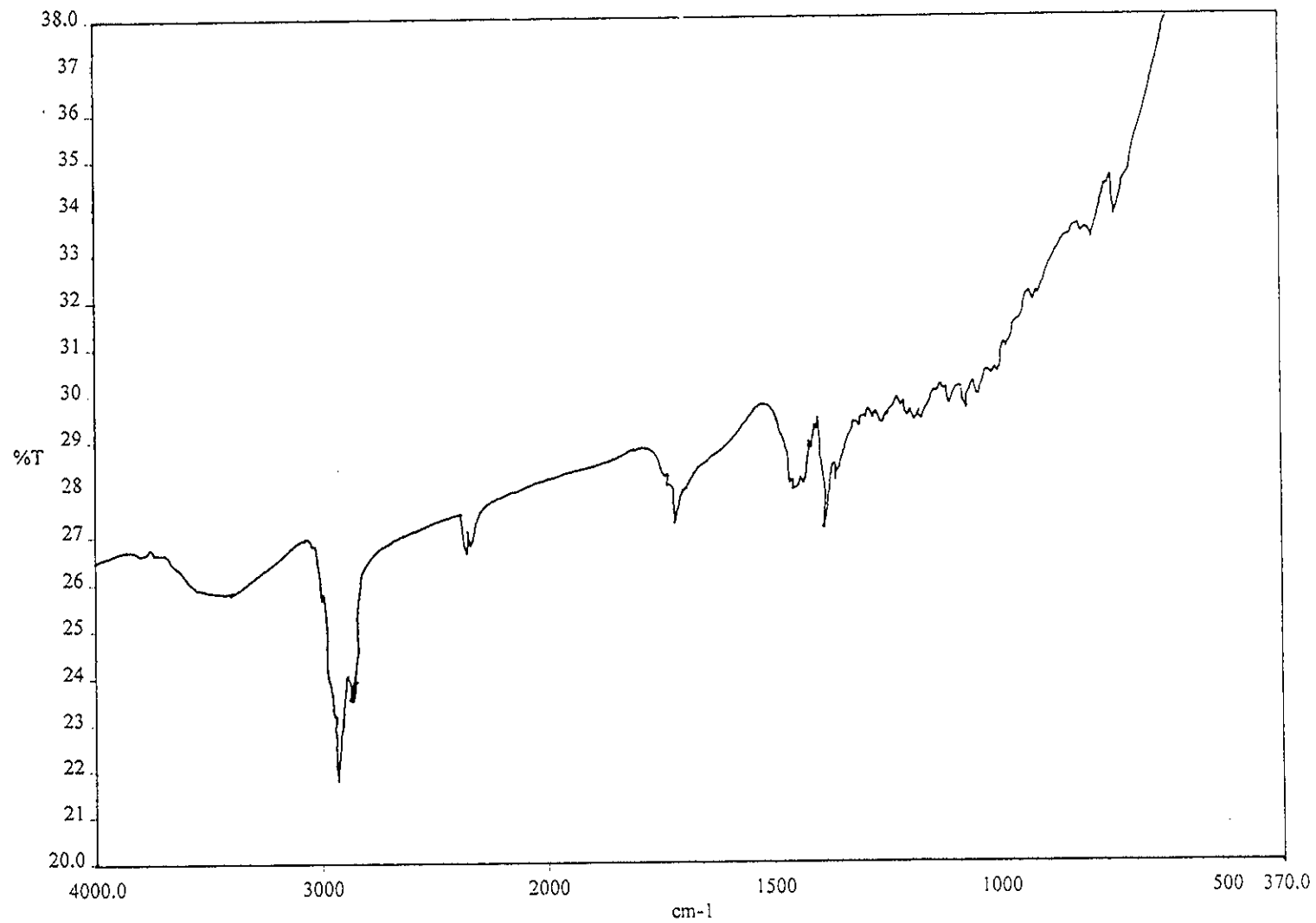


Figure 80 FT-IR (neat) spectrum of DD6

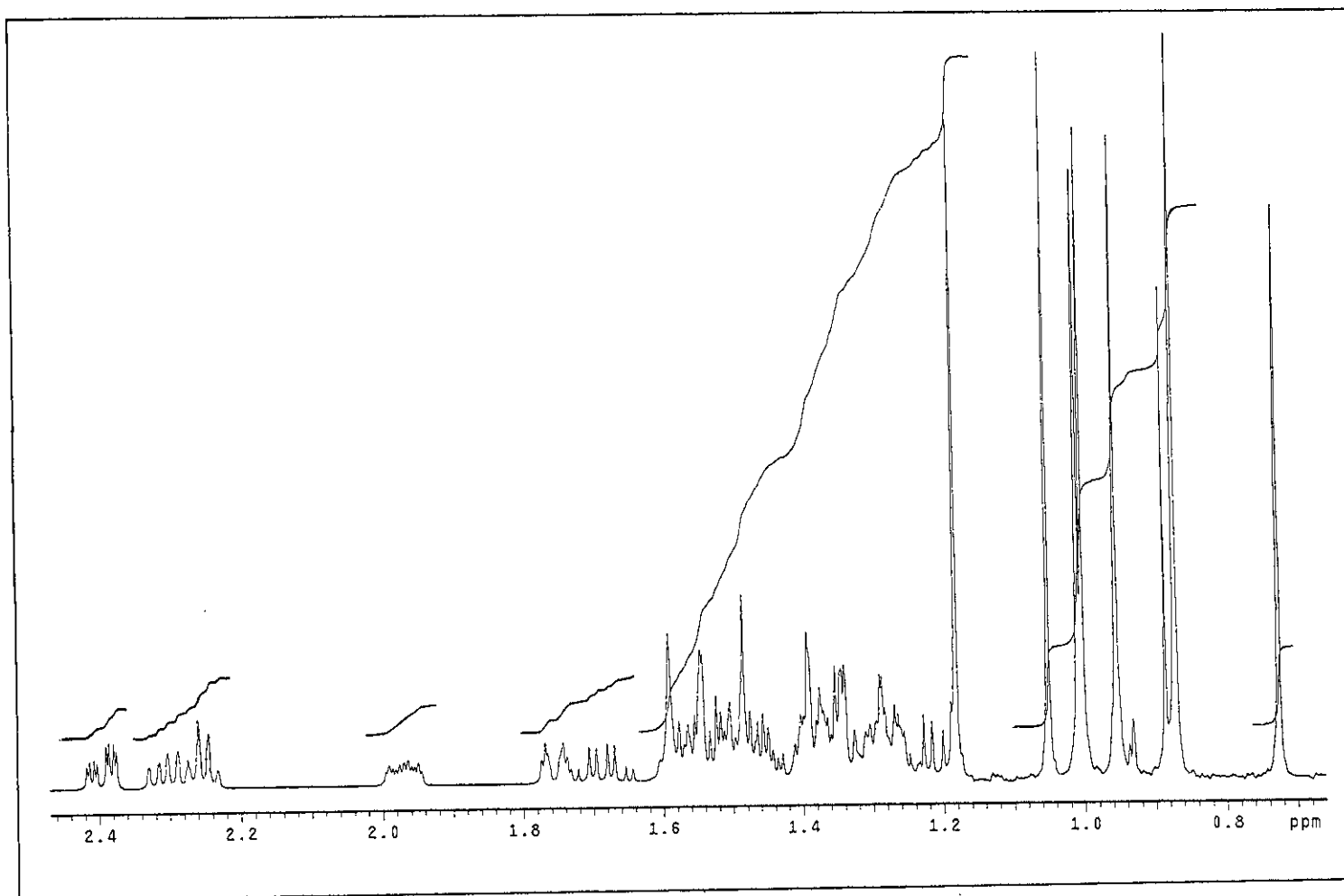


Figure 81 ¹H NMR (500 MHz) (CDCl₃) spectrum of DD6

Bibliography

เต็ม สมิตินันท์. 2523. “ชื่อพันธุ์ไม้แห่งประเทศไทย (ชื่อพฤกษศาสตร์-ชื่อพื้นเมือง)”.
กรมป่าไม้กรุงเทพฯ : พันธุ์พลับพลึง.

Adawadkar, P. D., Srinivasan, R. and Yemul, S. S. 1976. “Coloring matters of *Garcinia morella* : Part VIII. Morellinol, dihydromorelloflavone and morelloflavone-7^{''}- β -glucoside”, *Indian J. Chem.* 14B(1), 19-21.

Asano, J., Chiba, K., Tada, M. and Yoshii, T. 1996. “Cytotoxic xanthonenes from *Garcinia hanburyi*”, *Phytochemistry.* 41(3), 815-820.

Babu, V., Mashhood A. and Ilyas, M. 1988. “A biflavonoid from *Garcinia nervosa*”, *Phytochemistry.* 27(10), 3332-3335.

Bhat, H. B., Nair, P. M. and Venkataraman, K. 1964. “The coloring matters of *Garcinia morella* V. Isolation of deoxymorellin and dihydroisomorellin”, *Indian J. Chem.* 2(10), 405-410.

Bringi, N. V., Shah, K. H. and Venkataraman, K. 1955. “The coloring matters of *Garcinia morella* I.”, *J. Sci. Ind. Research (India).* 14B, 135-152.

Cao, S-G., Wu, X-H., Sim, K-Y., Tan, B. H. K., Pereira, J. T., Wong, W. H., Hew, N. F. and Goh, S. H. 1998a. “Cytotoxic caged tetraprenylated xanthonoids from

Garcinia gaudichaudii (Guttiferae)", *Tetrahedron Letters*. 39, 3353-3356.

Cao, S-G., Sng, V. H. L., Wu, X-H., Sim, K-Y., Tan, B. H. K., Pereira, J. T. and Goh, S. H. 1998b. "Novel cytotoxic polyprenylated xanthonoids from *Garcinia gaudichaudii* (Guttiferae)", *Tetrahedron*. 54, 10915-10924.

Cường, N. M., Sung, T. V. and Taylor, W. C. 1999. "Phân lập và xác định cấu trúc một sesquiterpen ancol có khung germacran từ cây cóm rượu (*Glycosmis petelotii*)", *Tap chí Hóa học*. 37(3), 52-55.

Fukuyama, Y., Kaneshi, A., Tani, N. and Kodama, M. 1993. "Subellinone, a polyisoprenylated phloroglucinol derivative from *Garcia subelliptica*", *Phytochemistry*. 33(2), 483-485.

Gopalakrishnan, G., Banumathi, B. and Suresh, G. 1997. "Evaluation of the antifungal activity of natural xanthenes from *Garcinia mangostana* and their synthetic derivatives", *J. Nat. Prod.* 60(5), 519-524.

Gunatilaka, A. A. L., Sriyani, H. T. B., Sotheeswaran, S. and Waight, E. S. 1983. "2,5-Dihydroxy-1,6-dimethoxyxanthone and biflavonoids of *Garcinia thwaitesii*", *Phytochemistry*. 22(1), 233-235.

Gustafson, K. R., Blunt, J. W., Munro, M. H. G., Fuller, R. W., McKee, T. C., Cardellina II, J. H., McMahon, J. B., Cragg, M. C. and Boyd, M. R. 1992. "The guttiferones, HIV-inhibitory benzophenones from *Symphonia*

globulifera, *Garcinia livingstonei*, *Garcinia ovalifolia* and *Clusia rosea*", *Tetrahedron*. 48(46), 10093-10102.

Hooker, J. D. 1875. "The Flora of British India", Vol. I (Ranunculaceae to Sapindaceae), L. Reeve & Co Ltd., The Oast House, Brook, NR. Ashford, Kent, England.

Iinuma, M., Tosa, H., Tanaka, T., Kanamaru, S., Asai, F., Kobayashi, Y., Miyauchi, K. and Shimano, R. 1996. "Antibacterial activity of some *Garcinia* benzophenone derivatives against Methicillin-Resistant *Staphylococcus aureus*", *Bio. Pharm. Bull.* 19(2), 311-314.

Ilyas, M., Kamil, M., Parveen, M. and Khan, M. S. 1994. "Isoflavones from *Garcinia nervosa*", *Phytochemistry*. 36(3), 807-809.

Ilyas, M., Perveen, M., Shafiullah and Ahmad, S. M. 2002. "A novel chalcone from *Garcinia nervosa*", *Journal of Chemical Research, Synopses*. (5), 231-233.

Ito, C., Miyamoto, Y., Nakayama, M., Kawai, Y., Rao, K. S. and Furukawa, H. 1997. "A novel depsidone and some new xanthenes from *Garcinia Species*", *Chem. Pharm. Bull.* 45(9), 1403-1413.

Ito, C., Itoigawa, M., Furukawa, H., Rao, K. S., Enjo, F., Bu, P., Takayasu, J., Tokuda, H. and Nishino, H. 1998. "Xanthenes as inhibitors of Epstein-Barr virus activation", *Cancer letters*. 132, 113-117.

- Kaewnok, W. 1999. "Chemical constituents from twigs of *Garcinia scortechinii*", M. Sc. Thesis, Prince of Songkla University, Thailand.
- Karanjgaonkar, C. G., Nair, P. M. and Venkataraman, K. 1966. "The coloring matters of *Garcinia morella* VI. Morellic, isomorellic and gambogic acid", *Tetrahedron Letters*. (7), 687-691.
- Kartha, G., Ramachandran, G. N., Bhat, H. B., Nair, P. M., Raghavan, K. V. and Venkataraman, K. 1963. "The constitution of morellin", *Tetrahedron Letters*. 7, 459-472.
- Kosela, S., Hu, L-H., Rachmatia, T., Hanafi, M. and Sim, K-Y. 2000. "Dulxanthones F-H, three new pyranoxanthones from *Garcinia dulcis*", *J. Nat. Prod.* 63(3), 406-407.
- Leong, Y-W., Harrison, L. J., Bennett, G. J. and Tan, H. T. W. 1996. "Forbesione, a modified xanthone from *Garcinia forbesii*", *J. Chem. Res., Synop.* (8), 392-393.
- Lin, L. J., Lin, L. Z., Pezzuto, J. M., Cordell, G. A. and Ruangrunsi, N. 1993. "Isogambogic acid and isomorellinol from *Garcinia hanburyi*", *Magn. Reson. Chem.* 31(4), 340-347.
- Lin, Y-M., Anderson, H., Flavin, M. T., Pai, Y-H. S., Mata-Greenwood, E., Pengsuparp, T., Pezzuto, M. J., Schinazi, R. F., Hughes, S. H. and Chen, F-

C. 1997. "In vitro anti-HIV activity of biflavonoids isolated from *Rhus succedanea* and *Garcinia multiflora*", *J. Nat. Prod.* 60(9), 884-888.

Likhitwitayawuid, K., Phadungcharoen, T. and Krungkrai, J. 1998a. "Antimalarial xanthenes from *Garcinia cowa*", *Planta Medica.* 64(1), 70-72.

Likhitwitayawuid, K., Chanmahasathien, W., Ruangrunsi, N. and Krungkrai, J. 1998b. "Xanthenes with antimalarial activity from *Garcinia dulcis*", *Planta Medica.* 64(3), 281-282.

Mackeen, M. M., Ali, A. M., Lajis, N. Hj., Kawazu, K., Kikuzaki, H. and Nakatani, N. 2002. "Antifungal garcinia acid esters from the fruits of *Garcinia atroviridis*", *Journal of Biosciences.* 57(3/4), 291-295.

Minami, H., Kuwayama, A., Yoshizawa, T. and Fukuyama, Y. 1996. "Novel prenylated xanthenes with antioxidant property from the wood of *Garcinia subelliptica*", *Chem. Pharm. Bull.* 44(11), 2103-2106.

Minami, H., Hamaguchi, K., Kubo, M. and Fukuyama, Y. 1998. "A Benzophenone and a xanthone from *Garcinia subelliptica*", *Phytochemistry.* 49(6), 1783-1785.

Murty, D. V. K. and Rao, P. L. N. 1953. "Antibiotic principles of *Garcinia morella* III. Moreollin, a new pigment", *J. Sci. Ind. Research (India).* 12B, 565-566.

- Nilar and Harrison, L. J. 2002. "Xanthenes from the heartwood of *Garcinia mangostana*", *Phytochemistry*. 60, 541-548.
- Nyemba, A-M., Mpondo, T. N., Connolly, J. D. and Rycroft, D. S. 1990. "Cycloartane derivatives from *Garcinia lucida*", *Phytochemistry*. 29(3), 994-997.
- Ollis, W. D., Ramsay, M. V. J. and Sutherland, I. O. 1965. "The constitution of gambogic acid", *Tetrahedron*. 21, 1453-1470.
- Phainuphong, P. 2002. "Caged-polyprenylated xanthenes from the latex and the stem bark of *Garcinia scortechinii*", M. Sc. Thesis, Prince of Songkla University, Thailand.
- Parveen, M., Khan, N. U., Achari, B. and Dutta, P. K. 1991. "A triterpene from *Garcinia mangostana*", *Phytochemistry*. 30(1), 361-362.
- Pelter, A., Warren, R., Chexal, K. K., Handa, B. K. and Rahman, W. 1971. "Biflavonyls from Guttiferae-*Garcinia livingstonii*", *Tetrahedron*. 27, 1625-1634.
- Peres, V., Nagem, T. J. and Oliveira, F. F. 2000. "Tetraoxygenated naturally occurring xanthenes", *Phytochemistry*. 55, 683-710.

- Permana, D., Lajis, N. H., MacKeen, M. M., Ali, A. M., Aimi, N., Kitajima, M. and Takayama, H. 2001. "Isolation and bioactives of constituents of the roots of *Garcinia atroviridis*", *J. Nat. Prod.* 64(7), 976-979.
- Rao, B. S. 1937. "Morellin, a constituent of the seeds of *Garcinia morella*", *J. Chem. Soc.* 853-855.
- Rao, G. S. R. S., Mala, S. R., Surendranath, V., Gupta, V. S. and Rao, N. 1974. "The structure of moreollin", *Tetrahedron Letters.* (14), 1259-1262.
- Ritthiwigrom, T. 2002. "Xanthones from the stem bark of *Garcinia nigrolineata*", M. Sc. Thesis, Prince of Songkla University, Thailand.
- Rukachaisirikul, V., Kaewnok, W., Koysomboon, S., Phongpaichit, S. and Taylor, W. C. 2000a. "Caged-tetraprenylated xanthones from *Garcinia scortechinii*", *Tetrahedron.* 56, 8539-8543.
- Rukachaisirikul, V., Adiar, A., Dampawan, P., Taylor, W. C. and Turner, P. C. 2000b. "Lanostanes and friedolanostanes from the pericarp of *Garcinia hombroniana*", *Phytochemistry.* 55, 183-188.
- Spino, C., Lal, J., Sotheeswaran, S. and Aalbersberg, W. 1995. "Three prenylated phenolic benzophenones from *Garcinia myrtifolia*", *Phytochemistry.* 38(1), 233-236.

- Suksamrarn, S., Suwannapoch, N., Ratananukul, P., Aroonlerk, N. and Suksamrarn, A. 2002. "Xanthones from the green fruit hulls of *Garcinia mangostana*", *J. Nat. Prod.* 65, 761-763.
- Sukpondma, Y. 2002. "Chemical constituents from the fruits of *Garcinia scortechinii*", Unpublished data, Prince of Songkla University, Thailand.
- Terashima, K., Kondo, Y., Mohammad, A. and Niwa, M. 1999. "A new xanthone from the stems of *Garcinia kola*", *Nat. Prod. Lett.* 14(2), 91-97.
- Thoison, O., Fahy, J., Dumontet, V., Chiaroni, A., Riche, C., Tri, M. V. and Sevenet, T. 2000. "Cytotoxic prenylxanthones from *Garcinia bracteata*", *J. Nat. Prod.* 63(4), 441-446.
- Waterman, P. G. and Crichton, E. G. 1980. "Xanthones and biflavonoids from *Garcinia densivenia*", *Phytochemistry.* 19, 2723-2726.
- Wu, X-H., Tan, B. K. H., Cao, S-G., Sim, K-Y. and Goh, S. H. 2000. "Two minor, cytotoxic caged xanthonoids from *Garcinia gaudichaudii*", *Natural Product Letters.* 14(6), 453-458.
- Wu, J., Xu, Y-J., Cheng, X-F., Harrison, L. J., Sim, K-Y. and Goh, S. H. 2001. "A highly rearranged tetraprenylxanthonoid from *Garcinia gaudichaudii* (Guttiferae)", *Tetrahedron Letters.* 42, 727-729.

Xu, Y. J., Yip, S. C., Kosela, S., Fitri, E., Hana, M., Goh, S. H. and Sim, K. Y. 2000.

“Novel cytotoxic, polyprenylated heptacyclic xanthonoids from Indonesian *Garcinia gaudichaudii* (Guttiferae)”, *Organic Letters*. 2(24), 3945-3948.

Yates, P., Karmarkar, S. S., Rosenthal, D., Stout, G. H. and Stout, V. F. 1963.

“Acetyl- α -gambogic acid”, *Tetrahedron Letters*. 24, 1623-1629.

Vitae

Name Miss Dudsadee Sukavisite

Birth Date 21 April 1978

Place of Birth Phuket, Thailand

Educational Attainment

Degree	Name of Institution	Year of Graduation
Bachelor of Science (Chemistry)	Prince of Songkla University	1996-2000
Master of Science (Organic Chemistry)	Prince of Songkla University	2000-2003

Scholarship Awards during Enrolment

1. The partial support from Higher Education Development Project : Postgraduate Education and Research Program in Chemistry, funded by The Royal Thai Government
2. The partial support from the Graduate School, Prince of Songkla University